frontiers | Research Topics

Insights in vascular physiology 2024

Edited by
Christopher Garland, Irena Levitan and
Luis A. Martinez-Lemus

Published in
Frontiers in Physiology

ISSN 1664-8714
ISBN 978-2-8325-6457-8
DOI 10.3389/978-2-8325-6457-8

About Frontiers

Frontiers is more than just an open access publisher of scholarly articles: it is a pioneering approach to the world of academia, radically improving the way scholarly research is managed. The grand vision of Frontiers is a world where all people have an equal opportunity to seek, share and generate knowledge. Frontiers provides immediate and permanent online open access to all its publications, but this alone is not enough to realize our grand goals.

Frontiers journal series

The Frontiers journal series is a multi-tier and interdisciplinary set of open-access, online journals, promising a paradigm shift from the current review, selection and dissemination processes in academic publishing. All Frontiers journals are driven by researchers for researchers; therefore, they constitute a service to the scholarly community. At the same time, the *Frontiers journal series* operates on a revolutionary invention, the tiered publishing system, initially addressing specific communities of scholars, and gradually climbing up to broader public understanding, thus serving the interests of the lay society, too.

Dedication to quality

Each Frontiers article is a landmark of the highest quality, thanks to genuinely collaborative interactions between authors and review editors, who include some of the world's best academicians. Research must be certified by peers before entering a stream of knowledge that may eventually reach the public - and shape society; therefore, Frontiers only applies the most rigorous and unbiased reviews. Frontiers revolutionizes research publishing by freely delivering the most outstanding research, evaluated with no bias from both the academic and social point of view. By applying the most advanced information technologies, Frontiers is catapulting scholarly publishing into a new generation.

What are Frontiers Research Topics?

Frontiers Research Topics are very popular trademarks of the *Frontiers journals series*: they are collections of at least ten articles, all centered on a particular subject. With their unique mix of varied contributions from Original Research to Review Articles, Frontiers Research Topics unify the most influential researchers, the latest key findings and historical advances in a hot research area.

Find out more on how to host your own Frontiers Research Topic or contribute to one as an author by contacting the Frontiers editorial office: frontiersin.org/about/contact

Insights in vascular physiology: 2024

Topic editors

Christopher Garland — University of Oxford, United Kingdom
Irena Levitan — University of Illinois Chicago, United States
Luis A. Martinez-Lemus — University of Missouri, United States

Citation

Garland, C., Levitan, I., Martinez-Lemus, L. A., eds. (2025). *Insights in vascular physiology: 2024*. Lausanne: Frontiers Media SA. doi: 10.3389/978-2-8325-6457-8

Table of contents

frontiers | Frontiers in Physiology

TYPE Editorial
PUBLISHED 29 May 2025
DOI 10.3389/fphys.2025.1628173

OPEN ACCESS

EDITED AND REVIEWED BY
Osama F. Harraz,
University of Vermont, United States

*CORRESPONDENCE
Irena Levitan,
levitan@uic.edu

RECEIVED 13 May 2025
ACCEPTED 14 May 2025
PUBLISHED 29 May 2025

CITATION
Martinez-Lemus LA, Garland C and Levitan I (2025) Editorial: Insights in vascular physiology 2024.
Front. Physiol. 16:1628173.
doi: 10.3389/fphys.2025.1628173

Editorial: Insights in vascular physiology 2024

Luis A. Martinez-Lemus[1], Christopher Garland[2] and Irena Levitan[3]*

[1]Department of Medical Pharmacology and Physiology, University of Missouri, Colombia, MO, United States, [2]The Vascular Pharmacology Group, Department of Pharmacology, University of Oxford, Oxford, United Kingdom, [3]Department of Medicine, Pulmonary Section, University of Illinois Chicago, Chicago, IL, United States

KEYWORDS

endothelial cells, ion channels, aging, kinases, hemodynamic forces

Editorial on the Research Topic
Insights in vascular physiology 2024

In this special issue, we present recent discoveries in vascular physiology, focusing on the regulation of blood flow and hemodynamic forces, ion channels, metabolism, LIM kinases and aging.

Blood flow is known to be regulated by the mechanical forces of shear stress via endothelial mechano-transduction. However, the role of stiffness of vascular smooth muscle cells (VSMCs) in the regulation of blood flow is virtually unknown. In this Research Topic, McCallinhart et al. presented a groundbreaking study "*Coronary Cytoskeletal Modulation of Coronary Blood Flow in the Presence and Absence of Type 2 Diabetes: The Role of Cofilin*" demonstrating that cytoskeleton remodeling of VSMCs in type 2 diabetes results in the softening of coronary resistance arteries, which augments coronary blood flow. Mechanistically, the authors showed that the softening of the VSMCs is mediated by the actin-binding protein cofilin, which promotes the disassembly of filamentous actin (F-actin), resulting in a loss of F-actin architecture. This mechanism is proposed to be compensatory to a decrease in coronary blood flow, a known complication of diabetes. Notably, this is in contrast to large arteries, which stiffen under diabetic conditions. This has a deleterious effect on cardiovascular function. This is the first indication that direct modulation of VSMCs' cytoskeletal structure can regulate blood flow *in vivo*. The role of hemodynamic forces in vascular physiology is also addressed in this issue by Kuang et al. In their study "*Fundamental Equations and Hypotheses Governing Glomerular Hemodynamics*". They presented a new mathematical model of the glomerular hemodynamics in the Hypothesis and Theory category, which helps to understand the physics governing glomerular filtration in a more holistic way. Finally, a review article by Chen et al. discussed recent advances in understanding the mechanisms by which low and oscillatory flow disrupts the endothelial barrier. The authors cover the complex interactions between the endothelial glycocalyx, the cytoskeleton and the junctional architecture, leading to a better understanding of how pro-inflammatory flow disrupts the barrier.

Potassium channels play a fundamental role in regulating arterial VSMCs and endothelial cell signaling via nitric oxide (NO) and EDH. Recent research has identified

a key role for one form of the delayed rectifier K^+ channel, $K_V1.3$, in the development of intimal hyperplasia during type 2 diabetes, including in human arteries. Since low-grade inflammation is ubiquitous in T2D, the paper by Peraza et al. titled "*A sex-dependent role of Kv1.3 channels from macrophages in metabolic syndrome*" investigated whether other metabolic syndrome-related effects are ameliorated by inhibiting $K_V1.3$ and demonstrated that blocking these channels had a primary effect against the infiltration of macrophages in female mice. Another form of K^+-channel, the BK_{Ca} channel, which is found in VSMCs, not endothelial cells, was found to be linked to spontaneous calcium sparks, with activity suppressing vascular reactivity. These channels can also be influenced by NO. The study by Shvetsova et al. titled "*Dual Role of Calcium-Activated Potassium Channels of High Conductance: Facilitator or Limiter of NO-induced Arterial Relaxation?*" indicated that this is a dual effect in VSMCs, with BK_{Ca} limiting vasodilation to the NO-donor SNP in arteries stimulated with low concentrations of the vasoconstrictor methoxamine. In contrast, with higher concentrations of methoxamine BK_{Ca} activity was observed to enhance vasodilation to NO. The authors suggest that NO acts indirectly by inhibiting Ca^{2+} entry via VGCC, thereby limiting BK_{Ca} activity during low-level vasoconstriction. However, as vasoconstriction becomes more intense, the influence of BK_{Ca} increases, enhancing vasodilation to NO. BK_{Ca} channels are sensitive to voltage and calcium so it remains to be demonstrated whether VSM depolarization contributes to enhanced hyperpolarizing current and thus vasodilation.

A significant risk factor for the development of cardiovascular disease is hypertension. In pregnancy, it endangers the development of the embryo/fetus along with the health of the mother. Two prominent characteristics of hypertension are the presence of endothelial dysfunction and arterial stiffening. How these two characteristics of hypertension correlate in pregnant women with chronic hypertension or preeclampsia was revealed in the study by Kaihara et al. "*Differences between macrovascular and microvascular functions in pregnant women with chronic hypertension and preeclampsia: new insights into maternal vascular health*." Their results indicate that an increased carotid-femoral pulse wave velocity is consistently present in both chronic hypertension and preeclampsia. Meanwhile, reactive hyperemia was positively correlated with blood pressure and plasma nitrite (a surrogate of nitric oxide) only in preeclampsia. Since carotid-femoral pulse wave velocity represents large artery stiffness and reactive hyperemia represents microvascular function, Kaihara et al. proposed the explanation that microvascular endothelial function is preserved in preeclampsia due to its earlier onset compared to that of chronic hypertension. An additional explanation is that endothelial dysfunction is not the initial driver of hypertension in preeclampsia. Further investigation of the potential explanations that Kaihara et al. provided for their results could influence the therapeutic approaches for the treatment of preeclampsia.

This issue also includes review articles on targeting NO production and on using the zebrafish as a model of aging. "*Promotion of Nitric Oxide Production: Mechanisms, Strategies, and Possibilities*" by Gonzalez et al. provided a brief but highly comprehensive overview of the targetable mechanisms for promoting NO production. The authors discussed the strategies currently used in clinical practice and potential approaches with specific limitations, such as specificity issues and a lack of large-scale clinical data. These limitations are appropriately described in their review. In "Cerebrovascular ageing: how zebrafish can contribute to solving the puzzle", Malkinson and Henriques addressed the potentially impactful role of using zebrafish as a model for studying cerebrovascular aging. The researchers highlighted the advantages of assessing longitudinal cerebrovascular changes throughout the lifespan of the model and its capacity to image genetically modified and labeled targets in the whole zebrafish. Another important review article by Lateef et al. "*LIM kinases in cardiovascular health and disease*" provided a comprehensive review of the roles of LIM kinases, which regulate cytoskeleton dynamics, in cardiovascular cells. LIM kinases are known to be canonical substrates of small Rho-GTPases but despite accumulating evidence of their critical roles in the cardiovascular system, a comprehensive review has been lacking. Lateef et al. provided an in-depth analysis of the Research Topic.

Author contributions

LM-L: Writing – original draft, Writing – review and editing. CG: Writing – original draft, Writing – review and editing. IL: Writing – original draft, Writing – review and editing.

Funding

The author(s) declare that no financial support was received for the research and/or publication of this article.

Conflict of interest

The authors declare that the research was conducted in the absence of any commercial or financial relationships that could be construed as a potential conflict of interest.

The author(s) declared that they were an editorial board member of Frontiers, at the time of submission. This had no impact on the peer review process and the final decision.

Generative AI statement

The author(s) declare that no Generative AI was used in the creation of this manuscript.

Publisher's note

frontiers | Frontiers in Physiology

TYPE Hypothesis and Theory
PUBLISHED 14 August 2024
DOI 10.3389/fphys.2024.1440627

OPEN ACCESS

EDITED BY
Irena Levitan,
University of Illinois Chicago, United States

REVIEWED BY
Praghalathan Kanthakumar,
University of Missouri, United States
Elizabeth LeMaster,
University of Illinois Chicago, United States

*CORRESPONDENCE
Serena Y. Kuang,
kuang@oakland.edu

RECEIVED 29 May 2024
ACCEPTED 19 July 2024
PUBLISHED 14 August 2024

CITATION
Kuang SY, Ahmetaj B and Qu X (2024), Fundamental equations and hypotheses governing glomerular hemodynamics. *Front. Physiol.* 15:1440627. doi: 10.3389/fphys.2024.1440627

Fundamental equations and hypotheses governing glomerular hemodynamics

Serena Y. Kuang [1]*, Besjana Ahmetaj[1] and Xianggui Qu [2]

[1]Department of Foundational Medical Studies, Oakland University William Beaumont School of Medicine, Rochester, MI, United States, [2]Department of Mathematics and Statistics, Oakland University, Rochester, MI, United States

The glomerular filtration rate (GFR) is the outcome of glomerular hemodynamics, influenced by a series of parameters: renal plasma flow, resistances of afferent arterioles and efferent arterioles (EAs), hydrostatic pressures in the glomerular capillary and Bowman's capsule, and plasma colloid osmotic pressure in the glomerular capillary. Although mathematical models have been proposed to predict the GFR at both the single-nephron level and the two-kidney system level using these parameters, mathematical equations governing glomerular filtration have not been well-established because of two major problems. First, the two-kidney system-level models are simply extended from the equations at the single-nephron level, which is inappropriate in epistemology and methodology. Second, the role of EAs in maintaining the normal GFR is underappreciated. In this article, these two problems are concretely elaborated, which collectively shows the need for a shift in epistemology toward a more holistic and evolving way of thinking, as reflected in the concept of the complex adaptive system (CAS). Then, we illustrate eight fundamental mathematical equations and four hypotheses governing glomerular hemodynamics at both the single-nephron and two-kidney levels as the theoretical foundation of glomerular hemodynamics. This illustration takes two steps. The first step is to modify the existing equations in the literature and establish a new equation within the conventional paradigm of epistemology. The second step is to formulate four hypotheses through logical reasoning from the perspective of the CAS (beyond the conventional paradigm). Finally, we apply the new equation and hypotheses to comprehensively analyze glomerular hemodynamics under different conditions and predict the GFR. By doing so, some concrete issues are eliminated. Unresolved issues are discussed from the perspective of the CAS and a desinger's view. In summary, this article advances the theoretical study of glomerular dynamics by 1) clarifying the necessity of shifting to the CAS paradigm; 2) adding new knowledge/insights into the significant role of EAs in maintaining the normal GFR; 3) bridging the significant gap between research findings and physiology education; and 4) establishing a new and advanced foundation for physiology education.

KEYWORDS

glomerular hemodynamics, renal plasma flow, glomerular filtration rate, efferent arteriole, mathematical model, colloid osmotic pressure, net filtration pressure, complex adaptive system

1 Introduction

The mammalian kidney is a vital organ responsible for maintaining homeostasis by regulating fluid balance, electrolytes, and waste removal through urine production. It plays a crucial role in the overall health and functionality of the body. The kidney is unique in the body as it is the only organ that has two arterioles and two capillary beds aligned in a series. The renal autoregulation mechanisms (myogenic response and tubuloglomerular feedback [TGF]) keep the renal plasma flow (RPF) and glomerular filtration rate (GFR) stable when arterial blood pressure fluctuates within a broad range. This indicates the importance of maintaining a normal GFR that is critical to the homeostasis of the internal environment. Precise regulation of the GFR depends on the balance between the resistances of afferent arterioles (AAs) and efferent arterioles (EAs), which together determine the net filtration pressure (NetP) that drives glomerular filtration.

NetP is the sum of the four Starling forces across a glomerular capillary wall. The two Starling forces that favor glomerular filtration are the hydrostatic pressure in the glomerular capillary (P_{GC}) and the colloid osmotic pressure in Bowman's capsule (π_{BC}), where π_{BC} is zero or negligible in the normal situation and becomes significant in patients with various renal diseases. The two Starling forces that oppose glomerular filtration are the plasma colloid osmotic pressure in the glomerular capillary (π_{GC}) and the hydrostatic pressure in Bowman's capsule (P_{BC}). The filtration fraction (FF) is the ratio of the GFR/RPF and is about 20% in the normal situation. All of these parameters together characterize glomerular hemodynamics and determine the GFR.

The parameters of glomerular hemodynamics are well-known and have been used to establish mathematical models to predict the GFR at both the single-nephron (SN) level and the two-kidney system level (Deen et al., 1974; Huss et al., 1975; Brenner et al., 1976; Navar et al., 1977; Chang, 1978; Papenfuss and Gross, 1978; Tucker and Blantz, 1981; Sgouralis and Layton, 2015). Nevertheless, two major problems exist: first, the two-kidney system-level equations are simply extended from the equations at the SN level, which is inappropriate in epistemology and methodology. Second, EAs play an important role in glomerular hemodynamics and, thus, the GFR, but the role of EAs in the maintenance of the normal GFR is underappreciated. These two problems are elaborated in terms of a total of six concrete issues in the next section and collectively show the need for a shift in epistemology toward a more holistic and evolved way of thinking reflected in the concept of the complex adaptive system (CAS; Holland, 2006; Carmichael and Hadžikadić, 2019).

After this elaboration, we illustrate eight fundamental equations and four hypotheses that govern glomerular hemodynamics at both the SN and two-kidney system levels as the theoretical foundation of glomerular hemodynamics. This illustration modifies some equations in the literature, establishes a new equation in the conventional paradigm of epistemology, and formulates four new hypotheses through logical reasoning from the perspective of the CAS (beyond the conventional paradigm). Finally, we apply the new equation and hypotheses we established to comprehensively analyze glomerular hemodynamics under different conditions and predict the GFR. By doing so, some concrete issues are eliminated. Unresolved issues are discussed from the perspective of the CAS and a desinger's view. The methodology in this article is logical, largely quantitative, and systematic.

The significance of this article is as follows: 1) it makes clear the necessity of shifting the epistemology that guides research from a conventional paradigm toward a CAS paradigm; 2) it adds new knowledge/insights to understand the significant potential role of EAs in maintaining the normal GFR, which has been underappreciated; 3) it bridges the significant gap between research findings and physiology education; and 4) it establishes a new and advanced foundation for physiology education in which glomerular hemodynamics should be illustrated at the SN and two-kidney system levels.

2 How are system-level equations extended from the SN level, and why is the role of EAs in the GFR underappreciated?

Different from the pressure profile in the peripheral capillaries, the decrease in P_{GC} during glomerular filtration is insignificant, so P_{GC} is constant throughout glomerular filtration (Figure 1). Meanwhile, π_{GC} is a variable that increases linearly (Figure 1A) or nonlinearly (Figures 1B,C) during glomerular filtration (Brenner et al., 1976; Giebisch et al., 2017; Hall and Hall, 2021). The rising orange line labeled Q in Figure 1 shows the sum of the two opposing pressures to glomerular filtration: $\pi_{GC} + P_{BC}$. P_{BC} is constant under normal conditions (Giebisch et al., 2017) and in Figure 1, and π_{BC} is ignored under normal situations and, thus, not drawn. If the orange line rises, it means that π_{GC} increases because P_{BC} remains constant.

Based on Figure 1, multiple issues can be addressed as follows. In the literature, different symbols are used to refer to the parameters of glomerular hemodynamics. In this article, we deal with the equations that model glomerular hemodynamics at both the SN and system levels; hence, the parameters at these levels are clearly differentiated to avoid confusion, and new terms are defined when necessary.

2.1 Issue 1

The widely used equation, $NetP = P_{GC} - \pi_{GC} - P_{BC}$, is qualitative and vague. π_{GC} increases during glomerular filtration, so it is unclear which value of π_{GC}, such as an instantaneous π_{GC} or the mean π_{GC} throughout glomerular filtration ($\overline{\pi_{GC\_SN}}$), should be used in the equation. It is also unclear how $\overline{\pi_{GC\_SN}}$ should be quantified when it increases nonlinearly (Figures 1B,C). Subsequently, whether NetP is instantaneous or the total $NetP_{SN}$ or the mean NetP throughout glomerular filtration ($\overline{NetP_{SN}}$) is not addressed. These questions are sometimes addressed in research (Brenner et al., 1976; Navar et al., 1977; Papenfuss and Gross, 1978) but do not appear in physiology education, leaving the equation quantitatively inappropriate and useless.

2.2 Issue 2

Another widely used equation, $GFR = K_f(NetP) = K_f(P_{GC} - \pi_{GC} - P_{BC})$, where K_f refers to the filtration coefficient

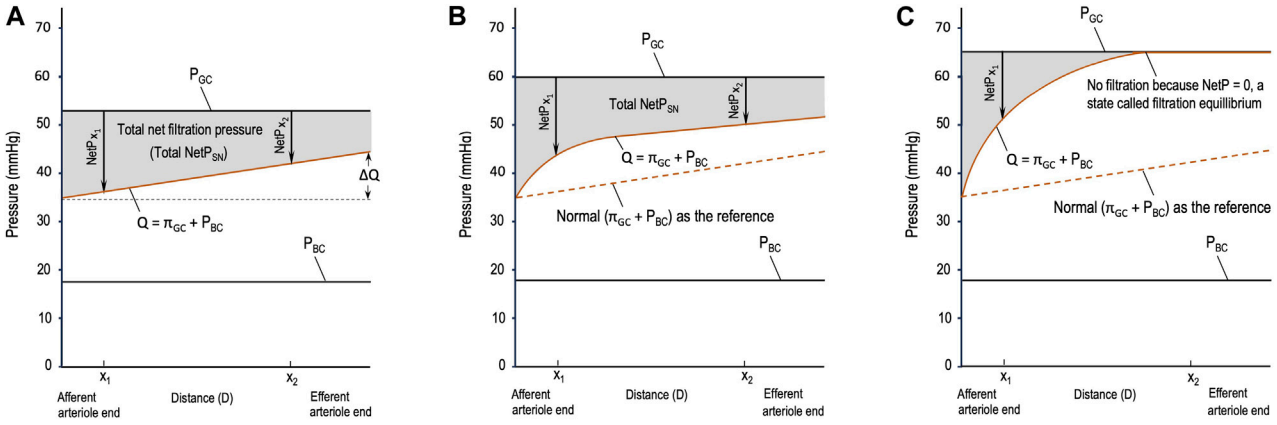

FIGURE 1
Starling forces across the wall of a glomerular capillary (GC) in three different situations. **(A)** Normal stable glomerular hydrostatic pressure (P_{GC}) and increasing plasma colloid osmotic pressure (π_{GC}); **(B)** initial moderate elevations in P_{GC} and π_{GC} due to moderate efferent arteriole (EA) constriction; and **(C)** initial significant elevations in P_{GC} and π_{GC} due to severe EA constriction. P_{BC}: hydrostatic pressure in Bowman's capsule, x_1 and x_2: distances in the capillary from the afferent arteriole end.

(Drumond and Deen, 1994; Leatherby et al., 2021), is more vague or ambiguous. It has the same problem addressed above. Moreover,

- P_{GC}, π_{GC}, and P_{BC} are pressures across a glomerular capillary wall, whereas the GFR is the filtration achieved by the two kidneys (with numerous nephrons) per unit time. It is inappropriate to calculate the GFR at the system level using these single-capillary-level pressures.
- The filtration coefficient is the product of the hydraulic permeability of the filtration membrane (K or L_PA) and the filtration area (Brenner et al., 1976; Tucker and Blantz, 1977; Hall and Hall, 2021). The total filtration area of the two kidneys is remarkably different from the filtration area of an SN. However, the symbols that refer to them are inconsistent: either SNK_f or K_f is used to refer to the filtration coefficient at the SN level (Brenner et al., 1976; Ott et al., 1976; Navar et al., 1977; Marchand and Mohrman, 1980; Savin and Terreros, 1981; Arendshorst and Gottschalk, 1985), whereas K_f also refers to the filtration coefficient at the two-kidney level (Giebisch et al., 2017; Hall and Hall, 2021). It should be noted that the unit of the filtration coefficient for the SN is nl/min/mmHg (Brenner et al., 1976; Navar et al., 1977; Marchand and Mohrman, 1980; Savin and Terreros, 1981) or nl/sec/mmHg (Tucker and Blantz, 1977; Chang, 1978; Arendshorst and Gottschalk, 1985), whereas the unit of the coefficient for the two-kidney system is ml/min/mmHg (Costanzo, 2018; Hall and Hall, 2021).
- It is unclear what NetP refers to in the equation. In other words, it remains unclear whether it should be $\overline{NetP_{SN}}$ averaged at the SN level or the mean NetP averaged from numerous nephrons at the system level ($\overline{NetP_{SYS}}$).
- If NetP in this equation applies to an SN, then it should be total $NetP_{SN}$ or $\overline{NetP_{SN}}$, the GFR should be SNGFR, and the filtration coefficient should be SNK_f. If NetP refers to $\overline{NetP_{SYS}}$, then the GFR should remain the GFR; the filtration coefficient should be K_f; and P_{GC}, π_{GC}, and P_{BC} should be averaged at the system levels $\overline{P_{GC\_SYS}}$, $\overline{\pi_{GC\_SYS}}$, and $\overline{P_{BC\_SYS}}$, respectively.

To the best of our knowledge, this is the first time that two sets of parameters have been defined and differentiated systematically to avoid confusion. Specifically, P_{GC}, P_{BC}, $d\pi_{GC}/dx$, $\overline{\pi_{GC\_SN}}$, SNK_f, d(NetP)/dx, total $NetP_{SN}$, SNRPF, SNGFR, and SNFF apply to the SN level, and RPF, GFR, FF, K_f, $\overline{NetP_{SYS}}$, $\overline{P_{GC\_SYS}}$, $\overline{\pi_{GC\_SYS}}$, and $\overline{P_{BC\_SYS}}$ apply to the system level.

2.3 Issue 3

Whether filtration equilibrium occurs in mammalian kidneys remains a continuous debate (Osgood et al., 1982; Arendshorst and Gottschalk, 1985). Filtration equilibrium refers to the phenomenon when NetP decreases to zero at a point before the blood reaches the EA so that no filtration occurs after this point (Figure 1C). Filtration equilibrium has been reported in some experimental studies on Munich–Wistar rats (Marchand and Mohrman, 1980) and squirrel monkeys (Maddox et al., 1974) but has not been observed in studies on dogs (Ott et al., 1976), Wistar rats (Seiller and Gertz, 1977), and rabbits (Denton and Anderson, 1991). In other words, glomerular filtration in the kidneys of these animals is characterized by filtration disequilibrium.

2.4 Issue 4

A critical gap in current research is the notable lack of research questions and efforts to investigate whether there is a direct and/or indirect communication between an upstream AA and its downstream EA. This situation may lead to missing crucial insights into glomerular hemodynamics. The advantages of these types of communication are obvious. For example, in the design of

artificial nephrons or kidneys, enabling these communications could potentially improve the coordination between AAs and EAs and lead to more efficient function. On the other hand, Davis (1991) reported that under certain circumstances, TGF may involve EA vasomotion either in the same or opposite direction of AA vasomotion. If there is no communication between EAs and AAs, necessary vasomotion of AAs and/or EAs to maintain the normal GFR may be mediated through the TGF. If so, it is neither efficient nor economical.

2.5 Issue 5

Physiologists often note that FF = GFR/RPF ≈ 20%. Obviously, this means that a much larger fraction of RPF (80%) is not filtered but exits through the EAs under normal conditions. This 80% fraction is apparently ignored because its implications for glomerular hemodynamics and maintaining the normal GFR are not mentioned, appreciated, or discussed in the literature. The importance of having 80% RPF exiting through EAs becomes clear gradually in this article, and its implications are addressed in *Conclusion*.

2.6 Issue 6

In terms of how AA resistance influences glomerular hemodynamics, there is no disagreement among physiologists in general. However, the explanations of how EA resistance influences glomerular hemodynamics are inconsistent, incomplete, and inappropriate:

- Some literature only introduce the effect of AA resistance on the GFR but not the effect of EA constriction (Pal et al., 2017; Kibble, 2020; Loscalzo et al., 2022; Eaton and Pooler, 2023).
- EA constriction may increase both P_{GC} and π_{GC} but may or may not reduce RPF. However, textbooks often merely mention that EA constriction increases P_{GC} and/or GFR and do not address how it influences RPF and/or π_{GC} (Bijlani and Manjunatha, 2011; Krishna, 2015; Koeppen and Stanton, 2018; Barrett et al., 2019).
- Some literature briefly note that EA constriction has a biphasic effect on the GFR depending on whether EA constriction reduces RPF and how significantly it increases π_{GC}. Specifically, if the EAs constrict slightly, which reduces RPF insignificantly or not at all, then the GFR increases slightly. However, if the EAs constrict severely (causing a threefold or more increase in the EA resistance), the RPF and GFR are both reduced because under this circumstance, the increase in π_{GC} ($\Delta\pi_{GC}$) becomes greater than the increase in P_{GC} (ΔP_{GC}), i.e., $\Delta\pi_{GC} > \Delta P_{GC}$ (Giebisch et al., 2017; Hall and Hall, 2021). This means that the role of each phase of the biphasic effect of EA constriction on the RPF and, thus, GFR is conditional.

Omitting the analysis of RPF, π_{GC}, and whether $\Delta\pi_{GC} > \Delta P_{GC}$ but stating that EA constriction increases or decreases the GFR, is logically flawed. The comparison between $\Delta\pi_{GC}$ and ΔP_{GC} is an indispensable step that determines whether the GFR increases or remains unchanged or decreases in response to a change in EA resistance. However, comparing the two is not appropriate because of the lack of logical rigor, as shown in issue 1 above. Theoretically, $\Delta\pi_{GC} > \Delta P_{GC}$ needs to be replaced by $\overline{\Delta\pi_{GC\_SN}} > \Delta P_{GC}$ or a comparison of the total $NetP_{SN}$ in a situation with the normal total $NetP_{SN}$ illustrated in Section 4 (see Hypothesis 1).

2.7 Summary

These issues, together, indicate the following:

- The qualitative, vague equations cause insufficient and confusing definitions of the parameters at both the SN and system levels.
- A system-level understanding of glomerular hemodynamics is mechanically extended from the SN level due to the lack of an appropriate epistemology.
- A comprehensive understanding of the role of the EAs as a type of resistance vessel on glomerular hemodynamics and, thus, the GFR has not been well-established.

3 Eight fundamental mathematical equations within the conventional paradigm of epistemology

The mathematical equations illustrated in this section can be reasoned out by anyone who understands the fundamentals of calculus or can be modified from the literature Eq. 1, Eq. 2, Eq. 6, and Eq. 7. SN-level parameters (SNRPF, d(NetP)/dx, total $NetP_{SN}$, $\overline{NetP_{SN}}$, $\overline{\pi_{GC\_SN}}$, SNK_f, SNGFR, and SNFF) and system-level parameters (RPF, $\overline{NetP_{SYS}}$, $\overline{P_{GC\_SYS}}$, $\overline{\pi_{GC\_SYS}}$, $\overline{P_{BC\_SYS}}$, K_f, GFR, and FF) are easy to differentiate. Following common practice in the literature, all capillaries in a glomerulus are considered one tube with the same filtration area as all the capillaries together (Brenner et al., 1976; Chang, 1978; Drumond and Deen, 1994).

Since π_{GC} is the function of the distance (x) from a point of glomerular filtration to the beginning of the filtration (the AA end of the capillary), the vague expression $NetP = P_{GC} - \pi_{GC} - P_{BC}$ needs to be derived to quantify a derivative NetP [d(NetP)/dx)] and the total $NetP_{SN}$ [the integration of d(NetP)/dx)]:

$$d(NetP)/dx = P_{GC} - \pi_{GC}(x) - P_{BC} \tag{1}$$

and

$$\begin{aligned} \text{Total } NetP_{SN} &= \int_{\text{AA end}}^{\text{EA end}} [P_{GC} - \pi_{GC}(x) - P_{BC}]dx \\ &= \int_{\text{AA end}}^{\text{EA end}} (P_{GC} - mQ)dx, \end{aligned} \tag{2}$$

where $Q = \pi_{GC} + P_{BC}$, $m = \frac{\Delta Q}{D}$ represents the slope of the orange line in Figure 1A, and D refers to the distance from the AA end to the end of glomerular filtration. The gray area in Figure 1A represents the total $NetP_{SN}$ determined by Eq. 2.

If the orange line is a curve (Figures 1B,C), integrating the total $NetP_{SN}$ becomes complex. It requires conducting experiments, setting points to collect data, and then performing mathematical modeling, which is beyond the scope of these fundamental equations. Nevertheless, regardless of whether the total $NetP_{SN}$

can be easily integrated using Eq. 2 or needs a complex model, the gray area in Figures 1A–C represents the total $NetP_{SN}$ determined by the line of P_{GC} and the orange line.

Furthermore, an instantaneous SNGFR can be reasoned out or modified from the equation provided by Brenner et al. (1976) or Navar et al. (1977) using the symbols at the SN level defined in this article:

$$\begin{aligned} D(SNGFR)/dx &= SNK_f\,[d(NetP)/dx] \\ &= SNK_f\,[P_{GC} - \pi_{GC}(x) - P_{BC}]. \end{aligned} \quad (3)$$

The total SNGFR can be reasoned out as follows or modified from the equation provided by Deen et al. (1974) or Sgouralis and Layton (2015) using the symbols at the SN level defined in this article:

$$\text{Total SNGFR} = SNK_f \int_{AA\ end}^{EA\ end} [P_{GC} - \pi_{GC}(x) - P_{BC}]dx. \quad (4)$$

Similarly, the vague expression $GFR = K_f(NetP) = K_f(P_{GC} - \pi_{GC} - P_{BC})$ needs to be derived to estimate the GFR using the symbols at the two-kidney system level defined in this article:

$$GFR = (K_f)\overline{NetP_{SYS}} = K_f\overline{P_{GC\_SYS}} - \overline{\pi_{GC\_SYS}} - \overline{P_{BC\_SYS}}). \quad (5)$$

Obviously, the many mean values in the equation can only be estimated for the millions of nephrons at the two-kidney level. This equation makes better sense than its original form [$GFR = K_f(NetP) = K_f(P_{GC} - \pi_{GC} - P_{BC})$]. It is theoretically meaningful but is still of no practical use. Practically and clinically, the GFR can be calculated using inulin clearance or estimated using creatinine clearance.

The following equation estimates K_f:

$$K_f = SNK_f \text{ x estimated total number of nephrons in the two kidneys} \quad (6)$$

Hladunewich et al. (2004) estimated K_f for pregnant women using this equation, where the estimated mean total number of nephrons for healthy women between the ages of 20 and 50 years is 1.4×10^6 (Nyengaard and Bendtsen, 1992).

The relationship between the GFR and SNGFR can be expressed as

$$GFR = \sum_1^{\text{Total number of glomeruli in two kidneys}} SNGFR. \quad (7)$$

Since RPF is the plasma flow that enters AAs and FF = GRF/RPF ≈ 20%, we establish the following equation to describe the distribution of RPF after entering AAs at the two-kidney system level:

$$RPF = GFR + RPF_{EA} \approx 20\%\,RPF + 80\%\,RPF. \quad (8)$$

Eq. 8 leads to the formulation of the last hypothesis in the next section and is critical to resolve issue 6 and understand the significant potential role of EAs in maintaining the normal GFR when renal autoregulation fails to maintain the normal RPF.

The two kidneys as a whole have numerous nephrons (about 30,000 in a rat kidney and 10^6 in a human kidney; Sgouralis and Layton, 2015). These nephrons not only have similarities in their structures and functions but also exhibit heterogeneity in their structural and functional aspects from the molecular level to the cellular, nephron, and regional levels. All of these contribute to the complexity of the system (the two kidneys).

Moreover, a system with numerous components exhibits emergent properties that its components or agents (in this context, single nephrons) do not possess, such as a great capacity of resilience and adaptability to internal and external perturbations, as well as nonlinearity. Nonlinearity means that the response of such a system toward a perturbation is often unproportional to the strength of the perturbation (Janson, 2012), and a perturbation to the system may cause a large nonproportional response, a proportional response, or no response at all. For instance, Denton et al. (2000) reported that administering intrarenal angiotensin II caused a decrease in RPF with a concomitant increase in FF in a dose-dependent manner so that the GFR does not decrease but is maintained with no change. Their research also showed the following observations:

- From the outer cortex to the juxtamedullary cortex, the diameters of the EAs show a gradient: those with the smallest diameters are in the outer cortex, whereas those with the largest diameters lie in the juxtamedullary cortex.
- The diameters of the EA in the outer and mid cortexes are smaller than those of the AA, but the diameters of the EA in the juxtamedullary cortex are similar to those of the AA.
- Such heterogeneity in the diameters of the EA seems to be one of the reasons that angiotensin II has differential degrees of vasoconstrictive effects on the AAs and EAs. According to Poiseuille's equation, which states that resistance is inversely proportional to the fourth power of the radius, it can be predicted that the EAs in the outer cortex with the smallest diameters can impact glomerular hemodynamics most substantially.
- Since outer and midcortical glomeruli account for about 90% of all glomeruli, in general, angiotensin II tends to cause a higher increase in EA resistance than in AA resistance.

Therefore, the sensitivity of glomerular hemodynamics to a minor change in EA resistance should not be ignored. In other words, the EAs possess great potential to regulate glomerular hemodynamics in various ways to maintain a normal GFR. If we consider the two kidneys a renal CAS (Holland, 2006; Carmichael and Hadžikadić, 2019) with both similarities and heterogeneities in its agents and emergent properties at the system level, it becomes clear why extending the SN-level equations to describe the system-level equations is inappropriate in epistemology and methodology. However, so far, mathematical modeling of a CAS is difficult and needs further advancement.

From the perspective of the CAS and a designer's view, the debate about whether filtration equilibrium does or does not occur in mammalian nephrons may be reconsidered to avoid a mechanical, mutually exclusive approach and facilitate a holistic and dynamic approach:

- "Fitness functions that are inherent in nature are always pushing the system, any system, toward more efficient use

of resources" (Carmichael and Hadžikadić, 2019). Filtration equilibrium makes a fraction of the capillary useless for filtration. Therefore, it is worth considering that filtration equilibrium might not be the normal condition and may occur only under specific circumstances. Theoretically, if SNRPF is low and/or SNK_f is high and/or the constriction of an EA is severe, filtration equilibrium may occur (Arendshorst and Gottschalk, 1985) in some glomeruli. Practically, multiple factors may encourage or prevent it. It is crucial to identify these factors and determine whether filtration equilibrium is more or less likely to occur in specific regions of the kidney.

- If we design an artificial kidney, it is important to determine whether it is beneficial for filtration equilibrium and disequilibrium to be mutually transformable under some conditions for the sole purpose of increasing the capacity of both resilience and adaptability of the kidneys. Alternatively, it should be assessed whether filtration equilibrium should be more likely to appear in some nephrons and less likely to occur in others for the same purpose.
- Renal heterogeneity could be a consequence of the past adaptive processes of the renal CAS toward internal and external perturbations for the purpose of maintaining a normal GFR. It is essential to explore whether renal heterogeneity should exhibit different patterns at various levels, from molecular to cellular, nephron, and system, in response to different perturbations.
- Developing methods to study and recognize different patterns of renal heterogeneity is critical for advancing our understanding of kidney function.

The eight equations given above are generally linear or simple models; thus, we consider them fundamental in the study of glomerular hemodynamics, or more specifically, glomerular filtration. To model other aspects of glomerular hemodynamics or, more broadly, renal hemodynamics, such as renal autoregulation (myogenic response and TGF) and coupled nephrons, much more complex mathematical models are needed, and readers may refer to the review article by Sgouralis and Layton (2015). Like the eight fundamental mathematical models mentioned above, complex models have the same problem, i.e., how the SN and two-kidney levels of models can be well-integrated by taking both the similarity and heterogeneity of nephrons into consideration in the direction of the CAS.

4 Four hypotheses from the perspective of the complex adaptive system

Obviously, the gray area in Figure 1C due to severe EA constriction is smaller than the normal gray area in Figure 1A. If the SNGFR were to be calculated for the condition in Figure 1C, it would be less than the normal SNGFR in Figure 1A. Depending on the concrete value of SNRPF, the exact degree of EA constriction, and the resulting P_{GC} and π_{GC}, the gray area due to moderate EA constriction (Figure 1B) may be greater than, equal to, or smaller than the normal gray area in Figure 1A. Note that in Figure 1B, before x_1, NetP ($x < x_1$) is greater than that in the normal situation (Figure 1A); after x_1, NetP ($x > x_1$) becomes smaller than normal; and at x_1, NetP (x_1, Figure 1B) = the normal (x_1 in Figure 1A)[1] (this analysis also applies to Figure 1C). The closer x_1 is to the AA end in Figure 1B, the more likely it is that the resulting gray area is smaller than the normal gray area in Figure 1A; on the contrary, the farther x_1 is from the AA end in Figure 1B, the more likely the gray area is to be equal to or greater than the normal gray area in Figure 1A. This analysis makes it clearer that a comparison of whether $\Delta\pi_{GC} > \Delta P_{GC}$ is not practical, but a comparison of a gray area with the normal gray area is doable. Hence, logically, the comparison of $\Delta\pi_{GC}$ and ΔP_{GC} should be replaced by Hypothesis 1:

Hypothesis 1: If the total $NetP_{NS}$ (the gray area) < or = or > the normal, then SNGFR < or = or > the normal. In other words, the SNGFR decreases or remains unchanged or increases.

Hypothesis 1 is qualitative and specifically useful for physiology education, which is so far not math-heavy. From now on, if the total $NetP_{SN}$ is reduced compared to the normal, it means that the mean increase in π_{GC} is greater than the increase in P_{GC}, i.e., $\overline{\Delta\pi_{GC\_SN}} > \Delta P_{GC}$. Subsequently,

Hypothesis 2: If the total $NetP_{SN}$ in a significant number of nephrons increases/decreases, $\overline{NetP_{sys}}$ increases/decreases so that the GFR increases/decreases.

Note that from the total $NetP_{SN}$ at the SN level to $\overline{NetP_{sys}}$ at the system level, the description "significant number of nephrons increases/decreases" reflects the CAS. Since renal autoregulation mechanisms conventionally involve the AA and macula densa, not the EA, from a designer's view, we hypothesize that there are unknown direct or indirect communications (mechanical, electrical, chemical, or biological) between an upstream AA and its downstream EA, or between a glomerulus and its downstream EA, or between the macula densa and its adjacent EA, so that these parties work efficiently and in coordination to precisely maintain the normal GFR as far as possible, especially when renal autoregulation mechanisms fail to maintain stable RPF:

Hypothesis 3: If the GFR is greater than the normal upper range, *generally speaking*, the AAs should constrict, or the EAs should dilate, or both; on the contrary, if the GFR is less than the normal lower range, the AAs should dilate or the EAs should constrict or both.

To date, the occasional involvement of the EA in TGF has been reported under some circumstances (Davis, 1991; Ren et al., 2001); some autocoids (e.g., nitric oxide and prostgalndins etc.) produced in the glomerulus may diffuse to influence EA vasomotion (Ito and Abe, 1997; Leipziger and Praetorius, 2020). Chilton et al. (2008) speculated a direct communication between an upstream AA and its downstream EA via electrical potential change in the smooth muscles of the EA. Denton et al. (2000) reported that angiotensin II changed the geometry of the glomerular pole including the extraglomerular mesangium, whereas Elger et al. (1998) suggested a direct functional influence of

1 $\Delta P_{GC} = P_{GC}$ (Figure 1B) $- P_{GC}$ (Figure 1A) = 60−53 = 7 (mmHg) and $\Delta Q(x_1) = Q(x_1)$ (Figure 1B) $- Q(x_1;)$ (Figure 1A) = 42−35 = 7 (mmHg), meaning at x_1, $\Delta Q(x_1) = \Delta P_{GC}$, instantaneous $NetP(x_1)$ (Figure 1B) = instantaneous $NetP(x_1)$ (Figure 1A).

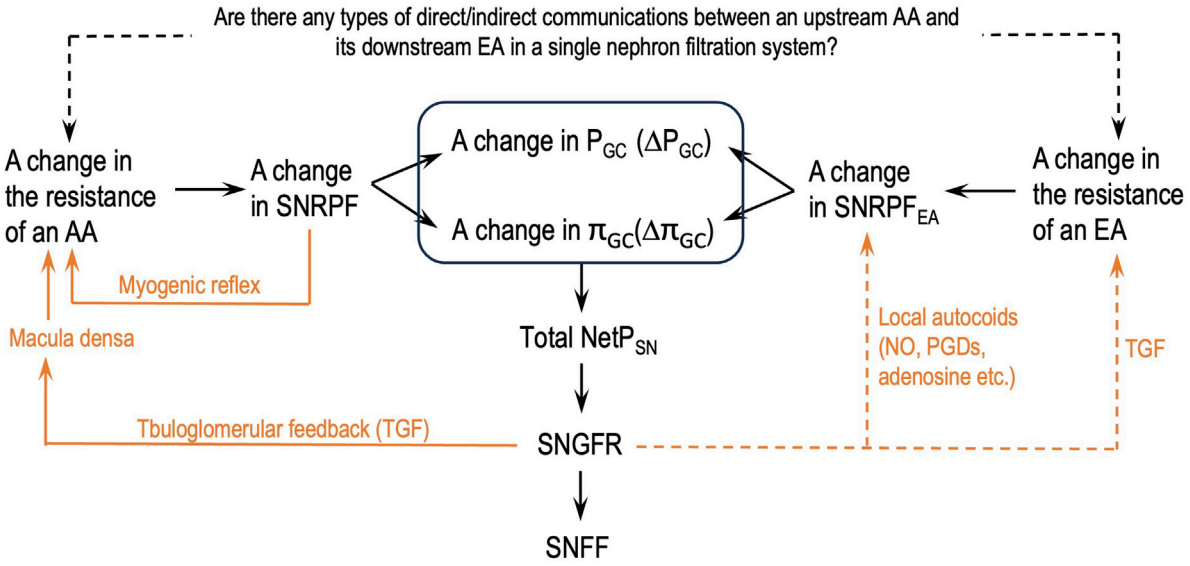

FIGURE 2
Logical steps to analyze the parameters of the glomerular hemodynamics of a single nephron after a change in the resistance of either an afferent arteriole (AA) or an efferent arteriole (EA) or both. SNGFR: single-nephron GFR; SNFF: single-nephron FF; orange lines: single-nephron autoregulation mechanisms; dashed orange lines: some supportive findings in the literature; dashed black line: authors' hypothesis.

an AA on an EA via the extraglomerular mesangium and the presence of a specific sheer stress receptor located in the intraglomerular portion of the EA. Further research to explore the hypothesized communications between an upstream AA and its downstream EA will be of great value. In Section 5, we show the pivotal role of this hypothesis in guiding our analyses of glomerular hemodynamics and GFR under various conditions and eventually resolve issue 6.

Next, we reason out Hypothesis 4 using the following data. If the RPF of a healthy man is approximately 600 mL/min, the GFR is approximately 125 mL/min, and FF is approximately 20%, then his RPF_{EA} (renal plasma flow that exits through the EAs) should be approximately 475 mL/min. Below, the unit ml/min is omitted for RPF, GFR, and RPF_{EA}. Assume that his blood pressure decreases too much for some reason so that renal autoreglation can no longer maintain stable RPF, e.g., RPF decreases to 300. In order to maintain the GFR at approximately 125, according to Eq. 8, the EAs should constrict to cause RPF_{EA} to be approximately 175. If RPF_{EA} > or <175, then GFR < or > normal, indicating that the total $NetP_{SN}$ in a significant number of nephrons in the two kidneys < or > their normal values. Hence, 175 is the critical point of RPF_{EA} in response to the primary change of RPF = 300. If RPF is approximately 400, then the critical point of RPF_{EA} should be approximately 275. Due to the heterogeneity of the nephrons, it is not easy to obtain or estimate the total $NetP_{SN}$ for the majority of the nephrons. The purpose of introducing the concept of the critical point of RPF_{EA} at the two-kidney level is to use it to estimate what is more likely to happen in the majority of the nephrons in terms of their total $NetP_{SN}$ when RPF is below normal:

Hypothesis 4a: If RPF_{EA} > or = or < a critical point in response to a particular value of RPF, the total $NetP_{SN}$ in a significant number of nephrons is < or = or > their normal values.

On the contrary, if EA vasomotion is the primary change, then RPF has a critical point in response to a particular EA resistance, which also predicts the total $NetP_{SN}$:

Hypothesis 4b: If RPF > or = or < a critical point in response to a particular value of RPF_{EA}, the total $NetP_{SN}$ in a significant number of nephrons is > or = or < their normal value.

Hypothesis 4 is inferred from Eq. 8. This is the first significance of Eq. 8.

The illustration of the equations and hypotheses leads to the criteria to define the following terms in this article:

- Slight EA constriction means that the EAs constrict slightly, which does not reduce RPF but redistributes it to the GFR and RPF_{EA}.
- Severe EA constriction means that the EAs constrict significantly, causing a threefold or more increase in EA resistance and reducing RPF, which results in the total $NetP_{SN}$ in the majority of the nephrons becoming smaller than normal (Figure 1C) and, thus, a decrease in $\overline{NetP_{sys}}$ and the GFR.
- Moderate EA constriction is between slight and severe constriction, which may lead to an increase or decrease or no change in the GFR depending on the resulting RPF, P_{GC}, π_{GC}, and total $NetP_{SN}$ in the majority of the nephrons, as shown in Figure 1B.

Figure 2 depicts a flowchart of how the parameters of the glomerular hemodynamics of a single nephron should be analyzed after a change in either AA or EA resistance or both without missing links. This flowchart will help eliminate the logical flaws addressed in issue 6.

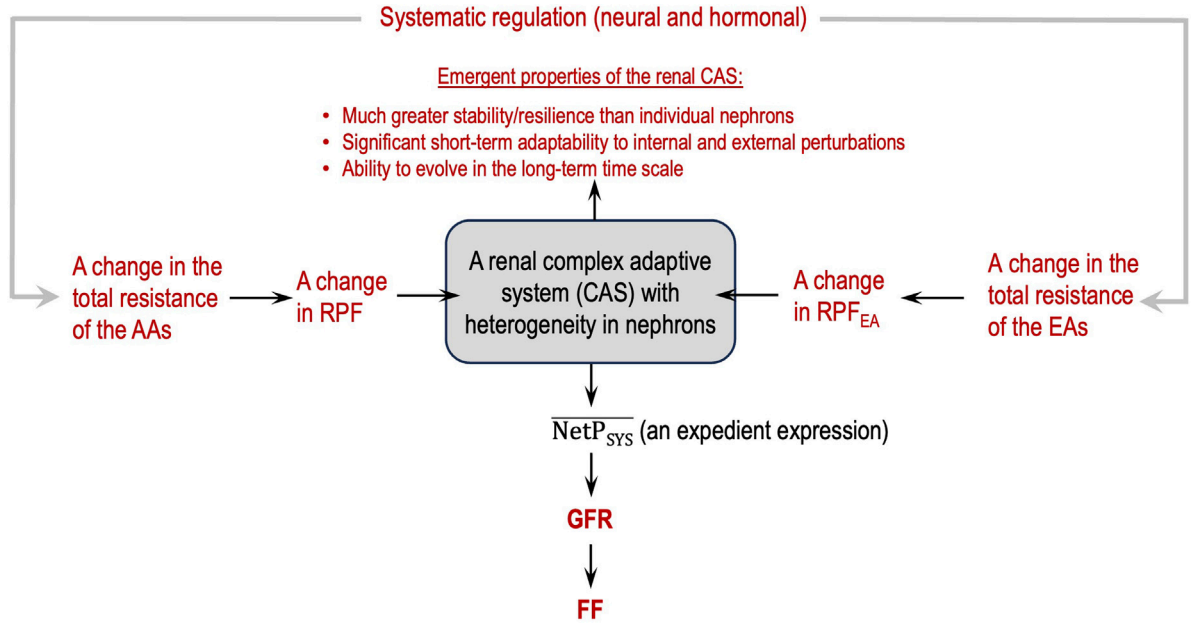

FIGURE 3
Renal complex adaptive system (CAS) for glomerular filtration with emergent, macroscopic properties (in red).

Figure 3 depicts a flowchart of how to view glomerular hemodynamics at the two-kidney level by considering the two kidneys as a renal CAS.

5 A comprehensive analysis to understand the impact of EA constriction on glomerular hemodynamics

Guided by the flowcharts given in Figures 2, 3, issue 6 is resolved in this section by applying Eq. 8 and Hypothesis 3 and Hypothesis 4b.

5.1 The essential roles of the EAs and EA baseline resistance

When renal autoregulation maintains stable RPF and GFR, why is the P_{GC} higher than that in the peripheral tissue and relatively stable throughout the glomerular filtration (Figure 1A)? A normal EA tone (a certain level of constant constriction) maintains the P_{GC} high and relatively constant (Savedchuk et al., 2023). This is the essential role of the EAs. This essential role is conditional upon the renal autoregulation of RPF functioning normally.

A normal EA tone results in normal EA resistance (level-0 resistance). This normal EA resistance is the baseline when renal autoregulation mechanisms function normally. EA constriction means that the EAs constrict more than the level of the normal EA tone; thus, EA resistance becomes higher than the baseline. EA dilation means that the EAs constrict less than the normal EA tone; thus, EA resistance becomes smaller than the baseline.

Throughout our analysis, each level of EA constriction sets a new baseline for EA resistance. EA constriction/dilation means that the EAs constrict more/less than a corresponding level of EA constriction.

5.2 Comprehensive analysis of the effect of EA constriction on glomerular hemodynamics

The data on RPF, GFR, and FF of the healthy man mentioned above when we addressed Hypothesis 4 are used to facilitate the analysis. Due to renal heterogeneity, glomerular hemodynamics is analyzed at the system level not the SN level.

5.2.1 Slight EA constriction, which sets a level-1 baseline EA resistance

This situation does not reduce RPF significantly or at all but redistributes RPF (~600) to RPF_{EA} and GFR (Eq. 8). The more the EAs constrict, the more $\overline{NetP_{SYS}}$, GFR, and FF increase. According to Hypothesis 3, the EA should stop constricting and dilate (with reference to level 1-EA baseline resistance) to reduce the GFR to normal.

5.2.2 Moderate EA constriction, which sets a level-2 baseline EA resistance, e.g., EA resistance ≈1.5-fold of level-0 EA baseline resistance or RPF_{EA} ≈ 316.7, 2/3 of the original (475)

This situation causes a reduction in RPF and an increase in both $\overline{P_{GC\_SYS}}$ and $\overline{\pi_{GC\_SYS}}$, in general. How it influences $\overline{NetP_{SYS}}$, GFR, and FF depends on the exact degree of EA constriction and the concrete RPF. If the resulting $\overline{NetP_{SYS}}$ is around normal, then the GFR is around normal, but FF increases because of a reduction in RPF. If RPF_{EA} remains approximately 316.7, RPF needs to be adjusted to 441.7 (441.7 = 125 + 316.7, Eq. 8) to maintain the GFR at approximately 125.

According to Hypothesis 4b, RPF of approximately 441.7 is the critical point for RPF_{EA} of approximately 316.7. If RPF > or <441.7, then GFR > or < normal, $\overline{NetP_{SYS}}$ > or < normal, and FF should decrease or increase. According to Hypothesis 3, the EA should dilate or constrict with reference to the level-2 baseline EA resistance. Therefore, level-2 EA constriction is certain to cause a reduction in RPF and an increase in FF but embraces multiple possibilities for the values of $\overline{NetP_{SYS}}$ and GFR.

5.2.3 Severe EA constriction, which sets a level-3 baseline EA resistance, e.g., EA resistance = or > 3-fold of level-0 EA baseline resistance or $RPF_{EA} \approx$ 158.3 (1/3 of 475)

This situation causes significant reduction in RPF and $\overline{NetP_{SYS}}$, which leads to a decrease in the GFR and an increase in FF. Under such circumstances (most likely, renal autoregulation mechanisms have failed to maintain the normal, stable RPF), the critical point of RPF with regard to RPF_{EA} of approximately 158.3 is 278.3 (278.3 = 125 + 158.3, Eq. 8), if possible. If RPF > or <278.3, then the EA should dilate or constrict with reference to the level-3 baseline EA resistance to adjust the GFR to be not too far from normal. This means, logically, that even though RPF is reduced significantly, as long as the EA can constrict more, it still has the potential to maintain the normal GFR. FF should always increase at level-3 EA constriction. Practically, the EAs may not be able to constrict more, especially if they are smaller in diameter. In addition, it should be noted that if the reduction of RPF is not due to EA constriction, but due to other reasons, the analysis should still revolve around how to maintain the normal GFR by applying Eq. 8, Hypothesis 3 and Hypothesis 4a.

5.2.4 More severe EA constriction that causes RPF (e.g., 100) < normal GFR (e.g., ~120)

This situation can occur under some pathological conditions such as acute renal failure, when both the AAs and EAs constrict significantly as part of systemic vascular constriction. Regardless of how severely the EAs constrict, a normal GFR cannot be maintained. Therefore, administering vasodilator(s) to the AA and EA is a preventive action if acute renal failure is likely to occur and life-saving if acute renal failure is already occurring. This is an exception to Hypothesis 3.

5.2.5 Summary

The analyses in this section are guided by the logical relationships shown in Figures 2, 3, Eq. 8, and Hypothesis 3 and Hypothesis 4b. They are much more comprehensive than those in the literature and in standard physiology textbooks, without logical errors, an address the following two important points:

- The impact of EA constriction on glomerular hemodynamics is quite conditional, depending on concrete situations.
- The parameters that should and should not be analyzed must be differentiated in this context in consideration of renal heterogeneity.

6 Conclusion

This article presents the following outcomes. First, it makes clear the need for a shift in epistemology to adopt the concept of the CAS and a designer's view.

Second, some fundamental equations are modified/improved, and one new equation is established in the conventional paradigm. Four new hypotheses are formulated from the perspective of the CAS with guiding significance for future research.

Third, new insights to understand the role of EAs as resistance arterioles are developed, specifically:

- RPF_{EA} (80% RPF) serves as an adequate reserve of the normal GFR. This reserve becomes significant when renal autoregulation fails to maintain normal RPF, and RPF is significantly low. Theoretically, as long as RPF > normal GFR, EA constriction has the potential to adjust EA resistance to maintain the GFR at a normal level. Therefore, the distribution of 80% RPF to EAs, in particular, plays a protective role in the maintenance of the normal GFR. If the fractions of a normal GFR and RPF_{EA} in RPF are reversed, i.e., normal GFR ≈80% RPF and $RPF_{EA} \approx$ 20% RPF, the EA will not be able to effectively protect the normal GFR in any scenario. This is the second significance of Eq. 8.
- Having an EA aligned in series with an AA and a glomerulus for each nephron is the *necessary condition* to maintain the normal GFR, whereas having 80% RPF entering the EAs as a significant reserve to maintain the normal GFR when renal autoregulation fails to maintain the normal stable RPF is the *sufficient condition* to maintain the normal GFR. Without the sufficient condition, the kidney will lack resilience and adaptability and will be unable to cope with various internal and external perturbations. This analysis of *necessary and sufficient conditions* is borrowed from cybernetics. It theorizes our understanding of renal autoregulation of many of its functions at the philosophical level. If biomedical research studies adopt this perspective, more insights into the biomedical disciplines will emerge.
- It is possible that if the pre-glomerular resistance increases or decreases inappropriately, the EAs have the sensitivity and potential to constrict or dilate to a certain degree to correct the error. This is because the heterogeneity in the diameters of the EAs and the distribution of EAs with different diameters in the renal cortex in contrast to AAs suggest the substantial power and potential of the EAs in the regulation of glomerular hemodynamics in various ways to maintain the normal GFR.

Future research on glomerular hemodynamics should focus on recognizing patterns of renal heterogeneity in response to various perturbations, dynamic interactions among nephrons, and the emergent properties of the renal CAS.

Data availability statement

The original contributions presented in the study are included in the article further inquiries can be directed to the corresponding authors.

Author contributions

SK: conceptualization, formal analysis, investigation, methodology, project administration, resources, supervision, validation, visualization, writing–original draft, and writing–review and editing. BA: investigation, resources,

validation, and writing–review and editing. XQ: conceptualization, investigation, methodology, resources, supervision, validation, visualization, and writing–review and editing.

Funding

The author(s) declare that no financial support was received for the research, authorship, and/or publication of this article.

Acknowledgments

The authors thank Cody Bailey-Crow for modifying Figure 1 and Savanna Lavander for helping with the literature.

Conflict of interest

The authors declare that the research was conducted in the absence of any commercial or financial relationships that could be construed as a potential conflict of interest.

Publisher's note

All claims expressed in this article are solely those of the authors and do not necessarily represent those of their affiliated organizations, or those of the publisher, the editors, and the reviewers. Any product that may be evaluated in this article, or claim that may be made by its manufacturer, is not guaranteed or endorsed by the publisher.

References

Arendshorst, W. J., and Gottschalk, C. W. (1985). Glomerular ultrafiltration dynamics: historical perspective. *Am. J. Physiol.* 248 (2 Pt 2), F163–F174. doi:10.1152/ajprenal.1985.248.2.F163

Barrett, K. E., Barman, S. M., Brooks, H. L., and Yuan, J. X.-J. (2019). "Renal function and micturition," in *Ganong's review of medical physiology*. 26th ed. (New York: McGraw Hill Education), 1548.

Bijlani, R. L., and Manjunatha, S. (2011). "Mechanism of urine formation," in *Understanding medical physiology: a textbook for medical students*. Editors R. L. Bijlani and S. Manjunatha 4th ed. (New Delhi, India: Jaypee Brothers Medical Publishers), 428.

Brenner, B. M., Deen, W. M., and Robertson, C. R. (1976). Determinants of glomerular filtration rate. *Annu. Rev. Physiol.* 38, 11–19. doi:10.1146/annurev.ph.38.030176.000301

Carmichael, T., and Hadžikadić, M. (2019). "The fundamentals of complex adaptive systems," in *Complex adaptive systems*. Editors T. Carmichael, A. J. Collins, and M. Hadžikadić (Cham: Springer), 1–16. doi:10.1007/978-3-030-20309-2_1

Chang, R. L. (1978). A model to study the dynamics of glomerular ultrafiltration and glomerular capillary permselectivity characteristics. *Microvasc. Res.* 16 (1), 141–150. doi:10.1016/0026-2862(78)90050-x

Chilton, L., Loutzenhiser, K., Morales, E., Breaks, J., Kargacin, G. J., and Loutzenhiser, R. (2008). Inward rectifier K(+) currents and Kir2.1 expression in renal afferent and efferent arterioles. *J. Am. Soc. Nephrol.* 19 (1), 69–76. doi:10.1681/ASN.2007010039

Costanzo, L. S. (2018). "Renal physiology," in *Physiology*. 6th ed. (Philadelphia: Elsevier), 263–265.

Davis, J. M. (1991). Role of the efferent arteriole in tubuloglomerular feedback. *Kidney Int. Suppl.* 32, S71–S73.

Deen, W. M., Maddox, D. A., Robertson, C. R., and Brenner, B. M. (1974). Dynamics of glomerular ultrafiltration in the rat. VII. Response to reduced renal mass. *Am. J. Physiol.* 227 (3), 556–562. doi:10.1152/ajplegacy.1974.227.3.556

Denton, K. M., and Anderson, W. P. (1991). Glomerular ultrafiltration in rabbits with superficial glomeruli. *Pflügers Arch.* 419, 235–242. doi:10.1007/BF00371101

Denton, K. M., Anderson, W. P., and Sinniah, R. (2000). Effects of angiotensin II on regional afferent and efferent arteriole dimensions and the glomerular pole. *Am. J. Physiol. Regul. Integr. Comp. Physiol.* 279 (2), R629–R638. doi:10.1152/ajpregu.2000.279.2.R629

Drumond, M. C., and Deen, W. M. (1994). Structural determinants of glomerular hydraulic permeability. *Am. J. Physiol.* 266 (1 Pt 2), F1–F12. doi:10.1152/ajprenal.1994.266.1.F1

Eaton, D. C., and Pooler, J. P. (2023). "Renal blood flow and glomerular filtration," in *Vander's renal physiology*. Editors M. Weitz and C. M. Thomas 10th ed. (New York, New York: McGraw Hill Medicine). ch. 2, ebook version.

Elger, M., Sakai, T., and Kriz, W. (1998). The vascular pole of the renal glomerulus of rat. *Adv. Anat. Embryol. Cell Biol.* 139, 1–98. doi:10.1007/978-3-642-80449-6

Giebisch, G., Windhager, E. E., and Aronson, P. S. (2017). "Glomerular filtration and renal blood flow," in *Medical physiology*. Editors W. F. Boron and E. L. Boulpaep 3rd ed. (Philadelphia, PA: Elsevier), 743–747.

Hall, J. E., and Hall, M. E. (2021). "Glomerular filtration, renal blood flow, and their control," in *Guyton and Hall textbook of medical physiology*. 14th ed. (Philadelphia, PA: Elsevier), 333–335.

Hladunewich, M. A., Lafayette, R. A., Derby, G. C., Blouch, K. L., Bialek, J. W., Druzin, M. L., et al. (2004). The dynamics of glomerular filtration in the puerperium. *Am. J. Physiol. Ren. Physiol.* 286 (3), F496–F503. doi:10.1152/ajprenal.00194.2003

Holland, J. H. (2006). Studying complex adaptive systems. *J. Sys Sci. Complex* 19 (1), 1–8. doi:10.1007/s11424-006-0001-z

Huss, R. E., Marsh, D. J., and Kalaba, R. E. (1975). Two models of glomerular filtration rate and renal blood flow in the rat. *Ann. Biomed. Eng.* 3 (1), 72–99. doi:10.1007/BF02584490

Ito, S., and Abe, K. (1997). Contractile properties of afferent and efferent arterioles. *Clin. Exp. Pharmacol. Physiol.* 24, 532–536. doi:10.1111/j.1440-1681.1997.tb01241.x

Janson, N. B. (2012). Non-linear dynamics of biological systems. *Contemp. Phys.* 53 (2), 137–168. doi:10.1080/00107514.2011.644441

Kibble, J. D. (2020). "Renal physiology & acid-base balance," in *Physiology medical course and 1 step review*. Editors W. Weitz and P. J. Boyle, 2nd ed. (New York, NY: McGraw Hill). ch. 6, ebook version.

Koeppen, B. M., and Stanton, B. A. (2018). "Elements of renal function," in *Berne & levy physiology*. 7th ed. (Philadelphia, PA: Elsevier), 596–599.

Krishna, A. P. (2015). "Excretory system," in *Textbook of medical physiology*. 2nd revised ed. (New Delhi, India: MedTec), 731–732.

Leatherby, R., Theodorou, C., and Dhanda, R. (2021). Renal physiology: blood flow, glomerular filtration and plasma clearance. *Anaesth. Intensive Care Med.* 22 (7), 439–442. doi:10.1016/j.mpaic.2021.05.003

Leipziger, J., and Praetorius, H. (2020). Renal autocrine and paracrine signaling: A story of self-protection. *Physiol. Rev.* 100, 1229–1289. doi:10.1152/physrev.00014.2019

Loscalzo, J., Fauci, A., Kasper, D., Hauser, S., Longo, D., and Jameson, L. (2022). "Cell biology and physiology of the kidney," in *Harrison's principles of internal medicine*. Editors J. Loscalzo, D. L. Kasper, D. L. Longo, A. S. Fauci, S. L. Hauser, and J. L. Jameson 21st ed. (New York, NY: McGraw Hill Medicine). ch. 309, ebook version.

Maddox, D. A., Deen, W. M., and Brenner, B. M. (1974). Dynamics of glomerular ultrafiltration. VI. Studies in the primate. *VI. Stud. primate. Kidney Int.* 5 (4), 271–278. doi:10.1038/ki.1974.36

Marchand, G. R., and Mohrman, D. E. (1980). Glomerular filtration rate as a function of the net transcapillary hydrostatic pressure. *Life Sci.* 27 (25–26), 2571–2576. doi:10.1016/0024-3205(80)90541-X

Navar, L. G., Bell, P. D., White, R. W., Watts, R. L., and Williams, R. H. (1977). Evaluation of the single nephron glomerular filtration coefficient in the dog. *Kidney Int.* 12 (2), 137–149. doi:10.1038/ki.1977.91

Nyengaard, J. R., and Bendtsen, T. F. (1992). Glomerular number and size in relation to age, kidney weight, and body surface in normal man. *Anat. Rec.* 232 (2), 194–201. PMID: 1546799. doi:10.1002/ar.1092320205

Osgood, R. W., Reineck, H. J., and Stein, J. H. (1982). Methodologic considerations in the study of glomerular ultrafiltration. *Am. J. Physiol.* 242 (1), F1–F7. doi:10.1152/ajprenal.1982.242.1.F1

Ott, C. E., Marchand, G. R., Diaz-Buxo, J. A., and Knox, F. G. (1976). Determinants of glomerular filtration rate in the dog. *Am. J. Physiol.* 231 (1), 235–239. doi:10.1152/ajplegacy.1976.231.1.235

Pal, G. K., Pravati, P., and Nanda, N. (2017). "Glomerular filtration," in Comprehensive Textbook of Medical Physiology, New Delhi, India (New Delhi, India: JayPee The Health Sciences Publisher), 676–678.

Papenfuss, H. D., and Gross, J. F. (1978). Analytic study of the influence of capillary pressure drop and permeability on glomerular ultrafiltration. *Microvasc. Res.* 16 (1), 59–72. doi:10.1016/0026-2862(78)90045-6

Ren, Y., Garvin, J. L., and Carretero, O. A. (2001). Efferent arteriole tubuloglomerular feedback in the renal nephron. *Kidney Int.* 59 (1), 222–229. doi:10.1046/j.1523-1755.2001.00482.x

Savedchuk, S., Phachu, D., Shankar, M., Sparks, M. A., and Harrison-Bernard, L. M. (2023). Targeting glomerular hemodynamics for kidney protection. *Adv. Kidney Dis. Health* 30 (2), 71–84. doi:10.1053/j.akdh.2022.12.003

Savin, V. J., and Terreros, D. A. (1981). Filtration in single isolated mammalian glomeruli. *Kidney Int.* 20 (2), 188–197. doi:10.1038/ki.1981.121

Seiller, W., and Gertz, K. H. (1977). Single nephron filtration, luminal flow and tubular fluid reabsorption along the proximal convolution and the pars recta of the rat kidney as influenced by luminal pressure changes. *Pflügers Arch.* 371, 235–243. doi:10.1007/BF00586263

Sgouralis, I., and Layton, A. T. (2015). Mathematical modeling of renal hemodynamics in physiology and pathophysiology. *Math. Biosci.* 264, 8–20. doi:10.1016/j.mbs.2015.02.016

Tucker, B. J., and Blantz, R. C. (1977). An analysis of the determinants of nephron filtration rate. *Am. J. Physiol.* 232 (6), F477–F483. doi:10.1152/ajprenal.1977.232.6.F477

Tucker, B. J., and Blantz, R. C. (1981). Effects of glomerular filtration dynamics on the glomerular permeability coefficient. *Am. J. Physiol.* 240 (3), F245–F254. doi:10.1152/ajprenal.1981.240.3.F245

frontiers | Frontiers in Physiology

TYPE Review
PUBLISHED 09 September 2024
DOI 10.3389/fphys.2024.1432719

OPEN ACCESS

EDITED BY
Irena Levitan,
University of Illinois Chicago, United States

REVIEWED BY
Sang Joon Ahn,
University of Illinois Chicago, United States
Zhe Sun,
University of Missouri, United States

*CORRESPONDENCE
Da-Zhuo Shi,
shidazhuo_hua@yeah.net
Ying Zhang,
echo993272@sina.com

†These authors have contributed equally to this work

RECEIVED 14 May 2024
ACCEPTED 28 August 2024
PUBLISHED 09 September 2024

CITATION
Chen L, Qu H, Liu B, Chen B-C, Yang Z, Shi D-Z and Zhang Y (2024) Low or oscillatory shear stress and endothelial permeability in atherosclerosis.
Front. Physiol. 15:1432719.
doi: 10.3389/fphys.2024.1432719

Low or oscillatory shear stress and endothelial permeability in atherosclerosis

Li Chen[1,2†], Hua Qu[1,3†], Bin Liu[4†], Bing-Chang Chen[5], Zhen Yang[1,2], Da-Zhuo Shi[1,2*] and Ying Zhang[1,2*]

[1]Xiyuan Hospital, China Academy of Chinese Medical Sciences, Beijing, China, [2]National Clinical Research Center for Chinese Medicine Cardiology, Beijing, China, [3]NMPA Key Laboratory for Clinical Research and Evaluation of Traditional Chinese Medicine, Beijing, China, [4]The First Affiliated Hospital, Hainan Medical University, Haikou, China, [5]Graduate school, Shanxi University of Chinese Medicine, Taiyuan, China

Endothelial shear stress is a tangential stress derived from the friction of the flowing blood on the endothelial surface of the arterial wall and is expressed in units of force/unit area (dyne/cm^2). Branches and bends of arteries are exposed to complex blood flow patterns that generate low or oscillatory endothelial shear stress, which impairs glycocalyx integrity, cytoskeleton arrangement and endothelial junctions (adherens junctions, tight junctions, gap junctions), thus increasing endothelial permeability. The lipoproteins and inflammatory cells penetrating intima due to the increased endothelial permeability characterizes the pathological changes in early stage of atherosclerosis. Endothelial cells are critical sensors of shear stress, however, the mechanisms by which the complex shear stress regulate endothelial permeability in atherosclerosis remain unclear. In this review, we focus on the molecular mechanisms of the endothelial permeability induced by low or oscillatory shear stress, which will shed a novel sight in early stage of atherosclerosis.

KEYWORDS

shear stress, endothelial permeability, glycocalyx, cytoskeleton arrangement, endothelial junctions, atherosclerosis

Introduction

The vascular endothelium maintains the homeostasis of the exchanges of solutes and cells between circulating blood and vascular tissues. Small molecules access to intimal layer by their concentration gradients, while larger molecules and cells pass through intimal layer via vesicles and receptors, or the injured intimal layer with higher permeability (Mundi et al., 2018). Increased endothelial permeability initiates a dysregulated transendothelial flux, leading to abnormal deposition of lipids and infiltration of inflammatory cells in the intima, which promotes the progression of atherosclerosis (Peng et al., 2019; Sedding et al., 2018; Hurtubise et al., 2016). Atherosclerosis is a major pathology of coronary artery disease, stroke, and peripheral arterial disease, which have become a principal consideration of morbidity and mortality worldwide (Libby et al., 2016; Herrington et al., 2016). Therefore, it's crucial to elaborate the mechanisms of increased endothelial permeability in atherogenesis.

The interactions of blood flow with complex vessel geometry generate hemodynamic characteristics, including the heterogeneous spatial and temporal mechanical forces acting on the vessel wall (Zhou et al., 2014; Souilhol et al., 2020). The patterns of blood flow and the

changes of hemodynamics are not consistent in the vascular system (Yamashiro and Yanagisawa, 2020). The blood flow of vertical parts in the arterial tree is usually laminar, leading to high and directed wall shear stress; while blood flow in branches and curvatures is constantly changeable and result in low or oscillatory wall shear stress (Marchio et al., 2019). Vascular endothelial cells (ECs) are constantly exposed to shear stress and respond to the changes of shear stress to regulate endothelial function. The low or oscillatory shear stress accelerates vascular dysfunction and atherogenesis, in contrast to high shear stress (Kwak et al., 2014). Chatzizisis et al. (2007) elaborated the definition of endothelial shear stress that is proportional to the product of the blood viscosity (μ) and the spatial gradient of blood velocity at the wall (endothelial shear stress = μ × dv/dy) (Chatzizisis et al., 2007). Of them, low endothelial shear stress refers to endothelial shear stress that is unidirectional at any given point but has a periodically fluctuating magnitude that results in a low time-average (approximately<10–12 dyne/cm^2); Oscillatory endothelial shear stress is characterized by significant changes in both direction (bidirectional) and magnitude between systole and diastole, resulting in a very low time-average, usually close to 0.

Many risk factors, including hyperlipidemia, obesity, overweight, smoking, etc., are closely associated with atherogenesis. The atherosclerosis is primarily occurred near bifurcation and bends of arterial tree, where generates low or oscillatory shear stress due to disturbed blood flow (Kwak et al., 2014). The disturbed blood flow mediates the initiation of atherosclerosis by inducing vascular inflammation and excessive endothelial cell death (Souilhol et al., 2020). The initial exposure to the blood flow is arterial endothelium, which has critical role in preserving the integrity and homeostasis of blood vessel in response to hemodynamic forces and chemical signals (Davies, 2009; Heo et al., 2011). The endothelial cells are gradually changeable by low or oscillatory shear stress and then switch to atheroprone phenotype (Wang et al., 2013). Understanding the effects of low or oscillatory shear stress on endothelial cells provide mechanistic insights into the roles of complex flow patterns in increased endothelial permeability during the early stage of atherosclerosis. Therefore, this review focuses that the roles of low or oscillatory shear stress on increased endothelial permeability, which is associated with the injury of glycocalyx integrity, cytoskeleton arrangement and cell-cell junctions.

Shear stress and glycocalyx

The glycocalyx is the extracellular covering and exists on the luminal surface of the plasma membrane. The thickness and structure of the glycocalyx vary from different species and is approximately 0.5–5.0 μm in humans (Alphonsus and Rodseth, 2014). The glycocalyx comprises of proteoglycans (PG), glycoproteins bound with sialic acid, glycosaminoglycans (GAG), and adherent plasma proteins (Reitsma et al., 2007). The glycocalyx acts as a negatively charged molecular sieve to maintain the integrity of endothelial barrier (Zhang et al., 2018). Moreover, glycocalyx, as a highly delicate surface structure of endothelial cells, is constantly exposed to shear stress. Low shear stress not only downregulates two major GAGs of the endothelial glycocalyx, heparan sulfate and hyaluronic acid, but also reduces the expression of PG, glycoproteins and adherent plasma proteins, thus resulting in the degradation of glycocalyx layer. Glycocalyx degradation is accompanied by increased endothelial permeability (Zhang et al., 2018) (Figure 1).

Glycocalyx integrity is dependent on blood flow patterns along the walls of the vasculature. Bai and Wang (2014) observed that the glycocalyx relocated near the edge of endothelial cells after HUVECs were subjected to 24 h low shear stress of 12 dyne/cm^2. Following the removal of the shear stress, the glycocalyx redistributed and gradually appeared in the apical region of the cell membrane. The study showed that low shear stress decreased the distribution of sialic acid of the glycocalyx on the cell membrane, but static flow didn't affect the distribution. The results indicated that low shear stress caused lower spatial distribution of glycocalyx layer on endothelial cell membranes compared with static flow, thus degrading glycocalyx and increasing endothelial permeability (Bai and Wang, 2014). Yao et al. (2007) examined the role of the glycocalyx in mechanotransduction by studying the well-characterized responses of endothelial cells to fluid shear stress of 15 dyne/cm^2 for 24 h. The results showed that the glycocalyx redistribution induced by the redistribution of heparan sulfate proteoglycan from a uniform surface profile to a distinct periphery on cell surface after flow application. Moreover, endothelial cells alignment and proliferation were suppressed by removing the glycocalyx compared with normal cells after flow application, suggesting that the glycocalyx plays a pivotal role in mechanotransduction of applied shear (Yao et al., 2007). These results showed that glycocalyx played an important role in endothelial permeability when the endothelial cells exposed to different shear stress. These observations are consistent with the findings of previous studies (Giantsos-Adams et al., 2013; Koo et al., 2013) showing that glycocalyx components are synthesized at a higher rate in arteries with high shear stress compared to those with low shear stress which downregulated heparan sulfate and hyaluronic acid (Mitra et al., 2017).

Moreover, low shear stress also induces endothelial glycolysis, which is a process that releases energy by breaking down the sugar glucose and closely associated with endothelial permeability. Wu et al. (2017) found that HIF-1α activation significantly reduced the basal glycolysis and glycolytic capacity in endothelial cells subjected to low shear stress, thus increasing endothelial permeability (Wu et al., 2017). Feng et al. (2017). showed that low shear stress activates HIF 1α to increase excessive endothelial cell proliferation and permeability via nuclear factor-κB and Cezanne by the induction of glycolysis enzymes (Feng et al., 2017). Another key gene RhoA is also involved in low shear stress-induced endothelial glycolysis. Wu et al. (2021) also revealed that low shear stress induced cell activation and increased endothelial permeability by inducing endothelial glycolysis, which was associated with the activation of RhoA (Wu et al., 2021). Han et al. (2021) showed that pulsatile shear stress downregulated glycolysis in endothelial cells by KLF4-mediated epigenetic and transcriptional upregulation of GCKR expression, which increased endothelial permeability (Han et al., 2021).

Shear stress and cytoskeleton arrangement

The cytoskeleton has three major functions, including the spatial organization of cells' contents, the connection of cell with the

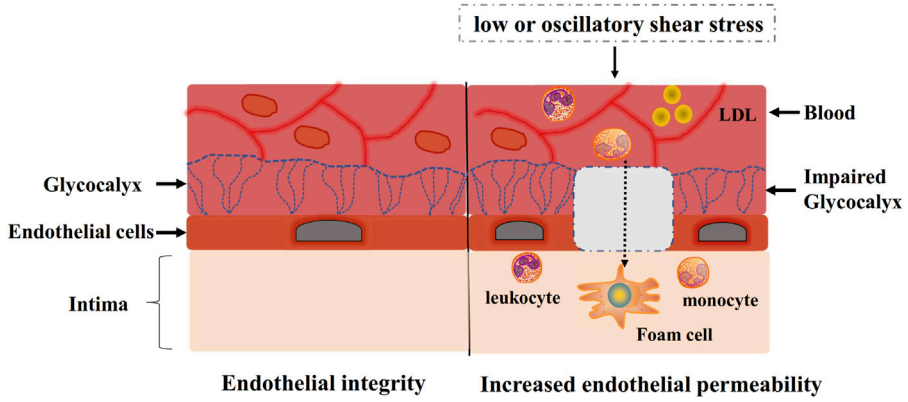

FIGURE 1
Endothelial integrity and increased endothelial permeability. Low or oscillatory shear stress impairs glycocalyx integrity, thus increasing endothelial permeability. Inflammatory cells and LDL infiltrate into intima due to increased endothelial permeability, which causes progression of atherosclerosis.

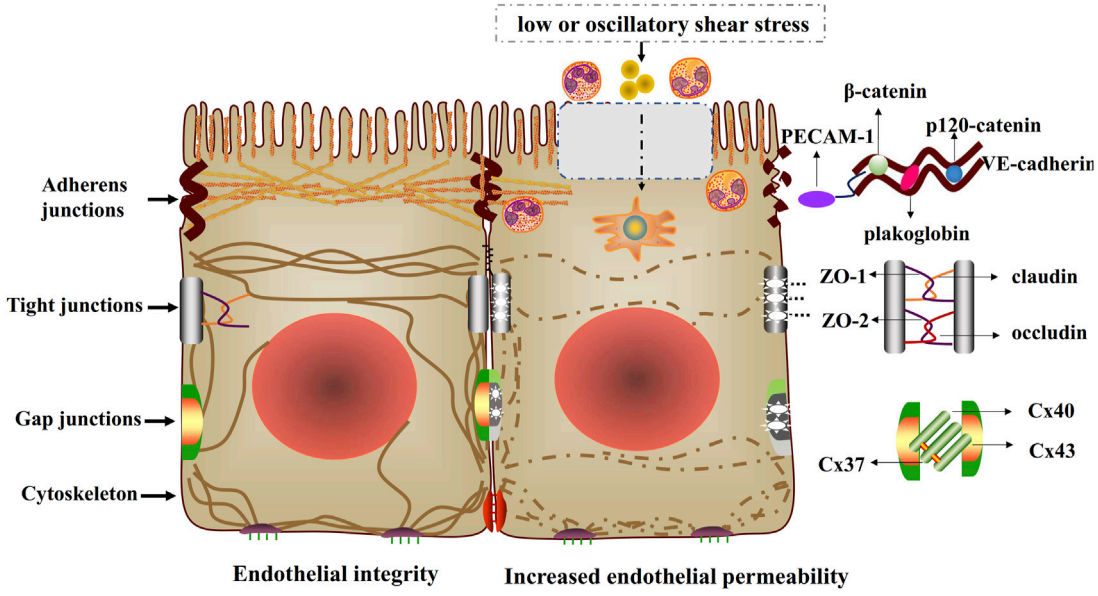

FIGURE 2
Endothelial integrity and increased endothelial permeability. Low or oscillatory shear stress impairs cell-cell junctions and cytoskeletal arrangement, thus increasing endothelial permeability. The injured cell-cell junctions include adherens junctions (VE-cadherin binds to p120-catenin, β-catenin or plakoglobin), tight junctions (occludin, claudin and ZO) and gap junctions (Cx37, Cx40 and Cx43).

external environment, and coordinating ability to promote cells' change and movement (Fletcher and Mullins, 2010). The cytoskeleton is a dynamic and adaptive structure whose component polymers and regulatory proteins are in constant flux (Fletcher and Mullins, 2010). Cytoskeleton arrangement is disrupted and endothelial permeability is increased when endothelial cells exposed to low or oscillatory shear stress (Figure 2).

Actin filaments, the fundamental structure of the membrane cytoskeleton, play an important role in cytoskeleton arrangement and endothelial integrity. The following studies described the critical roles of actin filaments in maintaining endothelial integrity during endothelial cells exposure to shear stress. Ting et al. (2012) found that low endothelial shear stress of 0.75 dyne/cm^2 decreases cytoskeletal tension and disrupts distribution for actin filaments in endothelial cells, which compromises the assembly of cell-cell junctions and increases endothelial integrity (Ting et al., 2012). The mechanism is that PAK and RhoA signaling pathways are activated by low endothelial shear stress, and in turn, regulate endothelial permeability (Ting et al., 2012). Slee and Lowe-Krentz (2013) observed that fluid shear stress of 15 dyne/cm^2 stimulates the disruptions of actin realignment in endothelial cells, which impairs VE-cadherin/β-catenin adhesions and endothelial integrity (Slee and Lowe-Krentz, 2013). The mechanism is that the phosphorylation of cofilin (an actin severing protein) decreases in the cytoplasm and increases in the nucleus, resulting in decreased correct actin realignment during endothelial cells

exposed to fluid shear stress (Slee and Lowe-Krentz, 2013). Blocking stress kinases JNK and p38 reduces phospho-cofilin during fluid shear stress exposure, indicating the significance of exact actin realignment in endothelial integrity during fluid shear stress (Slee and Lowe-Krentz, 2013). Moreover, Verma et al. (2012) used stress sensitive fluorescence resonance energy transfer (FRET) sensors to measure cytoskeletal stresses in α-actinin and rearrangement of the actin cytoskeleton in endothelial cells subjected to low shear stress of 0.74 dyne/cm^2 (Verma et al., 2012). The study showed that low shear stress decreases average actinin stress and cytoskeletal tension, which are accompanied by rearrangement of actin cytoskeleton from parallel F-actin bundles to peripheral bundles, thus increasing endothelial permeability (Verma et al., 2012). The mechanism is associated with Ca^{2+} increase and Rho GTPases signaling activation (Verma et al., 2012). These results showed that low shear stress-induced elongation and orientation of endothelial cells is due to reorganization of actin filaments and actin cytoskeleton, which accelerates an increase in endothelial permeability.

Moreover, there are some key elements involved in the regulation of shear stress in endothelial permeability. One of the key elements is transcription factor FOXC2 which controls endothelial cytoskeleton organization and thus ensures cell-cell junction stability and endothelial integrity under disturbed flow conditions. Sabine et al. (2015) found that transcription factor FOXC2 knockdown in endothelial cells subjected to oscillatory shear stress not only disrupts β-catenin link VE-cadherin to the actin cytoskeleton, but also impairs tight junctions (ZO-1) (Sabine et al., 2015). The study further demonstrated that junction stability is maintained by a FOXC2-dependent fine-tuning of the intercellular tensional cytoskeletal forces and the mechanism is associated with regulation of RhoA/ROCK/MLC signaling. These results illustrated that FOXC2 plays a critical role in maintaining endothelial integrity during oscillatory shear stress (Sabine et al., 2015). CD97, another key element, is the most broadly expressed member with roles in cell adhesion, migration and regulation of intercellular junctions. Hilbig et al. (2018) revealed that mechanical forces rapidly induce phosphorylation of CD97/ADGRE5 (pCD97) at its intracellular C-terminal PDZ-binding motif (PBM). And this phosphorylation disrupts CD97 binding to PDZ domains of the scaffold protein DLG1. Endothelial cells expressing CD97 without the PBM are more deformable, and subjected to shear stress of 1–10 dyne/cm^2, these cells lost cell contacts and impairs actin cytoskeleton, indicating CD97 linked to cytoskeleton arrangement and affects endothelial integrity (Hilbig et al., 2018). These observations indicated that above key elements play critical role in low or oscillatory shear stress-induced increased endothelial permeability.

Shear stress and adherens junctions

Endothelial cell-cell adherens junctions supervise fundamental vascular functions, such as controlling permeability and transmigration of circulating leukocytes, and maintaining the function of existing vessels and formation of new ones (Rudini and Dejana, 2008). The adherens junctions are particularly important for endothelial integrity and are prerequisite for the assembly of other junctional complexes. Vascular endothelial cadherin (VE-cadherin), the basic component of adherens junctions, is connected via its cytoplasmic domain to p120-catenin and β-catenin or plakoglobin (Brüser and Bogdan, 2017). Some complexes can be formed by the interaction of VE-cadherin and distinct transmembrane signaling systems, such as vascular endothelial growth factor receptor 2 (VEGFR2), vascular endothelial phosphotyrosine phosphatase (VE-PTP), and transforming growth factor (TGF) β receptor complex (Lampugnani et al., 2018). These complexes are important in regulating cell–cell junctions. Low shear stress contributes to the injury of adherens junctions, which increases endothelial permeability (Giannotta et al., 2013) (Figure 2).

Previous studies applied many advanced technologies to investigate the effects of shear stress on adherens junctions and endothelial permeability (Hur et al., 2012; Miao et al., 2005; Hofer et al., 2018). For example, Hur et al. (2012) applied 3D inter-/intracellular force microscopy technique to measure the cell-cell junctional and intracellular tensions in vascular endothelial cells monolayers under shear flow conditions. The study observed that cell-cell junctional tensions are increased by shear stress of 12 dyne/cm^2, which are concomitant with elongated cell morphology and stress fibers, and reorganization of adherens junction proteins, such as VE-cadherin and catenins (Hur et al., 2012). This tension-mediated directional reorganization of the adherens junctions indicates that directional mechanotransduction is necessary for the ECs to regulate endothelial permeability in response to changes flow shear. Miao et al. (2005) also found that endothelial cells exposed to low shear stress (12 dyne/cm^2) causes the reorganization of VE-cadherin in endothelial monolayers, which impairs adherens junctions (Miao et al., 2005). Hofer et al. (2018) applied an adenoviral vector with VE-cadherin-EGFP to investigate the dynamic alteration of VE-cadherin in endothelial cells subjected to low shear stress of 12 dyn/cm^2 (Hofer et al., 2018). The results showed that cell junction remodeling during low shear stress is accompanied by VE-cadherin plaque formation, which is associated with endothelial integrity (Hofer et al., 2018).

Moreover, there are some key elements involves in shear stress-mediated increased endothelial permeability by impairing adherens junctions. Rap1, a key modulator of integrin- and cadherin-regulated processes, is indispensable for vascular stability and the formation of functional vasculature in endothelium. Lakshmikanthan et al. (2018) showed that Rap1 plays crucial roles in regulating VEGFR2-mediated angiogenesis and shear stress-induced endothelial responses (Lakshmikanthan et al., 2018). The study observed that deleting Rap1 isoform impairs *de novo* adherens junctions (VE-cadherin and β-catenin) formation and recovery from disturbed shear, indicating the important role of Rap1 in endothelial permeability (Lakshmikanthan et al., 2018). Src, a proto-oncogene, plays key roles in cell morphology, motility, proliferation, and survival. Spindel et al. (2014) found that fluid shear stress decreases Src activity and stress fiber formation in endothelial cells, whereas it increases the expression of thioredoxin-interacting protein (TXNIP) (Spindel et al., 2014). TXNIP, a biomechanical regulator, involves in the activation of Src and formation of EC stress fibers. Under low shear stress of 2 dyne/cm^2, high expression of TXNIP increases Src Y527 phosphorylation and reduces Src activity, which impairs VE-cadherin-Src complex and F-actin stress fibers formation,

thus increasing endothelial permeability (Spindel et al., 2014). Moreover, IQ domain GTPase activating protein 1 (IQGAP1) is a scaffold protein which couples cell signaling to the actin and microtubule cytoskeletons and participates in cell migration and adhesion (Rami et al., 2013). Rami et al. (2013) observed that low shear stress (1.2 dyne/m^2) in endothelial cells induces the interaction of IQGAP1/β-catenin, which is concomitant with the impaired interactions between VE-cadherin/IQGAP1 and VE-cadherin/β-catenin. The mechanism is that IQGAP1 interacting with β-catenin causes the separation of VE-cadherin and β-catenin, thus impairing the adherent junction and endothelial integrity (Rami et al., 2013). Endothelial-to-mesenchymal transition (EndMT) is a process that low shear stress stimulates the differentiation of endothelial cells. Mahmoud et al. (2017) explored the function of Snail in low shear stress-induced EndMT, and found that exposed to low shear stress (5 dyne/cm^2) induces Snail expression in cultured endothelial cells (Mahmoud et al., 2017). Gene silencing Snail revealed that Snail has positive regulation of EndMT markers expression (Slug, N-cadherin, α-SMA) and increases endothelial permeability to macromolecules, indicating that Snail is a necessary driver of EndMT under low shear stress and may promote early atherogenesis by enhancing vascular permeability (Mahmoud et al., 2017). Baratchi et al. (2017) showed that transient receptor potential vanilloid 4 (TRPV4) channels are expressed in preclustered structures and in a complex with β-catenin (Baratchi et al., 2017). Stimulated endothelial cells with low shear stress of 10 dyne/cm^2 for 6 h, TRPV4 channels relocates from the basolateral membrane to basal membrane and loses the interaction with β-catenin. β-catenin is the main adapter protein of the adherens junctions at the point of cell-cell contact that is proposed to transmit the shear stress to the cell interior and cytoskeleton. These results indicated that TRPV4 might increase endothelial permeability after shear stress stimulation by relocating TRPV4 channels from adherens junctions and reducing TRPV4 with β-catenin (Baratchi et al., 2017). These results suggested that above key elements play critical roles in the impairment of adherens junctions and increased endothelial permeability due to low shear stress in endothelial cells.

Except for observing morphological changes and key molecules in adherens junctions, we also demonstrate the mechanisms of low shear stress-mediated adherens junctions damnification (Ukropec et al., 2002; Kang et al., 2014). Ukropec et al. (2002) demonstrated that the composition of the junctional complexes, such as β-catenin or α-catenin associated with VE-cadherin, are obviously decreased in endothelial cells subjected to fluid shear stress of 10 dyne/cm^2 (Ukropec et al., 2002). The mechanism is that the impairment of α-catenin from the junctional and elevating tyrosine phosphorylation of β-catenin relates with VE-cadherin (Ukropec et al., 2002). The alteration of β-catenin phosphorylation is associated with the dissociation of protein tyrosine phosphatase SHP-2 from VE-cadherin complexes, which is mediated by low shear stress and increases endothelial permeability (Ukropec et al., 2002). Kang et al. (2014) observed that endothelial monolayers exposure to shear stress of 12 dyne/cm^2 lowers the expression of VE-cadherin, which increases water flux and LDL leakage. However, treating endothelial cells with NO inhibitor (L-NMMA) blocks these changes, suggesting that low shear stress impairs adherens junctions and endothelial permeability by an NO dependent mechanism (Kang et al., 2014).

In addition, endothelial adherens junctions can adapt to the changes of shear stress to maintain the endothelial integrity. Noria et al. (1999) revealed that endothelial cells exposed to 15 dyne/cm^2 of shear stress by using a parallel plate flow chamber, in order to illustrate the function of altered shear stress on the disassembly of adherens junction protein complexes (Noria et al., 1999). The results showed that shear stress contributes to partial disassembly of the adherens junction complex (α/β-catenin with VE-cadherin). Which play an important role in endothelial permeability barrier (Noria et al., 1999). Seebach et al. (2000) observed shear stress-induced change in transendothelial electrical resistance (TER) is associated with changes in cell motility and cell shape as a function of morphodynamics and accompanied by a reorganization of catenins that regulate endothelial adherens junctions. The endothelial cells exposed to shear stress of 2–50 dyne/cm^2 and the results demonstrated that endothelial monolayers exposed to laminar shear stress respond with a shear stress-dependent regulation of permeability and a reorganization of junction-associated proteins, whereas monolayer integrity remains unaffected (Seebach et al., 2000). These different observations from above studies indicated that the endothelial monolayer has the fascinating capability to adapt accordingly to these changeable shear stress while maintaining its crucial vascular barrier function. Failure of the endothelial monolayer to adapt to changes in the magnitude or direction of forces has direct consequences on endothelial permeability (Shah and Katira, 2023), and is, therefore, regarded as an important cause of atherogenesis.

Shear stress and tight junctions

Tight junctions play critical roles in maintaining the barrier homostasis of different compartments, and act as paracellular gates that restrict diffusion on the basis of size and charge (Zihni et al., 2016). Tight junction proteins include the claudin family that possesses barrier characteristics, and MARVEL family that conduces to barrier regulation. Besides, JAM molecules belong to tight junctions as well and regulate organization and diapedesis of the junctions (Díaz-Coránguez et al., 2019). What's more, MAGUK family members, such as zonula occludens (ZO), contribute to the formation of scaffold, which is related with cells signaling molecules and cytoskeleton arrangement (Shen et al., 2011). Previous studies have demonstrated that the damage of tight junction proteins increase endothelial permeability under low or oscillatory shear stress conditions, which impairs the endothelial barrier function and accelerates early atherosclerotic development (DeMaio et al., 2001; Conklin et al., 2007; Conklin et al., 2002; Okano and Yoshida, 1992) (Figure 2).

Occludin is a major component of the tight junctions. Phosphorylation/dephosphorylation plays a major role in regulation of occludin and tight junctions. DeMaio et al. (2001) revealed that occludin phosphorylation increases and occludin total content decreases when endothelial cells expose to shear stress of 10 dyne/cm^2. Alterations of phosphorylation state and total content in occludin impairs tight junction, thus increasing endothelial permeability (DeMaio et al., 2001). Conklin et al. (2002) found that low shear stress of 1.5 dyne/cm^2 decreases occludin expression and increases endothelial cells VEGF expression, which is associated

with increased endothelial permeability (Conklin et al., 2002). Moreover, Conklin et al. (2007) further found that low shear stress of 1.5 dyne/cm^2 increases the endothelial permeability to LDL particles by using a highly controlled artery perfusion culture system (Conklin et al., 2007). The changes in endothelial permeability corresponds to an approximately 50% reduction of occludin expression, illustrating that occludin plays important roles in low shear stress-mediated increased endothelial permeability (Conklin et al., 2007). Okano and Yoshida (1992) revealed that the hip of the flow dividers of branching, a relatively low shear stress region, is covered by ellipsoidal cells with intermittent tight junctions and abnormal gap junctions in hyperlipidemic rabbits (Okano and Yoshida, 1992). The results suggested that endothelial cells exposed to relatively low shear stress may be activated, leading to increased endothelial permeability (Okano and Yoshida, 1992). These findings illustrated that occludin is not only a key player in shear stress but may also be a significant structural element in the construction of endothelial permeability within tight junctions. Except for occludin, ZO-1 is another tight junction involved in low shear stress-induced increased permeability. Besides, ZO-1 present to interact with occludin, allowing occludin to function as a seal or a gate, which would explain the increase in TER and slight reduction in cellular permeability.

Therefore, we then discussed ZO-1 in endothelial permeability-induced by low shear stress. There are plenty of advanced technologies applied to investigate the effects of different shear stress on tight junctions. Berardi and Tarbell (2009) used a hemodynamic simulator to explore the associative effects of wall shear stress and circumferential stress on EC junctions (Berardi and Tarbell, 2009). The study showed that low shear stress of 10 dyne/cm^2 reduces the protein expression of ZO-1 and increases leaky junctions, which accelerates lipoprotein into the intima. The results indicate that shear stress impairs tight junctions stability and increases endothelial permeability (Berardi and Tarbell, 2009). Chen et al. (2019) applied a gelatin-based perfusable endothelial 3D carotid artery model to investigate the endothelial response to shear stress (Chen et al., 2019). The study observed that low shear stress (less than 0.4 dyne/cm^2) induces the downregulation of ZO-1 levels and disorganization of F-actin cytoskeleton, which increases endothelial permeability (Chen et al., 2019). The mechanism might be associated with the increase of n ZO-1itric oxide (NO) and prostacyclin (PGI2) release, and inhibition of endothelin-1 (ET-1) release (Chen et al., 2019). Himburg et al. (2004) used a novel technique to test the interaction between fluid shear stress and endothelial permeability to macromolecules in cultured endothelial cells (Himburg et al., 2004). The results showed that low shear stress of 10 dyne/cm^2 promotes lipoprotein infiltration into intima via an increased endothelial permeability, which might be related with increased VEGF expression and decreased occludin expression (Himburg et al., 2004).

The mechanisms of low shear stress increasing endothelial permeability by impairing tight junctions have been illustrated as followed. Rac1 has been found to be involved in a variety of cellular processes such as cell–cell or cell–substrate adhesion, apicobasal polarity, migration, invasion, and proliferation. Walsh et al. (2011) observed that 10 dyne/cm^2 shear stress reduces membrane localization of ZO-1 and claudin-5, thus increasing endothelial permeability (Walsh et al., 2011). Treating endothelial cells with VE-cadherin inhibitor (VE-cad ΔEXD) attenuates shear-induced Rac1 activation and increased endothelial permeability (Walsh et al., 2011). The mechanism is that VE-cadherin inhibition disrupts the distribution of tight junction proteins (such as claudin-5 and ZO-1) by repressing Rac1 signaling under low shear stress (Walsh et al., 2011). Ho et al. (2019) illustrated that flow shear stress of 6 dyne/cm^2 induces the activation of proline-rich receptor-1 (IGPR-1) compared with static flow, which modulates endothelial cells remodeling and stimulates actin stress fiber assembly by regulating ZO-1, thus increasing endothelial permeability (Ho et al., 2019). Mechanistically, shear stress activates AKT Ser/Thr kinase 1 (AKT1), resulting in phosphorylation of IGPR-1 at Ser-220. Suppressing the phosphorylation prevents low shear stress-stimulated actin fiber assembly and increased endothelial permeability. Dickkopf1 (DKK1) is a comprehensive regulator of the Wnt pathway of which activation is associated with cell proliferation and apoptosis. Li et al. (2016) found that oscillatory shear stress induces DKK1 expression and impairs endothelial tight junctions, which increases endothelial permeability and can be counteracted by siRNA knockdown or silencing DKK1 in ApoE$^{-/-}$ mice (Li et al., 2016). The mechanism is that activating endothelial proteinase-activated receptor 1 (PAR1) and its downstream transcription factor, cAMP response element-binding protein (CREB), increases expression of DKK1 under oscillatory shear stress (Li et al., 2016). However, Gross identified a new mechanism by which endothelial cells adapt to laminar shear stress by up-regulating Sox18 to prevent the disruption of the endothelial barrier. The study demonstrated that laminar shear stress (20 dyne/cm^2) increases the protein expression of Claudin-5 in a Sox18 dependent pattern (Gross et al., 2014). Sox18 is a transcription factor involved in endothelial barrier integrity, and knockdown of Sox18 causes the dysfunction of endothelial barrier during shear stress (Gross et al., 2014). The results indicated that laminar shear stress increases the expression of Sox18 and Claudin-5, thus protecting endothelial barrier function (Gross et al., 2014). The different results of shear stress on endothelial barrier further demonstrated the different roles of low or oscillatory shear stress on tight junctions. Low or oscillatory shear stress increasing endothelial permeability by impair tight junctions, such as decreasing occludin and ZO-1, while high laminar shear stress maintaining tight junctions by increasing Claudin-5.

Shear stress and gap junctions

Gap junctions, integral membrane proteins, not only directly promote cytoplasmic exchange of ions, but also regulate low molecular weight metabolites of adjacent cells (Nielsen et al., 2012). Gap junctions play significant roles in physiological functions, such as propagating electrical signals and coordinating cell signaling through interacting with second messengers (Nielsen et al., 2012). Gap junction comprises of two connexons (hexamers of connexins, Cx) that align in the extracellular space (Harris, 2001). Previous studies have authenticated nearly 21 human connexin genes, such as Cx40, Cx43 and Cx37 expressed in the endothelium (Harris, 2001; Molica et al., 2014). Previous researches have illustrated that low or oscillatory shear stress increasing endothelial permeability by regulating gap junctions

(Kwak et al., 2005; Gabriels and Paul, 1998; Inai et al., 2004) (Figure 2).

There is growing evidence that Cx proteins play an important role in atherosclerosis development. Cx43 is normally absent in the aortic endothelium of healthy individuals; however, it is located at branching sites of the arterial tree, which are highly susceptible to atherosclerosis development (Ramadan et al., 2012). High Cx43 expression was reported at regions of disturbed blood flow in rat aortic endothelial cells, and increased Cx43 expression was also observed in various *in vivo* studies using a model that simulates human arterial shear stress. For example, Kwak et al. (2005) showed that low shear stress of 6 dyne/cm^2 significantly increases Cx43 expression in endothelial cells (Kwak et al., 2005). High-expressed endothelial Cx43 is at flow dividers, upstream of valves and at the shoulder of atherosclerotic plaques (Kwak et al., 2005). In such regions, the endothelium is characterized by an increased permeability and a decreased expression of endothelial nitric oxide synthase (Kwak et al., 2005). Gabriels and Paul (1998) investigate the relationship between shear stress and Cx43 expression in a segment of abdominal aorta. The study showed that Cx43 is highly localized at the downstream edge of the ostia of branching vessels and at flow dividers, regions that experience turbulent shear stress and endothelial permeability increases (Gabriels and Paul, 1998). Inai et al. (2004) revealed that Cx43 was highly localized to the sites subjected to disturbed shear from turbulent flow (Inai et al., 2004). This specific site increases Cx43 expression, and consequently supports the notion that shear stress regulate endothelial permeability by controlling Cx43 expression in endothelial cells (Inai et al., 2004). DePaola et al. (1999) used a model of controlled disturbed flows in endothelial cells to investigates the effects of low shear stress on endothelial gap junction protein Cx43. The study showed that low shear stress of 0–8.5 dyne/cm^2 significantly increases endothelial Cx43 expression compared with no-flow controls. The results indicated that upregulation of Cx43 transcripts, sustained disorganization of Cx43 protein, and increased endothelial permeability suggest that low shear stress gradients in regions of disturbed flow regulate endothelial permeability through the expression and function of Cx43. (DePaola et al., 1999). Moreover, Xu et al. (2017) found that in blood perfused vessels, low shear stress of 1.1 or 3.2 dyne/cm^2 acting on red blood cells (RBCs) stimulates shear dependent release of ATP, which increases EC $[Ca^{2+}]_i$ and endothelial gap formation, thus increasing endothelial permeability (Xu et al., 2017). These observations illustrated that high Cx43 expression at regions of low or oscillatory shear stress plays a critical role in atherogenesis by increasing endothelial permeability.

Shear stress and PECAM-1

Platelet endothelial cell adhesion molecule (PECAM-1), a type 1 transmembrane glycoprotein of the immunoglobulin (Ig) superfamily of cell adhesion molecules, acts as vascular mechanosensor and plays an important role in angiogenesis and vascular remodeling. When endothelial cells are exposed to fluid shear stress, PECAM-1 has been shown to be tyrosine phosphorylated (Tzima et al., 2005; Lertkiatmongkol et al., 2016). Given the subcellular localization of PECAM-1 to regions of high mechanical tension, shear-induced PECAM-1 signaling may result from force-induced deformational changes in the molecule (Tzima et al., 2005), suggesting a role in sensing atheroprone hemodynamics flow. Moreover, VE-cadherin, PECAM-1 and VEGF receptor 2 form a mechanosensory complex that is in charge of shear stress sensing in endothelial cells (Conway et al., 2013) (Figures 1–3).

The following studies illustrated that PECAM-1 is a critical mediator of atherosclerosis under low shear stress. Otte et al. (2009) observed that in endothelial cells, temporal gradients in shear stress of 0–14 dyne/cm^2 lead to a rapid dissociation of the Gαq/11–PECAM-1 complex, whereas fluid flow devoid of temporal gradients does not disrupt the complex. And fluid shear-dependent Gαq/11–PECAM-1 complex dissociation increases endothelial permeability (Otte et al., 2009). dela Paz et al. (2014) also found that Gαq/11 is rapidly dissociated from PECAM-1 followed by re-association when endothelial cells exposed to shear stress of 14 dyne/cm^2, thus increasing endothelial permeability (dela Paz et al., 2014). Biswas et al. (2006) found that PECAM-1-null mice enhances endothelial permeability during inflammatory intervention. And in PECAM-1-null endothelial cells, β-catenin remains tyrosine phosphorylated and is accompanied by a continuous augmentation in endothelial permeability (Biswas et al., 2006). The mechanism is associated with activation of β-catenin/glycogen synthase kinase 3 (GSK-3β) signaling (Biswas et al., 2006). However, Xie et al. (2020) revealed that low shear stress of 2 dyne/cm^2 upregulates PECAM-1 expression, leading to endothelial apoptosis and monocyte adhesion that subsequently increases endothelial permeability (Xie et al., 2020). The mechanism is that PECAM-1 siRNA transfection increases Akt and forkhead box O1 phosphorylation under low shear stress conditions. These different roles of PECAM-1-iduced by shear stress on endothelial permeability indicated that more studies are needed to investigate the exact role and mechanism of PECAM-1 in endothelial permeability under different shear stress conditions.

Conclusion

Atherosclerosis, a progressive inflammatory disease of large and medium-sized arteries, is the main pathological changes of cardiovascular diseases (Sanz and Fayad, 2008). Vascular endothelial cells are subjected to hemodynamic forces that can activate mechanotransduction and regulate homeostasis. Pro-atherogenic low or oscillatory shear stress and atheroprotective pulsatile shear stress are two vital hemodynamic forces that modulate endothelial cells dysfunction and function (Lee and Chiu, 2019). Endothelial cells dysfunctions, including turnover enhancement, glycocalyx injury, cell-cell junction disruption, and inflammation, have been found to play vital roles in the initiation of atherosclerosis (Lee and Chiu, 2019). These responses can disrupt the intact structure of the endothelium to increase endothelial permeability and allow the penetration of lipoproteins and inflammatory monocytes to promote the progression of atherosclerosis (Wang et al., 2020; Heo et al., 2014). In this review we focus on the mechanisms that low or oscillatory shear stress increases endothelial permeability by impairing glycocalyx integrity, cytoskeleton arrangement and cell-cell junctions.

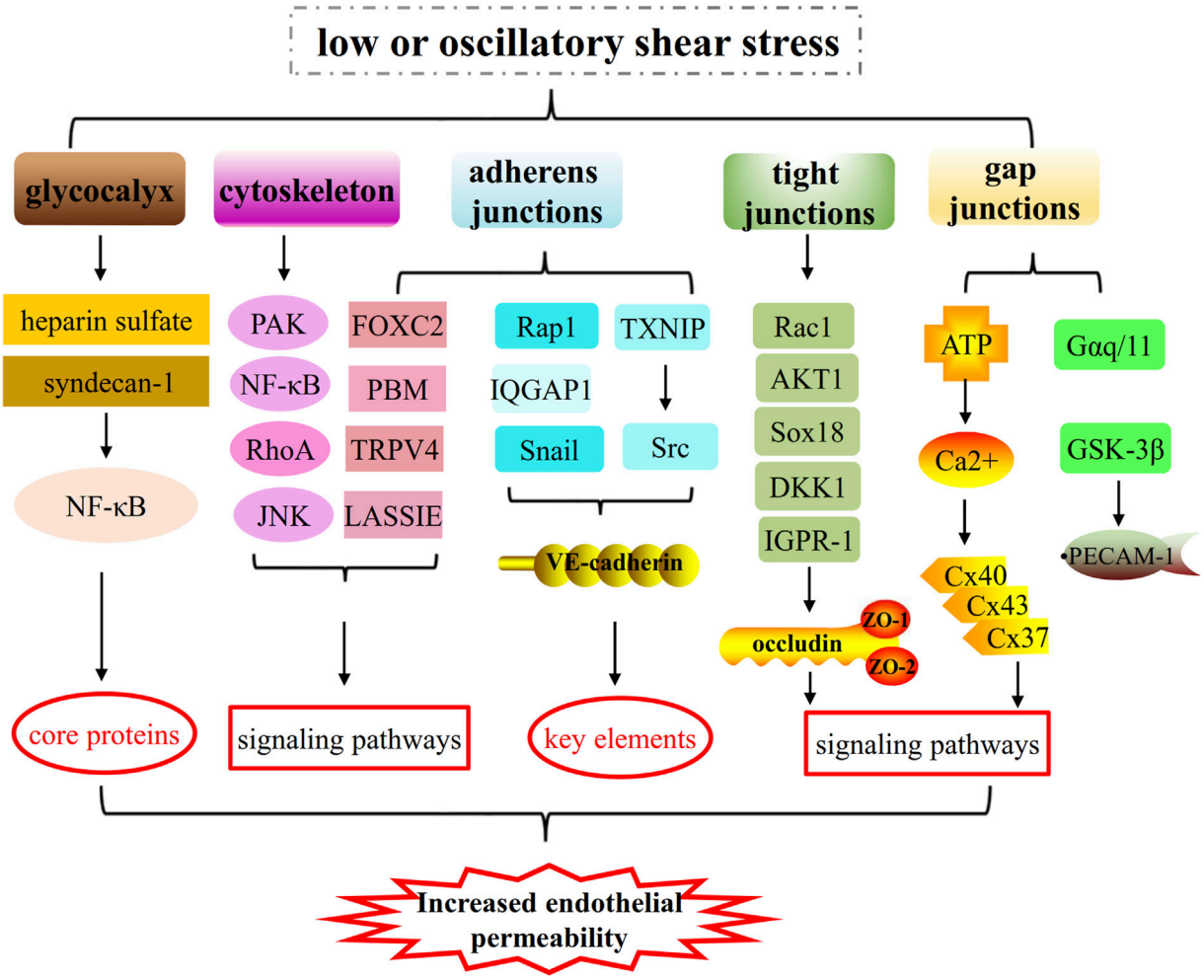

FIGURE 3
The mechanisms of low or oscillatory shear stress on increased endothelial permeability by impairing glycocalyx integrity, cytoskeletal arrangement and cell-cell junctions (such as, adherens junctions, tight junctions and gap junctions). 1) Low or oscillatory shear stress increases endothelial permeability by regulating core proteins of glycocalyx and key elements of cytoskeleton and cell-cell junctions (adherens junctions and tight junctions). 2) Low or oscillatory shear stress increases endothelial permeability by regulating PAK/NF-κB signaling, RhoA signaling, JNK signaling pathways and so on.

The pulsatile nature of the arterial blood flow in combination with the complex geometric configuration of the coronaries determines the endothelial shear stress patterns, which are characterized by direction and magnitude. In geometrically irregular regions, where disturbed laminar flow occurs, pulsatile flow generates low and/or oscillatory endothelial shear stress (Chatzizisis et al., 2007; Chiu and Chein, 2011; Wu et al., 2007). The low or oscillatory shear stress injures glycocalyx, cytoskeleton and cell-cell junctions, such as adherens junctions, tight junctions and gap junctions, thus leading to a leakage of the endothelial permeability barrier. The glycocalyx plays significant roles in transferring fluid shear stress to the actin cytoskeleton and initiating intracellular signaling. And cytoskeletal reorganization and biochemical responses during disturbed shear are dependent by the structural integrity of the glycocalyx and can be almost blocked if the glycocalyx is not integral (Massou et al., 2020). The interaction between cytoskeleton and cell-cell junctions is critical for tissue development and physiology, and takes part in the molecular mechanisms, such as regulating cell shape, motility and growth (Charras and Yap, 2018). Low or oscillatory shear stress injures the function of the actin cytoskeleton in the organization and function of cell–cell junctions, thus increasing endothelial permeability, while high shear stress might play a beneficial role. KLF2 are core shear-stress dependent transcription factors which regulate cell-cell junctions, and Huang et al. (2017) showed that high shear stress induces KLF2 which act to promote adherens and tight junctions. When the glycocalyx is damaged by low or oscillatory shear stress, the subsequent dysfunctions of cytoskeleton and cell-cell junctions will also occur, forming a malignant circle, thus increasing endothelial permeability and accelerating atherosclerotic development.

The vascular barrier is essential for normal tissue homeostasis. The barrier is formed by tight junctions, adherens junctions and gap junctions that join endothelial cells, with additional contributions from the endothelial cell glycocalyx and cell cytoskeleton on the luminal surface and basement membrane and mural cells on the abluminal surface (Wettschureck et al., 2019). Barrier disruption is accompanied by an increase in endothelial permeability, which

occurs in early stages of atherogenesis. These pathological findings are important when considering therapeutic strategies for treating early stage of atherosclerosis. Preventing the entry and subsequent intimal retention of ApoB-containing lipoprotein, particularly at an early stage of atherosclerosis, are critical in the prevention of atherosclerosis. For example, statins lower the plasma concentration of lipoproteins and can reduce the entry of lipoproteins in the intima (Nakashima et al., 2008). Targeting of inflammatory pathways also provide an additional treatment in early stage of atherosclerosis. Dexamethasone (DXM), an anti-inflammatory steroid drug, can inhibit atherosclerosis development via decreasing intimal macrophage recruitment and foam cell formation (Zhang et al., 2017).

Considering the critical roles of low or oscillatory shear stress in endothelial permeability during early stage of atherogenesis, some problems need to be solved urgently. Many unknown knowledge still needs to be uncovered to develop endothelial barrier-targeted therapies in atherosclerosis (Peruzzi et al., 2018). Especially, applying the therapeutic strategies to promote normal shear stress in the branches and bends of arteries, which may contribute to maintain glycocalyx integrity, cytoskeleton arrangement and cell-cell junctions (Peruzzi et al., 2018; Tarbell and Cancel, 2016). First, as novel potential therapeutic targets are increasingly distinguished, including EndoMT reversal, the assumption to treat atherosclerosis via above targets might be proposed and ultimately applied in human trial (Li et al., 2018). Second, studies have showed that low shear stress (3–6 dyne/cm^2) increases PCSK9 expression, and lipid-induced increase in PCSK9 expression is higher at low shear stress (Yurtseven et al., 2020; Ason et al., 2014). PCSK9 inhibitors might contribute to improve endothelial dysfunction-induced by low shear stress. Moreover, a principal challenge in the region is the integration of a large quantity of data on endothelial cells subjected to disturbed shear flow at the molecular level, and then to identify the shear stress-specific endothelial gene expression and phenotype (Monfoulet et al., 2017). Therefore, understanding the mechanisms of low or oscillatory shear stress in increased endothelial permeability promotes to find new diagnostic markers and develop novel therapies.

Author contributions

LC: Writing–review and editing, Writing–original draft, Validation, Methodology, Funding acquisition, Data curation. HQ: Writing–review and editing, Validation, Resources. BL: Visualization, Supervision, Writing–review and editing, Investigation. B-CC: Writing–review and editing, Software, Methodology. ZY: Writing–review and editing, Validation, Conceptualization. D-ZS: Writing–review and editing, Visualization, Funding acquisition. YZ: Writing–review and editing.

Funding

The author(s) declare that financial support was received for the research, authorship, and/or publication of this article. This work was supported by the Fundamental Research Funds for the Central public welfare research institutes (No. ZZ16-XRZ-005) and the National Natural Science Foundation of China (Nos 81774141 and 82074418).

Conflict of interest

The authors declare that the research was conducted in the absence of any commercial or financial relationships that could be construed as a potential conflict of interest.

Publisher's note

References

Alphonsus, C. S., and Rodseth, R. N. (2014). The endothelial glycocalyx: a review of the vascular barrier. *Anaesthesia* 69 (7), 777–784. doi:10.1111/anae.12661

Ason, B., van der Hoorn, J. W., Chan, J., Lee, E., Pieterman, E. J., Nguyen, K. K., et al. (2014). PCSK9 inhibition fails to alter hepatic LDLR, circulating cholesterol, and atherosclerosis in the absence of ApoE. *J. Lipid Res.* 55 (11), 2370–2379. doi:10.1194/jlr.M053207

Bai, K., and Wang, W. (2014). Shear stress-induced redistribution of the glycocalyx on endothelial cells *in vitro*. *Biomech. Model Mechanobiol.* 13 (2), 303–311. doi:10.1007/s10237-013-0502-3

Baratchi, S., Knoerzer, M., Khoshmanesh, K., Mitchell, A., and McIntyre, P. (2017). Shear stress regulates TRPV4 channel clustering and translocation from adherens junctions to the basal membrane. *Sci. Rep.* 7 (1), 15942. doi:10.1038/s41598-017-16276-7

Berardi, D. E., and Tarbell, J. M. (2009). Stretch and shear interactions affect intercellular junction protein expression and turnover in endothelial cells. *Cell Mol. Bioeng.* 2 (3), 320–331. doi:10.1007/s12195-009-0073-7

Biswas, P., Canosa, S., Schoenfeld, D., Schoenfeld, J., Li, P., Cheas, L. C., et al. (2006). PECAM-1 affects GSK-3beta-mediated beta-catenin phosphorylation and degradation. *Am. J. Pathol.* 169 (1), 314–324. doi:10.2353/ajpath.2006.051112

Brüser, L., and Bogdan, S. (2017). Adherens junctions on the move-membrane trafficking of E-cadherin. *Cold Spring Harb. Perspect. Biol.* 9 (3), a029140. doi:10.1101/cshperspect.a029140

Charras, G., and Yap, A. S. (2018). Tensile forces and mechanotransduction at cell-cell junctions. *Curr. Biol.* 28 (8), R445–R457. doi:10.1016/j.cub.2018.02.003

Chatzizisis, Y. S., Coskun, A. U., Jonas, M., Edelman, E. R., Feldman, C. L., and Stone, P. H. (2007). Role of endothelial shear stress in the natural history of coronary atherosclerosis and vascular remodeling: molecular, cellular, and vascular behavior. *J. Am. Coll. Cardiol.* 49 (25), 2379–2393. doi:10.1016/j.jacc.2007.02.059

Chen, R., Wang, B., Liu, Y., He, J., Lin, R., and Li, D. (2019). Gelatin-based perfusable, endothelial carotid artery model for the study of atherosclerosis. *Biomed. Eng. Online* 18 (1), 87. doi:10.1186/s12938-019-0706-6

Chiu, J. J., and Chien, S. (2011). Effects of disturbed flow on vascular endothelium: pathophysiological basis and clinical perspectives. *Physiol. Rev.* 91 (1), 327–387. doi:10.1152/physrev.00047.2009

Conklin, B. S., Vito, R. P., and Chen, C. (2007). Effect of low shear stress on permeability and occludin expression in porcine artery endothelial cells. *World J. Surg.* 31 (4), 733–743. doi:10.1007/s00268-006-0735-8

Conklin, B. S., Zhong, D. S., Zhao, W., Lin, P. H., and Chen, C. (2002). Shear stress regulates occludin and VEGF expression in porcine arterial endothelial cells. *J. Surg. Res.* 102 (1), 13–21. doi:10.1006/jsre.2001.6295

Conway, D. E., Breckenridge, M. T., Hinde, E., Gratton, E., Chen, C. S., and Schwartz, M. A. (2013). Fluid shear stress on endothelial cells modulates mechanical tension across VE-cadherin and PECAM-1. *Curr. Biol.* 23 (11), 1024–1030. doi:10.1016/j.cub.2013.04.049

Davies, P. F. (2009). Hemodynamic shear stress and the endothelium in cardiovascular pathophysiology. *Nat. Clin. Pract. Cardiovasc Med.* 6 (1), 16–26. doi:10.1038/ncpcardio1397

dela Paz, N. G., Melchior, B., Shayo, F. Y., and Frangos, J. A. (2014). Heparan sulfates mediate the interaction between platelet endothelial cell adhesion molecule-1 (PECAM-1) and the Gαq/11 subunits of heterotrimeric G proteins. *J. Biol. Chem.* 289 (11), 7413–7424. doi:10.1074/jbc.M113.542514

DeMaio, L., Chang, Y. S., Gardner, T. W., Tarbell, J. M., and Antonetti, D. A. (2001). Shear stress regulates occludin content and phosphorylation. *Am. J. Physiol. Heart Circ. Physiol.* 281 (1), H105–H113. doi:10.1152/ajpheart.2001.281.1.H105

DePaola, N., Davies, P. F., Pritchard, W. F., Florez, L., Harbeck, N., and Polacek, D. C. (1999). Spatial and temporal regulation of gap junction connexin43 in vascular endothelial cells exposed to controlled disturbed flows *in vitro*. *Proc. Natl. Acad. Sci. U. S. A.* 96 (6), 3154–3159. doi:10.1073/pnas.96.6.3154

Díaz-Coránguez, M., Liu, X., and Antonetti, D. A. (2019). Tight junctions in cell proliferation. *Int. J. Mol. Sci.* 20 (23), 5972. doi:10.3390/ijms20235972

Feng, S., Bowden, N., Fragiadaki, M., Souilhol, C., Hsiao, S., Mahmoud, M., et al. (2017). Mechanical activation of hypoxia-inducible factor 1α drives endothelial dysfunction at atheroprone sites. *Arterioscler. Thromb. Vasc. Biol.* 37 (11), 2087–2101. doi:10.1161/ATVBAHA.117.309249

Fletcher, D. A., and Mullins, R. D. (2010). Cell mechanics and the cytoskeleton. *Nature* 463 (7280), 485–492. doi:10.1038/nature08908

Gabriels, J. E., and Paul, D. L. (1998). Connexin43 is highly localized to sites of disturbed flow in rat aortic endothelium but connexin37 and connexin40 are more uniformly distributed. *Circ. Res.* 83 (6), 636–643. doi:10.1161/01.res.83.6.636

Giannotta, M., Trani, M., and Dejana, E. (2013). VE-cadherin and endothelial adherens junctions: active guardians of vascular integrity. *Dev. Cell* 26 (5), 441–454. doi:10.1016/j.devcel.2013.08.020

Giantsos-Adams, K. M., Koo, A. J., Song, S., Sakai, J., Sankaran, J., Shin, J. H., et al. (2013). Heparan sulfate regrowth profiles under laminar shear flow following enzymatic degradation. *Cell Mol. Bioeng.* 6 (2), 160–174. doi:10.1007/s12195-013-0273-z

Gross, C. M., Aggarwal, S., Kumar, S., Tian, J., Kasa, A., Bogatcheva, N., et al. (2014). Sox18 preserves the pulmonary endothelial barrier under conditions of increased shear stress. *J. Cell Physiol.* 229 (11), 1802–1816. doi:10.1002/jcp.24633

Han, Y., He, M., Marin, T., Shen, H., Wang, W. T., Lee, T. Y., et al. (2021). Roles of KLF4 and AMPK in the inhibition of glycolysis by pulsatile shear stress in endothelial cells. *Proc. Natl. Acad. Sci. U. S. A.* 118 (21), e2103982118. doi:10.1073/pnas.2103982118

Harris, A. L. (2001). Emerging issues of connexin channels: biophysics fills the gap. *Q. Rev. Biophys.* 34 (3), 325–472. doi:10.1017/s0033583501003705

Heo, K. S., Fujiwara, K., and Abe, J. (2011). Disturbed-flow-mediated vascular reactive oxygen species induce endothelial dysfunction. *Circ. J.* 75 (12), 2722–2730. doi:10.1253/circj.cj-11-1124

Heo, K. S., Fujiwara, K., and Abe, J. (2014). Shear stress and atherosclerosis. *Mol. Cells* 37 (6), 435–440. doi:10.14348/molcells.2014.0078

Herrington, W., Lacey, B., Sherliker, P., Armitage, J., and Lewington, S. (2016). Epidemiology of atherosclerosis and the potential to reduce the global burden of atherothrombotic disease. *Circ. Res.* 118 (4), 535–546. doi:10.1161/CIRCRESAHA.115.307611

Hilbig, D., Sittig, D., Hoffmann, F., Rothemund, S., Warmt, E., Quaas, M., et al. (2018). Mechano-dependent phosphorylation of the PDZ-binding motif of CD97/ADGRE5 modulates cellular detachment. *Cell Rep.* 24 (8), 1986–1995. doi:10.1016/j.celrep.2018.07.071

Himburg, H. A., Grzybowski, D. M., Hazel, A. L., LaMack, J. A., Li, X. M., and Friedman, M. H. (2004). Spatial comparison between wall shear stress measures and porcine arterial endothelial permeability. *Am. J. Physiol. Heart Circ. Physiol.* 286 (5), H1916–H1922. doi:10.1152/ajpheart.00897.2003

Ho, R. X., Tahboub, R., Amraei, R., Meyer, R. D., Varongchayakul, N., Grinstaff, M., et al. (2019). The cell adhesion molecule IGPR-1 is activated by and regulates responses of endothelial cells to shear stress. *J. Biol. Chem.* 294 (37), 13671–13680. doi:10.1074/jbc.RA119.008548

Hofer, I., Schimp, C., Taha, M., Seebach, J., Aldirawi, M., Cao, J., et al. (2018). Advanced methods for the investigation of cell contact dynamics in endothelial cells using fluorescence-based live cell imaging. *J. Vasc. Res.* 55 (6), 350–364. doi:10.1159/000494933

Huang, R. T., Wu, D., Meliton, A., Oh, M. J., Krause, M., Lloyd, J. A., et al. (2017). Experimental lung injury reduces krüppel-like factor 2 to increase endothelial permeability via regulation of RAPGEF3-rac1 signaling. *Am. J. Respir. Crit. Care Med.* 195 (5), 639–651. doi:10.1164/rccm.201604-0668OC

Hur, S. S., del Álamo, J. C., Park, J. S., Li, Y. S., Nguyen, H. A., Teng, D., et al. (2012). Roles of cell confluency and fluid shear in 3-dimensional intracellular forces in endothelial cells. *Proc. Natl. Acad. Sci. U. S. A.* 109 (28), 11110–11115. doi:10.1073/pnas.1207326109

Hurtubise, J., McLellan, K., Durr, K., Onasanya, O., Nwabuko, D., and Ndisang, J. F. (2016). The different facets of dyslipidemia and hypertension in atherosclerosis. *Curr. Atheroscler. Rep.* 18 (12), 82. doi:10.1007/s11883-016-0632-z

Inai, T., Mancuso, M. R., McDonald, D. M., Kobayashi, J., Nakamura, K., and Shibata, Y. (2004). Shear stress-induced upregulation of connexin 43 expression in endothelial cells on upstream surfaces of rat cardiac valves. *Histochem Cell Biol.* 122 (5), 477–483. doi:10.1007/s00418-004-0717-6

Kang, H., Cancel, L. M., and Tarbell, J. M. (2014). Effect of shear stress on water and LDL transport through cultured endothelial cell monolayers. *Atherosclerosis* 233 (2), 682–690. doi:10.1016/j.atherosclerosis.2014.01.056

Koo, A., Dewey, C. F., Jr., and García-Cardeña, G. (2013). Hemodynamic shear stress characteristic of atherosclerosis-resistant regions promotes glycocalyx formation in cultured endothelial cells. *Am. J. Physiol. Cell Physiol.* 304 (2), C137–C146. doi:10.1152/ajpcell.00187.2012

Kwak, B. R., Bäck, M., Bochaton-Piallat, M. L., Caligiuri, G., Daemen, M. J., Davies, P. F., et al. (2014). Biomechanical factors in atherosclerosis: mechanisms and clinical implications. *Eur. Heart J.* 35 (43), 3013–3020d. doi:10.1093/eurheartj/ehu353

Kwak, B. R., Silacci, P., Stergiopulos, N., Hayoz, D., and Meda, P. (2005). Shear stress and cyclic circumferential stretch, but not pressure, alter connexin43 expression in endothelial cells. *Cell Commun. Adhes.* 12 (5-6), 261–270. doi:10.1080/15419060500514119

Lakshmikanthan, S., Sobczak, M., Li Calzi, S., Shaw, L., Grant, M. B., and Chrzanowska-Wodnicka, M. (2018). Rap1B promotes VEGF-induced endothelial permeability and is required for dynamic regulation of the endothelial barrier. *J. Cell Sci.* 131 (1), jcs207605. doi:10.1242/jcs.207605

Lampugnani, M. G., Dejana, E., and Giampietro, C. (2018). Vascular endothelial (VE)-Cadherin, endothelial adherens junctions, and vascular disease. *Spring Harb. Perspect. Biol.* 10 (10), a029322. doi:10.1101/cshperspect.a029322

Lee, D. Y., and Chiu, J. J. (2019). Atherosclerosis and flow: roles of epigenetic modulation in vascular endothelium. *J. Biomed. Sci.* 26 (1), 56. doi:10.1186/s12929-019-0551-8

Lertkiatmongkol, P., Liao, D., Mei, H., Hu, Y., and Newman, P. J. (2016). Endothelial functions of platelet/endothelial cell adhesion molecule-1 (CD31). *Curr. Opin. Hematol.* 23 (3), 253–259. doi:10.1097/MOH.0000000000000239

Li, M., Liu, X., Zhang, Y., Di, M., Wang, H., Wang, L., et al. (2016). Upregulation of Dickkopf1 by oscillatory shear stress accelerates atherogenesis. *J. Mol. Med. Berl.* 94 (4), 431–441. doi:10.1007/s00109-015-1369-9

Li, Y., Lui, K. O., and Zhou, B. (2018). Reassessing endothelial-to-mesenchymal transition in cardiovascular diseases. *Nat. Rev. Cardiol.* 15 (8), 445–456. doi:10.1038/s41569-018-0023-y

Libby, P., Bornfeldt, K. E., and Tall, A. R. (2016). Atherosclerosis: successes, surprises, and future challenges. *Circ. Res.* 118 (4), 531–534. doi:10.1161/CIRCRESAHA.116.308334

Mahmoud, M. M., Serbanovic-Canic, J., Feng, S., Souilhol, C., Xing, R., Hsiao, S., et al. (2017). Shear stress induces endothelial-to-mesenchymal transition via the transcription factor Snail. *Sci. Rep.* 7 (1), 3375. doi:10.1038/s41598-017-03532-z

Marchio, P., Guerra-Ojeda, S., Vila, J. M., Aldasoro, M., Victor, V. M., and Mauricio, M. D. (2019). Targeting early atherosclerosis: a focus on oxidative stress and inflammation. *Oxid. Med. Cell Longev.* 2019, 8563845. doi:10.1155/2019/8563845

Massou, S., Nunes Vicente, F., Wetzel, F., Mehidi, A., Strehle, D., Leduc, C., et al. (2020). Cell stretching is amplified by active actin remodelling to deform and recruit proteins in mechanosensitive structures. *Nat. Cell Biol.* 22 (8), 1011–1023. doi:10.1038/s41556-020-0548-2

Miao, H., Hu, Y. L., Shiu, Y. T., Yuan, S., Zhao, Y., Kaunas, R., et al. (2005). Effects of flow patterns on the localization and expression of VE-cadherin at vascular endothelial cell junctions: *in vivo* and *in vitro* investigations. *J. Vasc. Res.* 42 (1), 77–89. doi:10.1159/000083094

Mitra, R., O'Neil, G. L., Harding, I. C., Cheng, M. J., Mensah, S. A., and Ebong, E. E. (2017). Glycocalyx in atherosclerosis-relevant endothelium function and as a therapeutic target. *Curr. Atheroscler. Rep.* 19 (12), 63. doi:10.1007/s11883-017-0691-9

Molica, F., Meens, M. J., Morel, S., and Kwak, B. R. (2014). Mutations in cardiovascular connexin genes. *Biol. Cell* 106 (9), 269–293. doi:10.1111/boc.201400038

Monfoulet, L. E., Mercier, S., Bayle, D., Tamaian, R., Barber-Chamoux, N., Morand, C., et al. (2017). Curcumin modulates endothelial permeability and monocyte transendothelial migration by affecting endothelial cell dynamics. *Free Radic. Biol. Med.* 112, 109–120. doi:10.1016/j.freeradbiomed.2017.07.019

Mundi, S., Massaro, M., Scoditti, E., Carluccio, M. A., van Hinsbergh, V., Iruela-Arispe, M. L., et al. (2018). Endothelial permeability, LDL deposition, and cardiovascular risk factors-a review. *Cardiovasc Res.* 114 (1), 35–52. doi:10.1093/cvr/cvx226

Nakashima, Y., Wight, T. N., and Sueishi, K. (2008). Early atherosclerosis in humans: role of diffuse intimal thickening and extracellular matrix proteoglycans. *Cardiovasc Res.* 79 (1), 14–23. doi:10.1093/cvr/cvn099

Nielsen, M. S., Axelsen, L. N., Sorgen, P. L., Verma, V., Delmar, M., Holstein-Rathlou, N. H., et al. (2012). Gap junctions. *Compr. Physiol.* 2 (3), 1981–2035. doi:10.1002/cphy.c110051

Noria, S., Cowan, D. B., Gotlieb, A. I., and Langille, B. L. (1999). Transient and steady-state effects of shear stress on endothelial cell adherens junctions. *Circ. Res.* 85 (6), 504–514. doi:10.1161/01.res.85.6.504

Okano, M., and Yoshida, Y. (1993). Influence of shear stress on endothelial cell shapes and junction complexes at flow dividers of aortic bifurcations in cholesterol-fed rabbits. *Front. Med. Biol. Eng.* 5 (2), 95–120.

Otte, L. A., Bell, K. S., Loufrani, L., Yeh, J. C., Melchior, B., Dao, D. N., et al. (2009). Rapid changes in shear stress induce dissociation of a G alpha(q/11)-platelet endothelial cell adhesion molecule-1 complex. *J. Physiol.* 587 (Pt 10), 2365–2373. doi:10.1113/jphysiol.2009.172643

Peng, Z., Shu, B., Zhang, Y., and Wang, M. (2019). Endothelial response to pathophysiological stress. *Arterioscler. Thromb. Vasc. Biol.* 39 (11), e233–e243. doi:10.1161/ATVBAHA.119.312580

Peruzzi, G., Sinibaldi, G., Silvani, G., Ruocco, G., and Casciola, C. M. (2018). Perspectives on cavitation enhanced endothelial layer permeability. *Colloids Surf. B Biointerfaces* 168, 83–93. doi:10.1016/j.colsurfb.2018.02.027

Ramadan, R., Baatout, S., Aerts, A., and Leybaert, L. (2012). The role of connexin proteins and their channels in radiation-induced atherosclerosis. *Cell Mol. Life Sci.* 78 (7), 3087–3103. doi:10.1007/s00018-020-03716-3

Rami, L., Auguste, P., Thebaud, N. B., Bareille, R., Daculsi, R., Ripoche, J., et al. (2013). IQ domain GTPase-activating protein 1 is involved in shear stress-induced progenitor-derived endothelial cell alignment. *PloS one* 8 (11), e79919. doi:10.1371/journal.pone.0079919

Reitsma, S., Slaaf, D. W., Vink, H., van Zandvoort, M. A., and oude Egbrink, M. G. (2007). The endothelial glycocalyx: composition, functions, and visualization. *Pflugers Arch.* 454 (3), 345–359. doi:10.1007/s00424-007-0212-8

Rudini, N., and Dejana, E. (2008). Adherens junctions. *Curr. Biol.* 18 (23), R1080–R1082. doi:10.1016/j.cub.2008.09.018

Sabine, A., Bovay, E., Demir, C. S., Kimura, W., Jaquet, M., Agalarov, Y., et al. (2015). FOXC2 and fluid shear stress stabilize postnatal lymphatic vasculature. *J. Clin. Invest.* 125 (10), 3861–3877. doi:10.1172/JCI80454

Sanz, J., and Fayad, Z. A. (2008). Imaging of atherosclerotic cardiovascular disease. *Nature* 451 (7181), 953–957. doi:10.1038/nature06803

Sedding, D. G., Boyle, E. C., Demandt, J., Sluimer, J. C., Dutzmann, J., Haverich, A., et al. (2018). Vasa vasorum angiogenesis: key player in the initiation and progression of atherosclerosis and potential target for the treatment of cardiovascular disease. *Front. Immunol.* 9, 706. doi:10.3389/fimmu.2018.00706

Seebach, J., Dieterich, P., Luo, F., Schillers, H., Vestweber, D., Oberleithner, H., et al. (2000). Endothelial barrier function under laminar fluid shear stress. *Lab. Invest.* 80 (12), 1819–1831. doi:10.1038/labinvest.3780193

Shah, N., and Katira, B. H. (2023). Role of cardiopulmonary interactions in development of ventilator-induced lung injury-Experimental evidence and clinical Implications. *Front. Physiol.* 14, 1228476. doi:10.3389/fphys.2023.1228476

Shen, L., Weber, C. R., Raleigh, D. R., Yu, D., and Turner, J. R. (2011). Tight junction pore and leak pathways: a dynamic duo. *Annu. Rev. Physiol.* 73, 283–309. doi:10.1146/annurev-physiol-012110-142150

Slee, J. B., and Lowe-Krentz, L. J. (2013). Actin realignment and cofilin regulation are essential for barrier integrity during shear stress. *J. Cell Biochem.* 114 (4), 782–795. doi:10.1002/jcb.24416

Souilhol, C., Serbanovic-Canic, J., Fragiadaki, M., Chico, T. J., Ridger, V., Roddie, H., et al. (2020). Endothelial responses to shear stress in atherosclerosis: a novel role for developmental genes. *Nat. Rev. Cardiol.* 17 (1), 52–63. doi:10.1038/s41569-019-0239-5

Spindel, O. N., Burke, R. M., Yan, C., and Berk, B. C. (2014). Thioredoxin-interacting protein is a biomechanical regulator of Src activity: key role in endothelial cell stress fiber formation. *Circ. Res.* 114 (7), 1125–1132. doi:10.1161/CIRCRESAHA.114.301315

Tarbell, J. M., and Cancel, L. M. (2016). The glycocalyx and its significance in human medicine. *J. Intern Med.* 280 (1), 97–113. doi:10.1111/joim.12465

Ting, L. H., Jahn, J. R., Jung, J. I., Shuman, B. R., Feghhi, S., Han, S. J., et al. (2012). Flow mechanotransduction regulates traction forces, intercellular forces, and adherens junctions. *Am. J. Physiol. Heart Circ. Physiol.* 302 (1), H2220–H2229. doi:10.1152/ajpheart.00975.2011

Tzima, E., Irani-Tehrani, M., Kiosses, W. B., Dejana, E., Schultz, D. A., Engelhardt, B., et al. (2005). A mechanosensory complex that mediates the endothelial cell response to fluid shear stress. *Nature* 437 (7057), 426–431. doi:10.1038/nature03952

Ukropec, J. A., Hollinger, M. K., and Woolkalis, M. J. (2002). Regulation of VE-cadherin linkage to the cytoskeleton in endothelial cells exposed to fluid shear stress. *Exp. Cell Res.* 273 (2), 240–247. doi:10.1006/excr.2001.5453

Verma, D., Ye, N., Meng, F., Sachs, F., Rahimzadeh, J., and Hua, S. Z. (2012). Interplay between cytoskeletal stresses and cell adaptation under chronic flow. *PloS one* 7 (9), e44167. doi:10.1371/journal.pone.0044167

Walsh, T. G., Murphy, R. P., Fitzpatrick, P., Rochfort, K. D., Guinan, A. F., Murphy, A., et al. (2011). Stabilization of brain microvascular endothelial barrier function by shear stress involves VE-cadherin signaling leading to modulation of pTyr-occludin levels. *J. Cell Physiol.* 226 (11), 3053–3063. doi:10.1002/jcp.22655

Wang, G., Kostidis, S., Tiemeier, G. L., Sol, W., de Vries, M. R., Giera, M., et al. (2020). Shear stress regulation of endothelial glycocalyx structure is determined by glucobiosynthesis. *Arterioscler. Thromb. Vasc. Biol.* 40 (2), 350–364. doi:10.1161/ATVBAHA.119.313399

Wang, X., Fang, X., Zhou, J., Chen, Z., Zhao, B., Xiao, L., et al. (2013). Shear stress activation of nuclear receptor PXR in endothelial detoxification. *Proc. Natl. Acad. Sci. U. S. A.* 110 (32), 13174–13179. doi:10.1073/pnas.1312065110

Wettschureck, N., Strilic, B., and Offermanns, S. (2019). Passing the vascular barrier: endothelial signaling processes controlling extravasation. *Physiol. Rev.* 99 (3), 1467–1525. doi:10.1152/physrev.00037.2018

Wu, C. C., Li, Y. S., Haga, J. H., Kaunas, R., Chiu, J. J., Su, F. C., et al. (2007). Directional shear flow and Rho activation prevent the endothelial cell apoptosis induced by micropatterned anisotropic geometry. *Proc. Natl. Acad. Sci. U. S. A.* 104 (4), 1254–1259. doi:10.1073/pnas.0609806104

Wu, D., Harrison, D. L., Szasz, T., Yeh, C. F., Shentu, T. P., Meliton, A., et al. (2021). Single-cell metabolic imaging reveals a SLC2A3-dependent glycolytic burst in motile endothelial cells. *Nat. Metab.* 3 (5), 714–727. doi:10.1038/s42255-021-00390-y

Wu, D., Huang, R. T., Hamanaka, R. B., Krause, M., Oh, M. J., Kuo, C. H., et al. (2017). HIF-1α is required for disturbed flow-induced metabolic reprogramming in human and porcine vascular endothelium. *eLife* 6, e25217. doi:10.7554/eLife.25217

Xie, X., Wang, F., Zhu, L., Yang, H., Pan, D., Liu, Y., et al. (2020). Low shear stress induces endothelial cell apoptosis and monocyte adhesion by upregulating PECAM-1 expression. *Mol. Med. Rep.* 21 (6), 2580–2588. doi:10.3892/mmr.2020.11060

Xu, S., Li, X., LaPenna, K. B., Yokota, S. D., Huke, S., and He, P. (2017). New insights into shear stress-induced endothelial signalling and barrier function: cell-free fluid versus blood flow. *Cardiovasc Res.* 113 (5), 508–518. doi:10.1093/cvr/cvx021

Yamashiro, Y., and Yanagisawa, H. (2020). The molecular mechanism of mechanotransduction in vascular homeostasis and disease. *Clin. Sci. (Lond).* 134 (17), 2399–2418. doi:10.1042/CS20190488

Yao, Y., Rabodzey, A., and Dewey, C. F., Jr (2007). Glycocalyx modulates the motility and proliferative response of vascular endothelium to fluid shear stress. *Am. J. Physiol. Heart Circ. Physiol.* 293 (2), H1023–H1030. doi:10.1152/ajpheart.00162.2007

Yurtseven, E., Ural, D., Baysal, K., and Tokgözoğlu, L. (2020). An update on the role of PCSK9 in atherosclerosis. *J. Atheroscler. Thromb.* 27 (9), 909–918. doi:10.5551/jat.55400

Zhang, J., Zu, Y., Dhanasekara, C. S., Li, J., Wu, D., Fan, Z., et al. (2017). Detection and treatment of atherosclerosis using nanoparticles. *Wiley Interdiscip. Rev. Nanomed Nanobiotechnol.* 9(1) doi:10.1002/wnan.1412

Zhang, X., Sun, D., Song, J. W., Zullo, J., Lipphardt, M., Coneh-Gould, L., et al. (2018). Endothelial cell dysfunction and glycocalyx - a vicious circle. *Matrix Biol.* 71-72, 7–431. doi:10.1016/j.matbio.2018.01.026

Zhou, J., Li, Y. S., and Chien, S. (2014). Shear stress-initiated signaling and its regulation of endothelial function. *Arterioscler. Thromb. Vasc. Biol.* 34 (10), 2191–2198. doi:10.1161/ATVBAHA.114.303422

Zihni, C., Mills, C., Matter, K., and Balda, M. S. (2016). Tight junctions: from simple barriers to multifunctional molecular gates. *Nat. Rev. Mol. Cell Biol.* 17 (9), 564–580. doi:10.1038/nrm.2016.80

frontiers | Frontiers in Physiology

TYPE Original Research
PUBLISHED 13 November 2024
DOI 10.3389/fphys.2024.1487775

OPEN ACCESS

EDITED BY
Luis A. Martinez-Lemus,
University of Missouri, United States

REVIEWED BY
William F. Jackson,
Michigan State University, United States
Alexander Widiapradja,
West Virginia University, United States

*CORRESPONDENCE
M. Teresa Pérez-Garcia,
tperez@uva.es

‡These authors share senior authorship

RECEIVED 28 August 2024
ACCEPTED 28 October 2024
PUBLISHED 13 November 2024

CITATION
Peraza DA, Benito-Salamanca L, Moreno-Estar S, Alonso E, López-López JR, Pérez-Garcia MT and Cidad P (2024) A sex-dependent role of Kv1.3 channels from macrophages in metabolic syndrome. *Front. Physiol.* 15:1487775. doi: 10.3389/fphys.2024.1487775

A sex-dependent role of Kv1.3 channels from macrophages in metabolic syndrome

Diego A. Peraza [1,2], Lucía Benito-Salamanca[1,2], Sara Moreno-Estar[1,2], Esperanza Alonso[1,2], José R. López-López[1,2‡], M. Teresa Pérez-Garcia[1,2*‡] and Pilar Cidad[1,2‡]

[1]Departamento de Bioquímica y Biología Molecular y Fisiología, Universidad de Valladolid, Valladolid, Spain, [2]Unidad de Excelencia, Instituto de Biología y Genética Molecular (IBGM), Universidad de Valladolid y Consejo Superior de Investigaciones Científicas (CSIC), Valladolid, Spain

Introduction: Coronary artery disease (CAD) is the foremost single cause of mortality and disability globally. Patients with type 2 diabetes (T2DM) have a higher incidence of CAD, and poorer prognosis. The low-grade inflammation associated to T2DM contributes to increased morbidity and worst outcomes after revascularization. Inflammatory signaling in the vasculature supports endothelial dysfunction, leukocyte infiltration, and macrophage activation to a metabolic disease (MMe) specific phenotype, which could contribute to the metabolic disorders and ascular damage in T2DM. We have previously found that K_v1.3 blockers inhibit the development of intimal hyperplasia, thereby preventing restenosis. This inhibition was enhanced in a mouse model of T2DM, where systemic K_v1.3 blockers administration also improve metabolic dysfunction by acting on unidentified cellular targets other than vascular smooth muscle. Here we characterize the MMe phenotype in our T2DM model with a focus on macrophage K_v1.3 channels, to explore their contribution to vascular disease and their potential role as targets to ameliorate T2DM vascular risk.

Methods and Results: Male and female BPH mice fed on high-fat diet (HFD) develop metabolic syndrome (MetS) and T2DM. mRNA levels of several K^+ channels (K_v1.3, K_{Ca}3.1, K_{ir}2.1) and macrophage markers (TNFα, NOS2, CD36) were analyzed. The MMe phenotype associated with increased CD36 expression. Channel-specific fingerprinting highlights a gender-specific increase of K_V1.3 mRNA fold change in LPS stimulated macrophages from HFD compared to standard diet (SD). K_V1.3 functional expression was also significantly increased after LPS stimulation in female HFD macrophages compared to SD. Functional studies showed that macrophage's K_V1.3 channels of BPH female mice did not contribute to phagocytosis or metabolic profile but were relevant in cell migration rate.

Conclusion: Altogether, our data suggest that by inhibiting macrophage infiltration, Kv1.3 blockers could contribute to disrupt the vicious cycle of inflammation and insulin resistance, offering a novel approach to prevent MetS, T2DM and its associated cardiovascular complications in females.

KEYWORDS

bone marrow-derived macrophages, Kv1.3 channels, metabolic syndrome, cell migration, electrophysiology, macrophage phenotype, sex-dependent differences

1 Introduction

Type 2 diabetes mellitus (T2DM) significantly increases the risk of cardiovascular diseases (CVD), including coronary artery disease and restenosis following angioplasty or stenting. A key factor in the development of atherosclerotic and restenotic lesions is the abnormal proliferation and migration of vascular smooth muscle cells (VSMCs). Consequently, pharmaceutical interventions targeting VSMCs growth and migration represent a promising approach to treating T2DM-associated CVD.

Recent research has identified Kv1.3 channels in VSMCs as novel targets for treating undesirable vascular remodeling (Cidad et al., 2010; Cheong et al., 2011). Selective Kv1.3 blockade inhibits VSMCs remodeling and prevents restenosis in both animal models (Cidad et al., 2014; Bobi et al., 2020) and human vessels (Arévalo-Martínez et al., 2019). Notably, Kv1.3 inhibitors demonstrate increased efficacy in preventing restenosis in human T2DM vessels and in a mouse model of metabolic syndrome and T2DM (Arevalo-Martinez et al., 2021).

The benefits of Kv1.3 inhibition extend beyond vascular remodeling. In T2DM mice, Kv1.3 blockade reduces weight gain and associated inflammation, improves glucose tolerance, and eliminates insulin resistance (Upadhyay et al., 2013; Arevalo-Martinez et al., 2021). These beneficial effects are thought to result from increased energy expenditure and reduced obesity-induced inflammation in abdominal adipose tissue (Upadhyay et al., 2013). While Kv1.3 channels are known to play a crucial role in cytokine production and cholesterol accumulation in macrophages (Vicente et al., 2003; Yang et al., 2013), their specific contribution to macrophage function in T2DM remains unexplored.

Metabolic diseases like T2DM and obesity are characterized by low-grade chronic inflammation, leading to various complications (Hotamisligil, 2006). This inflammatory state is associated with the recruitment of pro-inflammatory monocytes and macrophages to various organs, including adipose tissue, liver, and blood vessel walls. The infiltration of macrophages into adipose tissue is a key initiating event in obesity-induced inflammation and insulin resistance. In conditions of over-nutrition, adipocytes secrete chemokines that attract monocytes to adipose tissue, where they differentiate into adipose tissue macrophages (ATMs). These pro-inflammatory ATMs, in turn, secrete additional chemokines, creating a self-perpetuating cycle of inflammation (Olefsky and Glass, 2010; Osborn and Olefsky, 2012). This feed-forward process significantly contributes to the progression of metabolic disorders and associated cardiovascular complications, although the functional involvement of macrophages in systemic metabolism is unclear (Hotamisligil, 2006).

Early studies attempting to classify macrophage inflammatory polarization as either inflammatory (M1) or anti-inflammatory (M2) oversimplified their complex and plastic biology. However, it is evident that macrophages in lean and obese tissues differ not only in number but also in functional properties. A plasma-membrane proteomic approach in both human and murine subjects, demonstrated that classical M1 inflammatory markers did not accurately define ATMs in obesity (Kratz et al., 2014), and a "metabolically-activated" macrophage (MMe) phenotype has been proposed to better characterize macrophages in high glucose/high fat environments. These pro-inflammatory ATMs exhibit a unique metabolic signature in obesity that promotes inflammatory cytokine release (Boutens et al., 2018). Similarly, fundamental differences in the regulation of genes linked to specific inflammatory triggers have been observed in bone marrow-derived macrophages (BMDM) (Robblee et al., 2016). Saturated fatty acid treatment of BMDM regulated the inflammasome, but the identity and expression time course of inflammatory mediators were distinct from those induced by the classical M1 pro-inflammatory stimulus, lipopolysaccharide (LPS), illustrating the complexity of macrophage activation in metabolic disorders. These observations highlight the need for a more detailed understanding of macrophage phenotypes in obesity and related metabolic conditions, beyond the simplistic M1/M2 dichotomy, which could potentially offer new targets for therapeutic interventions in obesity-related inflammation and its associated complications.

Here we characterized the phenotype of macrophages from a mouse model of MetS and T2DM (Arevalo-Martinez et al., 2021), using both BMDM (*ex vivo* differentiated from stem cells) and fresh peritoneal macrophages (*in vivo* differentiated). We explored the association between HFD-induced changes in the macrophages phenotype and changes in the functional expression of Kv1.3 channels, and we analyzed the potential impact of Kv1.3 changes in macrophage-integrated functions such as phagocytosis, migration and metabolism. Male and female mice were studied separately, as sex dependent differences in the low-grade chronic inflammation associated to metabolic diseases have been demonstrated before, and in some cases independently of steroid hormones (Gal-Oz et al., 2019; Li et al., 2023).

Functional expression of Kv1.3 channels was significantly upregulated in BMDM from HFD females (but not in males) upon LPS treatment. We did not find changes in oxygen consumption rate in BMDM from HFD females. In contrast, they displayed increased migration rate and phagocytic activity, but only migration rate was dependent on Kv1.3 expression and activity. As migration of pro-inflammatory macrophages into adipose tissue represents the initial step in obesity-induced inflammation and insulin resistance, our data suggest that inhibiting macrophage chemotaxis with Kv1.3 blockers could provide therapeutic benefits in MetS females without inhibiting other innate immune functions.

2 Material and methods

2.1 Animal model

Colonies of BPH/2J (blood pressure high) and BPN/3J mice (blood pressure normal, both from Jackson Laboratories, Bar Harbor, ME, United States) were housed in the animal facility of the School of Medicine of Valladolid, maintained by inbreeding crossing under temperature-controlled conditions (21°C) and with unlimited access to water and food. All procedures were approved by the Animal Care and Use Committee of the University of Valladolid (Project 505649), in accordance with the European Community guides (Directive 2010/63/UE).

To generate a mouse model of metabolic syndrome and type-2 diabetes mellitus (MetS/T2DM), 6 weeks old BPH mice were fed with a standard rodent chow diet (SD; Research Diets, #D12450J, 10% fat) or high-fat diet (HFD; Research Diets, #D12492,

60% fat) for 12 weeks. Weight was determined weekly, fasting blood glucose, cholesterol, insulin plasma level and blood pressure were obtained every 4 weeks and intraperitoneal glucose tolerance test (ipGTT), and intraperitoneal insulin tolerance test (ipITT) were determined every 6 weeks, as described elsewhere (Arevalo-Martinez et al., 2021).

2.2 Cell cultures

Animals were euthanized with isofluorane overdose (5%) in an anesthetic-gases chamber. BMDM were differentiated from mononuclear phagocytic precursor cells obtained after flushing bone marrow of femurs and tibiae of control (SD) or MetS/T2DM (HFD) BPH mice with RPMI. Precursor cells were propagated in suspension by culturing in RMPI supplemented with 10% FBS, 1% PSF, 1% L-glutamine and 10% L-929 supernatant in tissue-culture dishes. The precursor cells became adherent within 7–9 days of culture (Meana et al., 2014). Peritoneal macrophages (PM) were also obtained and cultured as previously described (Olivencia et al., 2021). PM were kept in culture overnight (16 h) in control media (control, resting macrophages) or in the presence of LPS (100 ng/mL; LPS-activated macrophages) before electrophysiological recordings.

2.3 RNA expression

Total RNA was extracted from BMDM culture with TRIzol® (Ambion). mRNA expression of $K_V1.3$, $K_{Ca}3.1$, $K_{ir}2.1$, $P2X_7$, TNF-α, NOS2 and CD36 (Table 1) was determined with qPCR with Taqman® and SYBR Green assays (Applied Biosystems) using RPL18 (ribosomal protein L18) as housekeeping (Arevalo-Martinez et al., 2019). qPCR was performed in a Rotor-Gene 3,000 instrument, and the relative quantification method ($2^{-\Delta\Delta CT}$) was used to express mRNA levels (Livak and Schmittgen, 2001; Cidad et al., 2010). The information regarding commercial assays and/or primers sequences is listed in Supplementary Table SI.

2.4 Electrophysiological methods

Ionic currents were recorded at room temperature using whole-cell configuration of the patch clamp technique as previously described (Lordén et al., 2017; Cidad et al., 2020; Olivencia et al., 2021). BMDM and PM were plated on the bottom of a small recording chamber (0.2 mL) on the stage of an inverted microscope and perfused by gravity. The composition of the bath solution was (in mM): 141 NaCl, 4.7 KCl, 1.2 $MgCl_2$, 1.8 $CaCl_2$, 10 glucose, and 10 HEPES, pH 7.4 with NaOH. Recording pipettes were pulled to obtain resistances ranging from 2 to 4 MΩ when filled with an internal solution containing (in mM): 125 KCl, 4 $MgCl_2$, 10 HEPES, 10 EGTA, 5 MgATP, pH 7.2 with KOH.

Total current amplitude was explored with either 500 ms voltage ramps from −140 to +60 mV every 5 s or current/voltage (I/V) curves with 200 ms pulses from −80 to +60 mV in 10 mV steps. C-type inactivation was explored by analyzing use-dependent block, using trains of pulses of 250 ms duration from −80 to +40 mV at a frequency of 2 Hz. Pharmacological characterization of the currents was carried out by recording ramps after perfusing the cells with bath solutions containing the Kv1.3 blocker PAP-1 (100 nM, Sigma #P6124), the $K_{Ca}3.1$blocker TRAM-34 (100 nM; Sigma # T-6700) the nonselective K channel blocker TEA (5 mM, Sigma, # 177806), or a solution containing 100 μM Ba_2Cl to block inward rectifier K^+ currents (Miguel-Velado et al., 2005; Cidad et al., 2010; Tajada et al., 2012). Purinergic currents were obtained in continuous recording from a holding potential of 0 mV, by perfusing macrophages with an external solution containing 2 mM ATP (Sigma # A-2383) or the specific $P2X_7$ activator-BzATP (700 μM; Alomone #: A-385).

2.5 Phagocytic activity

Phagocytosis was assessed using zymosan A fluorescent particles and flow cytometry. Briefly, BMDM were detached with 5 mM EDTA in HBSS for 30 min at 37°C in a humidified 5% $C0^2$ incubator and 2.5×10^5 cells/condition were resuspended in PBS with the corresponding treatments. LPS (100 ng/mL) and PAP-1 (200 nM) were added 18 h and 30 min before the addition of zymosan respectively. Alexa Fluor 594 zymosan A (Molecular probes) particles were added to the cell suspension at a ratio of 1:5 (particles:cells). The mixture was incubated at 37°C for 15 min in a humidified 5% $C0_2$ incubator to allow phagocytosis to occur. Following incubation, cells were washed twice with cold PBS to remove non-phagocytosed particles and fixed using 4% paraformaldehyde for 10 min. Cells were kept at 4°C before and after the 15 min incubations to avoid unwanted phagocytosis. Samples were then analyzed using an Aurora flow cytometer (Cytek Biosciences). The percentage of Alexa Flour-positive cells was determined using Kaluza Analysis 2.1 software (Beckman Coulter). Negative controls (cells without zymosan) were included in each experiment.

2.6 Seahorse Cell Mito Stress Test

The oxygen consumption rate (OCR) was measured in real-time using a Seahorse XF24 Analyzer (Agilent, California, CA, United States) with Seahorse XF Cell Mito Stress Test Kit (Agilent, cat#: 103015-100), following manufacturer's instructions, using the respiratory chain inhibitors oligomycin (10 μM), FCCP (25 μM), rotenone (10 μM) and antimycin A, (25 μM). The seahorse analyzer was calibrated with a calibrating Seahorse XF solution (Agilent, 102342-100).

Briefly, BMDM were seeded in 24-well Seahorse assay plates at a concentration of 4×10^4 cells/well and cultured overnight with control media or media with 100 ng/mL LPS 100 nM PAP-1 was also present in some experimental groups of control or LPS-treated cells overnight. Next day, macrophages were washed, and the medium was replaced with Seahorse XF RPMI (Agilent, cat#: 103576-100) supplemented with 10 mM glucose (Agilent, cat#: 103577-100), 1 mM pyruvate (Agilent, cat#: 103578-100) and 2 mM glutamine (Agilent, cat#: 103579-100). Hoechst (Invitrogen, H3570) was used to evaluate cell viability and normalize readings from the Seahorse XF Analyzer.

10.3389/fphys.2024.1487775

TABLE 1 mRNA expression levels of several phenotype markers (upper rows) and ion channels (lower rows) were determined with qPCR in BMDM from male and female mice subjected to SD or HFD. mRNA levels are expressed as normalized abundance ($2^{-\Delta Ct}$) using Rpl18 as the housekeeping gene. Statistical comparisons were carried out using two-way ANOVA followed by Tukey's test in the case of normal distributions and equal variances; alternatively Kruskal-Wallis analysis followed by Dunn's test was used. Red numbers indicate p-values of significant differences compared to SD, and blue numbers indicated the p-value for the significant differences between males and females. Values are mean ± SEM of 8–12 triplicate determinations, obtained from two batches of SD and HFD mice in each group (male and female). A graphical representation of these data is available in the supplemental file.

Gen	Sex	SD-control	HFD-control	SD-LPS fold change	HFD-LPS fold change
Tnf-α	Female	1.28 ± 0.16	1.31 ± 0.11	6.31 ± 1,99	5.01 ± 1.89
	Male	0.42 ± 0.07	0.38 ± 0.04 (0.0001)	1.91 ± 029	2.71 ± 0.33
Nos2	Female	2.91E-03 ± 0.97E-03	1.56E-03 ± 0.37E-03	113 ± 30,82	153.9 ± 45.8
	Male	0.335E-03 ± 0.88E-03	0.34E-03 ± 0.076E-03	99.54 ± 17.03	107.92 ± 30.08
Cd36	Female	37.53 ± 4.97	53.48 ± 4.36 (0.011)	0,25 ± 0,03	0.24 ± 0.05
	Male	22.71 ± 3.07	18.96 ± 3.08 (0.000)	0.25 ± 0.061	0.28 ± 0.05
Gen		SD-control	HFD-control	SD-LPS fold change	HFD-LPS fold change
Kcna3	Female	2.19E-03 ± 0.22E-03	1.43E-03 ± 0.15E-03	8,04 ± 1,41	20,18 ± 4,48 (0.025)
	Male	1.88E-03 ± 0.17E-03	1.86E-03 ± 0.27E-03	2.23 ± 0.44	3.11 ± 0.48 (0.000)
Kcnn4	Female	1.52 ± 0.15	1.12 ± 0.13	0.62 ± 0.13	0.59 ± 0.07
	Male	1.15 ± 0.18	1.05 ± 0.07	0.36 ± 0.045	0.30 ± 0.038 (0.03)
Kcnj2	Female	25.06E-03 ± 1.9E-03	55.9E-0.3 ± 6.3E-03 (0.000)	0.4 ± 0.12	0.19 ± 0.02 (0.02)
	Male	30.35E-03 ± 0.19E-03	60.59E-03 ± 4.8E-03 (0.000)	0.13 ± 0.037 (0.003)	0.06 ± 0.011 (0.03)
P2rx7	Female	0.297 ± 0,033	0.299 ± 0,024	1.05 ± 0,11	1.07 ± 0,16
	Male	0.170 ± 0.012	0.194 ± 0.02	0.94 ± 0.20	0.92 ± 0.20

2.7 Migration assays

Scratch migration assay was carried out in confluent BMDM cultures plated in 24 well plates. BMDM were incubated for 24 h in serum-free media, and LPS-stimulated macrophages were incubated the last 16 h with 100 ng/mL LPS. Next day, after creating a wound in the macrophage monolayer with a 10 µL tip, the medium was refreshed and 100 nM PAP-1 was added to some wells. Images of the same areas were taken at different time points (from 0 to 12 h) and ImageJ (Fiji) software was used to calculate the fraction of free area (normalized area) as A_X/A_0, where A_0 is the area at t = 0 and A_X is the area at the selected time point. The area under the curve (AUC) in each condition was calculated and used for statistical comparisons among conditions.

2.8 Statistical analysis

Statistical analysis was carried out using Origin 2023b and Microsoft Excel software. The combined data were presented as mean values ±standard error of the mean (SEM) derived from multiple experiments. P-values<0.05 were considered significantly different. For comparisons between two groups with normal distribution, Student's t-test, for paired or unpaired data as required, was used to determined p-values. For comparisons among several groups, one-way, two-way or three-way ANOVA followed by Tukey's test was employed in the case of normal distributions and equal variances; alternatively Kruskal-Wallis analysis followed by Dunn's test was used. Shapiro-Wilk test and Levene´s or Bartlett's test were used to test normality and homogeneity of variances respectively.

3 Results

3.1 Characterization of the MetS/T2DM mouse model in male and female

To develop a MetS/T2DM model, 6 weeks old BPH male or female mice were fed with SD or HFD for 12 weeks. BPH mice are hypertensive as compared to their controls BPN (Mean BP values in male were BPN = 70.39 ± 3.8 mmHg and BPH = 101.19 ± 1.3 mmHg and in female BPN = 75.16 ± 1.9 mmHg and BPH = 95.38 ± 2.1 mmHg), and HFD did not induce significant changes in BP (mean BP in HFD male = 101.01 ± 2.9 mmHg and in HFD female = 97.67 ± 3.8 mmHg). However, mice fed with HFD exhibited significant weight gain (Figure 1A), and developed

10.3389/fphys.2024.1487775

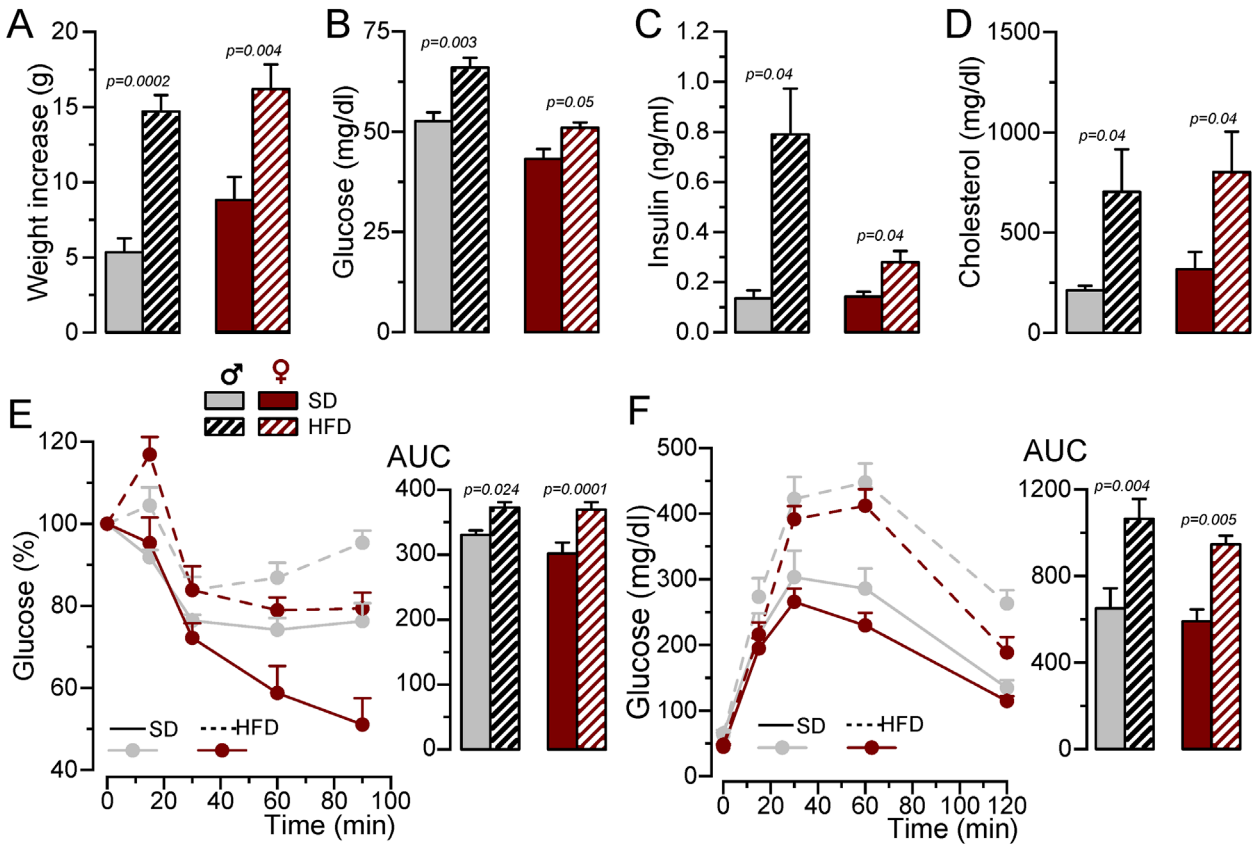

FIGURE 1
Generation of a MetS/T2DM mouse model. **(A)**. Average weight gain of BPH/SD and BPH/HFD male (grey) and female (red) mice. Mean ± SEM data from 8 to 12 mice per group, Kruskal-Wallis analysis followed by Dunn´s test and Student's t-test, respectively, were used to estimate significance between SD and HFD. **(B)**. Fasting blood glucose levels after 12 weeks in SD or HFD; n = 8-12 animals in each group; Kruskal-Wallis analysis followed by Dunn´s test (for male data) and and Student's t-test (for female). **(C)**. Basal insulin blood levels determined with an ELISA assay, n = 4-5 animals per group Kruskal-Wallis analysis followed by Dunn´s test. **(D)**. Blood cholesterol levels determined by spectrophotometry at the end of the 12-week treatment with SD or HFD. Student's t-test to estimate mean differences, n = 5-11 per group. **(E)**. IpGTT after 12 weeks of SD or HFD, male BPH/SD (n = 9), male BPH/HFD (n = 11, female BPH/SD (n = 8) and female BPH/HFD (n = 12), both the time course of blood glucose level after glucose overload in fasting animals and the area under the curve (AUC) are represented, p-values are from Student's t-test. **(F)**. IpITT after 12 weeks of HFD obtained from the same animals as in **(E)**. The plots show the time course of changes in blood glucose (100% = glucose at t = 0) after insulin load, and the area under the curve (AUC), p-values are from Student's t-test.

an increase in fasting glucose, basal insulin levels and plasma cholesterol (Figures 1B–D), together with glucose intolerance and insulin resistance (Figures 1E, F).

3.2 BMDM phenotype in MetS/T2DM model in male and female

Next, we explored the phenotypic changes in BMDM obtained from our HFD mice. mRNA expression profile of markers of pro-inflammatory macrophages (TNF-α, NOS2) or MMe metabolically-activated macrophages (CD36; Kratz et al., 2014) were determined in male and female BMDM both at rest and after LPS treatment (Supplementary Table SI; Supplementary Figure SI). While TNFα and NOS2 increased in pro-inflammatory macrophages, LPS treatment decreased CD36. No significant sex-dependent differences in these markers could be observed in control (SD) conditions, but upon HFD levels of TNFα and CD36 were significantly higher in female compared to male. However, the only diet-induced change in these markers was the upregulation of CD36 in control BMDM in HFD females (Figure 2A). The upregulation of CD36 in these conditions was confirmed at the protein level using flow cytometry (Supplementary Figure SII)

Many functional ion channels have been described in macrophages, and some of them can be regarded as potential therapeutic targets in several immune disease, as they have been shown to contribute to macrophage polarization towards pro-inflammatory or anti-inflammatory phenotype also referred as M1 or M2 respectively. The expression levels of mRNA encoding for some previously described K^+ channels (which can also serve as phenotypic markers), were determined in BMDM. LPS treatment led to upregulation of Kv1.3 mRNA (Kcna3, Figure 2B) and concomitant downregulation of Kir2.1 mRNA [Kcnj2 (Vicente et al., 2003; Chen et al., 2022), Supplementary Table SI]. We also found a LPS-induced downregulation of $K_{Ca}3.1$ (Kcnn4), whose role in macrophage polarization is more controversial (Xu et al., 2017).

10.3389/fphys.2024.1487775

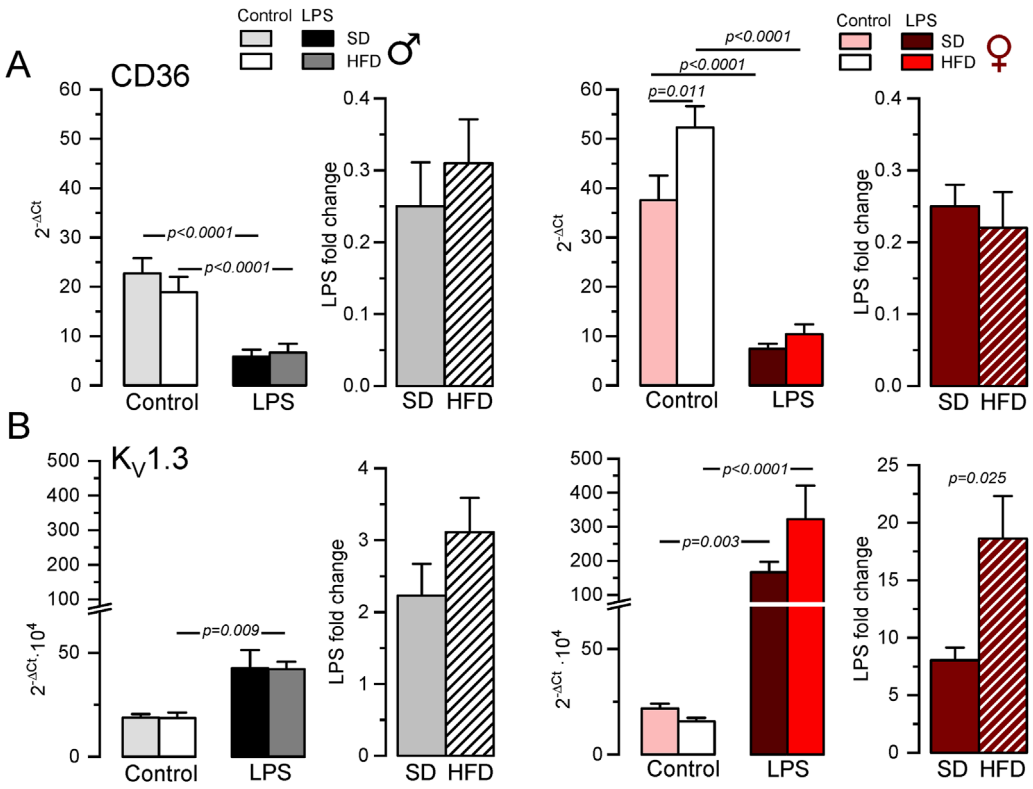

FIGURE 2
Gene expression changes in BMDM from the MetS/T2DM mice model. **(A)** mRNA expression levels of CD36 were determined in male (left plot, grey scale colors) and female (right plot, red scale colors) BMDM obtained from SD and HFD-fed mice. In both groups, mRNA expression levels under resting conditions (control) and after LPS treatment for 16 h (LPS) were obtained, and the differences between these two conditions are plotted as LPS-fold change. mRNA values were normalized using Rrl18 as housekeeping gene and expressed as $2^{-\Delta Ct}$. Data are mean ± SEM of 8–12 triplicate determinations, obtained from two batches of SD and HFD mice in each group (male and female). P-values were obtained with a two-way ANOVA followed by Tukey´s post-hoc test. **(B)**. The same analysis as in A was carried out for mRNA expression levels of KCNA3 gene (Kv1.3), with mRNA data obtained from the same samples. Kruskal-Wallis analysis followed by Dunn's test was used to estimate significance between control and LPS-treated BMDMs mRNA levels, and one-way ANOVA followed by Tukey´s post-hoc test was used for LPS-fold change data.

Finally, we explored the expression levels of the ATP-activated receptor $P2X_7$ (P2rx7) that has been proposed as a marker of MMe phenotype (Kratz et al., 2014), although its functional contribution is not clearly established (Sun et al., 2012). With the exception of $P2X_7$, which showed no sex- diet- or LPS-induced changes in mRNA expression, LPS-fold changes in HFD were always significantly larger in female compared to male BMDMs (Table 1, p-values in blue). Moreover, HFD treatment led to a significant increase in Kcnj2 expression in both male and female in control, unstimulated BMDMs, with no significant changes in Kcna3 and Kcnn4 expression. In the case of Kcna3 in females, HFD appears to both reduce its expression in control and enhance LPS-induced upregulation, leading to a significant diet-induced fold change increase upon LPS activation (Figure 2B).

3.3 Modulation of outward K^+ currents in macrophages from MetS/T2DM model in male and female

The functional contribution of the changes in K^+ currents was next explored with electrophysiological techniques both in BMDM and in fresh PM from SD and HFD mice. The summary data obtained from male and female BMDM are shown in Figure 3. In control macrophages, K^+ current amplitudes were smaller in HFD BMDM in both sexes (Figures 3A, B). However, in LPS-treated macrophages the effect of HFD was sex dependent, and current density was smaller in males and larger in females. These changes in female BMDM are in good agreement with the observed differences in Kv1.3 mRNA expression levels (Figure 2B). To further confirm this extent, kinetic and pharmacological analysis of these currents was carried out. Kv1.3 channels exhibit a characteristic C-type inactivation (Vennekamp et al., 2004; Kurata and Fedida, 2006) that translates into a use-dependent block (UDB) upon repetitive stimulation. This UDB was taken as a kinetic parameter to explore Kv1.3 contribution to total outward K^+ currents in macrophages (Figures 3C, D). No significant differences were found in control macrophages, but LPS-stimulated BMDM from HFD females (but not males) showed a significant increase of UDB compared to SD BMDM, suggesting an increased Kv1.3 functional expression in these cells. Finally, a pharmacological dissection of the outward K^+ currents was performed in a group of cells, using sequential application of PAP-1 (100 nM) to block Kv1.3 currents, TRAM34 (100 nM) to block $K_{Ca}3.1$ and TEA (5 mM) to block Kv2 and Kv3

10.3389/fphys.2024.1487775

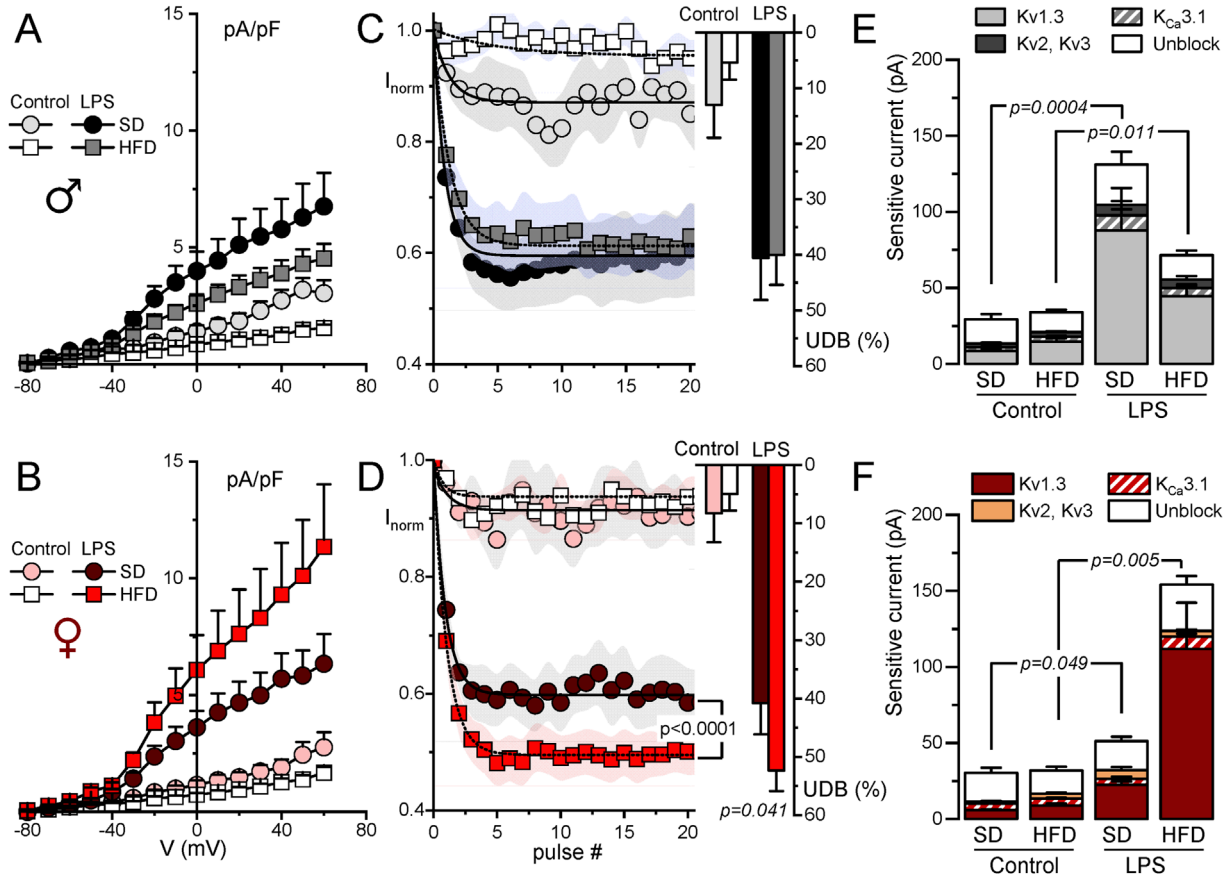

FIGURE 3
Electrophysiological characterization of outward K^+ currents from BMDM. Kinetic and pharmacological studies were carried out in BMDM obtained from female (red scale colors, lower plots) and male mice (upper plots, grey scale colors). In all cases, BMDM obtained from SD and HFD-fed mice were studied at rest (control) and after16 h treatment with 100 ng/mL LPS (LPS) as indicated. **(A, B)**. Current density to voltage relationships were constructed from peak outward current amplitudes obtained in 200 ms pulses from −80 to +60 mV in 10 mV steps, from a holding potential of −80 mV. Data are mean ± SEM of 15–25 cells in each group, obtained from at least six different animals. **(C, D)**. Peak current amplitude was obtained from trains of 40 pulses of 250 ms from −80 mV to +40 mV applied every 0.5 s, and normalized to the amplitude of the first pulse. The symbol graphs show the mean ± SEM of the first 20 pulses fitted to a one-exponential decay function, and the bars plots on the right were obtained by averaging the normalized amplitude (expressed as %) of the last 20 pulses in each group. P values were obtained from F-test comparison between the fits (for the normalized current plot) and with one-way ANOVA for the % of UDB. Data are mean ± SEM of 10–20 cells per group, from at least 5 different cultures. **(E, F)**. Average peak current amplitude for the PAP-1 sensitive (Kv1.3 current), the TRAM34-sensitive ($K_{Ca}3.1$ current) the 5 mM TEA-sensitive (Kv2-Kv3 current) and the insensitive outward K current (unblock) in each of the conditions. 7–11 BMDM obtained from at least 4 different animals were used for each determination Statistical analysis was carried out with Kruskal-Wallis analysis followed by Dunn's test to compare the fraction of Kv1.3-sensitive current in each condition.

currents. Kv1.3-sensitive current represented the largest fraction of K^+ current in all cases, and the main contributor to the outward current upregulation of LPS-treated BMDM (Figures 3E, F). The increase of the Kv1.3-current fraction in LPS-treated macrophages parallels the data shown in A and B, being significantly larger in HFD BMDM from females compared to SD. In contrast, a reduction of Kv1.3 currents in HFD macrophages stimulated with LPS was observed in male BMDM.

Electrophysiological characterization of BMDM also confirm expression data for $P2X_7$ receptors (Figures 4A, B). BzATP is a $P2X_7$ receptor agonist used to explore the activity of these currents. As shown in the figure, we did not find any change BzATP-activated currents dependent either on macrophage activation or sex. However, discrepancies between mRNA expression and protein function (determined by electrophysiological recordings) were found in the case of inward rectifier K^+ currents (Kir2.1 channels). Figure 4C shows the effect of 100 μM $BaCl_2$ and PAP-1 on K^+ currents obtained in male BMDM in SD from resting (control) and LPS-stimulated macrophages. A decrease of inward currents in LPS-stimulated BMDM is evident. However, with regards to diet, while mRNA shows a significant upregulation upon HFD treatment, (see Table 1), we found a tendency to a decreased $BaCl_2$-sensitive current when comparing control SD versus control HFD in both sexes (Figure 4D), that reached statistical significance in female BMDM.

The characterization of the outward K^+ currents was also carried out in peritoneal macrophages (PM) (Supplementary Figure SIII). As in BMDM, outward K^+ currents in control PM were decreased in HFD-fed mice (figure IIA and D), most likely due to a decreased contribution of Kv1.3, as suggested by the significant reduction

10.3389/fphys.2024.1487775

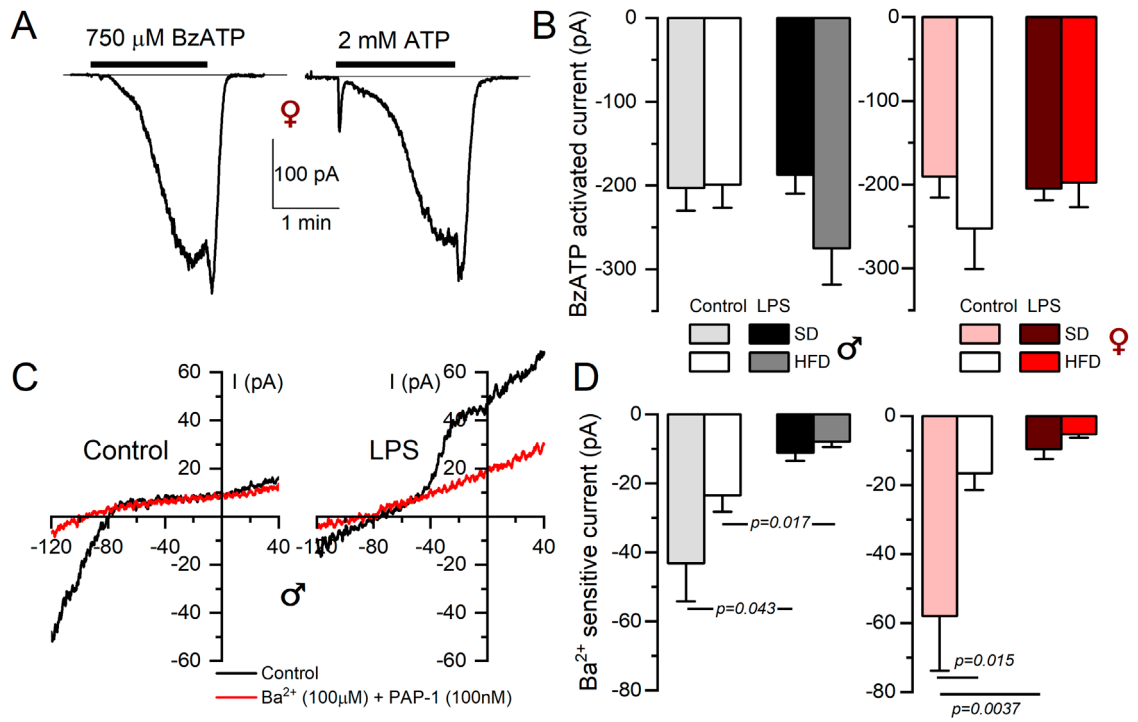

FIGURE 4
Electrophysiological characterization of $P2X_7$ and inward rectifier K^+ currents from BMDM. **(A)** Representative currents obtained from a female control BMDM upon application of either BzATP (750 μM) or 2 mM ATP during the indicated time to show the kinetics and amplitude of the P2X7-mediated currents. Holding potential was kept at 0 mV. **(B)** The right panels show de average current amplitude elicited by 750 μM BzATP in BMDM from the indicated groups obtained from female (red scale) or male (gray scale) mice. Each column is mean ± SEM of 12–20 cells in each group, obtained from 4 to 6 different animals. A two-way ANOVA did not show significant differences. **(C)** Representative recordings of the current elicited in one control and one LPS-treated BMDM SD male with voltage ramps from a holding potential of −80 mV with control solution (black traces) or in the presence of a baths solution containing 100 nM PAP-1 and 100 μM $BaCl_2$ to block Kv1.3 and Kir2.1 currents respectively (red traces). **(D)** The amplitude of the $BaCl_2$-sensitive current was measured at −120 mV, and the averaged values obtained in all experimental conditions are plotted in the right graphs, both in female (red color scale) and male (gray colors) BMDM. Statistical analyses were carried out with a two-way ANOVA followed by Tukey´s post-hoc test (in the females group) and with a Kruskal-Wallis analysis followed by Dunn's test in the males group. Mean ± SEM, n = 8-12 cells per group from at least 4 different cultures.

of UDB in these conditions, both in male and female (Figure IIB y E). The activation with LPS elicited larger increases in Kv current density in female than in male PM, but in both cases were reduced in HFD-treated PM. Altogether, the electrophysiological characterization of PM did not show the Kv1.3 changes observed in female BMDM from HFD. However, in this latter preparation changes expression and function of Kv1.3 channels exhibit a good correlation.

3.4 MetS/T2DM female BMDM show Kv1.3-independent increased phagocytosis

As the previous data exploring HFD-associated changes in Kv1.3 channels and metabolic markers indicated sex-dependent significant differences only in female mice, we focused on female BMDM to further explore the functional impact of these changes in several macrophage´s integrated responses. We studied phagocytosis using flow cytometry to measure the number of cells that uptake Alexa Fluor 594-labelled zymosan A particles (Figure 5). In SD BMDM, there was no difference in the number of zymosan-labelled cells upon LPS treatment. In contrast, LPS-stimulated HFD cells showed increased phagocytosis compared to LPS-stimulated SD or control HFD macrophages. However, Kv1.3 blockade had no effect in any condition, indicating that the increased phagocytic capacity of LPS-activated BMDM from MetS/T2DM female mice is independent of Kv1.3 channels.

3.5 BMDM from MetS/T2DM females did not show changes in O_2 consumption rate

Potential changes in energy metabolism between BMDM from SD and HFD female mice were explored using a Seahorse analyzer to study oxygen consumption rate (OCR). We assessed OCR in control media and after the sequential addition of oligomycin (ATP synthase inhibitor), carbonyl cyanide 4-(trifluoromethoxy)phenylhydrazone (FCCP, a H^+ ionophore) and rotenone/antymicin A (complex I and III inhibitors respectively) to calculate basal respiration, ATP-linked respiration and spare respiratory capacity. Average data obtained in both groups, analyzing also the effects of LPS activation and PAP-1 treatment are depicted in Figure 6. We found no differences in basal respiration among the different experimental conditions. The analysis of the ATP-linked respiration indicates

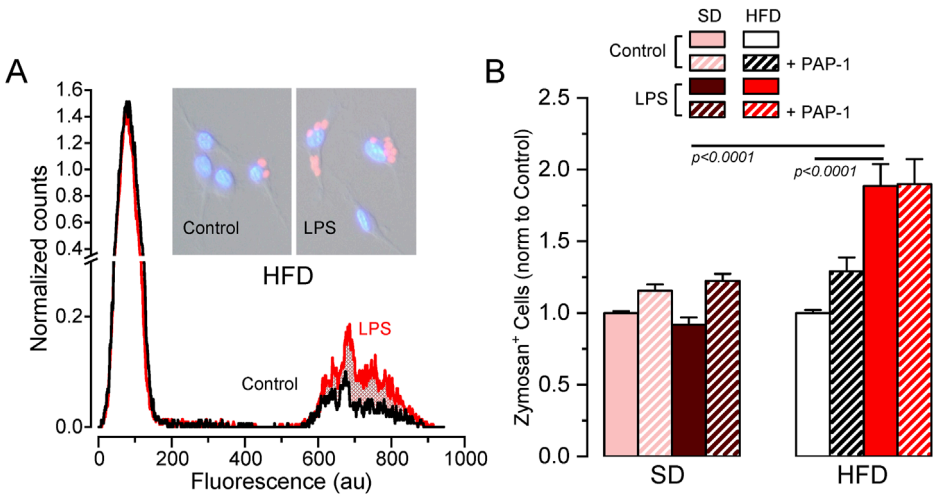

FIGURE 5
Effects of HFD on female BMDM phagocytosis. **(A)**. Example of a flow cytometer experiment in a control (black line) and LPS-treated (red line) BMDM population from a HFD female to determine phagocytosis. The graph shows the normalized counts for each cell population (obtained by normalizing the running area integral of each experiment, to correct for the total number of cells), against fluorescence intensity. An increase in the number of cells showing fluorescence from Alexa Fluor 594-labelled zymosan was observed in HFD LPS-treated cells (red area). Representative pictures of control and LPS cells with labelled zymosan particles are also shown. **(B)**. Average data (mean ± SEM) obtained from 4-7 independent experiments in each condition, carried out with BMDM from different mice. In this case, the percentage of zymosan-labelled cells was normalized to its own control, untreated cells in each experiment. Statistical significance was obtained with a three-way ANOVA followed by Tukey´s post-hoc test.

that this parameter is dependent on Kv1.3 in resting (control) macrophages in SD but this dependence is lost in HFD, which is consistent with the reduced functional expression of Kv1.3 channels after HFD treatment (Figure 3). However, ATP-linked respiration increases significantly upon LPS-activation in HFD, matching Kv1.3 upregulation, but in this case, it is PAP-1 insensitive, suggesting a change in the mechanism(s) involved in respiration in activated BMDMs. The spare respiratory capacity was increased after LPS stimulation in both BMDM from SD and HFD and it was Kv1.3-dependent only in HFD macrophages.

3.6 BMDM from MetS/T2DM females show Kv1.3-dependent increased migration

A key to an efficient and optimally regulated macrophage´s response is their ability to shift between a resting and activated mobile state rapidly, combined with stringent regulation of cell migration during the activated state. Consequently, mechanisms controlling macrophage mobility and migration play a key role in the efficiency of their immune or inflammatory responses. For this reason, we explore the role of Kv1.3 channels in the migration of BMDM from both SD and HFD female mice (Figure 7). As in the previous experiments, PAP-1 treatment was used to infer Kv1.3 contribution. The representative plots (Figure 7A) show the time course of the changes in the invaded area in experiments in SD and HFD BMDM in all the conditions tested. Control BMDM migration was inhibited by PAP-1 in SD cells but not in HFD cells. LPS-stimulated BMDM exhibit an increased migration rate (compared to control) that was sensitive to PAP-1 in both groups. The averaged area under the curve (AUC) obtained in pooled experiments confirmed these results (note that larger AUCs represent slower migration rates). These data suggest that differences in migration rate between SD and HFD macrophages are dependent on Kv1.3 expression levels, as the magnitude of PAP-1 effects shows a good correlation with Kv1.3 expression levels in each condition (Figure 7B).

4 Discussion

4.1 Macrophage phenotype contribution to metabolic syndrome and T2DM

The metabolic syndrome (MetS) is a cluster of clinical disorders including central obesity, dyslipidemia, glucose intolerance and hypertension. It is known that these disorders not only increase the chances of developing T2DM, but also Cardiovascular diseases (CVD). Insulin resistance has been considered at the root of the problem to explain the metabolic abnormalities within this syndrome, but new evidence points to several pro-inflammatory cytokines, reactive oxygen species and free fatty acid intermediates as key elements in sustaining and perpetuating the development of the MetS and its CVD complications.

Macrophages are a well-established key player in cardiovascular disease, particularly in atherosclerotic plaque formation and remodeling (Aparicio-Vergara et al., 2012; Simon-Chica et al., 2022). Recent findings show that they also accumulate in adipose tissue of obese mice, contributing to chronic low-grade inflammation and disrupting glucose and lipid metabolism leading to MetS and CVD. The mechanism involves mononuclear cells migrating to white adipose tissue, releasing pro-inflammatory cytokines, and promoting insulin resistance in skeletal muscle, liver, and other tissues (Donath and Shoelson, 2011). Clinical observations reveal

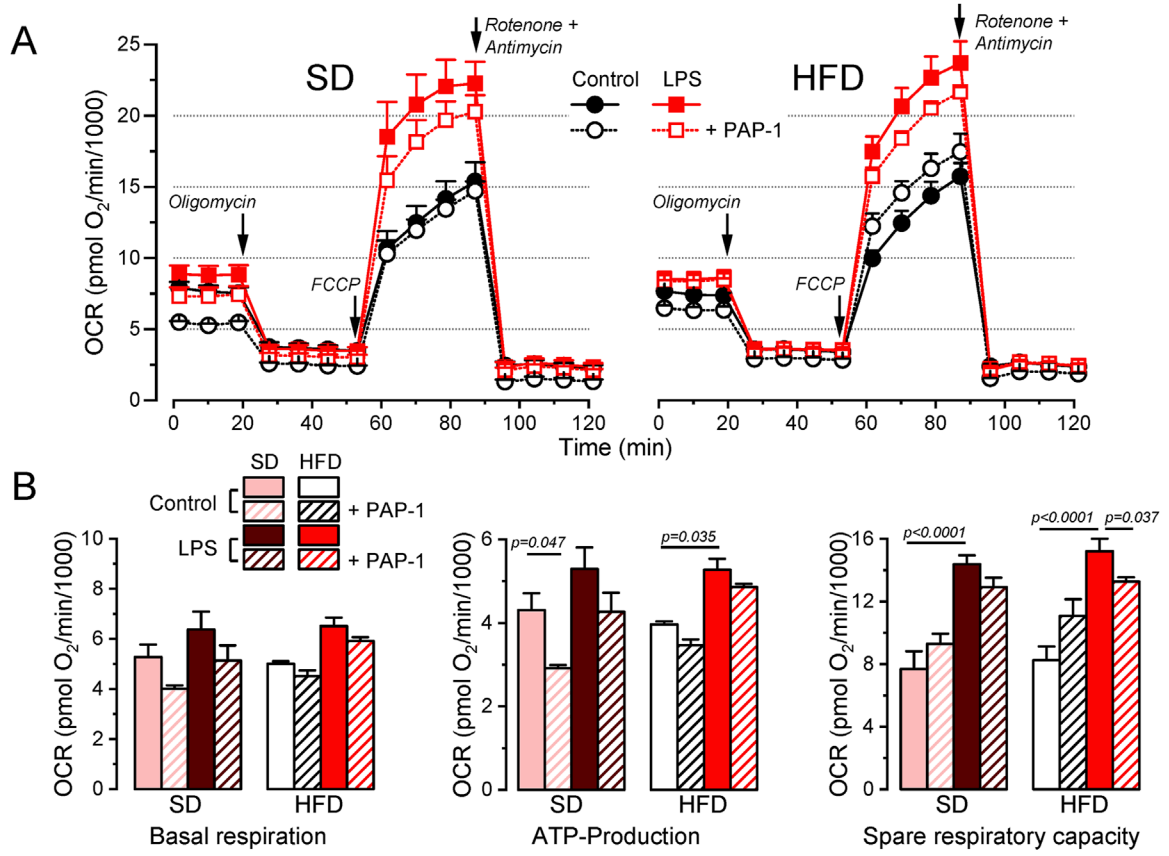

FIGURE 6
Metabolic profile of SD and HFD BMDM from female mice. **(A)**. Average data from Seahorse XF Cell Mito Stress Test experiments carried out in BMDM from SD (left) and HFD (right) female mice, using resting (control) and activated (LPS) cells with or without overnight treatment with 100 nM PAP-1 as indicated. The Cell Mito Stress Test profile was obtained by sequential application of the drugs indicated (see methods for details). Data was normalized by counting of cells and expressed as pmol O_2/min/1,000 cells. **(B)**. Quantification of several standard parameters in the Seahorse analysis. The plots show the average (mean ± SEM) data of OCR in basal respiration (before oligomycin application), ATP-linked respiration (the difference in OCR between basal respiration and oligomycin) and spare respiratory capacity (OCR difference between basal and FCCP). Data were obtained from 3 independent experiments, each one containing 3 replicates and analyzed with a 3-way ANOVA followed by Tukey´s post-hoc test.

that MetS subjects show higher circulating levels of inflammatory cytokines and greater macrophage infiltration compared to healthy controls (Andersen, et al., 2016). Notably, deletion of the insulin receptor in myeloid cells reduces macrophage infiltration during HFD, decreases circulating levels of TNF-α and protects against HFD-induced insulin resistance, highlighting insulin's potential negative role in innate immune responses during MetS.

4.2 Kv1.3 channels contribution to metabolic syndrome and T2DM

It is well established that Kv1.3 channels influence body weight regulation. Kv1.3-KO mice exhibit higher metabolic rates, improved insulin sensitivity, and resistance to diet-induced obesity (Xu et al., 2004). Kv1.3 blockers mitigate the effects of HFD, reducing weight gain and inflammation while improving glucose tolerance in animal models (Upadhyay et al., 2013). In this line, our previous research in the MetS/T2DM model shows that local Kv1.3 blocker treatment after carotid ligation ameliorates vessel remodeling and eliminates HFD-induced insulin resistance and weight gain (Arevalo-Martinez et al., 2021). Interestingly, HFD enhances sensitivity to Kv1.3 inhibition, as Kv1.3 blockade did not affect weight gain in SD mice. Based on these findings, we have explored the contribution of macrophages to the development of MetS, focusing on the potential role of Kv1.3 channels.

Macrophage polarization induces a differential K^+ channel expression pattern with the upregulation of Kv1.3 channels, which contribute to proliferation, migration and secretion of pro-inflammatory cytokines (Feske et al., 2015; Di Lucente et al., 2018). However, Kv1.3 channel expression and function in macrophages vary significantly depending on factors such as culture conditions, stimulation mode and organ and species source, among others (Nguyen et al., 2017; Simon-Chica et al., 2022).

4.3 Contribution of Kv1.3 channels to the MMe phenotype of BMDM

Our data from BMDM from SD and HFD fed mice revealed sex-dependent differences in their susceptibility to develop a metabolically activated (MMe) phenotype. Notably, the MMe

10.3389/fphys.2024.1487775

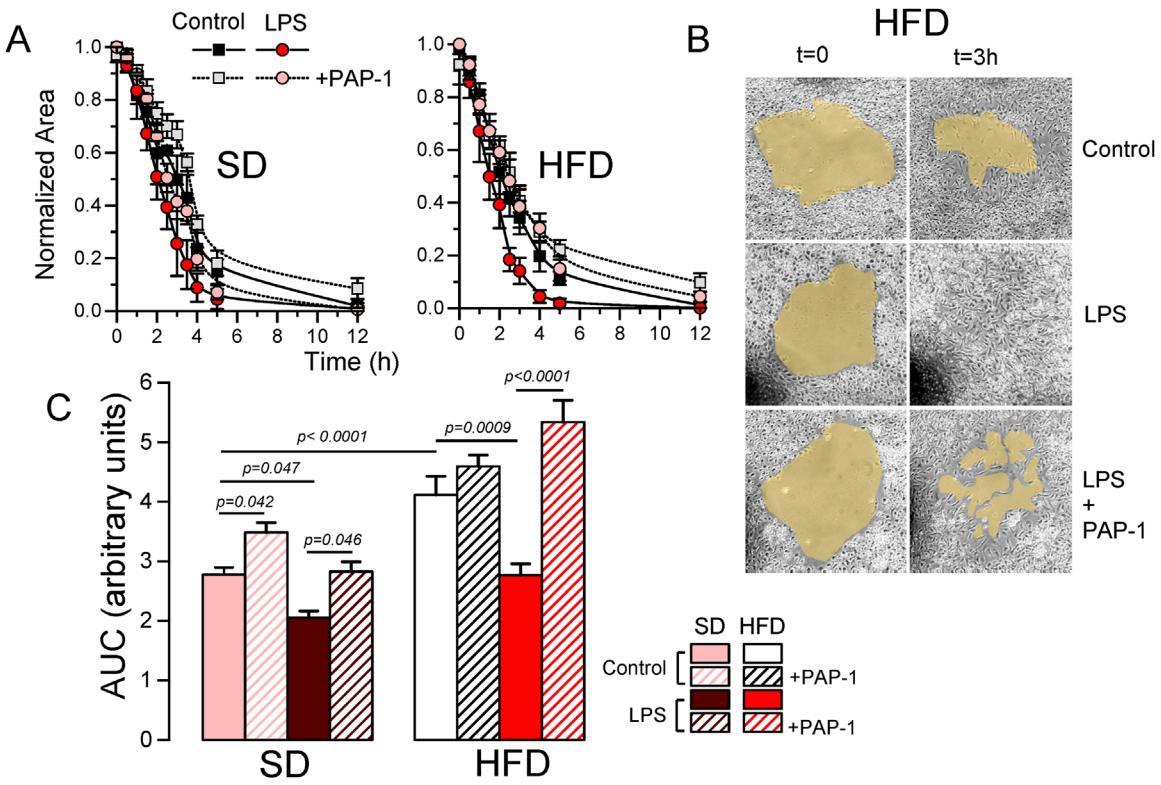

FIGURE 7
Effects of HFD on the migration of BMDM from female mice. **(A)**. Representative examples of a migration experiment using BMDM from SD (left) or HFD (right) female mice. In each experiment the four indicated conditions (Control and LPS-treated with or without PAP-1) were analyzed using three independent replicates. The time course of the invaded area up to 12 h was determined at the indicated times, to obtain the area free of cells, which was normalized to the initial area. **(B)**. Sample images obtained at t = 0 and after 3 h in control, LPS and LPS + PAP-1 in one experiment carried out with BMDM from a HFD female mouse. **(C)**. The bars plot represents the averaged area under the curve obtained in 4-6 independent experiments as the ones shown in A, each one from a different cell culture. Statistical significance was obtained from a three-way ANOVA followed by Tukey´s post-hoc test.

marker CD36 was significantly upregulated only in female mice. Similarly, diet-related changes in Kv1.3 channels functional expression were observed exclusively in female BMDM, becoming particularly pronounced upon LPS-induced polarization, with significantly enhanced Kv1.3 upregulation in HFD BMDM (Figure 3). However, the functional impact of this increased Kv1.3 expression in female HFD BMDMs was only apparent when examining their migration rate (Figure 7).

We observed that the combination of diet and LPS induced changes in the phagocytic activity independent of Kv1.3 (Figure 5). The increased phagocytic activity in our MMe BMDMs aligns with previous studies showing CD36 as an important macrophage receptor for apoptotic cell recognition and phagocytosis (Pennathur et al., 2015).

Our metabolic profile analysis indicated that oxygen consumption rate (OCR) remained essentially unchanged across diets (Figure 6). We also found higher extracellular acidification rates (ECAR) in LPS-treated macrophages (Supplementary Figure SIV), indicating an LPS-induced shift towards glycolysis. The glycolytic preference of M1 macrophages has been previously reported in murine models (Zhao et al., 2013; Bess et al., 2023; Gobelli et al., 2023). Interestingly, we also found increased spare respiratory capacity in both SD and HFD LPS-stimulated BMDM (Figure 6), suggesting enhanced oxidative phosphorylation (OXPHOS). While the glycolysis-OXPHOS paradigm has been used to define pro-inflammatory and anti-inflammatory macrophage phenotypes, it is somewhat oversimplified, much like the M1/M2 paradigm. Different pro-inflammatory stimuli mediate different metabolic responses, and different disease states are characterized by different immunometabolic profiles (Mouton et al., 2020). This dual metabolic capability (i.e., increased glycolysis alongside maintained oxidative capacity) has been observed in pro-inflammatory macrophages depending on the activating stimulus (Ishida et al., 2023). Moreover, mouse strain differences can also account for differences in the metabolic response to the same stimulus (Supplementary Figure SV). In parallel experiments using BMDM from BPH and C57 female mice we found an increase in OXPHOS metabolism in response to LPS-treatment in BPH mice, but a decreased OCR in C57 mice.

Regarding HFD treatment, and consistent with our findings, it has been described that in obese mice, adipose tissue macrophages assume a pro-inflammatory phenotype and show both increased glycolytic and OXPHOS metabolism, while peritoneal macrophages

do not alter their metabolism, suggesting that the microenvironment drives immunometabolic adaptations during obesity (Boutens et al., 2018). Such metabolic flexibility may allow activated macrophages to adapt to specific environmental conditions, potentially supporting both immediate and sustained inflammatory responses.

4.4 Sex-dependent differences in macrophage phenotype in MetS/T2DM mice

Sexual dimorphisms have been documented in immunity; in fact, clinical manifestations of infectious or autoimmune diseases and malignancy differ between females and males, and they are very much dependent on differences in the innate immunity system (Jaillon et al., 2017). A recent study characterized sex differences in the immune system with RNA and ATAC sequence profiling at baseline and after interferon-induced stimulation in 11 immune cell lineages. Surprisingly, only one cell type displayed differences between sexes, namely, the macrophages (Gal-Oz et al., 2019). In agreement with our data (see Table 1), they found that females exhibit a more highly activated innate immune pathways prior to pathogen presentation, and an increased response to interferon stimulus (which can correlate with the response to LPS activation). This female immune alertness makes them less vulnerable to infections but comes at the price of females being more prone to autoimmune diseases. Genes related to lipoprotein metabolism were also upregulated in female macrophages, in agreement with lipid metabolism exhibiting sexual dimorphism (Wang et al., 2011). The stronger inflammatory response in female may contribute to age-related disease developments and life expectancy and can be at the root of the sex-dependent development of the MMe phenotype in our MetS/T2DM model.

4.5 Kv1.3 channels as targets against macrophage infiltration in MetS/T2DM

Kv1.3 channels have been shown to contribute to macrophage migration and infiltration in various studies, both *in vivo* and *in vitro*. For instance, Wu et al. (2020) showed that blockage of Kv1.3 with Margatoxin (MgTx) can inhibiting macrophages infiltration in damaged liver tissues. Their *in vitro* studies with RAW264.7 cells suggested that MgTx treatment induced the downregulation of δ-catenin, a protein associated with macrophage migration, indicating that Kv1.3 inhibition represents a potential therapeutic strategy. In the context of CVD, Kv1.3 blockers have been shown to correct AngII induced macrophage infiltration and endothelial dysfunction in small and large vessels (Olivencia et al., 2021). This effect appears to be independent of electrophysiological changes in VSMCs, suggesting a role for Kv1.3 channels in the macrophage-dependent endothelial dysfunction induced by AngII in mice. Kan et al. (2016) proposed a role for Kv1.3 channels in atherosclerosis based on increased Kv1.3 channel expression in macrophages from acute coronary syndrome patients. In RAW264.7 cells, Kv1.3 small interfering RNA suppressed cell migration and reduced ERK1/2 phosphorylation, while Kv1.3 overexpression had the opposite effects. This suggest that Kv1.3 channels may stimulate macrophage migration through activating the ERK1/2-dependent signaling pathway. Interestingly, Kv1.3 induced proliferation in vascular smooth muscle cells and in heterologous expression system also depends on the ERK1/2 signaling pathway (Cidad et al., 2015; 2020; Jiménez-Pérez et al., 2016). Collectively, these findings highlight the importance of Kv1.3 channels in macrophage function and their potential as therapeutic targets in various pathological conditions.

The differences observed between BMDM and PM warrant further analysis. PM, differentiated *in vivo*, typically show modest responses when stimulated *ex vivo*. In contrast, BMDM, differentiated *in vitro*, respond rapidly and robustly to both pro-inflammatory and pro-resolving stimuli, making them the preferred cell type for studying macrophage plasticity (Zajd et al., 2020). BMDM are generally more phagocytic, both in terms of rate and amount of material ingested. They also respond more strongly to polarization, as evidenced by changes in surface molecule expression, gene regulation, and cytokine/chemokine release. For these reasons, we focused our study on the contribution of Kv1.3 to integrated macrophage responses and their changes in MetS/T2DM models using BMDM from female mice.

In our electrophysiological studies comparing both populations, we found that while the ion channel signature was very similar in both cell types, there were differences in the relative amplitude of the components and in their responses to polarization or HFD treatment. However, the low numbers of PM available precluded a thorough characterization of mRNA expression patterns, which would have allowed us to explore expression-function correlations in this cell population. Regarding their role in vascular diseases, it has been reported that PM and BMDM are phenotypically distinct and differ from macrophages in atherosclerotic lesions in terms of M1/M2 marker expression and lipid metabolism genes (Bisgaard et al., 2016). It is important to note that neither PM nor BMDM perfectly match the heterogeneity observed *in vivo*. In fact, their inherent heterogeneity and capacity to polarize rapidly in response to subtle micro-environmental changes may make it impossible to generate a perfect model.

4.6 Concluding remarks

Signal-dependent pro-inflammatory stimulation typically activates a broad range of overlapping intracellular cascades. Therefore, the most effective strategies to prevent insulin resistance and T2DM will probably be targeted at proximal and common steps in these pathways. In this scenario, unravelling the mechanisms responsible for monocyte and macrophage migration and infiltration can be relevant for our understanding of the pathophysiological progression to insulin resistance and T2DM. Kv1.3 channels may represent a promising therapeutic target for mitigating inflammation-driven metabolic disorders. By interfering with macrophage migration, Kv1.3 inhibition could potentially disrupt the vicious cycle of inflammation and insulin resistance, offering a novel approach to managing MetS and preventing its progression to T2DM and its associated CV complications. In addition, our findings reveal important sex-specific differences in macrophage function, which can contribute to design more effective and personalized interventions.

Data availability statement

The raw data supporting the conclusions of this article will be made available by the authors, without undue reservation.

Ethics statement

The animal study was approved by Animal Care and Use Committee of the University of Valladolid (Project 505649). The study was conducted in accordance with the local legislation and institutional requirements.

Author contributions

DP: Conceptualization, Data curation, Formal Analysis, Investigation, Methodology, Resources, Software, Validation, Writing–original draft, Writing–review and editing. LB-S: Data curation, Formal Analysis, Investigation, Methodology, Writing–original draft, Writing–review and editing, Visualization. SM-E: Data curation, Formal Analysis, Investigation, Methodology, Visualization, Writing–original draft, Writing–review and editing. EA: Data curation, Formal Analysis, Investigation, Methodology, Visualization, Writing–original draft, Writing–review and editing. JL-L: Data curation, Formal Analysis, Investigation, Methodology, Visualization, Writing–original draft, Writing–review and editing, Conceptualization, Funding acquisition, Resources, Software, Validation. MP-G: Conceptualization, Data curation, Formal Analysis, Funding acquisition, Investigation, Methodology, Resources, Software, Validation, Visualization, Writing–original draft, Writing–review and editing, Project administration, Supervision. PC: Conceptualization, Data curation, Formal Analysis, Investigation, Methodology, Resources, Software, Supervision, Validation, Visualization, Writing–original draft, Writing–review and editing.

Funding

The author(s) declare that financial support was received for the research, authorship, and/or publication of this article. This work was supported by grants PID2020-118517RB-I00 and PID2023-146750OB-I00 from the Spanish Agencia Estatal de Investigación (MICIU/AEI/10.13039/501100011033) and VA172P20 and VA186P24 from the Junta de Castilla y León (JCyL). DAP has a postdoctoral Juan de la Cierva training grant, FJC2021-046455-I, financed by the Spanish Government, MCIN/AEI/10.13039/501100011033, and by the European Union "NextGenerationEU/PRTR" and SME had a JCyL predoctoral contract.

Acknowledgments

We want to thank Alvaro Martin Muñoz for his help with all the flow cytometer experiments, and Clara Meana for her valuable advice and discussions. We are also grateful to all the members of the laboratory for their helpful discussions.

Conflict of interest

The authors declare that the research was conducted in the absence of any commercial or financial relationships that could be construed as a potential conflict of interest.

The author(s) declared that they were an editorial board member of Frontiers, at the time of submission. This had no impact on the peer review process and the final decision.

Publisher's note

Supplementary material

The Supplementary Material for this article can be found online at: https://www.frontiersin.org/articles/10.3389/fphys.2024.1487775/full#supplementary-material

References

Andersen, C. J., Murphy, K. E., and Fernandez, M. L. (2016). Impact of obesity and metabolic syndrome on immunity. *Adv. Nutr. Am. Soc. Nutr.* 7 (1), 66–75. doi:10.3945/an.115.010207

Aparicio-Vergara, M., Shiri-Sverdlov, R., Koonen, D. P. Y., and Hofker, M. H. (2012). Bone marrow transplantation as an established approach for understanding the role of macrophages in atherosclerosis and the metabolic syndrome. *Curr. Opin. Lipidol.* 23 (2), 111–121. doi:10.1097/MOL.0B013E3283508C4F

Arévalo-Martínez, M., Cidad, P., García-Mateo, N., Moreno-Estar, S., Serna, J., Fernández, M., et al. (2019). Myocardin-dependent Kv1.5 channel expression prevents phenotypic modulation of human vessels in organ culture. *Arteriosclerosis, Thrombosis, Vasc. Biol.* 39 (12), E273–E286. doi:10.1161/ATVBAHA.119.313492

Arevalo-Martinez, M., Cidad, P., Moreno-Estar, S., Fernández, M., Albinsson, S., Cózar-Castellano, I., et al. (2021). miR-126 contributes to the epigenetic signature of diabetic vascular smooth muscle and enhances antirestenosis effects of Kv1.3 blockers', *Molecular metabolism. Mol. Metab.* 53, 101306. doi:10.1016/J.MOLMET.2021.101306

Bess, S. N., Igoe, M. J., Denison, A. C., and Muldoon, T. J. (2023). Autofluorescence imaging of endogenous metabolic cofactors in response to cytokine stimulation of classically activated macrophages', *Cancer & Metabolism 2023 11:1. Biomed. Cent.* 11 (1), 1–16. doi:10.1186/S40170-023-00325-Z

Bisgaard, L. S., Mogensen, C. K., Rosendahl, A., Cucak, H., Nielsen, L. B., Rasmussen, S. E., et al. (2016). Bone marrow-derived and peritoneal macrophages have different inflammatory response to oxLDL and M1/M2 marker expression – implications for atherosclerosis research. *Sci. Rep.* 6, 35234. doi:10.1038/SREP35234

Bobi, J., Garabito, M., Solanes, N., Cidad, P., Ramos-Pérez, V., Ponce, A., et al. (2020). Kv1.3 blockade inhibits proliferation of vascular smooth muscle cells *in vitro* and intimal hyperplasia *in vivo*', *Translational research: the journal of laboratory and clinical medicine. Transl. Res.* 224, 40–54. doi:10.1016/J.TRSL.2020.06.002

Boutens, L., Hooiveld, G. J., Dhingra, S., Cramer, R. A., Netea, M. G., and Stienstra, R. (2018). Unique metabolic activation of adipose tissue macrophages in obesity promotes inflammatory responses. *Diabetol. Diabetol.* 61 (4), 942–953. doi:10.1007/S00125-017-4526-6

Chen, K., Man, Q., Miao, J., Xu, W., Zheng, Y., Zhou, X., et al. (2022). Kir2.1 channel regulates macrophage polarization via the Ca2+/CaMK II/ERK/NF-κB signaling pathway. *J. Cell Sci. Co. Biol. Ltd* 135 (13). doi:10.1242/jcs.259544

Cheong, A., Li, J., Sukumar, P., Kumar, B., Zeng, F., Riches, K., et al. (2011). Potent suppression of vascular smooth muscle cell migration and human neointimal hyperplasia by KV1.3 channel blockers. *Cardiovasc. Res.* 89 (2), 282–289. doi:10.1093/cvr/cvq305

Cidad, P., Alonso, E., Arévalo-Martínez, M., Calvo, E., de la Fuente, M. A., Pérez-García, M. T., et al. (2020). Voltage-dependent conformational changes of Kv1.3 channels activate cell proliferation. *J. Cell. Physiology* 236, 4330–4347. Wiley. doi:10.1002/jcp.30170

Cidad, P., Miguel-Velado, E., Ruiz-McDavitt, C., Alonso, E., Jiménez-Pérez, L., Asuaje, A., et al. (2015). Kv1.3 channels modulate human vascular smooth muscle cells proliferation independently of mTOR signaling pathway. *Pflügers Archiv - Eur. J. Physiology* 467 (8), 1711–1722. doi:10.1007/s00424-014-1607-y

Cidad, P., Moreno-Domínguez, A., Novensá, L., Roqué, M., Barquín, L., Heras, M., et al. (2010). Characterization of ion channels involved in the proliferative response of femoral artery smooth muscle cells. *Arteriosclerosis, Thrombosis, Vasc. Biol.* 30 (6), 1203–1211. doi:10.1161/ATVBAHA.110.205187

Cidad, P., Novensà, L., Garabito, M., Batlle, M., Dantas, A. P., Heras, M., et al. (2014). K+ channels expression in hypertension after arterial injury, and effect of selective Kv1.3 blockade with PAP-1 on intimal hyperplasia formation. *Cardiovasc. Drugs Ther.* 28 (6), 501–511. doi:10.1007/s10557-014-6554-5

Di Lucente, J., Nguyen, H. M., Wulff, H., Jin, L. W., and Maezawa, I. (2018). The voltage-gated potassium channel Kv1.3 is required for microglial pro-inflammatory activation *in vivo*. *Glia* 66 (9), 1881–1895. doi:10.1002/glia.23457

Donath, M. Y., and Shoelson, S. E. (2011). Type 2 diabetes as an inflammatory disease. *Nat. Rev. Immunol. 2011 11:2* 11 (2), 98–107. doi:10.1038/nri2925

Feske, S., Wulff, H., and Skolnik, E. Y. (2015). Ion channels in innate and adaptive immunity. *Annu. Rev. Immunol.* 33, 291–353. doi:10.1146/annurev-immunol-032414-112212

Gal-Oz, S. T., Maier, B., Yoshida, H., Seddu, K., Elbaz, N., Czysz, C., et al. (2019). ImmGen report: sexual dimorphism in the immune system transcriptome. *Nat. Commun.* 10 (1), 4295. doi:10.1038/s41467-019-12348-6

Gobelli, D., Serrano-Lorenzo, P., Esteban-Amo, M. J., Serna, J., Pérez-García, M. T., Orduña, A., et al. (2023). The mitochondrial succinate dehydrogenase complex controls the STAT3-IL-10 pathway in inflammatory macrophages. *Iscience. iScience* 26 (8), 107473. doi:10.1016/J.ISCI.2023.107473

Hotamisligil, G. S. (2006). Inflammation and metabolic disorders. *Nat. 2006* 444, 860–867. doi:10.1038/nature05485

Ishida, K., Nagatake, T., Saika, A., Kawai, S., Node, E., Hosomi, K., et al. (2023). Induction of unique macrophage subset by simultaneous stimulation with LPS and IL-4. *Front. Immunol.* 14, 1111729. doi:10.3389/fimmu.2023.1111729

Jaillon, S., Berthenet, K., and Garlanda, C. (2017). Sexual dimorphism in innate immunity. *Clin. Rev. Allergy and Immunol.* 56 (3), 308–321. doi:10.1007/S12016-017-8648-X

Jiménez-Pérez, L., Cidad, P., Álvarez-Miguel, I., Santos-Hipólito, A., Torres-Merino, R., Alonso, E., et al. (2016). Molecular determinants of Kv1.3 potassium channels-induced proliferation', *Journal of Biological Chemistry*. *Am. Soc. Biochem. Mol. Biol. Inc.* 291 (7), 3569–3580. doi:10.1074/jbc.M115.678995

Kan, X. H., Gao, H. Q., Ma, Z. Y., Liu, L., Ling, M. Y., and Wang, Y. Y. (2016). Kv1.3 potassium channel mediates macrophage migration in atherosclerosis by regulating ERK activity. *Archives Biochem. Biophysics* 591, 150–156. doi:10.1016/J.ABB.2015.12.013

Kratz, M., Coats, B. R., Hisert, K. B., Hagman, D., Mutskov, V., Peris, E., et al. (2014). Metabolic dysfunction drives a mechanistically distinct proinflammatory phenotype in adipose tissue macrophages', *Cell metabolism*. *Cell Metab.* 20 (4), 614–625. doi:10.1016/J.CMET.2014.08.010

Kurata, H. T., and Fedida, D. (2006). A structural interpretation of voltage-gated potassium channel inactivation. *Prog. Biophysics Mol. Biol. Pergamon* 92 (2), 185–208. doi:10.1016/J.PBIOMOLBIO.2005.10.001

Li, J., Ruggiero-Ruff, R. E., He, Y., Qiu, X., Lainez, N., Villa, P., et al. (2023). Sexual dimorphism in obesity is governed by RELMα regulation of adipose macrophages and eosinophils. *Elife. eLife Sci. Publ. Ltd.* 12, e86001. doi:10.7554/ELIFE.86001

Livak, K. J., and Schmittgen, T. D. (2001). Analysis of relative gene expression data using real-time quantitative PCR and the 2(-Delta Delta C(T)) Method. *Methods* 25 (4), 402–408. doi:10.1006/meth.2001.1262

Lordén, G., Sanjuán-García, I., de Pablo, N., Meana, C., Alvarez-Miguel, I., Pérez-García, M. T., et al. (2017). Lipin-2 regulates NLRP3 inflammasome by affecting $P2X_7$receptor activation. *J. Exp. Med.* 214 (2), 511–528. doi:10.1084/jem.20161452

Meana, C., Peña, L., Lordén, G., Esquinas, E., Guijas, C., Valdearcos, M., et al. (2014). Lipin-1 integrates lipid synthesis with proinflammatory responses during TLR activation in macrophages. *J. Immunol.* 193 (9), 4614–4622. *(Baltimore, Md.* doi:10.4049/JIMMUNOL.1400238

Miguel-Velado, E., Moreno-Domínguez, A., Colinas, O., Cidad, P., Heras, M., Pérez-García, M. T., et al. (2005). Contribution of Kv channels to phenotypic remodeling of human uterine artery smooth muscle cells. *Circulation Res.* 97 (12), 1280–1287. doi:10.1161/01.RES.0000194322.91255.13

Mouton, A. J., Li, X., Hall, M. E., and Hall, J. E. (2020). Obesity, hypertension, and cardiac dysfunction: novel roles of immunometabolism in macrophage activation and inflammation', *Circulation research*. *NIH Public Access* 126 (6), 789–806. doi:10.1161/CIRCRESAHA.119.312321

Nguyen, H. M., Grössinger, E. M., Horiuchi, M., Davis, K. W., Jin, L. W., Maezawa, I., et al. (2017). Differential Kv1.3, KCa3.1, and Kir2.1 expression in "classically" and "alternatively" activated microglia', *Glia*. *Glia* 65 (1), 106–121. doi:10.1002/GLIA.23078

Olefsky, J. M., and Glass, C. K. (2010). Macrophages, inflammation, and insulin resistance. *Annu. Rev. Physiology is online A. T.* 72, 219–246. doi:10.1146/annurev-physiol-021909-135846

Olivencia, M. A., Martínez-Casales, M., Peraza, D. A., García-Redondo, A. B., Mondéjar-Parreño, G., Hernanz, R., et al. (2021). KV1.3 channels are novel determinants of macrophage-dependent endothelial dysfunction in angiotensin II-induced hypertension in mice. *Br. J. Pharmacol.* 178 (8), 1836–1854. doi:10.1111/bph.15407

Osborn, O., and Olefsky, J. M. (2012). The cellular and signaling networks linking the immune system and metabolism in disease', *Nature Medicine 2012 18:3*. *Nat. Publ. Group* 18 (3), 363–374. doi:10.1038/nm.2627

Pennathur, S., Pasichnyk, K., Bahrami, N. M., Zeng, L., Febbraio, M., Yamaguchi, I., et al. (2015). The macrophage phagocytic receptor CD36 promotes fibrogenic pathways on removal of apoptotic cells during chronic kidney injury. *Am. J. Pathology* 185 (8), 2232–2245. doi:10.1016/j.ajpath.2015.04.016

Robblee, M. M., Kim, C. C., Porter Abate, J., Valdearcos, M., Sandlund, K. L. M., Shenoy, M. K., et al. (2016). Saturated fatty acids engage an ire1α-dependent pathway to activate the NLRP3 inflammasome in myeloid cells', *Cell reports*. *Cell Rep.* 14 (11), 2611–2623. doi:10.1016/J.CELREP.2016.02.053

Simon-Chica, A., Fernández, M. C., Wülfers, E. M., Lother, A., Hilgendorf, I., Seemann, G., et al. (2022). Novel insights into the electrophysiology of murine cardiac macrophages: relevance of voltage-gated potassium channels. *Cardiovasc. Res. Oxf. Univ. Press* 118 (3), 798–813. doi:10.1093/CVR/CVAB126

Sun, S., Xia, S., Ji, Y., Kersten, S., and Qi, L. (2012). The ATP-P2X 7 signaling axis is dispensable for obesity-associated inflammasome activation in adipose tissue', *Diabetes*. *Diabetes* 61 (6), 1471–1478. doi:10.2337/db11-1389

Tajada, S., Cidad, P., Moreno-Domínguez, A., Pérez-García, M. T., and López-López, J. R. (2012). High blood pressure associates with the remodelling of inward rectifier K+ channels in mice mesenteric vascular smooth muscle cells. *J. physiology* 590 (Pt 23), 6075–6091. doi:10.1113/jphysiol.2012.236190

Upadhyay, S. K., Eckel-Mahan, K. L., Mirbolooki, M. R., Tjong, I., Griffey, S. M., Schmunk, G., et al. (2013). Selective Kv1.3 channel blocker as therapeutic for obesity and insulin resistance. *Proc. Natl. Acad. Sci.* 110 (24), E2239–E2248. doi:10.1073/pnas.1221206110

Vennekamp, J., Wulff, H., Beeton, C., Calabresi, P. A., Grissmer, S., Hänsel, W., et al. (2004). Kv1.3-blocking 5-phenylalkoxypsoralens: a new class of immunomodulators. *Mol. Pharmacol. U. S.* 65 (6), 1364–1374. doi:10.1124/mol.65.6.1364

Vicente, R., Escalada, A., Coma, M., Fuster, G., Sánchez-Tilló, E., López-Iglesias, C., et al. (2003). Differential voltage-dependent K+ channel responses during proliferation and activation in macrophages. *J. Biol. Chem. U. S.* 278 (47), 46307–46320. doi:10.1074/jbc.M304388200

Wang, X., Magkos, F., and Mittendorfer, B. (2011). Sex differences in lipid and lipoprotein metabolism: it's not just about sex hormones. *J. Clin. Endocrinol. Metab.* 96 (4), 885–893. doi:10.1210/jc.2010-2061

Wu, B., Liu, J. d., Bian, E., Hu, W., Huang, C., Meng, X., et al. (2020). Blockage of Kv1.3 regulates macrophage migration in acute liver injury by targeting δ-catenin through RhoA signaling. *Int. J. Biol. Sci.* 16 (4), 671–681. doi:10.7150/IJBS.38950

Xu, J., Wang, P., Li, Y., Li, G., Kaczmarek, L. K., Wu, Y., et al. (2004). The voltage-gated potassium channel Kv1.3 regulates peripheral insulin sensitivity. *Proc. Natl. Acad. Sci. U. S. A.* 101 (9), 3112–3117. doi:10.1073/pnas.0308450100

Xu, R., Li, C., Wu, Y., Shen, L., Ma, J., Qian, J., et al. (2017). Role of KCa3.1 channels in macrophage polarization and its relevance in atherosclerotic plaque instability', *arteriosclerosis, thrombosis, and vascular biology*. *Arterioscler. Thromb. Vasc. Biol.* 37 (2), 226–236. doi:10.1161/ATVBAHA.116.308461

Yang, Y. Y., Wang, Y. F., Yang, X. F., Wang, Z. H., Lian, Y. T., and Yang, Y. (2013). Specific Kv1.3 blockade modulates key cholesterol-metabolism-associated molecules in human macrophages exposed to ox-LDL', *Journal of Lipid Research*. *Am. Soc. Biochem. Mol. Biol.* 54 (1), 34–43. doi:10.1194/jlr.M023846

Zajd, C. M., Ziemba, A. M., Miralles, G. M., Nguyen, T., Feustel, P. J., Dunn, S. M., et al. (2020). Bone marrow-derived and elicited peritoneal macrophages are not created equal: the questions asked dictate the cell type used. *Front. Immunol.* 11, 269. doi:10.3389/fimmu.2020.00269

Zhao, N., Dong, Q., Du, L. L., Fu, X. X., Du, Y. M., and Liao, Y. H. (2013). Potent suppression of Kv1.3 potassium channel and IL-2 secretion by diphenyl phosphine oxide-1 in human T cells. *PLOS ONE. Public Libr. Sci.* 8 (5), e64629. doi:10.1371/JOURNAL.PONE.0064629

frontiers | Frontiers in Physiology

TYPE Review
PUBLISHED 18 December 2024
DOI 10.3389/fphys.2024.1506356

OPEN ACCESS

EDITED BY
Tlili Barhoumi,
King Abdullah International Medical Research Center (KAIMRC), Saudi Arabia

REVIEWED BY
Titus J. Boggon,
Yale University, United States
Sebastian Mathea,
Goethe University Frankfurt, Germany

*CORRESPONDENCE
Luis A. Martinez-Lemus,
martinezlemusl@missouri.edu
Jaume Padilla,
padillaja@missouri.edu

RECEIVED 05 October 2024
ACCEPTED 28 November 2024
PUBLISHED 18 December 2024

CITATION
Lateef OM, Foote C, Power G, Manrique-Acevedo C, Padilla J and Martinez-Lemus LA (2024) LIM kinases in cardiovascular health and disease. *Front. Physiol.* 15:1506356. doi: 10.3389/fphys.2024.1506356

LIM kinases in cardiovascular health and disease

Olubodun M. Lateef[1,2], Christopher Foote[1], Gavin Power[1,3], Camila Manrique-Acevedo[1,4,5,6], Jaume Padilla[1,3,4]* and Luis A. Martinez-Lemus[1,2,6]*

[1]NextGen Precision Health, University of Missouri, Columbia, MO, United States, [2]Department of Medical Pharmacology and Physiology, University of Missouri Columbia, Columbia, MO, United States, [3]Department of Nutrition and Exercise Physiology, University of Missouri, Columbia, MO, United States, [4]Harry S. Truman Memorial Veterans' Hospital, Columbia, MO, United States, [5]Department of Medicine, Division of Endocrinology, Diabetes and Metabolism, Columbia, MO, United States, [6]Center for Precision Medicine, Department of Medicine, University of Missouri, Columbia, MO, United States

The Lim Kinase (LIMK) family of serine/threonine kinases is comprised of LIMK1 and LIMK2, which are central regulators of cytoskeletal dynamics via their well-characterized roles in promoting actin polymerization and destabilizing the cellular microtubular network. The LIMKs have been demonstrated to modulate several fundamental physiological processes, including cell cycle progression, cell motility and migration, and cell differentiation. These processes play important roles in maintaining cardiovascular health. However, LIMK activity in healthy and pathological states of the cardiovascular system is poorly characterized. This review highlights the cellular and molecular mechanisms involved in LIMK activation and inactivation, examining its roles in the pathophysiology of vascular and cardiac diseases such as hypertension, aneurysm, atrial fibrillation, and valvular heart disease. It addresses the LIMKs' involvement in processes that support cardiovascular health, including vasculogenesis, angiogenesis, and endothelial mechanotransduction. The review also features how LIMK activity participates in endothelial cell, vascular smooth muscle cell, and cardiomyocyte physiology and its implications in pathological states. A few recent preclinical studies demonstrate the therapeutic potential of LIMK inhibition. We conclude by proposing that future research should focus on the potential clinical relevance of LIMK inhibitors as therapeutic agents to reduce the burden of cardiovascular disease and improve patient outcomes.

KEYWORDS

cardiovascular disease, vascular remodeling, arterial stiffening, atrial fibrillation, atherosclerosis, hypertension

1 Introduction

The LIM (Lin-11, Islet-1, and Mec-3) kinase (LIMK) family of enzymes is considered a key regulator of cytoskeletal dynamics due to the ability of its members to promote actin polymerization. As multiple fundamental mechanisms of cellular function depend on proper actin cytoskeletal dynamics, it is crucial to understand the physiological, pathological, and potential therapeutic implications of LIMK activation and activity modulation. The LIMKs are canonical downstream substrates of the Rho-family small GTPase members, RhoA, Cdc42, and Rac1. In turn, the primary target of the LIMKs is the Actin Depolymerizing Factor (ADF)/Cofilin family of proteins, including cofilin 1, 2, and

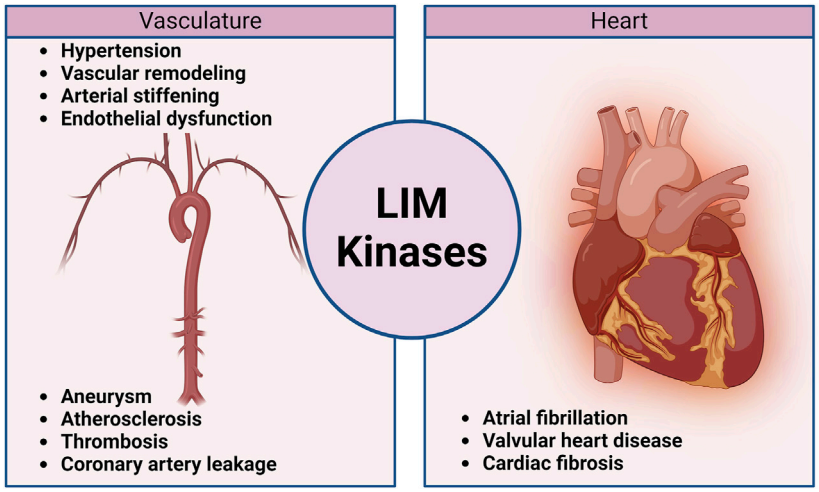

GRAPHICAL ABSTRACT
Schematic diagram illustrating the contribution of LIM kinases to the pathophysiology of cardiovascular diseases.

destrin, which will be referred to as cofilin in this review. The LIMKs can phosphorylate serine and tyrosine residues and have been demonstrated to phosphorylate cofilin at Ser3 as a primary target (Yang et al., 1998; Lagoutte et al., 2016; Salah et al., 2019). Ser3 phosphorylation of cofilin is an unusual but highly specific target of LIMK activity (Lagoutte et al., 2016; Salah et al., 2019) that inactivates cofilin and allows for filamentous actin (F-actin) to accumulate, as has been demonstrated with the use of LIMK overexpression or phospho Ser3 cofilin mimetics (Suurna et al., 2006; Zhao et al., 2008; Slee and Lowe-Krentz, 2013; Power et al., 2024b). In the cardiovascular system, F-actin is essential for maintaining the structural and functional integrity of vascular endothelial cells, smooth muscle cells, and cardiomyocytes. Therefore, disruptions in the mechanisms that control actin cytoskeletal dynamics can contribute to several cardiovascular diseases (Gorovoy et al., 2009; Yamin and Morgan, 2012; Ward and Crossman, 2014; Fediuk and Dakshinamurti, 2015; Pan et al., 2022). Additional evidence suggests that the LIMKs modulate the microtubular network via Rho-ROCK signaling pathways and the interaction between actin stress fibers with microtubules (Birukova et al., 2004b; Gorovoy et al., 2005). Because microtubules and F-actin exert opposing tensile forces to the cellular structural framework (vectors vs. tensors, respectively), the LIMKs can be considered central regulators of cytoskeletal tensegrity, i.e., the capacity of the cytoskeleton to stabilize the cell's 3-dimensional structure by balancing forces of compression vs. tension, as poles, pegs and ropes do in a camping tent (Ingber, 2003b; Ingber, 2003a; Ingber et al., 2014; Gardiner, 2021). Overall, neuronal plasticity and cancer are the most extensive areas of study addressing the LIMKs' role in cytoskeletal dynamics. Diverse roles for the LIMKs in the pathogenesis of neurological disorders (Cuberos et al., 2015), cancer manifestation (Yoshioka et al., 2003), and skin disorders (Honma et al., 2006) are reported in the literature. Comprehensive reviews in these areas are available, including those by Cuberos et al. (2015); Ben Zablah et al. (2021). However, reviews focused on the roles that the LIMKs play in the cardiovascular system and the potential applicability of LIMK inhibitors as therapeutic agents for cardiovascular disease are lacking. This is particularly important considering that cytoskeletal dynamics play significant roles in maintaining cardiovascular health. The cytoskeleton serves as the structural framework of all cardiovascular cells, maintaining cellular shape, providing mechanical integrity and resistance, and supporting the stability of intracellular proteins and attachments to the extracellular matrix (Gotlieb, 1990; Sequeira et al., 2014; Tang, 2018; Davis et al., 2023). In addition, cytoskeletal changes, particularly those involving F-actin and microtubules, have been linked to the development of specific vascular and cardiac disorders (Hein et al., 2000; Fediuk and Dakshinamurti, 2015; Subramanian et al., 2015; Morales-Quinones et al., 2020; Fang et al., 2022; Soares et al., 2022). Thus, this review is focused on the roles that the LIMKs play in cytoskeletal dynamics during physiological and pathological processes of cardiovascular cells and their potential therapeutic applications.

2 Regulation of the LIMKs

The LIMK family consists of two closely related members (LIMK1 and LIMK2), which are well-characterized substrates of the Rho-associated protein kinases (ROCK1 and 2). Both LIMKs have a unique organization of signaling domains, with two N-terminal LIM domains, an internal PDZ-like domain, and proline/serine-rich regions, followed by a C-terminal protein kinase domain. LIMK1 and LIMK2 have similar sequences with the tyrosine kinases despite being initially classified as serine/threonine kinases (Okano et al., 1995). Indeed, LIMK1 has been shown to phosphorylate serine and tyrosine residues (Yang et al., 1998; Ohashi et al., 2014; Lagoutte et al., 2016; Salah et al., 2019). Although the LIMKs are very similar, especially when comparing their kinase domains, there is mounting evidence that their regulatory pathways differ and contribute to unique and overlapping cellular and developmental activities (Scott and Olson, 2007). Like many other kinases, the LIMKs' activity is enhanced by phosphorylation of their activation loop, and

evidence suggests that the PDZ domain plays a role in auto-inhibiting the C-terminal kinase domain, as mutations in the PDZ domain increase LIMK catalytic activity (Casanova-Sepulveda et al., 2023).

2.1 LIMKs activation

The LIMKs are predominantly activated by diverse kinases positioned downstream from members of the Rho family of small GTPases (Villalonga et al., 2023). The best-characterized activation process of the LIMKs is contingent upon RhoA GTPase activation of ROCK with the subsequent phosphorylation of LIMK1 and LIMK2 at Thr-508 and Thr-505, respectively (Ohashi et al., 2000; Amano et al., 2001). Activation of the LIMKs downstream of Cdc42 and Rac1 also occurs via intermediary kinases. Current data suggest that LIMKs' activation downstream of Cdc42 involves the myotonic dystrophy kinase-related Cdc42-binding kinases (MRCK), which phosphorylate LIMK2 at Thr-505 (Sumi et al., 2001). For both Cdc42 and Rac1, the effectors include the p21-activated kinases (PAK), which phosphorylate LIMK1 at Thr-508 (Edwards et al., 1999). Indeed, PAKs increase their activity when associated with GTP-bound Cdc42 or Rac1 through their Cdc42 and Rac1-binding domain, and PAKs' activity has been shown to phosphorylate and activate the LIMKs (Figure 1).

Evidence for additional pathways by which the LIMKs become activated includes data indicating that p38 mitogen-activated protein kinase (MAPK) regulates LIMKs' phosphorylation status via MAPK-activated protein kinase-2 (MAPKAPK-2) (Scott and Olson, 2007). In endothelial cells, such activation of LIMK1 does not require Thr-508 phosphorylation, as it has been shown that vascular endothelial growth factor (VEGF) stimulation leads to MAPKAPK-2-dependent phosphorylation of LIMK1 at Ser-323 between the PDZ and kinase domains (Kobayashi et al., 2006). Further evidence indicates that the LIMKs are also directly phosphorylated by p38 at Ser-310 and Ser-323; however, the effect of Ser-310 phosphorylation on LIMKs' activity appears negligible. This further suggests that kinases such as p38 activate the LIMKs indirectly via MAPKAPK-2 activity. Several additional kinases activate the LIMKs (Manetti, 2012; Villalonga et al., 2023), some with an apparent specificity for one of the two different isoforms. These kinases include protein kinase A (PKA), MKK6, and Aurora kinase A (AURKA). The LIMKs also appear to dimerize and undergo autophosphorylation or transphosphorylation processes induced by heat shock protein (HSP)-90 and tropomyosin-related kinase B (TrkB) (Li et al., 2006; Dong et al., 2012). These processes, in turn, favor the translocation of the LIMKs from the cytosol to the cell membrane. Additional

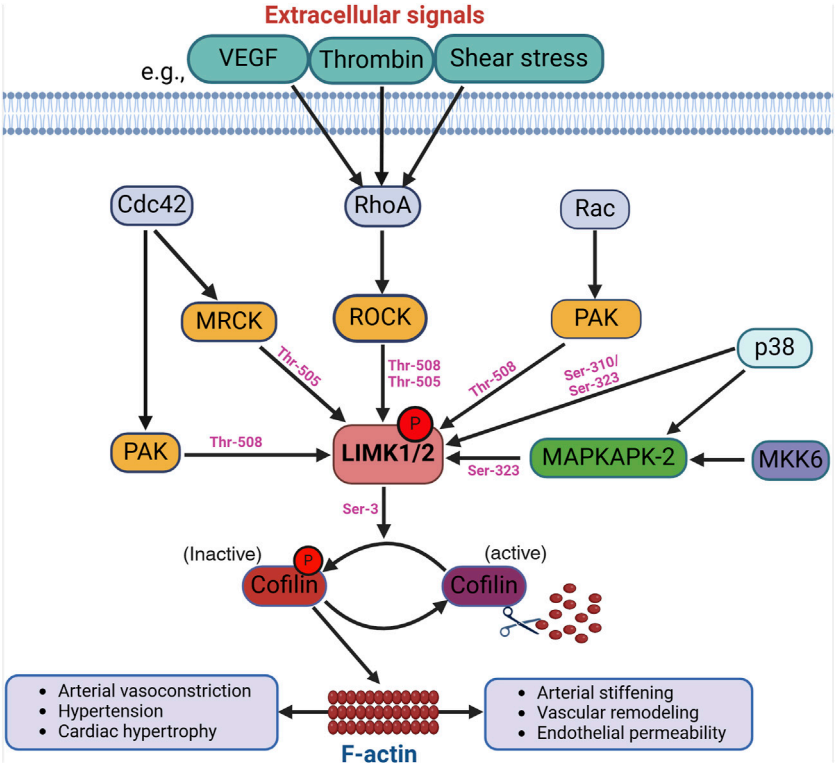

FIGURE 1
Activation of the LIMKs. Various upstream signaling pathways influence the LIMKs' activation. For example, extracellular signals like VEGF, thrombin, and shear stress trigger the activation of RhoA, which subsequently phosphorylates ROCK. LIMK1 and LIMK2 undergo phosphorylation and activation by ROCK, and other kinases such as MRCK, PAK, p38, and MAPKAPK-2 at different phosphorylation sites as shown in the figure. LIMK activation leads to cofilin phosphorylation at Ser-3 resulting in the accumulation of F-actin. (VEGF: Vascular endothelial growth factor; ROCK: Rho-associated protein kinase; MRCK: myotonic dystrophy kinase-related Cdc42-binding kinases; Cdc42: cell division control protein 42; PAK: p21-activated kinases; MAPKAPK-2: mitogen-activated protein kinase-activated protein kinase-2).

ways for the LIMKs to augment their capacity to phosphorylate cofilin include their increased expression resulting from p53 activity and the interaction of LIMK1 with the cyclin-dependent kinase inhibitor $p57^{krp2}$ (Hsu et al., 2010). It remains to be fully elucidated which activation pathways are specific for the different LIMK isoforms and the role of such pathways in cell-specific phenomena. In-depth recent reviews have been published on the diverse mechanisms that activate the LIMKs, how different mechanisms interact to increase or decrease the capacity of the LIMKs to phosphorylate cofilin, and which mechanisms require further corroboration or represent fruitful avenues for research endeavors (Chatterjee et al., 2022; Jiang et al., 2023; Villalonga et al., 2023; Casanova-Sepulveda and Boggon, 2024). Currently and consistent with their role in modulating cytoskeletal dynamics, the kinases downstream of Rho, Cdc42, and Rac1 are considered the primary activators of the LIMKs.

2.2 LIMKs inactivation

Typically, proteins subject to phosphorylation are dephosphorylated by phosphatases that return them to their unphosphorylated state. Slingshot 1 (SSH1), previously identified as a cofilin phosphatase, is among the phosphatases responsible for dephosphorylating and deactivating LIMK1 (Soosairajah et al., 2005; Gomez-Moron et al., 2024). In this process, SSH1 directly interacts with the kinase domain of LIMK1, facilitating the dephosphorylation of Thr-508 and consequently reducing the downstream phosphorylation of cofilin by LIMK1. Notably, SSH1 demonstrates a higher affinity for LIMK1 than LIMK2, suggesting that the phosphatase provides a differential regulation of these two kinases (Scott and Olson, 2007). Data also indicate that kinases that phosphorylate and activate the LIMKs further enhance LIMKs' activities by dampening SSH1's dephosphorylation capacity (Scott and Olson, 2007). For example, PAK4, which phosphorylates the LIMKs, also phosphorylates and inactivates SSH1 (Soosairajah et al., 2005). This indicates that the activity of the LIMKs is tuned by processes that finely control the phosphorylation status of the enzymes (Scott and Olson, 2007). These processes also include the status of the actin cytoskeleton, as low levels of F-actin in the cell can decrease SSH1 activity and thus promote the activation of LIMK1 and the polymerization of F-actin (Kurita et al., 2008).

Other mechanisms, in addition to the phosphatase activity of SSH1, reduce the capacity of the LIMKs to phosphorylate cofilin. For example, bone morphogenetic protein (BMP) and its type II receptor downregulate the activity of LIMK1 via the interaction of the enzyme with the intracellular tail of BMPR-II. This inhibits LIMK1's capacity to phosphorylate cofilin, which can be reversed by adding a BMP ligand to disrupt the interaction between LIMK1 and BMPR-II, leading to the subsequent activation of the enzyme (Foletta et al., 2003). Other molecules also participate in inactivating the LIMKs either by sequestering the LIMKs, thereby preventing phosphorylation at Thr-508 or Thr-505, or by facilitating the dephosphorylation of those activation sites (Figure 2). For example, Nischarin, a scaffolding protein that interacts with integrin α5β1 and participates in intracellular signaling (Alahari et al., 2000), also interacts and forms a complex with LIMK1 (Ding et al., 2008). This interaction leads to LIMK1 dephosphorylation and inactivation (Ding et al., 2008). Large tumor suppressor kinase 1 (LATS1) also interacts with LIMK1, rendering the enzyme inactive and reducing the phosphorylation level of downstream cofilin. Other cellular components that interact with the LIMKs and reduce their lifespan or kinase capacity include β-arrestin, the RING finger E3 ubiquitin ligase Rnf6, and PAR-3 (a protein involved in forming tight junctions) (Tursun et al., 2005; Chen and Macara, 2006; Zoudilova et al., 2007). Ultimately, processes that impede the phosphorylation of the LIMKs increase the capacity of phosphatases to dephosphorylate the enzymes, reduce their stability and half-life, or dephosphorylate cofilin to promote the severance of F-actin commonly associated with LIMKs' inhibition. Phosphatases that directly dephosphorylate cofilin include SSH1, protein phosphatase-1 and -2A (PP1, PP2A), and chronophin (Villalonga et al., 2023).

3 LIMKs' roles in the vasculature

The actin cytoskeleton is constantly remodeling via actin polymerization and depolymerization processes that fortify or weaken (degrade) F-actin stress fibers. Although this is particularly evident in motile cells and cells that constantly protrude and retract cellular extensions, vascular differentiated and de-differentiated cells also undergo constant changes in actin polymerization and depolymerization. Consequently, studies on the roles of LIMKs in the vasculature have focused on the effects of actin cytoskeletal dynamics in vascular remodeling and function, including but not limited to arterial stiffening, vasoconstriction, and vascular permeability. Most mechanistic studies in these research areas have been performed using LIMK inhibitors and not via knock down, knock out, or overexpression of the LIMKs' gene products. The cardiovascular pathology present in Williams–Beuren syndrome (a genetic disorder caused by heterozygous deletion of genes including *LIMK1* at chromosome 7q11.23) appears to depend on the heterozygous deletion of the elastin gene and not that of LIMK1. In addition, published data on knock-out models do not indicate that deletion of LIMK1 or LIMK2 produces an overt vascular phenotype. However, to the best of our knowledge, no specific analyses of vascular structure and function under basal or stressed conditions have been reported using such genetic models. It is also unclear which isoforms of the LIMKs or cofilin predominate in each vascular cell type. Although data using LIMK inhibitors indicate that LIMK activity modulation affects vascular function and structure, most of the inhibitors used do not distinguish family members, limiting the attribution of the phenomena studied to a specific LIMK isoform.

3.1 LIMKs and arterial remodeling

Arterial remodeling plays a critical role in cardiovascular physiological adaptations and the development and progression of cardiovascular diseases. Remodeling constitutes an overall important adaptive feature for maintaining blood vessel integrity. In broad terms, arterial remodeling refers to any change in vessel wall structure. However, it has been further defined as a change in the internal passive diameter of a vessel while under a specific

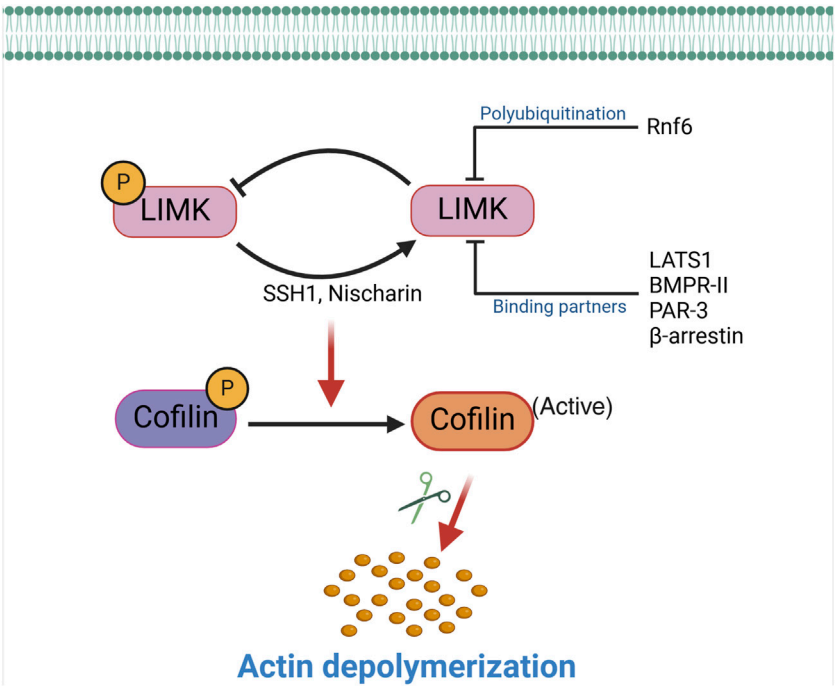

FIGURE 2
Inactivation of the LIMKs. The activity of the LIMKs is inhibited through dephosphorylation by SSH1, Nischarin. LIMKs are polyubiquitinated and degraded by Rnf6, while interactions with binding partners (LATS1, BMPR-II, PAR-3, and β-arrestin) inhibit their phosphorylation and prevent them from phosphorylating cofilin. This negative regulation of LIMK reduces cofilin phosphorylation, thereby enhancing the actin-severing activity of cofilin. (SSH1: Slingshot 1; LATS1: Large tumor suppressor kinase 1; PAR-3: Protease-activated receptor-3; Rnf6: Ring finger protein 6; BMPR-II: Bone morphogenetic protein receptor II).

intravascular pressure (Mulvany et al., 1996). Thus, a smaller passive internal diameter in a vessel represents inward remodeling, while a larger diameter represents outward remodeling. This is further characterized by the wall's cross-sectional area (CSA), such that a reduction in CSA is classified as hypotrophic, no change as eutrophic, and an increase as hypertrophic remodeling. This definition of vascular remodeling was first put forth by Mulvany et al. (1996) and has been mostly used for blood vessels in the microcirculation. In larger arteries where the presence of atherosclerotic plaques or neointimal formation may confound the internal diameter of an artery, the terms outward or inward remodeling are more commonly used to describe changes in the CSA contained within the external elastic lamina (Ward et al., 2000). Arterial remodeling is initiated by complex pathophysiological mechanisms that directly impact the vascular wall's cellular and non-cellular (extracellular matrix, ECM) components. These mechanisms include endothelial cell dysfunction, elastin and collagen content changes, vascular smooth muscle cell (VSMC) structure and function impairment, fibrosis, and calcification (Van Varik et al., 2012). Furthermore, multiple publications indicate that arterial remodeling precedes and participates in the development and progression of cardiovascular conditions such as hypertension (Weisbrod et al., 2013), aneurysm (Perissiou et al., 2019), or atherosclerosis (Palombo and Kozakova, 2016) and that changes in actin polymerization within VSMCs play an essential part in the early phases of arterial remodeling as well as in the maintenance of the remodeled state. In this regard, LIMK activity has been studied in vascular remodeling, as it highlights its capacity to enhance the formation and stabilization of F-actin by phosphorylating cofilin and suppressing its F-actin severing activity (Foote et al., 2016; Morales-Quinones et al., 2020).

Inward remodeling of the arterial vasculature is commonly associated with arterial stiffening. The stiffening of the vasculature has been widely attributed to elastin fragmentation, excessive collagen deposition, and crosslinking (Zhang et al., 2016; Hayashi and Hirayama, 2017; Aroor et al., 2019). However, an increasing body of evidence indicates that the mechanical properties of VSMCs also contribute to arterial stiffness (Sehgel et al., 2015; Martinez-Lemus et al., 2017). For example, Staiculescu et al. (2013) demonstrated that inhibition of VSMC actin polymerization prevents the development of inward remodeling in resistance arteries and further showed that F-actin depolymerization increased arterial passive diameter in inwardly remodeled vessels. This indicates that actin polymerization is a critical player in the mechanical processes that increase arterial stiffness and inward vascular remodeling. The polymerization and depolymerization of actin are tightly controlled processes, and many signaling factors, including kinase/phosphatase activity, temperature, Ca^{2+}, and pH, affect the function of different actin-binding proteins. All eukaryotic cells express the actin depolymerization cofilin family of proteins needed for actin filament turnover. These proteins weakly sever actin filaments without capping their ends, thereby increasing the number of uncapped filament ends available for polymerization and depolymerization (Goyal et al., 2013). As cofilin's primary activity is to sever F-actin cytoskeletal stress fibers, inactivation of

LIMK activity as the upstream regulator of cofilin phosphorylation may offer potential therapeutic strategies for preventing vascular inward remodeling and arterial stiffening. Indeed, recent research by Morales-Quinones et al. shows that LIMK inhibition reduces vasoconstriction-induced arterial stiffening by lowering the amount of F-actin and the stiffness of VSMCs (Morales-Quinones et al., 2020). Moreover, inhibition of LIMK prevented arterial stiffening and inward remodeling in isolated human visceral arteries exposed to prolonged vasoconstriction (Morales-Quinones et al., 2020). In that study, fluorescence images of omental arteries from hypertensive subjects showed increased F-actin stress fiber content and cofilin phosphorylation compared to non-hypertensive patients. LIMK inhibition also prevented the increased cortical stiffness observed after prolonged exposure to vasoconstrictor agonists in cultured VSMCs. Using a mouse model of hypertension, contralateral ears treated with a LIMK inhibitor prevented the reduction in vascular diameter following prolonged angiotensin II infusion (Morales-Quinones et al., 2020). In addition, recent findings by Power et al. (2024b) indicate that LIMK inhibition reduces endothelial cell stiffness by decreasing phosphorylated cofilin levels and consequently reducing F-actin stress fibers. These data suggest that targeting LIMK may lead to novel strategies to modulate arterial stiffness and ameliorate vascular remodeling in hypertension.

Arterial stiffening is correlated with end-organ damage, and several cardiovascular diseases are associated with increased vascular stiffness due to consequent increases in impedance and impaired vascular elasticity (Cheung, 2010). Changes in the characteristics of major vessel wall components, such as elastin, VSMCs, and collagen, cause aging-associated arterial stiffening. However, cumulative data on aging and obesity indicate that VSMC stiffness is a major driver of arterial stiffening (Qiu et al., 2010; Zhu et al., 2012; Ramirez-Perez et al., 2022). Therefore, considering that VSMC stiffness is modulated by cofilin phosphorylation through the RhoA-ROCK-LIMK signaling axis (Bravo-Cordero et al., 2013; Swiatlowska et al., 2022), modulation of LIMK activity may represent a novel therapeutic target to reduce arterial stiffness associated with aging and obesity.

3.2 LIMKs and arterial aneurysms

Aortic or intracranial aneurysms are defined as structural dilations that occur at weak points along the aorta or the cerebral vasculature, respectively. Four events are considered leading to aneurysm formation, including lymphocyte and macrophage infiltration into the vessel wall, vascular wall elastin and collagen destruction by proteases, VSMC loss within the media, and neovascularization (Ailawadi et al., 2003). Notably, rupture of aortic aneurysms has been associated with a mortality ranging from 50% to 80%, while subarachnoid hemorrhage is the most common consequence of intracranial aneurysm rupture, with a mortality rate of 27%–44% (Zhang et al., 2003; Kuivaniemi et al., 2015). Given the importance of the structural integrity of the vascular wall in precipitating aneurysm, the role of the cytoskeleton and its regulators has been investigated. LIMK has been demonstrated to promote aneurysmal formation. Single nucleotide polymorphisms in LIMK1 at chromosome 7q11 may cause intracranial aneurysm formation by affecting the structural support of the vascular wall (Akagawa et al., 2006). More specifically, the single nucleotide polymorphism rs6460071 in LIMK1 was associated with an increased risk of intracranial aneurysm formation (Low et al., 2011). This mutation reduces the promoter activity of *LIMK1* and a consequent decrease in LIMK1 protein levels, leading to the malformation of cerebral blood vessels and an increased incidence of intracranial aneurysms (Akagawa et al., 2006). However, it remains to be determined whether a reduction in LIMK activity alone can promote aneurysm formation. In a mouse model of ascending aortic aneurysms, both SSH1 abundance and cofilin dephosphorylation were increased during the phase of aneurysm initiation. This coincided with a reduction in F-actin and increased G-actin content within the developing aneurysm in the ascending aorta (Yamashiro et al., 2015). Paradoxically, there were also increases in RhoA abundance and activity and LIMK phosphorylation in the ascending aortas, ascribed to increased angiotensin II signaling in the mouse model of aneurysm used. The activity of LIMK is not well characterized in other models of aneurysm formation. However, reductions in F-actin and increases in G-actin are plausible mechanistic hypotheses for the weakening process that occurs in the aortic wall during the initiation stage of aneurysm development, which would likely implicate changes in the modulation of cofilin by the LIMKs.

In support of a prominent role for enzymes that affect both the cytoskeleton and ECM in aneurysm pathophysiology, tissue-type transglutaminase (TG2) expression was shown to be increased in the maximally dilated portion of human abdominal aorta aneurysmal samples compared to nondilated segments of the aorta (Shin et al., 2013). TG2 has been shown to inhibit MMP-2, -9, and tumor necrosis factor (TNF)-α in primary cultures of human abdominal aortic aneurysm-derived smooth muscle cells, supporting the notion that TG2 stabilizes the ECM and prevents the progression of abdominal aortic aneurysm (Shin et al., 2013). There is further evidence that members of a TG2-Rho-ROCK-LIMK-cofilin pathway may be involved in arterial aneurysm development, but how TG2 directly regulates LIMK activity in aneurysm development and progression remains poorly understood. In a mouse model of abdominal aortic aneurysm induced by intraluminal elastase and extraluminal calcium chloride exposure *in vivo*, TG2, TNF-α, MMP-2, and MMP-9 mRNA expression were increased in the acute phase compared to the chronic phase of the disease (Munezane et al., 2010). The mRNA expression of key factors promoting aneurysm formation, such as TNF-α, MMP-2, and MMP-9 in cultured aneurysmal tissue was decreased by exogenous TG2 exposure and increased by cystamine, a competitive inhibitor of TG2. This suggests a role for TG2 activity in ECM protection during the chronic phase of aneurysmal progression (Munezane et al., 2010). Because TG2 activity has also been shown to participate in VSMC actin dynamics and modulation of LIMK activity (Munezane et al., 2010), TG2 activation likely provides additional protection against aneurysmal development and progression via VSMC cytoskeletal modulation. In this scenario, inhibition or decreased expression of TG2 promotes the weakening of the vessel wall, leading to aneurysmal formation, while activation of TG2 protects against the development, progression, and potential rupture of the aneurysm. A few studies have examined the role of TG2 in

abdominal aortic aneurysms (Munezane et al., 2010; Shin et al., 2013; Griffin et al., 2021), but there is a lack of information on how LIMK directly regulates the aneurysmal process. Further studies should determine the molecular mechanisms by which a TG2-dependent LIMK activity pathway participates in aneurysm pathophysiology.

3.3 LIMKs and atherosclerosis

The dynamic remodeling of the actin cytoskeleton via LIMK activity is crucial for cell migration, gene expression, and morphogenesis (Scott and Olson, 2007; Manetti, 2012; Mizuno, 2013; Ohashi et al., 2014). Cell migration is essential for maintaining and establishing cellular organization, wound repair, tissue homeostasis, and a proper immune response (Trepat et al., 2012). Nonspecific electrostatic interactions and specific binding molecules such as cadherins, selectins, and integrins mediate cell adhesion to the ECM or nearby cells (Trepat et al., 2012). Cytoskeletal proteins such as α-actinin (Choi et al., 2008), filamin (Nagano et al., 2002), talin (Burridge and Connell, 1983), and tensin (Lo et al., 1994) link integrins to the actin cytoskeleton. Accordingly, the actin cytoskeleton is remodeled during VSMC migration in response to signals from cell surface receptors such as the integrins. This reorganization of the ECM-integrin-cytoskeleton axis causes the leading edge of VSMCs to protrude either along a path of variable adherence to the ECM or in the direction of a chemotactic signal (Gerthoffer, 2007). In addition to remodeling the cytoskeleton and focal adhesion disintegration at the trailing edge, contraction caused by actomyosin molecules in the cytoplasm propels the cell forward. By severing F-actin and expanding the number of F-actin portions available for actin polymerization, LIMK activity plays a significant role in cell proliferation and migration.

Indeed, modulation of LIMK activity and its associated pathways affects cell migration, including that of VSMCs. For example, use of the non-selective inhibitor of LIMK activity, damnacanthal, reduced breast carcinoma cells migration and invasion (Ohashi et al., 2014). Treatment with damnacanthal also prevented CXCL12-induced lamellipodium formation and suppressed migration in Jurkat cells through inhibition of LIMK1. A similar phenotype was reported by Nishita et al., who showed that LIMK1 knockdown suppressed chemokine-induced lamellipodium formation and cell migration (Nishita et al., 2005). Chemokine-like factor 1 (CKLF1) and chemokine receptor-8 (CCR8) have been shown to play an essential role in the migration and proliferation of VSMCs in vascular inflammation (Haque et al., 2004; Zhang et al., 2013) (Figure 3), and inhibition of CKLF1 can be used as a therapeutic target for the prevention of atherosclerosis. Furthermore, RhoA activates ROCK1 and ROCK2 in VSMCs, and non-selective inhibition of ROCK by fasudil or C3 exoenzyme impairs VSMC migration (Negoro et al., 1999; Seasholtz et al., 1999; Liu et al., 2002). The myosin binding component of myosin light chain phosphatase is phosphorylated by ROCK, which lowers phosphatase activity. ROCK can also directly phosphorylate Ser19 on myosin light chains *in vitro* (Amano et al., 1996), and in addition to its effects on myosin II phosphorylation (Gerthoffer, 2007), ROCK enhances actin polymerization by activating LIMK. Thus, various VSMC chemotactic signals that induce RhoA/ROCK activation, cytoskeletal remodeling, and VSMC migration (Raines, 2004) are potentially present in atherosclerosis and neointimal formation and represent processes likely modulated by LIMK activity.

The primary physiological functions of VSMC migration are vascular development and the maintenance of vascular integrity (Gerthoffer, 2007). In contrast, the pathophysiological migration and proliferation of VSMCs occur in response to vascular injury and atherogenesis (Gerthoffer, 2007). In this context, the differentiation and migration of VSMCs contribute to the pathological thickening of the arterial intima. Indeed, at the root of atherosclerosis and restenosis is the migration of VSMCs from the medial to the intimal layer of vessels (Chava et al., 2009; Gomez and Owens, 2012). Evidence indicates dynamic variations in LIMK expression and cofilin activity in VSMCs exist (Dai et al., 2006). However, new research on the role of LIMK activity in regulating VSMC migration in atherosclerotic plaque development and neointimal formation is warranted. In addition, vascular tone may be modulated by the differentiation of VSMCs from their contractile to a secretory or osteogenic phenotype. This promotes vascular wall calcification and secretion of proinflammatory cytokines such as platelet-derived growth factor (PDGF) (Winkles and Gay, 1991; Chang et al., 2014), critical characteristics of atherosclerosis development, progression, and complication.

PDGF plays a crucial role in atherosclerosis, vascular healing, and restenosis by promoting VSMC migration. While the stimulation of VSMC migration by PDGF is accompanied by cofilin activation, it has been demonstrated that dual regulation of cofilin activity by LIMK and SSH1 controls PDGF-induced migration of VSMCs (San Martin et al., 2008). PDGF activates both LIMK and the novel phosphatase SSH1L, but the activity of SSH1L supersedes LIMK activity, leading to the dephosphorylation of cofilin and VSMC migration. Indeed, inhibition of cofilin dephosphorylation by siSSH1L prevents cell migration, suggesting that the dual regulation of cofilin activity represents a finely tuned control of directional migration in which SSH1L plays a significant role in the maintenance of cofilin activity during PDGF-induced VSMC migration (San Martin et al., 2008). Similarly, in CXCL12-induced cell migration, LIMK1 and SSH1L are both activated in the process and mediate spatiotemporal regulation of cofilin. Ablation of either LIMK1 or SSH1L impairs chemokine-mediated cell migration (Nishita et al., 2005). LIMK1 is implicated in lamellipodium formation early in the migratory process. In contrast, the subsequent activation of SSH1L is posited to serve a dual purpose in restricting lamellipodia extension to one direction by retarding the growth of additional lamellipodia at other areas of the cell and then becoming discretely active at the leading edge of the lamellipodia to facilitate cyclic retraction and extension of the remaining lamellipodia. This proposed mechanism of cell migration induced by chemokines is more nuanced than that of several other studies that demonstrate cofilin phosphorylation promotes F-actin formation and cell migration.

VSMC migration induced by PDGF has also been associated with the activity of Rac-dependent induction of peripheral actin accumulation and membrane ruffling (Doanes et al., 1998). LIMK1 is involved in the lamellipodia formation induced by Rac1 (Sumi et al., 1999), while inflammation-activated Rac2 cooperates with the cytokine-inducible scaffold protein and

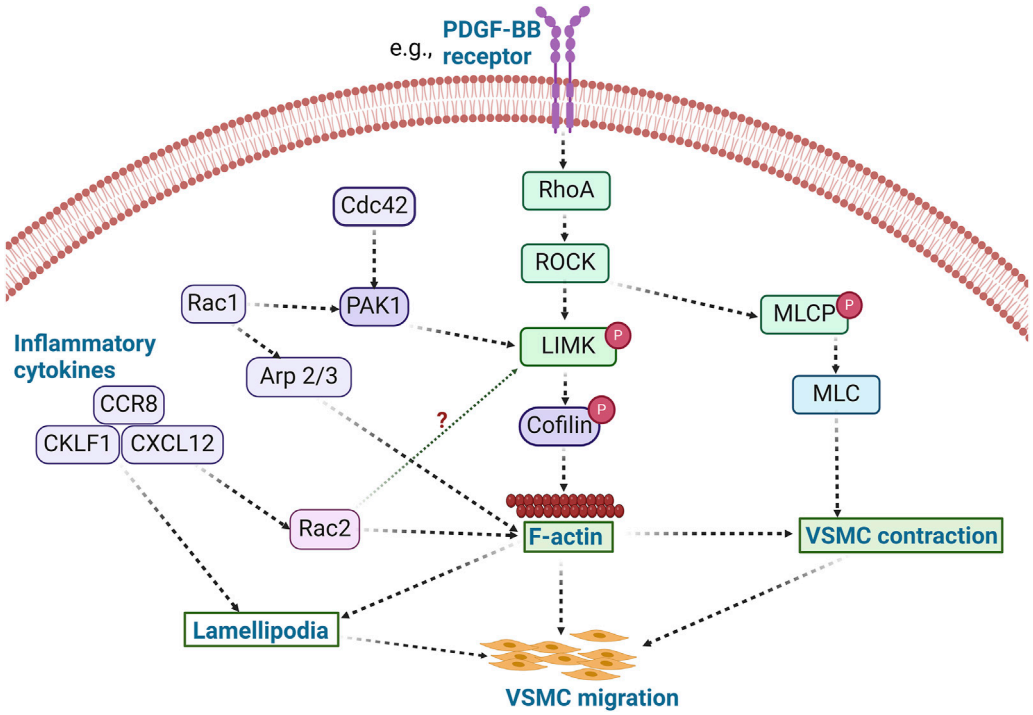

FIGURE 3
LIMK activity promotes VSMC migration. The activation of RhoA/ROCK by stimuli such as PDFG-BB leads to the phosphorylation of LIMK and inactivation of cofilin, thereby promoting actin polymerization. Concurrently, ROCK phosphorylates MLCP and inhibits its activity, resulting in increased phosphorylation of MLC and subsequent VSMC contraction. Activation of inflammatory cytokines such as CCR8, CKLF1, and CXCL12 also modulates cell migration via lamellipodia formation. These inflammatory processes likely promote VSMC migration in a LIMK-dependent manner. Whether inflammatory cytokines activate LIMK via Rac2 activation remains unknown. (PDFG-BB: Platelet derived growth factor BB; Arp 2/3: Actin related protein 2/3; CCR8: chemokine receptor-8; CKLF1: Chemokine-like factor 1; CXCL12: C-X-C motif chemokine 12; MLCP: Myosin light chain phosphatase).

allograft inflammatory factor to facilitate VSMC migration (Tian and Autieri, 2007). Similarly, PAK activity contributes to VSMC migration through Rac/Cdc42 GTPase signaling (Edwards et al., 1999). PAK phosphorylates LIMK and promotes actin polymerization when LIMK phosphorylates cofilin. In contrast, myosin phosphorylation is prevented when PAK phosphorylates myosin light-chain kinase (Edwards et al., 1999). Although it has been shown that VSMC migration is significantly inhibited by the expression of kinase-inactive PAK (Dechert et al., 2001), the predominant positive or negative effects of PAK and downstream LIMK activity on cytoskeletal filaments, myosin, and focal adhesions during VSMC migration remain poorly understood. All these indicate that Rac/Cdc42 and RhoA signaling are active participants in VSMC migration. Further studies should be conducted to accurately decipher the spatiotemporal activation of the LIMKs during the regulation of VSMC migration in response to diverse stimuli associated with atherosclerosis and neointima formation.

3.4 LIMKs and endothelial cell mechanotransduction

The survival and functional maintenance of living cells are linked to the cells' ability to perceive and respond to mechanical forces and the characteristics of their immediate extracellular microenvironment (Ingber, 2006; Janmey and McCulloch, 2007). The vascular endothelium plays critical homeostatic roles such as modulating macromolecular permeability, inflammatory responses, regulation of vascular remodeling, thrombosis, and vascular tone regulation in response to mechanical and chemical stimuli (Chiu and Chien, 2011; Davis et al., 2023). The two main mechanical forces acting upon the endothelium are the stretch caused by blood vessel deformation and the shear stress brought about by blood flow (Ali and Schumacker, 2002; Davis et al., 2023; Power et al., 2024a). These mechanical forces and associated mechanotransduction responses maintain endothelial cell morphology, signaling, and function under physiological conditions. However, during pathological conditions, altered mechanical forces and cellular responses participate in remodeling the structure of the ECM and the endothelium (Ingber, 2002). As a result, endothelial cells change their expression of molecules, such as the integrin receptors at cell-cell junctions and cell-matrix adhesions, to modulate the detection of mechanical stimuli, convert them into electrical or biochemical signals, and impact endothelial cell function (Dorland and Huveneers, 2017; Seetharaman and Etienne-Manneville, 2018). During this process, the RhoA/ROCK/LIMK pathway transduces mechanical signals from integrins to the cytoskeleton. Shear stress-induced ROCK/LIMK activity also facilitates endothelial cell migration by enhancing the traction force between the endothelial plasmalemma and the underlying substrate (Liu et al., 2018). Indeed, a growing body of evidence shows that the

relationship between integrins, Rho GTPases, and the actin cytoskeleton is crucial for the mechanotransduction of shear stress (Shyy and Chien, 2002) and that endothelial shear stress is essential for maintaining vascular wall homeostasis (Davies, 1995; Power et al., 2024a).

Shear stress induces Rho activation via multiple pathways, one of which includes integrins bound to fibronectin (Lin et al., 2003). It also causes a rapid increase in the kinase activity of ROCK and a sustained activation of LIMK2 (Lin et al., 2003). In cultured endothelial cells, integrin activation by shear engages the Rho-ROCK-LIMK-cofilin pathway to regulate the activity of sterol regulatory element binding proteins (SREBPs), which are important transcription factors responsible for the regulation of fatty acid, cholesterol, and triglyceride synthesis (Lin et al., 2003). Lin et al. showed that ROCK, LIMK, and cofilin are important mediators of shear stress-induced Rho activation of SREBP2 and that dominant negative Rho, RhoN19, prevents shear stress-induced SREBP2 nuclear translocation (Lin et al., 2003). The activation of SREBPs by shear stress may represent a novel mechanism by which mechanotransduction can be used as a tool to regulate SREBPs activity and the synthesis of lipids and sterols *in vivo* (Lin et al., 2003). This may be achieved via modulation of the Rho-ROCK-LIMK signaling cascade, as shear stress activates SREBPs via Rho by triggering the upstream mechanosensing process that involves integrins and ECM proteins. Indeed, Rho activity must be adequately regulated for shear stress to promote cell alignment and the creation of stress fibers, as either inhibition of Rho or activation of its mutant (RhoV14) causes a reduction in cell alignment (Li et al., 1999; Tzima et al., 2001). Thus, it is plausible that endothelial remodeling and lipid and sterol homeostasis may be regulated by tuning the Rho-ROCK-LIMK-cofilin pathway.

3.5 LIMKs in endothelial cell migration, vasculogenesis, and angiogenesis

Endothelial cell migration is essential for both angiogenesis and vasculogenesis and for restoring vessel integrity after damage (Michaelis, 2014). The migration of endothelial cells is regulated by mechanotactic, haptotactic, and chemotactic stimuli that modulate the progression and directionality of the migrating cells. This motile process requires the activation of various signaling cascades that converge on cytoskeletal remodeling (Lamalice et al., 2007). Thus, actin remodeling and focal adhesion dynamics are critical components of endothelial cell migration. Indeed, cell migration depends on the constant remodeling of the actin cytoskeleton into lamellipodia, stress fibers, and filopodia. Accordingly, endothelial cell migration is regulated by ROCK and requires the contraction of actomyosin, the rearrangement of stress fibers, and the dynamic formation and disassembly of focal adhesions (Lin et al., 2003; Wehrle-Haller, 2012).

VEGF is a potent mediator of vasculogenesis and angiogenesis, partly due to its ability to initiate cell migratory processes. In VEGF-stimulated endothelial cells, ROCK phosphorylation of LIMK leads to actin polymerization and stress fiber rearrangement (Gong et al., 2004). Notably, the induction of cell migration by VEGF involves actin reorganization, including intracellular localized actin polymerization and depolymerization processes. During angiogenesis, VEGF functions as a strong cell chemoattractant for mediating directional endothelial cell migration (Yoshida et al., 1996; Ferrara et al., 2003). Various cellular processes are required for such migration to occur. These include actin polymerization (Rousseau et al., 2000), focal adhesion turnover (Abedi and Zachary, 1997), and changes in cell binding interactions to the ECM that are enhanced by the high-affinity binding of VEGF to its cell surface receptor, kinase insert domain receptor (KDR) (Eliceiri et al., 2002) (Figure 4). In addition, the binding partner of PAK, the non-catalytic tyrosine kinase adaptor protein (NCK), has been shown to play critical roles in mediating focal adhesion turnover to promote cell migration (Stoletov et al., 2001; Gong et al., 2004). The PAK/NCK complex is recruited to the cell surface, where it activates PAK-kinase and promotes PAK redistribution to focal adhesions. Activation of PAK then inhibits actin depolymerization by activating LIMK (Edwards et al., 1999). Indeed, a report by Gong et al. further shows that NCK participates in VEGF-induced regulation of actin dynamics by activating LIMK and promoting cofilin phosphorylation (Gong et al., 2004). NCK regulates actin dynamics by two mechanisms: one includes activation of PAK and the resulting inhibition of F-actin depolymerization via LIMK activation, and the second enhances the activity of actin nucleation-promoting factors leading to the nucleation of nascent actin filaments (Gong et al., 2004). Both mechanisms modulate endothelial cell migration during vascular formation.

Another mechanism by which VEGF promotes endothelial cell migration, proliferation, and tube formation includes the activation of LIMK1 by MAPKAPK-2 (Kobayashi et al., 2006). Kobayashi and colleagues showed that VEGF-stimulated endothelial cells activate LIMK through phosphorylation of LIMK1 by MAPKAPK-2 in a signaling pathway composed of p38-MAPKAPK-2-LIMK1 (Kobayashi et al., 2006). Notably, it was observed that LIMK1 was activated downstream of p38 MAPK by phosphorylation at Ser-323. Furthermore, it was demonstrated that Thr508 was dispensable for LIMK1 activation by VEGF, as a T508V LIMK1 mutant could still phosphorylate cofilin. Moreover, the phosphorylation of Ser-323 in LIMK1 was deemed essential for VEGF-induced cell migration and stress fiber formation, as inhibition of MAPKAPK-2 suppressed VEGF-induced LIMK1 activation and prevented endothelial cell migration (Kobayashi et al., 2006). This is consistent with a previous study that showed the p38-MAPKAPK-2 signaling pathway is involved in VEGF-induced actin reorganization and cell migration through phosphorylation of HSP-27 (Rousseau et al., 2000). Unphosphorylated HSP-27 behaves as an F-actin cap-binding protein that prevents actin polymerization. HSP-27 phosphorylation by MAPKAPK-2 modifies its supramolecular structure. It enables its release from the capped filaments, generating new polymerization sites and allowing the addition of new actin monomers needed to increase actin polymerization (Rousseau et al., 2000). A similar study showed that annexin 1 regulates endothelial cell migration in response to VEGF via p38-MAPKAPK-2 (Cote et al., 2010). Annexin 1 is a protein whose phosphorylation is enhanced by VEGF and impaired by p38 inhibition. It was shown that LIMK1 phosphorylates annexin

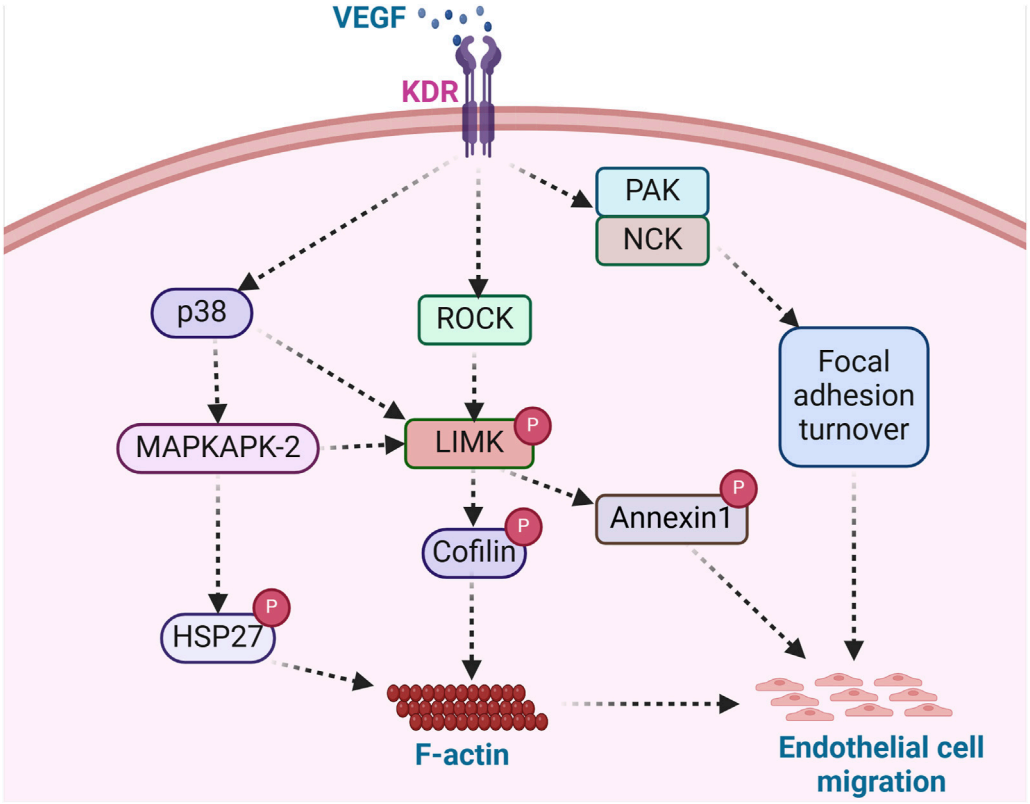

FIGURE 4
LIMK acts as an integral regulator of endothelial cell migration. Angiogenesis modulators such as VEGF bind surface receptors in endothelial cells and trigger the activation of ROCK, PAK/NCK, and p38 signaling pathways. ROCK activation, stimulated by VEGF, facilitates LIMK-induced cofilin deactivation and subsequent actin polymerization, while PAK/NCK activation reinforces focal adhesion turnover. LIMK-mediated annexin1 phosphorylation and enhanced focal adhesion turnover promote endothelial cell migration. The phosphorylation of Hsp27, a key regulator of actin dynamics, further stimulates actin polymerization, contributing to endothelial cell migration. This signaling cascade exemplifies the role of angiogenic factors in orchestrating cellular processes involved in endothelial cell migration. (KDR: Kinase insert domain receptor; NCK: non-catalytic tyrosine kinase adaptor protein; HSP27: Heat shock protein 27).

1 downstream of the p38-MAPKAPK-2 pathway in response to VEGF. Therefore, the phosphorylation of annexin 1 is considered a vital process required for sustained cell migration and angiogenesis (Martin et al., 2008). This indicates that LIMK regulates endothelial cell migration through the phosphorylation of cofilin and via the phosphorylation of annexin 1 to promote cell movement and vascular formation.

3.6 LIMKs and endothelial permeability

The vascular endothelium plays a vital role in regulating tissue fluid balance by forming a semipermeable barrier that allows for the selective exchange of various solutes between the circulation and the interstitial space. The primary determinant of vascular permeability is the integrity of interendothelial junctions, which include adherens junctions, gap junctions, and tight junctions [for review, see Komarova et al. (2017)]. Under inflammatory conditions, maintenance of the interendothelial junctions is impaired, leading to increased vascular permeability. Due to the expression variance of several receptors for inflammatory cytokines in different regions of the vascular tree, microvascular permeability is particularly increased in post-capillary venules under inflammatory conditions (Michel and Curry, 1999). The primary mechanism by which inflammatory mediators increase vascular permeability is by forming gaps between endothelial cells (Spindler et al., 2010). During this process, adherens junctions and tight junctions are disrupted, thereby increasing fluid flow across intercellular gaps. Maintaining endothelial barrier properties also requires a finely tuned balance between actin polymerization and depolymerization, as both hyperpolymerization by jasplakinolide and depolymerization by cytochalasin D increase microvascular permeability *in vivo* (Waschke et al., 2005). Accordingly, a group of GTPases, including RhoA, Cdc42, Rac1, and Rap1 regulate cell adhesion partially by reorganizing the junction-associated cortical actin cytoskeleton (Spindler et al., 2010), which inherently implies the intervention of LIMK activity and cofilin during inflammation-induced vascular permeability (Pober and Sessa, 2007; Skaria et al., 2016).

Recently, the mechanism by which LIMK2 contributes to disrupting barrier function and monolayer integrity through Wnt5A signaling in human coronary artery endothelial cells was determined (Skaria et al., 2017b; Skaria et al., 2017a). Wnt5A is a lipid-modified signaling protein present at high concentrations in the sera and bone marrow of patients with septic shock and severe systemic inflammation (Pereira et al., 2008; Angers and Moon,

TABLE 1 Representative studies on the role of LIMK in cardiovascular diseases.

CVD	Cells involved	LIMK isoform	References
Diabetes-associated vascular endothelial stiffening (Discussed in section 3.1)	Human umbilical vein endothelial cells	Unknown	Power et al. (2023), Power et al. (2024b)
Inward remodeling (Discussed in section 3.1)	VSMCs	Unknown	Foote et al. (2016)
Hypertension (Discussed in section 3.1)	VSMCs	Unknown	Morales-Quinones et al. (2020)
Intracranial aneurysms (Discussed in section 3.2)	VSMCs	LIMK1	Akagawa et al. (2006)
Vascular cell migration (Discussed in section 3.3 and 3.5)	Human umbilical vein endothelial cells and human aortic smooth muscle cells	LIMK1	Kobayashi et al. (2006), San Martin et al. (2008)
Coronary artery leakage (Discussed in section 3.6)	Human coronary artery endothelial cells	LIMK2	Skaria et al., (2017b), Skaria et al. (2017a)
Atrial fibrillation (Discussed in section 4)	Cardiac fibroblasts	LIMK1	Chen et al. (2019)
Ocular hypertension (Discussed in section 6)	Unknown	LIMK2	Harrison et al. (2009), Harrison et al. (2015)
Thrombsis (Discussed in section 5)	Platelets	LIMK1	Pandey et al. (2006), Antonipillai et al. (2019)

2009). Wnt5A targets and activates ROCK to phosphorylate LIMK2 and cofilin, thereby promoting the formation of actin stress fibers. This leads to the disruption of VE-cadherin and β-catenin at adherens junctions, forming interendothelial gaps and increasing the permeability of the endothelial monolayer (Skaria et al., 2017a). Wnt5A acts through the Ryk receptor to affect endothelial barrier function, as suppressing Ryk expression inhibits Wnt5A-induced hyperpermeability (Skaria et al., 2017b). Indeed, it was shown that Ryk-specific Wnt inhibitory factor 1 (WIF1) (Green et al., 2014) inhibited Wnt5A activity and reduced the development of F-actin stress fibers caused by Wnt5A (Skaria et al., 2016; Skaria et al., 2017b). As the cortical actin cytoskeleton spans the entire circumference of endothelial cells and comprises F-actin bundles that are associated with tight junctions and adherens junctions, it is potentially possible to improve endothelial barrier properties by enhancing junctional protein stability through strengthening of cortical actin (Spindler et al., 2010). There is a preponderance of evidence that supports this idea and shows that multiple GTPases use this method to control permeability, most notably Rac1 and Cdc42 (Adamson et al., 2002; Kouklis et al., 2004; Mehta and Malik, 2006; Baumer et al., 2008). Overall, intervening in this mechanism via modulation of LIMK activity may represent a potentially promising approach for treating vascular leakage resulting from inflammation.

4 LIMKs roles in the heart

The LIMKs are important participants in cardiomyocyte embryonic development, cardiomyocyte maintenance, and cardiac performance (Li et al., 2012). Furthermore, LIMK activity has been associated with the appropriate formation of cardiac organoids using human pluripotent stem cells in culture (Noh et al., 2023). The role of LIMK in cardiac organoid formation was determined using the potent LIMK inhibitor, LIMKi3, and appeared to involve the appropriate maturation and stabilization of both cardiomyocytes and blood vessels. Indeed, it has been well documented that RhoA-ROCK signaling provides cardioprotective effects. This appears to occur via the activity of LIMK on cofilin in cardiomyocytes (Kilian et al., 2021) in addition to the upstream stimulation of ECM-integrin cascades. As such, the LIMKs have been implicated in both physiological and pathological cardiac phenomena, providing an ample scenario for the roles that LIMKs play in CVD and the potential novel therapeutic use of LIMK inhibition to ameliorate CVD (Table 1).

LIMK activity has been particularly implicated in the development of atrial fibrillation and valvular heart disease. Atrial fibrillation is an irregular heart rhythm that begins at the upstream chambers of the heart (atria) and often causes an abnormally fast heart rate. Patients who suffer from recurrent atrial fibrillation are at an increased risk for valvular heart disease. The pathophysiology of atrial fibrillation is characterized by a gradual development of atrial fibrosis and abnormal electrical conduction of ventricular impulses. One key player in the development of atrial fibrillation is the profibrotic molecule, transforming growth factor-β (TGF-β). LIMK1 interacts with TGF-β to modulate actin cytoskeletal dynamics and microtubule stability. In addition, TGFβ1 promotes actin polymerization through the ROCK1-LIMK-cofilin phosphorylation pathway, which can be abolished via ROCK1 inhibition (Vardouli et al., 2005). It has also been shown that TGF-β promotes the differentiation of cardiac fibroblasts into myofibroblasts. Thus, activation of LIMK by TGF-β may be a mechanism by which LIMK promotes cardiac fibrosis. Considering the role of LIMK1 in tissue remodeling, Chen et al. collected clinical data and biopsies of the right atrial appendages from patients with valvular heart diseases to assess the role of LIMK1 in the pathophysiology of atrial fibrillation (Chen et al., 2019). Data from that study showed that LIMK1 expression was greater in patients with atrial fibrillation than in those with sinus rhythm.

It was further discovered that LIMK1 downregulation prevents collagen I and collagen II mRNA levels from increasing due to TGF-β interaction with LIMK1. This suggests that increased LIMK1 expression may promote fibrosis and ECM buildup, which could contribute to atrial fibrosis in atrial fibrillation. In addition, TGF-β promotes LIMK1 expression in primary cardiac fibroblasts, and LIMK1 downregulation has been used to prevent TGF-β driven cardiac fibroblast differentiation into myofibroblasts (Chen et al., 2019). Similar results were found in a prior work that demonstrated the downregulation of LIMK1 inhibited fibronectin expression and delayed cell migration in corneal fibroblasts (Gorovoy et al., 2008). LIMK interacts with TGF-β to promote cardiac fibrosis by increasing the deposition of ECM by cardiac fibroblasts and appears to regulate endothelial to mesenchymal transition of atrial endothelium to promote atrial fibrosis further (Lai et al., 2022). Therefore, LIMK inhibitors may represent a promising therapeutic strategy for the amelioration of atrial fibrosis, fibrillation, and associated valvular heart disease.

5 LIMKs and microtubules

Microtubules are filamentous polymers comprised of α- and β-tubulin heterodimers that participate in several cellular processes such as mitosis, migration, organelle trafficking, and protein transport (Gundersen and Cook, 1999; Waterman-Storer and Salmon, 1999). These dynamic polymers are regulated by a balance between microtubule-stabilizing and microtubule-destabilizing molecules (Andersen, 2000; Niethammer et al., 2007). In turn, microtubule dynamics can modulate intracellular signal transduction (Gundersen and Cook, 1999). For example, microtubule disruption enhances the formation of F-actin stress fibers and promotes cell contractility (Danowski, 1989). Indeed, it has been found that microtubule disruption by agents such as vinblastine and nocodazole promotes focal adhesion formation and rapid F-actin assembly. In contrast, microtubule stabilization with taxol prevents these effects (Bershadsky et al., 1996). It is also well documented that the Rho GTPases are necessary for microtubule-mediated regulation of the actin cytoskeleton (Wittmann and Waterman-Storer, 2001). However, little is known about the role of LIMK activity in microtubule stability. Some insights into the role of the LIMKs on the interaction between the formation and stability of the actin and microtubular cytoskeleton come from studies on the effects of thrombin in cells. Treatment of cells with thrombin promotes microtubule destabilization, leading to the formation of F-actin stress fibers. Thrombin is known to activate RhoA and ROCK (Essler et al., 1998). In contrast, inhibition of ROCK with Y27632 abolishes the effect of thrombin-induced F-actin stress fiber formation and prevents thrombin-induced destabilization of microtubules (Birukova et al., 2004a). This suggests that thrombin acts through the RhoA-ROCK pathway to promote microtubule destabilization. As mentioned, the LIMKs are downstream targets of ROCK. This implicates them in microtubule destabilization. In support of this thesis, thrombin induces both LIMK1 phosphorylation and cofilin phosphorylation in a time-dependent manner in human pulmonary artery endothelial cells (Leonard et al., 2013). In addition, it has been recently reported in a mouse neuroblast cell line that the destabilization of microtubules with nocodazole results in increased phosphorylation of LIMK1 (Roy et al., 2024). It has also been demonstrated in osteoclasts that nocodazole treatment increases cofilin phosphorylation (Zalli et al., 2016). This suggests a positive feedback loop may exist in which LIMK activation induces microtubule destabilization, and microtubule disruption increases LIMK activation (Gorovoy et al., 2005; Roy et al., 2024). Whether this feedback loop is part of cell biological processes is unknown and, if so, how it is controlled requires further investigation.

As further evidence of the link that microtubule regulation has with actin cytoskeleton reorganization, Gorovoy et al. showed that LIMK1 plays a major role in microtubule destabilization, favoring actin polymerization in human endothelial cells (Gorovoy et al., 2005). They determined that endogenous LIMK1 colocalizes with microtubules to form a complex with tubulin via the LIMK1 PDZ domain. The disruption of microtubules induced by nocodazole, or thrombin, reduced the colocalization of LIMK1 with microtubules but enhanced the interaction of LIMK1 with F-actin. This is consistent with a previous study demonstrating that LIMK inhibition with the compound Pyr1 stabilizes microtubules and abrogates neoplastic cell growth (Prudent et al., 2012). In a similar fashion, siRNA-mediated downregulation of endogenous LIMK1 has been shown to prevent thrombin-induced microtubule destabilization and inhibit thrombin-induced actin polymerization (Gorovoy et al., 2005). Interestingly, the interaction of LIMK1 with tubulin is drastically reduced when ROCK2 is expressed in endothelial cells but increases the interaction between LIMK1 and actin. Consequently, the knockdown of LIMK1 suppresses thrombin-induced microtubule destabilization and F-actin polymerization. This indicates that LIMK1 activity is necessary for orchestrating thrombin-induced actin polymerization and microtubule destabilization. Indeed, the crosstalk between the actin and microtubule cytoskeleton is needed for optimal cellular functions such as migration, cytokinesis, polarity, and locomotion (Rodriguez et al., 2003). Therefore, the findings summarized above provide insight into how LIMK crosstalk with ROCK mediates microtubule disassembly and promotes the formation of F-actin stress fibers.

6 LIMK inhibitors as therapeutic agents

As already established, the LIMKs contribute to a broad spectrum of cellular activities, including cell motility, proliferation, differentiation, gene expression, apoptosis, morphogenesis, etc., via the regulation of cytoskeletal dynamics (Scott and Olson, 2007; Prunier et al., 2017). Correspondingly, LIMK activity may be associated with a wide variety of pathologies, including hypertension (Morales-Quinones et al., 2020), aneurysm (Akagawa et al., 2006), erectile dysfunction (Park et al., 2021), glaucoma (Harrison et al., 2015), cancer resistance to microtubule-targeting chemotherapy (Acevedo et al., 2007; Mardilovich et al., 2015), pain (Yang et al., 2017), neuronal diseases (Ben Zablah et al., 2021), neurofibromatosis (Petrilli et al., 2014), etc. At the same time, its inhibition has emerged as a prospective therapeutic target for some of these diverse diseases. Several LIMK inhibitors have been developed for the treatment of conditions such as breast cancer (BMS3, LX7101, Pyr1) (Harrison et al., 2015; Prunier et al., 2016; Malvi et al., 2020), pancreatic cancer

(T56-LIMKi) (Rak et al., 2014), Alzheimer's disease (SR7826) (Henderson et al., 2019), Leukemia (Pyr1) (Prudent et al., 2012), Glaucoma and ocular hypertension (LX7101) (Harrison et al., 2009; Harrison et al., 2015). Although LIMK activity modulation appears to be a potential target for ameliorating the development and progression of cardiovascular disorders, no direct LIMK inhibitors have been approved for the treatment of CVD. Since the first report on the development of a selective inhibitor of LIMK activity by Bristol-Myers-Squibb in 2006, only one such molecule has reached clinical trials for treating glaucoma (Ross-Macdonald et al., 2008). The highly conserved chemical features of kinase ATP binding sites often make finding or developing selective LIMK inhibitors challenging (Simard and Rauh, 2014). Therefore, substances that interact with the ATP binding pocket in the LIMKs, such as type I and type II inhibitors, frequently have the same inhibitory activity across many kinases with little to no selectivity. Other novel compounds have been developed using a wide range of chemical scaffolds for LIMK inhibition, with excellent results (Manetti, 2012; Berabez et al., 2022; Bukhari et al., 2022). However, most of the LIMK inhibitors available today are type 1 kinase inhibitors that bind to the active conformation of the LIMKs in the ATP pocket (Manetti, 2012; Bukhari et al., 2022).

Owing to the role of the LIMKs in regulating cytoskeletal dynamics and their position as downstream effectors of numerous signaling cascades, we consider LIMK inhibition to be a promising approach for the treatment of cardiovascular disorders. Notably, it has been shown that LIMK inhibition destabilizes the intracellular cytoskeleton of platelets, thereby inhibiting platelet aggregation and adhesion to fibrinogen hence, promoting thrombolysis (Estevez et al., 2013; Antonipillai et al., 2019). Recently, Morales-Quinones et al. used the cell-permeable and potent LIMK inhibitor, LIMKi3, as a tool to stop the progression of arterial remodeling (Morales-Quinones et al., 2020). LIMKi3 effectively suppresses cellular LIMK-associated cofilin phosphorylation without affecting tubulin polymerization or inducing cytotoxicity. LIMK inhibition thus activates cofilin and promotes F-actin stress fiber depolymerization. In agreement with this, Morales-Quinones et al. found that LIMK inhibition reduced the stiffness caused by prolonged exposure to the vasoconstrictor agonists norepinephrine and angiotensin II in human VSMCs in culture and isolated human arteries under pressure myography. LIMKi3 also ameliorated arterial inward remodeling in mice with angiotensin II-induced hypertension (Morales-Quinones et al., 2020). Similarly, Foote et al. demonstrated that LIMK inhibition prevented the inward remodeling associated with the exposure of isolated arteries to the vasoconstrictor agonist serotonin combined with the nitric oxide synthase competitive inhibitor L-NAME (Foote et al., 2016). These studies provide strong evidence for considering LIMK inhibition as a potential therapeutic avenue to ameliorate aberrant arterial remodeling and its associated cardiovascular diseases.

More recent studies have been conducted on the use of LIMK inhibition for the treatment of multiple diseases. Several LIMK inhibitors have been synthesized and used to reduce intraocular pressure (Harrison et al., 2009; Boland et al., 2015; Yin et al., 2015). ROCK inhibitors can be used for that purpose, but they are associated with several side effects (Tanihara et al., 2008). This is overcome using the pyrrolopyrimidine class of LIMK 2 inhibitors, effectively lowering ocular pressure and associated glaucoma with reduced side effects (Harrison et al., 2009; Harrison et al., 2015). Berabez and colleagues recently reviewed several LIMK inhibitors that have progressed to the preclinical trial stage. However, none of them are specifically intended for the treatment of cardiovascular disorders (Berabez et al., 2022). New LIMK inhibitors have been developed, and their characteristics, including their selectivity, cell biological activity, and efficiency, have been described (Ariawan et al., 2021; Rybin et al., 2022; Champire et al., 2024). This furthers the notion that LIMK inhibition has promising therapeutic potential for multiple disease conditions. Some of the main concerns reported as preventing the advancement of LIMK into clinical trials are addressed with the new inhibitors (Manetti, 2018; Berabez et al., 2022; Champire et al., 2024). These improvements include a better selectivity of the inhibitors presenting little or no effects on kinases other than the LIMKs and even prefer one of the LIMKs, which would allow them to target cellular processes specific to one of the LIMK isoforms (Berabez et al., 2022; Champire et al., 2024). The capacity or incapacity of the LIMK inhibitors to cross the blood-brain barrier has also been a concern. In this regard, the inability of a compound to cross the blood-brain barrier may be an advantage for using LIMK inhibition to treat vascular diseases such as endothelial dysfunction, as the inability of compounds to cross the blood-brain barrier would limit neurological effects while maintaining endothelial targeting. Although all LIMK and cofilin isoforms appear to be expressed in smooth muscle, endothelium, and cardiomyocytes (Boengler et al., 2003; Bongalon et al., 2004; Pipp et al., 2004; Gorovoy et al., 2005; Goyal et al., 2005; Acevedo et al., 2006; Dai et al., 2006; Goyal et al., 2006; Kobayashi et al., 2006; Fazal et al., 2009; Cote et al., 2010; Lindstrom et al., 2011; Subramanian et al., 2015; Wang et al., 2016; Chatzifrangkeskou et al., 2018; Yu et al., 2021; Le Dour et al., 2022; Du et al., 2024), the level of expression of each enzyme isoform in different regions of the vascular tree, the heart, or specific cell types within those regions has not been thoroughly characterized. Such information would help choose the appropriate LIMK inhibitor to target a particular cellular type and pathophysiological process. This should be followed by testing the selected inhibitors in relevant preclinical animal models of cardiovascular diseases that involve actin polymerization derangements. Overall, research on the effects of LIMK inhibition indicates that LIMK inhibitors are still waiting to be harnessed in clinical settings and can potentially become effective treatments for cardiovascular disorders.

7 Conclusion

The LIMKs play preponderant roles in multiple cellular mechanisms. Due to the role that LIMK activity plays in cytoskeletal dynamics, it is considered particularly prominent in phenomena associated with cell migration, contraction, and stiffening. In the cardiovascular system, these phenomena are related to pathophysiological processes such as vascular remodeling, stiffening, permeability, angiogenesis, atrial stiffening, and fibrillation. Several LIMK inhibitors have been developed over the years, but these have been primarily tested as therapeutic agents for reducing intraocular pressure and cancer. Although the inhibition of LIMK activity should be considered a potential

avenue for treating several cardiovascular diseases, their efficacy and tolerance as therapeutic agents for this purpose remains to be determined.

Author contributions

OL: Conceptualization, Writing–original draft. CF: Writing–original draft. GP: Writing–original draft. CM-A: Writing–review and editing. JP: Conceptualization, Writing–review and editing. LM-L: Conceptualization, Writing–review and editing.

Funding

The author(s) declare that financial support was received for the research, authorship, and/or publication of this article. Content and ideas presented herein resulted from work supported, in part, by grants from the National Institutes of Health (R01HL088105 to LAM-L and R01082413 to CM-A, JP, and LM-L).

Conflict of interest

The authors declare that the research was conducted in the absence of any commercial or financial relationships that could be construed as a potential conflict of interest.

Generative AI statement

The author(s) declare that no Generative AI was used in the creation of this manuscript.

Publisher's note

References

Abedi, H., and Zachary, I. (1997). Vascular endothelial growth factor stimulates tyrosine phosphorylation and recruitment to new focal adhesions of focal adhesion kinase and paxillin in endothelial cells. *J. Biol. Chem.* 272, 15442–15451. doi:10.1074/jbc.272.24.15442

Acevedo, K., Li, R., Soo, P., Suryadinata, R., Sarcevic, B., Valova, V. A., et al. (2007). The phosphorylation of p25/TPPP by LIM kinase 1 inhibits its ability to assemble microtubules. *Exp. Cell Res.* 313, 4091–4106. doi:10.1016/j.yexcr.2007.08.012

Acevedo, K., Moussi, N., Li, R., Soo, P., and Bernard, O. (2006). LIM kinase 2 is widely expressed in all tissues. *J. Histochem Cytochem* 54, 487–501. doi:10.1369/jhc.5C6813.2006

Adamson, R. H., Curry, F. E., Adamson, G., Liu, B., Jiang, Y., Aktories, K., et al. (2002). Rho and rho kinase modulation of barrier properties: cultured endothelial cells and intact microvessels of rats and mice. *J. Physiology* 539, 295–308. doi:10.1113/jphysiol.2001.013117

Ailawadi, G., Eliason, J. L., and Upchurch, G. R. (2003). Current concepts in the pathogenesis of abdominal aortic aneurysm. *J. Vasc. Surg.* 38, 584–588. doi:10.1016/s0741-5214(03)00324-0

Akagawa, H., Tajima, A., Sakamoto, Y., Krischek, B., Yoneyama, T., Kasuya, H., et al. (2006). A haplotype spanning two genes, ELN and LIMK1, decreases their transcripts and confers susceptibility to intracranial aneurysms. *Hum. Mol. Genet.* 15, 1722–1734. doi:10.1093/hmg/ddl096

Alahari, S. K., Lee, J. W., and Juliano, R. L. (2000). Nischarin, a novel protein that interacts with the integrin alpha5 subunit and inhibits cell migration. *J. Cell Biol.* 151, 1141–1154. doi:10.1083/jcb.151.6.1141

Ali, M. H., and Schumacker, P. T. (2002). Endothelial responses to mechanical stress: where is the mechanosensor? *Crit. Care Med.* 30, S198–S206. doi:10.1097/00003246-200205001-00005

Amano, M., Ito, M., Kimura, K., Fukata, Y., Chihara, K., Nakano, T., et al. (1996). Phosphorylation and activation of myosin by Rho-associated kinase (Rho-kinase). *J. Biol. Chem.* 271, 20246–20249. doi:10.1074/jbc.271.34.20246

Amano, T., Tanabe, K., Eto, T., Narumiya, S., and Mizuno, K. (2001). LIM-kinase 2 induces formation of stress fibres, focal adhesions and membrane blebs, dependent on its activation by Rho-associated kinase-catalysed phosphorylation at threonine-505. *Biochem. J.* 354, 149–159. doi:10.1042/0264-6021:3540149

Andersen, S. S. (2000). Spindle assembly and the art of regulating microtubule dynamics by MAPs and Stathmin/Op18. *Trends Cell Biol.* 10, 261–267. doi:10.1016/s0962-8924(00)01786-4

Angers, S., and Moon, R. T. (2009). Proximal events in Wnt signal transduction. *Nat. Rev. Mol. Cell Biol.* 10, 468–477. doi:10.1038/nrm2717

Antonipillai, J., Rigby, S., Bassler, N., Peter, K., and Bernard, O. (2019). Pharmacological inhibition of LIM kinase pathway impairs platelets functionality and facilitates thrombolysis. *Exp. Cell Res.* 382, 111458. doi:10.1016/j.yexcr.2019.06.003

Ariawan, D., Au, C., Paric, E., Fath, T., Ke, Y. D., Kassiou, M., et al. (2021). The nature of diamino linker and halogen bonding define selectivity of pyrrolopyrimidine-based LIMK1 inhibitors. *Front. Chem.* 9, 781213. doi:10.3389/fchem.2021.781213

Aroor, A. R., Habibi, J., Nistala, R., Ramirez-Perez, F. I., Martinez-Lemus, L. A., Jaffe, I. Z., et al. (2019). Diet-induced obesity promotes kidney endothelial stiffening and fibrosis dependent on the endothelial mineralocorticoid receptor. *Hypertension* 73, 849–858. doi:10.1161/HYPERTENSIONAHA.118.12198

Baumer, Y., Burger, S., Curry, F. E., Golenhofen, N., Drenckhahn, D., and Waschke, J. (2008). Differential role of Rho GTPases in endothelial barrier regulation dependent on endothelial cell origin. *Histochem. Cell Biol.* 129, 179–191. doi:10.1007/s00418-007-0358-7

Ben Zablah, Y., Zhang, H., Gugustea, R., and Jia, Z. (2021). LIM-kinases in synaptic plasticity, memory, and brain diseases. *Cells* 10, 2079. doi:10.3390/cells10082079

Berabez, R., Routier, S., Benedetti, H., Ple, K., and Vallee, B. (2022). LIM kinases, promising but reluctant therapeutic targets: chemistry and preclinical validation *in vivo*. *Cells* 11, 2090. doi:10.3390/cells11132090

Bershadsky, A., Chausovsky, A., Becker, E., Lyubimova, A., and Geiger, B. (1996). Involvement of microtubules in the control of adhesion-dependent signal transduction. *Curr. Biol. CB* 6, 1279–1289. doi:10.1016/s0960-9822(02)70714-8

Birukova, A. A., Birukov, K. G., Smurova, K., Adyshev, D., Kaibuchi, K., Alieva, I., et al. (2004a). "Novel role of microtubules in thrombin-induced endothelial barrier dysfunction,", 18. FASEB journal: official publication of the Federation of American Societies for Experimental Biology, 1879–1890. doi:10.1096/fj.04-2328com

Birukova, A. A., Smurova, K., Birukov, K. G., Usatyuk, P., Liu, F., Kaibuchi, K., et al. (2004b). Microtubule disassembly induces cytoskeletal remodeling and lung vascular barrier dysfunction: role of Rho-dependent mechanisms. *J. Cell Physiol.* 201, 55–70. doi:10.1002/jcp.20055

Boengler, K., Pipp, F., Broich, K., Fernandez, B., Schaper, W., and Deindl, E. (2003). Identification of differentially expressed genes like cofilin2 in growing collateral arteries. *Biochem. Biophys. Res. Commun.* 300, 751–756. doi:10.1016/s0006-291x(02)02921-2

Boland, S., Bourin, A., Alen, J., Geraets, J., Schroeders, P., Castermans, K., et al. (2015). Design, synthesis and biological characterization of selective LIMK inhibitors. *Bioorg. and Med. Chem. Lett.* 25, 4005–4010. doi:10.1016/j.bmcl.2015.07.009

Bongalon, S., Dai, Y. P., Singer, C. A., and Yamboliev, I. A. (2004). PDGF and IL-1beta upregulate cofilin and LIMK2 in canine cultured pulmonary artery smooth muscle cells. *J. Vasc. Res.* 41, 412–421. doi:10.1159/000081247

Bravo-Cordero, J. J., Magalhaes, M. A., Eddy, R. J., Hodgson, L., and Condeelis, J. (2013). Functions of cofilin in cell locomotion and invasion. *Nat. Rev. Mol. Cell Biol.* 14, 405–415. doi:10.1038/nrm3609

Bukhari, S. N. A., Tandiary, M. A., Al-Sanea, M. M., Abdelgawad, M. A., Chee, C. F., and Hussain, M. A. (2022). Small molecules as LIM kinase inhibitors. *Curr. Med. Chem.* 29, 2995–3027. doi:10.2174/0929867328666211026120335

Burridge, K., and Connell, L. (1983). A new protein of adhesion plaques and ruffling membranes. *J. Cell Biol.* 97, 359–367. doi:10.1083/jcb.97.2.359

Casanova-Sepulveda, G., and Boggon, T. J. (2024). Regulation and signaling of the LIM domain kinases. *Bioessays*, e2400184. doi:10.1002/bies.202400184

Casanova-Sepulveda, G., Sexton, J. A., Turk, B. E., and Boggon, T. J. (2023). Autoregulation of the LIM kinases by their PDZ domain. *Nat. Commun.* 14, 8441. doi:10.1038/s41467-023-44148-4

Champire, A., Berabez, R., Braka, A., Cosson, A., Corret, J., Girardin, C., et al. (2024). Tetrahydropyridine LIMK inhibitors: structure activity studies and biological characterization. *Eur. J. Med. Chem.* 271, 116391. doi:10.1016/j.ejmech.2024.116391

Chang, S., Song, S., Lee, J., Yoon, J., Park, J., Choi, S., et al. (2014). Phenotypic modulation of primary vascular smooth muscle cells by short-term culture on micropatterned substrate. *PLoS ONE* 9, e88089. doi:10.1371/journal.pone.0088089

Chatterjee, D., Preuss, F., Dederer, V., Knapp, S., and Mathea, S. (2022). Structural aspects of LIMK regulation and pharmacology. *Cells* 11, 142. doi:10.3390/cells11010142

Chatzifrangkeskou, M., Yadin, D., Marais, T., Chardonnet, S., Cohen-Tannoudji, M., Mougenot, N., et al. (2018). Cofilin-1 phosphorylation catalyzed by ERK1/2 alters cardiac actin dynamics in dilated cardiomyopathy caused by lamin A/C gene mutation. *Hum. Mol. Genet.* 27, 3060–3078. doi:10.1093/hmg/ddy215

Chava, K. R., Karpurapu, M., Wang, D., Bhanoori, M., Kundumani-Sridharan, V., Zhang, Q., et al. (2009). CREB-mediated IL-6 expression is required for 15(S)-hydroxyeicosatetraenoic acid-induced vascular smooth muscle cell migration. *Arterioscler. Thromb. Vasc. Biol.* 29, 809–815. doi:10.1161/ATVBAHA.109.185777

Chen, Q., Gimple, R. C., Li, G., Chen, J., Wu, H., Li, R., et al. (2019). LIM kinase 1 acts as a profibrotic mediator in permanent atrial fibrillation patients with valvular heart disease. *J. Biosci.* 44, 16. doi:10.1007/s12038-018-9825-7

Chen, X., and Macara, I. G. (2006). Par-3 mediates the inhibition of LIM kinase 2 to regulate cofilin phosphorylation and tight junction assembly. *J. Cell Biol.* 172, 671–678. doi:10.1083/jcb.200510061

Cheung, Y.-F. (2010). "CHAPTER 6 - systemic circulation," in *Paediatric cardiology*. Editors R. H. Anderson, E. J. Baker, D. J. Penny, A. N. Redington, M. L. Rigby, G. Wernovsky, et al. Third Edition (Philadelphia: Churchill Livingstone), 91–116.

Chiu, J.-J., and Chien, S. (2011). Effects of disturbed flow on vascular endothelium: pathophysiological basis and clinical perspectives. *Physiol. Rev.* 91, 327–387. doi:10.1152/physrev.00047.2009

Choi, C. K., Vicente-Manzanares, M., Zareno, J., Whitmore, L. A., Mogilner, A., and Horwitz, A. R. (2008). Actin and alpha-actinin orchestrate the assembly and maturation of nascent adhesions in a myosin II motor-independent manner. *Nat. Cell Biol.* 10, 1039–1050. doi:10.1038/ncb1763

Cote, M. C., Lavoie, J. R., Houle, F., Poirier, A., Rousseau, S., and Huot, J. (2010). Regulation of vascular endothelial growth factor-induced endothelial cell migration by LIM kinase 1-mediated phosphorylation of annexin 1. *J. Biol. Chem.* 285, 8013–8021. doi:10.1074/jbc.M109.098665

Cuberos, H., Vallée, B., Vourc'h, P., Tastet, J., Andres, C. R., and Bénédetti, H. (2015). Roles of LIM kinases in central nervous system function and dysfunction. *FEBS Lett.* 589, 3795–3806. doi:10.1016/j.febslet.2015.10.032

Dai, Y.-P., Bongalon, S., Tian, H., Parks, S. D., Mutafova-Yambolieva, V. N., and Yamboliev, I. A. (2006). Upregulation of profilin, cofilin-2 and LIMK2 in cultured pulmonary artery smooth muscle cells and in pulmonary arteries of monocrotaline-treated rats. *Vasc. Pharmacol.* 44, 275–282. doi:10.1016/j.vph.2005.11.008

Danowski, B. A. (1989). Fibroblast contractility and actin organization are stimulated by microtubule inhibitors. *J. Cell Sci.* 93 (Pt 2), 255–266. doi:10.1242/jcs.93.2.255

Davies, P. F. (1995). Flow-mediated endothelial mechanotransduction. *Physiol. Rev.* 75, 519–560. doi:10.1152/physrev.1995.75.3.519

Davis, M. J., Earley, S., Li, Y.-S., and Chien, S. (2023). Vascular mechanotransduction. *Physiol. Rev.* 103, 1247–1421. doi:10.1152/physrev.00053.2021

Dechert, M. A., Holder, J. M., and Gerthoffer, W. T. (2001). p21-activated kinase 1 participates in tracheal smooth muscle cell migration by signaling to p38 Mapk. *Am. J. Physiology. Cell Physiology* 281, C123–C132. doi:10.1152/ajpcell.2001.281.1.C123

Ding, Y., Milosavljevic, T., and Alahari, S. K. (2008). Nischarin inhibits LIM kinase to regulate cofilin phosphorylation and cell invasion. *Mol. Cell Biol.* 28, 3742–3756. doi:10.1128/MCB.01832-07

Doanes, A. M., Irani, K., Goldschmidt-Clermont, P. J., and Finkel, T. (1998). A requirement for rac1 in the PDGF-stimulated migration of fibroblasts and vascular smooth cells. *Biochem. Mol. Biol. Int.* 45, 279–287. doi:10.1080/15216549800202652

Dorland, Y. L., and Huveneers, S. (2017). Cell-cell junctional mechanotransduction in endothelial remodeling. *Cell Mol. Life Sci.* 74, 279–292. doi:10.1007/s00018-016-2325-8

Dong, Q., Ji, Y. S., Cai, C., and Chen, Z. Y. (2012). LIM kinase 1 (LIMK1) interacts with tropomyosin-related kinase B (TrkB) and Mediates brain-derived neurotrophic factor (BDNF)-induced axonal elongation. *J. Biol. Chem.* 287 (50), 41720–41731. doi:10.1074/jbc.M112.405415

Du, Y., Zhu, P., Li, Y., Yu, J., Xia, T., Chang, X., et al. (2024). DNA-PKcs phosphorylates Cofilin2 to induce endothelial dysfunction and microcirculatory disorder in endotoxemic cardiomyopathy. *Res. Wash D.C.* 7, 0331. doi:10.34133/research.0331

Edwards, D. C., Sanders, L. C., Bokoch, G. M., and Gill, G. N. (1999). Activation of LIM-kinase by Pak1 couples Rac/Cdc42 GTPase signalling to actin cytoskeletal dynamics. *Nat. Cell Biol.* 1, 253–259. doi:10.1038/12963

Eliceiri, B. P., Puente, X. S., Hood, J. D., Stupack, D. G., Schlaepfer, D. D., Huang, X. Z., et al. (2002). Src-mediated coupling of focal adhesion kinase to integrin alpha(v)beta5 in vascular endothelial growth factor signaling. *J. Cell Biol.* 157, 149–160. doi:10.1083/jcb.200109079

Essler, M., Amano, M., Kruse, H.-J., Kaibuchi, K., Weber, P. C., and Aepfelbacher, M. (1998). Thrombin inactivates myosin light chain phosphatase via rho and its target rho kinase in human endothelial cells. *J. Biol. Chem.* 273, 21867–21874. doi:10.1074/jbc.273.34.21867

Estevez, B., Stojanovic-Terpo, A., Delaney, M. K., O'brien, K. A., Berndt, M. C., Ruan, C., et al. (2013). LIM kinase-1 selectively promotes glycoprotein Ib-IX-mediated TXA2 synthesis, platelet activation, and thrombosis. *Blood* 121, 4586–4594. doi:10.1182/blood-2012-12-470765

Fang, S., Wu, J., Reho, J. J., Lu, K. T., Brozoski, D. T., Kumar, G., et al. (2022). RhoBTB1 reverses established arterial stiffness in angiotensin II-induced hypertension by promoting actin depolymerization. *JCI Insight* 7, e158043. doi:10.1172/jci.insight.158043

Fazal, F., Bijli, K. M., Minhajuddin, M., Rein, T., Finkelstein, J. N., and Rahman, A. (2009). Essential role of cofilin-1 in regulating thrombin-induced RelA/p65 nuclear translocation and intercellular adhesion molecule 1 (ICAM-1) expression in endothelial cells. *J. Biol. Chem.* 284, 21047–21056. doi:10.1074/jbc.M109.016444

Fediuk, J., and Dakshinamurti, S. (2015). A role for actin polymerization in persistent pulmonary hypertension of the newborn. *Can. J. Physiol. Pharmacol.* 93, 185–194. doi:10.1139/cjpp-2014-0413

Ferrara, N., Gerber, H.-P., and Lecouter, J. (2003). The biology of VEGF and its receptors. *Nat. Med.* 9, 669–676. doi:10.1038/nm0603-669

Foletta, V. C., Lim, M. A., Soosairajah, J., Kelly, A. P., Stanley, E. G., Shannon, M., et al. (2003). Direct signaling by the BMP type II receptor via the cytoskeletal regulator LIMK1. *J. Cell Biol.* 162, 1089–1098. doi:10.1083/jcb.200212060

Foote, C. A., Castorena-Gonzalez, J. A., Staiculescu, M. C., Clifford, P. S., Hill, M. A., Meininger, G. A., et al. (2016). Brief serotonin exposure initiates arteriolar inward remodeling processes *in vivo* that involve transglutaminase activation and actin cytoskeleton reorganization. *Am. J. Physiol. Heart Circ. Physiol.* 310, H188–H198. doi:10.1152/ajpheart.00666.2015

Gardiner, J. (2021). Cytoskeletal tensegrity in microgravity. *Life (Basel)* 11, 1091. doi:10.3390/life11101091

Gerthoffer, W. T. (2007). Mechanisms of vascular smooth muscle cell migration. *Circ. Res.* 100, 607–621. doi:10.1161/01.RES.0000258492.96097.47

Gomez, D., and Owens, G. K. (2012). Smooth muscle cell phenotypic switching in atherosclerosis. *Cardiovasc Res.* 95, 156–164. doi:10.1093/cvr/cvs115

Gomez-Moron, A., Alegre-Gomez, S., Ramirez-Munoz, R., Hernaiz-Esteban, A., Carrasco-Padilla, C., Scagnetti, C., et al. (2024). Human T-cell receptor triggering requires inactivation of Lim kinase-1 by Slingshot-1 phosphatase. *Commun. Biol.* 7, 918. doi:10.1038/s42003-024-06605-8

Gong, C., Stoletov, K. V., and Terman, B. I. (2004). VEGF treatment induces signaling pathways that regulate both actin polymerization and depolymerization. *Angiogenesis* 7, 313–321. doi:10.1007/s10456-004-7960-2

Gorovoy, M., Han, J., Pan, H., Welch, E., Neamu, R., Jia, Z., et al. (2009). LIM kinase 1 promotes endothelial barrier disruption and neutrophil infiltration in mouse lungs. *Circ. Res.* 105, 549–556. doi:10.1161/CIRCRESAHA.109.195883

Gorovoy, M., Koga, T., Shen, X., Jia, Z., Yue, B. Y., and Voyno-Yasenetskaya, T. (2008). Downregulation of LIM kinase 1 suppresses ocular inflammation and fibrosis. *Mol. Vis.* 14, 1951–1959.

Gorovoy, M., Niu, J., Bernard, O., Profirovic, J., Minshall, R., Neamu, R., et al. (2005). LIM kinase 1 coordinates microtubule stability and actin polymerization in human endothelial cells. *J. Biol. Chem.* 280, 26533–26542. doi:10.1074/jbc.M502921200

Gotlieb, A. I. (1990). The endothelial cytoskeleton: organization in normal and regenerating endothelium. *Toxicol. Pathol.* 18, 603–617. doi:10.1177/019262339001804a10

Goyal, P., Pandey, D., Behring, A., and Siess, W. (2005). Inhibition of nuclear import of LIMK2 in endothelial cells by protein kinase C-dependent phosphorylation at Ser-283. *J. Biol. Chem.* 280, 27569–27577. doi:10.1074/jbc.M504448200

Goyal, P., Pandey, D., Brunnert, D., Hammer, E., Zygmunt, M., and Siess, W. (2013). Cofilin oligomer formation occurs *in vivo* and is regulated by cofilin phosphorylation. *PLoS One* 8, e71769. doi:10.1371/journal.pone.0071769

Goyal, P., Pandey, D., and Siess, W. (2006). Phosphorylation-dependent regulation of unique nuclear and nucleolar localization signals of LIM kinase 2 in endothelial cells. *J. Biol. Chem.* 281, 25223–25230. doi:10.1074/jbc.M603399200

Green, J., Nusse, R., and Van Amerongen, R. (2014). The role of Ryk and Ror receptor tyrosine kinases in Wnt signal transduction. *Cold Spring Harb. Perspect. Biol.* 6, a009175. doi:10.1101/cshperspect.a009175

Griffin, K. J., Simpson, K. R., Beckers, C. M. L., Newell, L. M., Cheah, L. T., Yuldasheva, N. Y., et al. (2021). Transglutaminase 2 moderates the expansion of mouse abdominal aortic aneurysms. *JVS Vasc. Sci.* 2, 95–109. doi:10.1016/j.jvssci.2021.04.002

Gundersen, G. G., and Cook, T. A. (1999). Microtubules and signal transduction. *Curr. Opin. Cell Biol.* 11, 81–94. doi:10.1016/s0955-0674(99)80010-6

Haque, N. S., Fallon, J. T., Pan, J. J., Taubman, M. B., and Harpel, P. C. (2004). Chemokine receptor-8 (CCR8) mediates human vascular smooth muscle cell chemotaxis and metalloproteinase-2 secretion. *Blood* 103, 1296–1304. doi:10.1182/blood-2002-05-1480

Harrison, B. A., Almstead, Z. Y., Burgoon, H., Gardyan, M., Goodwin, N. C., Healy, J., et al. (2015). Discovery and development of LX7101, a dual LIM-kinase and ROCK inhibitor for the treatment of glaucoma. *ACS Med. Chem. Lett.* 6, 84–88. doi:10.1021/ml500367g

Harrison, B. A., Whitlock, N. A., Voronkov, M. V., Almstead, Z. Y., Gu, K.-J., Mabon, R., et al. (2009). Novel class of LIM-kinase 2 inhibitors for the treatment of ocular hypertension and associated glaucoma. *J. Med. Chem.* 52, 6515–6518. doi:10.1021/jm901226j

Hayashi, K., and Hirayama, E. (2017). Age-related changes of wall composition and collagen cross-linking in the rat carotid artery - in relation with arterial mechanics. *J. Mech. Behav. Biomed. Mater.* 65, 881–889. doi:10.1016/j.jmbbm.2016.10.007

Hein, S., Kostin, S., Heling, A., Maeno, Y., and Schaper, J. (2000). The role of the cytoskeleton in heart failure. *Cardiovasc Res.* 45, 273–278. doi:10.1016/s0008-6363(99)00268-0

Henderson, B. W., Greathouse, K. M., Ramdas, R., Walker, C. K., Rao, T. C., Bach, S. V., et al. (2019). Pharmacologic inhibition of LIMK1 provides dendritic spine resilience against β-amyloid. *Sci. Signal* 12, eaaw9318. doi:10.1126/scisignal.aaw9318

Honma, M., Benitah, S. A., and Watt, F. M. (2006). Role of LIM kinases in normal and psoriatic human epidermis. *Mol. Biol. Cell* 17, 1888–1896. doi:10.1091/mbc.e05-12-1173

Hsu, F.-F., Lin, T.-Y., Chen, J.-Y., and Shieh, S.-Y. (2010). p53-Mediated transactivation of LIMK2b links actin dynamics to cell cycle checkpoint control. *Oncogene* 29, 2864–2876. doi:10.1038/onc.2010.40

Ingber, D. E. (2002). Mechanical signaling and the cellular response to extracellular matrix in angiogenesis and cardiovascular physiology. *Circ. Res.* 91, 877–887. doi:10.1161/01.res.0000039537.73816.e5

Ingber, D. E. (2003a). Tensegrity I. Cell structure and hierarchical systems biology. *J. Cell Sci.* 116, 1157–1173. doi:10.1242/jcs.00359

Ingber, D. E. (2003b). Tensegrity II. How structural networks influence cellular information processing networks. *J. Cell Sci.* 116, 1397–1408. doi:10.1242/jcs.00360

Ingber, D. E. (2006). Cellular mechanotransduction: putting all the pieces together again. *FASEB J. official Publ. Fed. Am. Soc. Exp. Biol.* 20, 811–827. doi:10.1096/fj.05-5424rev

Ingber, D. E., Wang, N., and Stamenovic, D. (2014). Tensegrity, cellular biophysics, and the mechanics of living systems. *Rep. Prog. Phys.* 77, 046603. doi:10.1088/0034-4885/77/4/046603

Janmey, P. A., and Mcculloch, C. A. (2007). Cell mechanics: integrating cell responses to mechanical stimuli. *Annu. Rev. Biomed. Eng.* 9, 1–34. doi:10.1146/annurev.bioeng.9.060906.151927

Jiang, X., Xu, Z., Jiang, S., Wang, H., Xiao, M., Shi, Y., et al. (2023). PDZ and LIM domain-encoding genes: their role in cancer development. *Cancers (Basel)* 15, 5042. doi:10.3390/cancers15205042

Kilian, L. S., Voran, J., Frank, D., and Rangrez, A. Y. (2021). RhoA: a dubious molecule in cardiac pathophysiology. *J. Biomed. Sci.* 28, 33. doi:10.1186/s12929-021-00730-w

Kobayashi, M., Nishita, M., Mishima, T., Ohashi, K., and Mizuno, K. (2006). MAPKAPK-2-mediated LIM-kinase activation is critical for VEGF-induced actin remodeling and cell migration. *EMBO J.* 25, 713–726. doi:10.1038/sj.emboj.7600973

Komarova, Y. A., Kruse, K., Mehta, D., and Malik, A. B. (2017). Protein interactions at endothelial junctions and signaling mechanisms regulating endothelial permeability. *Circ. Res.* 120, 179–206. doi:10.1161/CIRCRESAHA.116.306534

Kouklis, P., Konstantoulaki, M., Vogel, S., Broman, M., and Malik, A. B. (2004). Cdc42 regulates the restoration of endothelial barrier function. *Circ. Res.* 94, 159–166. doi:10.1161/01.RES.0000110418.38500.31

Kuivaniemi, H., Ryer, E. J., Elmore, J. R., and Tromp, G. (2015). Understanding the pathogenesis of abdominal aortic aneurysms. *Expert Rev. Cardiovasc Ther.* 13, 975–987. doi:10.1586/14779072.2015.1074861

Kurita, S., Watanabe, Y., Gunji, E., Ohashi, K., and Mizuno, K. (2008). Molecular dissection of the mechanisms of substrate recognition and F-actin-mediated activation of cofilin-phosphatase Slingshot-1. *J. Biol. Chem.* 283 (47), 32542–32552. doi:10.1074/jbc.M804627200

Lagoutte, E., Villeneuve, C., Lafanechere, L., Wells, C. M., Jones, G. E., Chavrier, P., et al. (2016). LIMK regulates tumor-cell invasion and matrix degradation through tyrosine phosphorylation of MT1-MMP. *Sci. Rep.* 6, 24925. doi:10.1038/srep24925

Lai, Y.-J., Tsai, F.-C., Chang, G.-J., Chang, S.-H., Huang, C.-C., Chen, W.-J., et al. (2022). miR-181b targets semaphorin 3A to mediate TGF-β-induced endothelial-mesenchymal transition related to atrial fibrillation. *J. Clin. Investigation* 132, e142548. doi:10.1172/JCI142548

Lamalice, L., Le Boeuf, F., and Huot, J. (2007). Endothelial cell migration during angiogenesis. *Circ. Res.* 100, 782–794. doi:10.1161/01.RES.0000259593.07661.1e

Le Dour, C., Chatzifrangkeskou, M., Macquart, C., Magiera, M. M., Peccate, C., Jouve, C., et al. (2022). Actin-microtubule cytoskeletal interplay mediated by MRTF-A/SRF signaling promotes dilated cardiomyopathy caused by LMNA mutations. *Nat. Commun.* 13, 7886. doi:10.1038/s41467-022-35639-x

Leonard, A., Marando, C., Rahman, A., and Fazal, F. (2013). Thrombin selectively engages LIM kinase 1 and slingshot-1L phosphatase to regulate NF-κB activation and endothelial cell inflammation. *Am. J. Physiology. Lung Cell. Mol. Physiology* 305, L651–L664. doi:10.1152/ajplung.00071.2013

Li, A., Ponten, F., and Dos Remedios, C. G. (2012). The interactome of LIM domain proteins: the contributions of LIM domain proteins to heart failure and heart development. *Proteomics* 12, 203–225. doi:10.1002/pmic.201100492

Li, R., Soosairajah, J., Harari, D., Citri, A., Price, J., Ng, H. L., et al. (2006). Hsp90 increases LIM kinase activity by promoting its homo-dimerization. *FASEB J.* 20 (8), 1218–1220. doi:10.1096/fj.05-5258fje

Li, S., Chen, B. P., Azuma, N., Hu, Y. L., Wu, S. Z., Sumpio, B. E., et al. (1999). Distinct roles for the small GTPases Cdc42 and Rho in endothelial responses to shear stress. *J. Clin. Investigation* 103, 1141–1150. doi:10.1172/JCI5367

Lin, T., Zeng, L., Liu, Y., Defea, K., Schwartz, M. A., Chien, S., et al. (2003). Rho-ROCK-LIMK-cofilin pathway regulates shear stress activation of sterol regulatory element binding proteins. *Circ. Res.* 92, 1296–1304. doi:10.1161/01.RES.0000078780.65824.8B

Lindstrom, N. O., Neves, C., Mcintosh, R., Miedzybrodzka, Z., Vargesson, N., and Collinson, J. M. (2011). Tissue specific characterisation of Lim-kinase 1 expression during mouse embryogenesis. *Gene Expr. Patterns* 11, 221–232. doi:10.1016/j.gep.2010.12.003

Liu, B., Itoh, H., Louie, O., Kubota, K., and Kent, K. C. (2002). The signaling protein Rho is necessary for vascular smooth muscle migration and survival but not for proliferation. *Surgery* 132, 317–325. doi:10.1067/msy.2002.125786

Liu, J., Wada, Y., Katsura, M., Tozawa, H., Erwin, N., Kapron, C. M., et al. (2018). Rho-associated coiled-coil kinase (ROCK) in molecular regulation of angiogenesis. *Theranostics* 8, 6053–6069. doi:10.7150/thno.30305

Lo, S. H., Janmey, P. A., Hartwig, J. H., and Chen, L. B. (1994). Interactions of tensin with actin and identification of its three distinct actin-binding domains. *J. Cell Biol.* 125, 1067–1075. doi:10.1083/jcb.125.5.1067

Low, S.-K., Zembutsu, H., Takahashi, A., Kamatani, N., Cha, P.-C., Hosono, N., et al. (2011). Impact of LIMK1, MMP2 and TNF-α variations for intracranial aneurysm in Japanese population. *J. Hum. Genet.* 56, 211–216. doi:10.1038/jhg.2010.169

Malvi, P., Janostiak, R., Chava, S., Manrai, P., Yoon, E., Singh, K., et al. (2020). LIMK2 promotes the metastatic progression of triple-negative breast cancer by activating SRPK1. *Oncogenesis* 9, 77. doi:10.1038/s41389-020-00263-1

Manetti, F. (2012). LIM kinases are attractive targets with many macromolecular partners and only a few small molecule regulators. *Med. Res. Rev.* 32, 968–998. doi:10.1002/med.20230

Manetti, F. (2018). Recent advances in the rational design and development of LIM kinase inhibitors are not enough to enter clinical trials. *Eur. J. Med. Chem.* 155, 445–458. doi:10.1016/j.ejmech.2018.06.016

Mardilovich, K., Baugh, M., Crighton, D., Kowalczyk, D., Gabrielsen, M., Munro, J., et al. (2015). LIM kinase inhibitors disrupt mitotic microtubule organization and impair tumor cell proliferation. *Oncotarget* 6, 38469–38486. doi:10.18632/oncotarget.6288

Martin, G. R., Perretti, M., Flower, R. J., and Wallace, J. L. (2008). Annexin-1 modulates repair of gastric mucosal injury. *Am. J. Physiology. Gastrointest. Liver Physiology* 294, G764–G769. doi:10.1152/ajpgi.00531.2007

Martinez-Lemus, L. A., Aroor, A. R., Ramirez-Perez, F. I., Jia, G., Habibi, J., Demarco, V. G., et al. (2017). Amiloride improves endothelial function and reduces vascular stiffness in female mice fed a western diet. *Front. Physiol.* 8, 456. doi:10.3389/fphys.2017.00456

Mehta, D., and Malik, A. B. (2006). Signaling mechanisms regulating endothelial permeability. *Physiol. Rev.* 86, 279–367. doi:10.1152/physrev.00012.2005

Michaelis, U. R. (2014). Mechanisms of endothelial cell migration. *Cell Mol. Life Sci.* 71, 4131–4148. doi:10.1007/s00018-014-1678-0

Michel, C. C., and Curry, F. E. (1999). Microvascular permeability. *Physiol. Rev.* 79, 703–761. doi:10.1152/physrev.1999.79.3.703

Mizuno, K. (2013). Signaling mechanisms and functional roles of cofilin phosphorylation and dephosphorylation. *Cell. Signal.* 25, 457–469. doi:10.1016/j.cellsig.2012.11.001

Morales-Quinones, M., Ramirez-Perez, F. I., Foote, C. A., Ghiarone, T., Ferreira-Santos, L., Bloksgaard, M., et al. (2020). LIMK (LIM kinase) inhibition prevents vasoconstriction- and hypertension-induced arterial stiffening and remodeling. *Hypertension* 76, 393–403. doi:10.1161/HYPERTENSIONAHA.120.15203

Mulvany, M. J., Baumbach, G. L., Aalkjaer, C., Heagerty, A. M., Korsgaard, N., Schiffrin, E. L., et al. (1996). Vascular remodeling. *Hypertens. Dallas, Tex.* 28, 505–506.

Munezane, T., Hasegawa, T., Tanaka, A., Okada, K., and Okita, Y. (2010). Activation of transglutaminase type 2 for aortic wall protection in a rat abdominal aortic aneurysm formation. *J. Vasc. Surg.* 52, 967–974. doi:10.1016/j.jvs.2010.04.049

Nagano, T., Yoneda, T., Hatanaka, Y., Kubota, C., Murakami, F., and Sato, M. (2002). Filamin A-interacting protein (FILIP) regulates cortical cell migration out of the ventricular zone. *Nat. Cell Biol.* 4, 495–501. doi:10.1038/ncb808

Negoro, N., Hoshiga, M., Seto, M., Kohbayashi, E., Ii, M., Fukui, R., et al. (1999). The kinase inhibitor fasudil (HA-1077) reduces intimal hyperplasia through inhibiting migration and enhancing cell loss of vascular smooth muscle cells. *Biochem. Biophysical Res. Commun.* 262, 211–215. doi:10.1006/bbrc.1999.1129

Niethammer, P., Kronja, I., Kandels-Lewis, S., Rybina, S., Bastiaens, P., and Karsenti, E. (2007). Discrete states of a protein interaction network govern interphase and mitotic microtubule dynamics. *PLoS Biol.* 5, e29. doi:10.1371/journal.pbio.0050029

Nishita, M., Tomizawa, C., Yamamoto, M., Horita, Y., Ohashi, K., and Mizuno, K. (2005). Spatial and temporal regulation of cofilin activity by LIM kinase and Slingshot is critical for directional cell migration. *J. Cell Biol.* 171, 349–359. doi:10.1083/jcb.200504029

Noh, J.-M., Choi, S.-C., Song, M.-H., Kim, K. S., Jun, S., Park, J. H., et al. (2023). The activation of the LIMK/cofilin signaling pathway via extracellular matrix-integrin interactions is critical for the generation of mature and vascularized cardiac organoids. *Cells* 12, 2029. doi:10.3390/cells12162029

Ohashi, K., Nagata, K., Maekawa, M., Ishizaki, T., Narumiya, S., and Mizuno, K. (2000). Rho-associated kinase ROCK activates LIM-kinase 1 by phosphorylation at threonine 508 within the activation loop. *J. Biol. Chem.* 275, 3577–3582. doi:10.1074/jbc.275.5.3577

Ohashi, K., Sampei, K., Nakagawa, M., Uchiumi, N., Amanuma, T., Aiba, S., et al. (2014). Damnacanthal, an effective inhibitor of LIM-kinase, inhibits cell migration and invasion. *Mol. Biol. Cell* 25, 828–840. doi:10.1091/mbc.E13-09-0540

Okano, I., Hiraoka, J., Otera, H., Nunoue, K., Ohashi, K., Iwashita, S., et al. (1995). Identification and characterization of a novel family of serine/threonine kinases containing two N-terminal LIM motifs. *J. Biol. Chem.* 270, 31321–31330. doi:10.1074/jbc.270.52.31321

Palombo, C., and Kozakova, M. (2016). Arterial stiffness, atherosclerosis and cardiovascular risk: pathophysiologic mechanisms and emerging clinical indications. *Vasc. Pharmacol.* 77, 1–7. doi:10.1016/j.vph.2015.11.083

Pan, C., Wang, S., Liu, C., and Ren, Z. (2022). Actin-binding proteins in cardiac hypertrophy. *Cells* 11, 3566. doi:10.3390/cells11223566

Pandey, D., Goyal, P., Bamburg, J. R., and Siess, W. (2006). Regulation of LIM-kinase 1 and cofilin in thrombin-stimulated platelets. *Blood* 107, 575–583. doi:10.1182/blood-2004-11-4377

Park, J., Kim, S. W., and Cho, M. C. (2021). The role of LIM kinase in the male urogenital system. *Cells* 11, 78. doi:10.3390/cells11010078

Pereira, C., Schaer, D. J., Bachli, E. B., Kurrer, M. O., and Schoedon, G. (2008). Wnt5A/CaMKII signaling contributes to the inflammatory response of macrophages and is a target for the antiinflammatory action of activated protein C and interleukin-10. *Arterioscler. Thromb. Vasc. Biol.* 28, 504–510. doi:10.1161/ATVBAHA.107.157438

Perissiou, M., Bailey, T. G., Windsor, M., Greaves, K., Nam, M. C. Y., Russell, F. D., et al. (2019). Aortic and systemic arterial stiffness responses to acute exercise in patients with small abdominal aortic aneurysms. *Eur. J. Vasc. Endovasc. Surg.* 58, 708–718. doi:10.1016/j.ejvs.2019.02.021

Petrilli, A., Copik, A., Posadas, M., Chang, L.-S., Welling, D. B., Giovannini, M., et al. (2014). LIM domain kinases as potential therapeutic targets for neurofibromatosis type 2. *Oncogene* 33, 3571–3582. doi:10.1038/onc.2013.320

Pipp, F., Boehm, S., Cai, W. J., Adili, F., Ziegler, B., Karanovic, G., et al. (2004). Elevated fluid shear stress enhances postocclusive collateral artery growth and gene expression in the pig hind limb. *Arterioscler. Thromb. Vasc. Biol.* 24, 1664–1668. doi:10.1161/01.ATV.0000138028.14390.e4

Pober, J. S., and Sessa, W. C. (2007). Evolving functions of endothelial cells in inflammation. *Nat. Rev. Immunol.* 7 (10), 803–815. doi:10.1038/nri2171

Power, G., Ferreira-Santos, L., Martinez-Lemus, L. A., and Padilla, J. (2024a). Integrating molecular and cellular components of endothelial shear stress mechanotransduction. *Am. J. Physiol. Heart Circ. Physiol.* 327, H989–H1003. doi:10.1152/ajpheart.00431.2024

Power, G., Gonzalez-Vallejo, J., Ramirez-Perez, F., Lateef, O., Manrique-Acevedo, C., Martinez-Lemus, L., et al. (2023). LIM kinase inhibition reduces endothelial cell cortical stiffness in diabetic arteries. *Physiology* 38, 5795981. doi:10.1152/physiol.2023.38.s1.5795981

Power, G., Lateef, O. M., Lazo-Fernandez, Y., Augenreich, M. A., Ferrieira-Santos, L., Ramirez-Perez, F. I., et al. (2024b). Reduced cofilin activity as a mechanism contributing to endothelial cell stiffening in type 2 diabetes. *Am. J. Physiology - Heart Circulatory Physiology*. doi:10.1152/ajpheart.00667.2024

Prudent, R., Vassal-Stermann, E., Nguyen, C.-H., Pillet, C., Martinez, A., Prunier, C., et al. (2012). Pharmacological inhibition of LIM kinase stabilizes microtubules and inhibits neoplastic growth. *Cancer Res.* 72, 4429–4439. doi:10.1158/0008-5472.CAN-11-3342

Prunier, C., Kapur, R., and Lafanechere, L. (2016). Targeting LIM kinases in taxane resistant tumors. *Oncotarget* 7, 50816–50817. doi:10.18632/oncotarget.10816

Prunier, C., Prudent, R., Kapur, R., Sadoul, K., and Lafanechère, L. (2017). LIM kinases: cofilin and beyond. *Oncotarget* 8, 41749–41763. doi:10.18632/oncotarget.16978

Qiu, H., Zhu, Y., Sun, Z., Trzeciakowski, J. P., Gansner, M., Depre, C., et al. (2010). Short communication: vascular smooth muscle cell stiffness as a mechanism for increased aortic stiffness with aging. *Circ. Res.* 107, 615–619. doi:10.1161/CIRCRESAHA.110.221846

Raines, E. W. (2004). PDGF and cardiovascular disease. *Cytokine and Growth Factor Rev.* 15, 237–254. doi:10.1016/j.cytogfr.2004.03.004

Rak, R., Haklai, R., Elad-Tzfadia, G., Wolfson, H. J., Carmeli, S., and Kloog, Y. (2014). Novel LIMK2 inhibitor blocks panc-1 tumor growth in a mouse xenograft model. *Oncoscience* 1, 39–48. doi:10.18632/oncoscience.7

Ramirez-Perez, F. I., Cabral-Amador, F. J., Whaley-Connell, A. T., Aroor, A. R., Morales-Quinones, M., Woodford, M. L., et al. (2022). Cystamine reduces vascular stiffness in Western diet-fed female mice. *Am. J. Physiology. Heart Circulatory Physiology* 322, H167–H180. doi:10.1152/ajpheart.00431.2021

Rodriguez, O. C., Schaefer, A. W., Mandato, C. A., Forscher, P., Bement, W. M., and Waterman-Storer, C. M. (2003). Conserved microtubule-actin interactions in cell movement and morphogenesis. *Nat. Cell Biol.* 5, 599–609. doi:10.1038/ncb0703-599

Ross-Macdonald, P., De Silva, H., Guo, Q., Xiao, H., Hung, C.-Y., Penhallow, B., et al. (2008). Identification of a nonkinase target mediating cytotoxicity of novel kinase inhibitors. *Mol. Cancer Ther.* 7, 3490–3498. doi:10.1158/1535-7163.MCT-08-0826

Rousseau, S., Houle, F., Kotanides, H., Witte, L., Waltenberger, J., Landry, J., et al. (2000). Vascular endothelial growth factor (VEGF)-driven actin-based motility is mediated by VEGFR2 and requires concerted activation of stress-activated protein kinase 2 (SAPK2/p38) and geldanamycin-sensitive phosphorylation of focal adhesion kinase. *J. Biol. Chem.* 275, 10661–10672. doi:10.1074/jbc.275.14.10661

Roy, A., Pathak, Z., and Kumar, H. (2024). Investigating LIM (Lin-11, isl-1, and mec-3) kinases and their correlation with pathological events and microtubule dynamics in an experimental model of spinal cord injury in rats. *ACS Pharmacol. and Transl. Sci.* 7, 667–679. doi:10.1021/acsptsci.3c00272

Rybin, M. J., Laverde-Paz, M. J., Suter, R. K., Affer, M., Ayad, N. G., Feng, Y., et al. (2022). A dual aurora and lim kinase inhibitor reduces glioblastoma proliferation and invasion. *Bioorg. and Med. Chem. Lett.* 61, 128614. doi:10.1016/j.bmcl.2022.128614

Salah, E., Chatterjee, D., Beltrami, A., Tumber, A., Preuss, F., Canning, P., et al. (2019). Lessons from LIMK1 enzymology and their impact on inhibitor design. *Biochem. J.* 476, 3197–3209. doi:10.1042/BCJ20190517

San Martin, A., Lee, M. Y., Williams, H. C., Mizuno, K., Lassegue, B., and Griendling, K. K. (2008). Dual regulation of cofilin activity by LIM kinase and Slingshot-1L phosphatase controls platelet-derived growth factor-induced migration of human aortic smooth muscle cells. *Circ. Res.* 102, 432–438. doi:10.1161/CIRCRESAHA.107.158923

Scott, R. W., and Olson, M. F. (2007). LIM kinases: function, regulation and association with human disease. *J. Mol. Med. Berlin, Ger.* 85, 555–568. doi:10.1007/s00109-007-0165-6

Seasholtz, T. M., Majumdar, M., Kaplan, D. D., and Brown, J. H. (1999). Rho and rho kinase mediate thrombin-stimulated vascular smooth muscle cell DNA synthesis and migration. *Circulation Res.* 84, 1186–1193. doi:10.1161/01.res.84.10.1186

Seetharaman, S., and Etienne-Manneville, S. (2018). Integrin diversity brings specificity in mechanotransduction. *Biol. Cell* 110, 49–64. doi:10.1111/boc.201700060

Sehgel, N. L., Sun, Z., Hong, Z., Hunter, W. C., Hill, M. A., Vatner, D. E., et al. (2015). Augmented vascular smooth muscle cell stiffness and adhesion when hypertension is superimposed on aging. *Hypertension* 65, 370–377. doi:10.1161/HYPERTENSIONAHA.114.04456

Sequeira, V., Nijenkamp, L. L., Regan, J. A., and Van Der Velden, J. (2014). The physiological role of cardiac cytoskeleton and its alterations in heart failure. *Biochim. Biophys. Acta* 1838, 700–722. doi:10.1016/j.bbamem.2013.07.011

Shin, S., Cho, Y.-P., Jun, H., Park, H., Hong, H. N., and Kwon, T.-W. (2013). Transglutaminase type 2 in human abdominal aortic aneurysm is a potential factor in the stabilization of extracellular matrix. *J. Vasc. Surg.* 57, 1362–1370. doi:10.1016/j.jvs.2012.09.062

Simard, J. R., and Rauh, D. (2014). FLiK: a direct-binding assay for the identification and kinetic characterization of stabilizers of inactive kinase conformations. *Methods Enzymol.* 548, 147–171. doi:10.1016/B978-0-12-397918-6.00006-9

Shyy, J. Y., and Chien, S. (2002). Role of integrins in endothelial mechanosensing of shear stress. *Circ. Res.* 91, 769–775. doi:10.1161/01.res.0000038487.19924.18

Skaria, T., Bachli, E., and Schoedon, G. (2017a). WIF1 prevents Wnt5A mediated LIMK/CFL phosphorylation and adherens junction disruption in human vascular endothelial cells. *J. Inflamm. (Lond)* 14, 10. doi:10.1186/s12950-017-0157-4

Skaria, T., Bachli, E., and Schoedon, G. (2017b). Wnt5A/Ryk signaling critically affects barrier function in human vascular endothelial cells. *Cell Adh Migr.* 11, 24–38. doi:10.1080/19336918.2016.1178449

Skaria, T., Burgener, J., Bachli, E., and Schoedon, G. (2016). IL-4 causes hyperpermeability of vascular endothelial cells through Wnt5A signaling. *PLoS One* 11, e0156002. doi:10.1371/journal.pone.0156002

Slee, J. B., and Lowe-Krentz, L. J. (2013). Actin realignment and cofilin regulation are essential for barrier integrity during shear stress. *J. Cell Biochem.* 114, 782–795. doi:10.1002/jcb.24416

Soares, R. N., Ramirez-Perez, F. I., Cabral-Amador, F. J., Morales-Quinones, M., Foote, C. A., Ghiarone, T., et al. (2022). SGLT2 inhibition attenuates arterial dysfunction and decreases vascular F-actin content and expression of proteins associated with oxidative stress in aged mice. *Geroscience* 44, 1657–1675. doi:10.1007/s11357-022-00563-x

Soosairajah, J., Maiti, S., Wiggan, O., Sarmiere, P., Moussi, N., Sarcevic, B., et al. (2005). Interplay between components of a novel LIM kinase-slingshot phosphatase complex regulates cofilin. *EMBO J.* 24, 473–486. doi:10.1038/sj.emboj.7600543

Spindler, V., Schlegel, N., and Waschke, J. (2010). Role of GTPases in control of microvascular permeability. *Cardiovasc. Res.* 87, 243–253. doi:10.1093/cvr/cvq086

Staiculescu, M. C., Galinanes, E. L., Zhao, G., Ulloa, U., Jin, M., Beig, M. I., et al. (2013). Prolonged vasoconstriction of resistance arteries involves vascular smooth muscle actin polymerization leading to inward remodelling. *Cardiovasc Res.* 98, 428–436. doi:10.1093/cvr/cvt034

Stoletov, K. V., Ratcliffe, K. E., Spring, S. C., and Terman, B. I. (2001). NCK and PAK participate in the signaling pathway by which vascular endothelial growth factor stimulates the assembly of focal adhesions. *J. Biol. Chem.* 276, 22748–22755. doi:10.1074/jbc.M009720200

Subramanian, K., Gianni, D., Balla, C., Assenza, G. E., Joshi, M., Semigran, M. J., et al. (2015). Cofilin-2 phosphorylation and sequestration in myocardial aggregates: novel pathogenetic mechanisms for idiopathic dilated cardiomyopathy. *J. Am. Coll. Cardiol.* 65, 1199–1214. doi:10.1016/j.jacc.2015.01.031

Sumi, T., Matsumoto, K., Takai, Y., and Nakamura, T. (1999). Cofilin phosphorylation and actin cytoskeletal dynamics regulated by rho- and Cdc42-activated LIM-kinase 2. *J. Cell Biol.* 147, 1519–1532. doi:10.1083/jcb.147.7.1519

Sumi, T., Matsumoto, K., Shibuya, A., and Nakamura, T. (2001). Activation of LIM kinases by myotonic dystrophy kinase-related Cdc42-binding kinase alpha. *J. Biol. Chem.* 276 (25), 23092–23096. doi:10.1074/jbc.C100196200

Suurna, M. V., Ashworth, S. L., Hosford, M., Sandoval, R. M., Wean, S. E., Shah, B. M., et al. (2006). Cofilin mediates ATP depletion-induced endothelial cell actin alterations. *Am. J. Physiol. Ren. Physiol.* 290, F1398–F1407. doi:10.1152/ajprenal.00194.2005

Swiatlowska, P., Sit, B., Feng, Z., Marhuenda, E., Xanthis, I., Zingaro, S., et al. (2022). Pressure and stiffness sensing together regulate vascular smooth muscle cell phenotype switching. *Sci. Adv.* 8, eabm3471. doi:10.1126/sciadv.abm3471

Tang, D. D. (2018). The dynamic actin cytoskeleton in smooth muscle. *Adv. Pharmacol.* 81, 1–38. doi:10.1016/bs.apha.2017.06.001

Tanihara, H., Inatani, M., Honjo, M., Tokushige, H., Azuma, J., and Araie, M. (2008). Intraocular pressure-lowering effects and safety of topical administration of a selective ROCK inhibitor, SNJ-1656, in healthy volunteers. *Archives Ophthalmol.* 126, 309–315. doi:10.1001/archophthalmol.2007.76

Tian, Y., and Autieri, M. V. (2007). Cytokine expression and AIF-1-mediated activation of Rac2 in vascular smooth muscle cells: a role for Rac2 in VSMC activation. *Am. J. Physiology. Cell Physiology* 292, C841–C849. doi:10.1152/ajpcell.00334.2006

Trepat, X., Chen, Z., and Jacobson, K. (2012). Cell migration. *Compr. Physiol.* 2, 2369–2392. doi:10.1002/cphy.c110012

Tursun, B., Schluter, A., Peters, M. A., Viehweger, B., Ostendorff, H. P., Soosairajah, J., et al. (2005). The ubiquitin ligase Rnf6 regulates local LIM kinase 1 levels in axonal growth cones. *Genes Dev.* 19, 2307–2319. doi:10.1101/gad.1340605

Tzima, E., Del Pozo, M. A., Shattil, S. J., Chien, S., and Schwartz, M. A. (2001). Activation of integrins in endothelial cells by fluid shear stress mediates Rho-dependent cytoskeletal alignment. *EMBO J.* 20, 4639–4647. doi:10.1093/emboj/20.17.4639

Van Varik, B., Rennenberg, R., Reutelingsperger, C., Kroon, A., De Leeuw, P., and Schurgers, L. (2012). Mechanisms of arterial remodeling: lessons from genetic diseases. *Front. Genet.* 3, 290. doi:10.3389/fgene.2012.00290

Vardouli, L., Moustakas, A., and Stournaras, C. (2005). LIM-kinase 2 and cofilin phosphorylation mediate actin cytoskeleton reorganization induced by transforming growth factor-beta. *J. Biol. Chem.* 280, 11448–11457. doi:10.1074/jbc.M402651200

Villalonga, E., Mosrin, C., Normand, T., Girardin, C., Serrano, A., Zunar, B., et al. (2023). LIM kinases, LIMK1 and LIMK2, are crucial node actors of the cell fate: molecular to pathological features. *Cells* 12, 805. doi:10.3390/cells12050805

Wang, H. J., Chen, S. F., and Lo, W. Y. (2016). Identification of cofilin-1 induces G0/G1 arrest and autophagy in angiotensin-(1-7)-treated human aortic endothelial cells from iTRAQ quantitative proteomics. *Sci. Rep.* 6, 35372. doi:10.1038/srep35372

Ward, M. L., and Crossman, D. J. (2014). Mechanisms underlying the impaired contractility of diabetic cardiomyopathy. *World J. Cardiol.* 6, 577–584. doi:10.4330/wjc.v6.i7.577

Ward, M. R., Pasterkamp, G., Yeung, A. C., and Borst, C. (2000). Arterial remodeling. Mechanisms and clinical implications. *Circulation* 102, 1186–1191. doi:10.1161/01.cir.102.10.1186

Waschke, J., Curry, F. E., Adamson, R. H., and Drenckhahn, D. (2005). Regulation of actin dynamics is critical for endothelial barrier functions. *Am. J. Physiol. Heart Circ. Physiol.* 288, H1296–H1305. doi:10.1152/ajpheart.00687.2004

Waterman-Storer, C. M., and Salmon, E. (1999). Positive feedback interactions between microtubule and actin dynamics during cell motility. *Curr. Opin. Cell Biol.* 11, 61–67. doi:10.1016/s0955-0674(99)80008-8

Wehrle-Haller, B. (2012). Assembly and disassembly of cell matrix adhesions. *Curr. Opin. Cell Biol.* 24, 569–581. doi:10.1016/j.ceb.2012.06.010

Weisbrod, R. M., Shiang, T., Al Sayah, L., Fry, J. L., Bajpai, S., Reinhart-King, C. A., et al. (2013). Arterial stiffening precedes systolic hypertension in diet-induced obesity. *Hypertension* 62, 1105–1110. doi:10.1161/HYPERTENSIONAHA.113.01744

Winkles, J. A., and Gay, C. G. (1991). Regulated expression of PDGF A-chain mRNA in human saphenous vein smooth muscle cells. *Biochem. Biophys. Res. Commun.* 180, 519–524. doi:10.1016/s0006-291x(05)81095-2

Wittmann, T., and Waterman-Storer, C. M. (2001). Cell motility: can Rho GTPases and microtubules point the way? *J. Cell Sci.* 114, 3795–3803. doi:10.1242/jcs.114.21.3795

Yamashiro, Y., Papke, C. L., Kim, J., Ringuette, L. J., Zhang, Q. J., Liu, Z. P., et al. (2015). Abnormal mechanosensing and cofilin activation promote the progression of ascending aortic aneurysms in mice. *Sci. Signal* 8, ra105. doi:10.1126/scisignal.aab3141

Yamin, R., and Morgan, K. G. (2012). Deciphering actin cytoskeletal function in the contractile vascular smooth muscle cell. *J. Physiol.* 590, 4145–4154. doi:10.1113/jphysiol.2012.232306

Yang, N., Higuchi, O., Ohashi, K., Nagata, K., Wada, A., Kangawa, K., et al. (1998). Cofilin phosphorylation by LIM-kinase 1 and its role in Rac-mediated actin reorganization. *Nature* 393, 809–812. doi:10.1038/31735

Yang, X., He, G., Zhang, X., Chen, L., Kong, Y., Xie, W., et al. (2017). Transient inhibition of LIMKs significantly attenuated central sensitization and delayed the development of chronic pain. *Neuropharmacology* 125, 284–294. doi:10.1016/j.neuropharm.2017.06.031

Yin, Y., Zheng, K., Eid, N., Howard, S., Jeong, J.-H., Yi, F., et al. (2015). Bis-aryl urea derivatives as potent and selective LIM kinase (limk) inhibitors. *J. Med. Chem.* 58, 1846–1861. doi:10.1021/jm501680m

Yoshida, A., Anand-Apte, B., and Zetter, B. R. (1996). Differential endothelial migration and proliferation to basic fibroblast growth factor and vascular endothelial growth factor. *Growth Factors Chur, Switz.* 13, 57–64. doi:10.3109/08977199609034566

Yoshioka, K., Foletta, V., Bernard, O., and Itoh, K. (2003). A role for LIM kinase in cancer invasion. *Proc. Natl. Acad. Sci. U. S. A.* 100, 7247–7252. doi:10.1073/pnas.1232344100

Yu, Q., Wu, C., Chen, Y., Li, B., Wang, R., Huang, R., et al. (2021). Inhibition of LIM kinase reduces contraction and proliferation in bladder smooth muscle. *Acta Pharm. Sin. B* 11, 1914–1930. doi:10.1016/j.apsb.2021.01.005

Zalli, D., Neff, L., Nagano, K., Shin, N. Y., Witke, W., Gori, F., et al. (2016). The actin-binding protein cofilin and its interaction with cortactin are required for podosome patterning in osteoclasts and bone resorption *in vivo* and *in vitro*. *J. Bone Min. Res.* 31, 1701–1712. doi:10.1002/jbmr.2851

Zhang, B., Fugleholm, K., Day, L. B., Ye, S., Weller, R. O., and Day, I. N. M. (2003). Molecular pathogenesis of subarachnoid haemorrhage. *Int. J. Biochem. and Cell Biol.* 35, 1341–1360. doi:10.1016/s1357-2725(03)00043-8

Zhang, J., Zhao, X., Vatner, D. E., Mcnulty, T., Bishop, S., Sun, Z., et al. (2016). Extracellular matrix disarray as a mechanism for greater abdominal versus thoracic aortic stiffness with aging in primates. *Arteriosclerosis, Thrombosis, Vasc. Biol.* 36, 700–706. doi:10.1161/ATVBAHA.115.306563

Zhang, T., Zhang, X., Yu, W., Chen, J., Li, Q., Jiao, Y., et al. (2013). Effects of chemokine-like factor 1 on vascular smooth muscle cell migration and proliferation in vascular inflammation. *Atherosclerosis* 226, 49–57. doi:10.1016/j.atherosclerosis.2012.09.023

Zhao, R., Du, L., Huang, Y., Wu, Y., and Gunst, S. J. (2008). Actin depolymerization factor/cofilin activation regulates actin polymerization and tension development in canine tracheal smooth muscle. *J. Biol. Chem.* 283, 36522–36531. doi:10.1074/jbc.M805294200

Zhu, Y., Qiu, H., Trzeciakowski, J. P., Sun, Z., Li, Z., Hong, Z., et al. (2012). Temporal analysis of vascular smooth muscle cell elasticity and adhesion reveals oscillation waveforms that differ with aging. *Aging Cell* 11, 741–750. doi:10.1111/j.1474-9726.2012.00840.x

Zoudilova, M., Kumar, P., Ge, L., Wang, P., Bokoch, G. M., and Defea, K. A. (2007). Beta-arrestin-dependent regulation of the cofilin pathway downstream of protease-activated receptor-2. *J. Biol. Chem.* 282, 20634–20646. doi:10.1074/jbc.M701391200

frontiers | Frontiers in Physiology

TYPE Review
PUBLISHED 23 January 2025
DOI 10.3389/fphys.2025.1545044

OPEN ACCESS

EDITED BY
Christopher Garland,
University of Oxford, United Kingdom

REVIEWED BY
Michael P. Massett,
Texas Tech University, United States
Giorgia Chinigò,
University of Turin, Italy

*CORRESPONDENCE
Quang-Kim Tran,
kim.tran@dmu.edu

RECEIVED 13 December 2024
ACCEPTED 07 January 2025
PUBLISHED 23 January 2025

CITATION
Gonzalez M, Clayton S, Wauson E, Christian D and Tran Q-K (2025) Promotion of nitric oxide production: mechanisms, strategies, and possibilities.
Front. Physiol. 16:1545044.
doi: 10.3389/fphys.2025.1545044

Promotion of nitric oxide production: mechanisms, strategies, and possibilities

Marcos Gonzalez, Sarah Clayton, Eric Wauson, Daniel Christian and Quang-Kim Tran*

Department of Physiology and Pharmacology, Des Moines University Medicine and Health Sciences, West Des Moines, IA, United States

The discovery of nitric oxide (NO) and the role of endothelial cells (ECs) in its production has revolutionized medicine. NO can be produced by isoforms of NO synthases (NOS), including the neuronal (nNOS), inducible (iNOS), and endothelial isoforms (eNOS), and via the non-classical nitrate-nitrite-NO pathway. In particular, endothelium-derived NO, produced by eNOS, is essential for cardiovascular health. Endothelium-derived NO activates soluble guanylate cyclase (sGC) in vascular smooth muscle cells (VSMCs), elevating cyclic GMP (cGMP), causing vasodilation. Over the past four decades, the importance of this pathway in cardiovascular health has fueled the search for strategies to enhance NO bioavailability and/or preserve the outcomes of NO's actions. Currently approved approaches operate in three directions: 1) providing exogenous NO, 2) promoting sGC activity, and 3) preventing degradation of cGMP by inhibiting phosphodiesterase 5 activity. Despite clear benefits, these approaches face challenges such as the development of nitrate tolerance and endothelial dysfunction. This highlights the need for sustainable options that promote endogenous NO production. This review will focus on strategies to promote endogenous NO production. A detailed review of the mechanisms regulating eNOS activity will be first provided, followed by a review of strategies to promote endogenous NO production based on the levels of available preclinical and clinical evidence, and perspectives on future possibilities.

KEYWORDS

nitric oxide, eNOS, endothelium, preclinical evidence, clinical trials

Nitric oxide bioavailability and the need to promote its endogenous production

NO synthases and general effects of NO

NO-containing compounds have been used in medicine for over 160 years; however, it was not until the early 1980s that NO was discovered as the ingredient that exerts the therapeutic effects and ECs as the key source of vascular NO (Katsuki et al., 1977; Arnold et al., 1977; Furchgott and Zawadzki, 1980; Ignarro et al., 1987; Palmer et al., 1987). We now know NO can be produced by three NO synthases and via nitrate-nitrite-NO conversion (Bredt et al., 1991; Janssens et al., 1992; Geller et al., 1993; Benjamin et al., 1994; Lundberg et al., 1994; Stuehr, 1997). The NO synthases are classified a neuronal NOS (encoded by *NOS1*), inducible NOS (encoded by *NOS2*), and eNOS (encoded by *NOS3*). Among these sources, endothelium-derived NO plays a vital role in regulating vascular tone, inhibiting inflammation, and preventing thrombosis

(Alheid et al., 1987; Forstermann et al., 1989; Bredt and Snyder, 1990; Mitchell et al., 1991; Forstermann et al., 1991). Endothelium-derived NO diffuses into the circulation and the underlying VSMCs, where it activates sGC, which enhances cGMP, causing vasodilation (Arnold et al., 1977; Ignarro et al., 1986a; Ignarro et al., 1986b; Forstermann et al., 1994). The critical role of eNOS in controlling vascular tone was documented by findings that pharmacological inhibition of NOS causes hypertension (Rees et al., 1989) and deletion of *NOS3* results in high blood pressure (Huang et al., 1995). Beyond activating sGC and enhancing cGMP, NO exerts numerous other effects. For example, endothelium-derived NO directly suppresses the electrical excitability of VSMCs by inhibiting the action of T-type and L-type voltage-gated Ca^{2+} channels in small arteries, and reduced NO availability can trigger transient depolarization in normally quiescent VSMCs leading to vasospasm (Smith et al., 2020). Actions of NO leading to smooth muscle relaxation are important for cardiovascular, respiratory, renal and digestive functions. NO is also critical in brain function as a neurotransmitter and immune responses.

Efforts to increase NO bioavailability

Dysfunction and uncoupling of eNOS are associated with cardiovascular diseases (CVD) (Janaszak-Jasiecka et al., 2023; Heitzer et al., 2000a; Munzel et al., 2005), and increased eNOS expression and reversal of eNOS uncoupling in experimental models improves vascular function (Li et al., 2006). Approaches to increase NO bioavailability have been intensively researched. Some studies suggest that diets that are high in *antioxidants or antioxidant supplementation* can help preserve vascular health and prevent CVD by reducing oxidative stress and improving endothelial function. However, a blanket recommendation has not been made in clinical guidelines as there are needs for stronger evidence and determinations of effective doses and specific patient populations that might benefit (Varadharaj et al., 2017). *Dietary nitrates and nitrites*, found in foods such as beetroot and leafy greens, can be converted to NO and have shown promising results in improving vascular function and lowering blood pressure. However, these are not yet recommended in clinical guidelines for prevention or management of CVD (Blekkenhorst et al., 2018). Current options in clinical practice guidelines focus mainly on downstream components of NO signaling, such as NO inhalation, use of NO donors, sGC stimulators/activators, or inhibition of phosphodiesterase (PDE) 5 (Chen et al., 2002; Rapoport et al., 1987; Bonderman et al., 2014; Ignarro et al., 1982; Kraehling and Sessa, 2017; Lundberg et al., 2015). However, challenges such as short-lived effects and the development of nitrate tolerance and endothelial dysfunction have limited their efficacy (Rapoport et al., 1987; Munzel et al., 1995a; Munzel et al., 1995b; Erdmann et al., 2013; Knorr et al., 2011; Munzel et al., 2014; Munzel et al., 2013; Oelze et al., 2013). There is thus a strong need to develop new and improve existing approaches to promote the endogenous production of NO.

The regulation of eNOS

eNOS is a ~133 kDa homo-dimeric oxidoreductase enzyme with an N-terminal oxygenase domain that binds L-arginine and tetrahydrobiopterin (BH_4) and a C-terminal reductase domain that transfers electrons from nicotinamide adenine dinucleotide phosphate (NADPH) via flavin adenine dinucleotide (FAD) and flavin mononucleotide (FMN) (Figure 1) (Stuehr, 1997; Palmer et al., 1988; Stuehr et al., 2005; Marsden et al., 1992). Dimerization is essential for eNOS function, stabilizing the enzyme and ensuring efficient electron transfer (List et al., 1997). Ca^{2+}-bound calmodulin (CaM) binds to the CaM-binding domain and initiates electron flow from the reductase domain to the oxygenase domain, where NO is synthesized from L-arginine (Busse and Mulsch, 1990; Venema et al., 1996). eNOS-mediated production of NO follows a two-step process: 1) hydroxylation of L-arginine to Nω-hydroxy-L-arginine, and 2) further oxidation to generate L-citrulline and NO. Tetrahydrobiopterin (BH_4) plays a vital role in this reaction by stabilizing the eNOS dimer and preventing the formation of superoxide, a potentially harmful byproduct, ensuring NO synthesis proceeds efficiently (Xia et al., 1998a; Xia et al., 1998b). eNOS regulation is a highly complex process, integrating multiple layers of control to fine-tune NO production according to physiological needs. These layers include transcriptional regulation, post-translational modifications, and protein-protein interactions.

Transcriptional regulation of eNOS

The *NOS3* gene is located on chromosome 7 (7q35-36) and is regulated by a promoter region containing binding sites for multiple transcription factors, including Krüppel-like Factor 2 (KLF2), Specificity protein 1 (Sp1), Specificity protein 3 (Sp3), Ets1, mothers against decapentaplegic homolog-2 (Smad2), and Nuclear factor erythroid 2-related factor (Nrf2), among others (Karantzoulis-Fegaras et al., 1999; Laumonnier et al., 2000; Balligand et al., 2009; Fish and Marsden, 2006). These factors dynamically regulate eNOS expression in response to physiological signals. Initially thought to be constitutively expressed, *NOS3* is now recognized to be highly responsive to various regulatory stimuli, which adjust its transcription to match the vascular environment's needs (Balligand et al., 2009; Black et al., 1998; Mattsson et al., 1997; Nadaud et al., 1996; Nishida et al., 1992; Ou et al., 2005; Searles, 2006). Transcriptional regulation of eNOS can be categorized into upregulating, downregulating, and dual-regulating factors (Figure 2).

Upregulating factors

Shear stress, the mechanical stimulus exerted on the endothelium by laminar blood flow, upregulates eNOS expression (Nadaud et al., 1996) by triggering PIEZO1 Ca^{2+} channels (Wang et al., 2016) and a mechanosensory complex leading to the activation of *KLF2*, which binds directly to the *NOS3* promoter (Wang et al., 2010; Lin et al., 2005). *Sp1* regulates basal *NOS3* expression and responds to stimuli like growth factors and hypoxia, enhancing NO production to maintain vascular tone (Tang et al., 1995; Wariishi et al., 1995). Additionally, *Nrf2*, activated by oxidative stress, enhances *NOS3* transcription by upregulating antioxidant response elements in the *NOS3* promoter (Wu et al., 2019).

Downregulating factors

NF-κB (Nuclear Factor kappa-light-chain-enhancer of activated B cells) represses eNOS expression, particularly in inflammation.

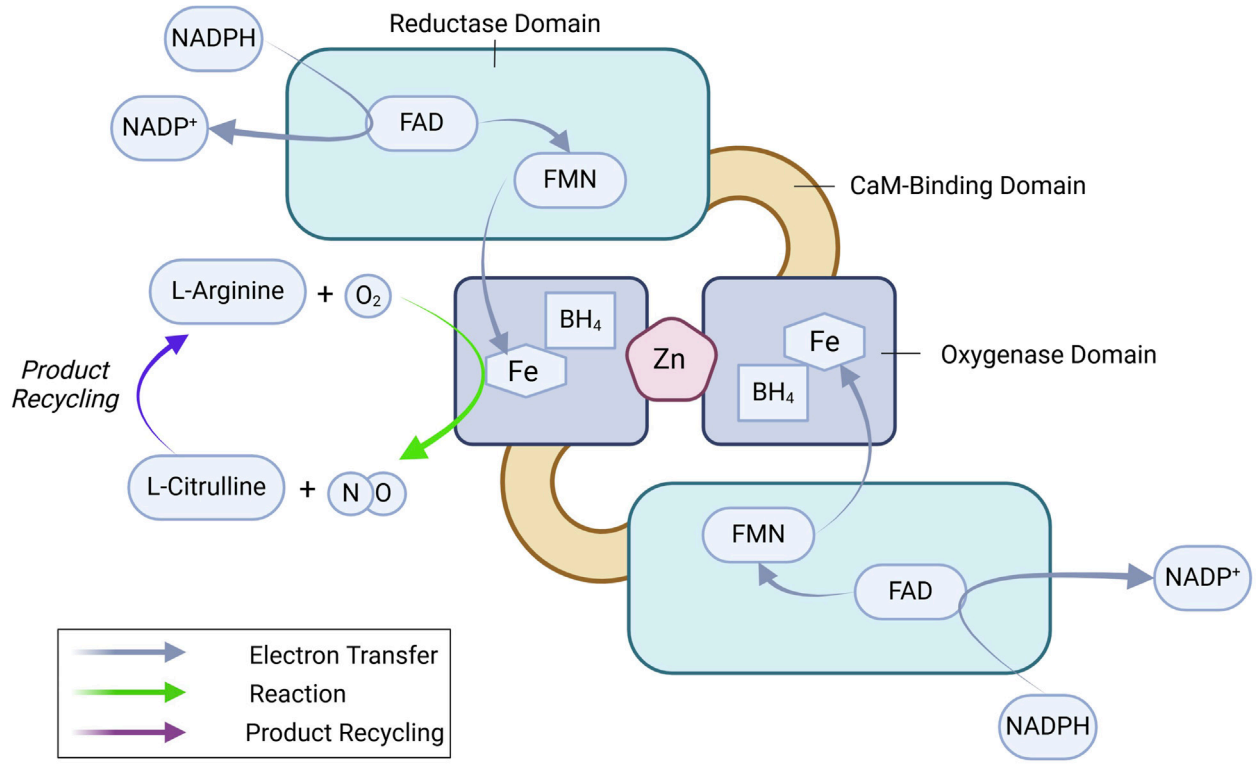

FIGURE 1
eNOS dimer and key enzymatic reactions leading to NO production. See text for details. BH_4, tetrahydrobiopterin; FAD, flavin adenine dinucleotide; FMN, flavin mononucleotide; NADPH, nicotinamide adenine dinucleotide phosphate.

NF-κB is activated by pro-inflammatory stimuli such as tumor necrosis factor-alpha (TNF-α), lipopolysaccharide (LPS), and oxidized low-density lipoprotein (ox-LDL). These molecules trigger signaling events that lead to NF-κB translocation into the nucleus, where it inhibits eNOS transcription (Nishida et al., 1992; Neumann et al., 2004). LPS and ox-LDL, both associated with oxidative stress and vascular inflammation, promote NF-κB activation, further repressing eNOS expression (Liao et al., 1995; Lu et al., 1996).

Dual-regulating factors

Certain factors can both up- or downregulate eNOS expression depending on cellular conditions. Tumor growth factor β (TGF-β)/Smad2 can enhance eNOS transcription in a healthy endothelium but suppress it in chronic inflammation or vascular injury (Saura et al., 2002). Hypoxia-inducible factor-1α (HIF-1α) also exhibits dual regulation: during acute hypoxia, it stimulates eNOS expression to ensure adequate NO production but may suppress eNOS in chronic hypoxia, causing maladaptive vascular changes (McQuillan et al., 1994; Fish et al., 2010).

Post-transcriptional mechanisms offer additional precision by modulating the stability and translation of eNOS mRNA. Elements such as miRNAs (e.g., miR-92a) and long non-coding RNAs (lncRNAs) can either enhance or suppress NO production in response to physiological conditions (Lin et al., 2005; Miao et al., 2018; Suarez et al., 2007; Man et al., 2018; Bonauer et al., 2009).

Post-translational modifications (PTMs) of eNOS

eNOS activity is also intricately regulated by various PTMs, including phosphorylation, acetylation, S-nitrosylation, and palmitoylation. These modifications play critical roles in modulating eNOS enzymatic activity, localization, and interactions with other cellular components (Figure 3).

Phosphorylation is a critical modification that modulates eNOS activity and is tightly regulated by various kinases and phosphatases in response to physiological cues such as shear stress, hypoxia, and growth factors. *Serine 1177* is located on the C-terminal reductase domain and when phosphorylated, enhances eNOS activity by facilitating electron flow from NADPH to the heme domain, contributing to NO production (Fulton et al., 1999; Scotland et al., 2002; Kashiwagi et al., 2013; Li Q. et al., 2013; Park et al., 2016). Ser1177 phosphorylation is key positive regulator of eNOS function (Dimmeler et al., 1999; Tomada et al., 2014). Stimuli such as shear stress, vascular endothelial growth factor (VEGF), and insulin activate kinases including protein kinase B (Akt), AMP-activated protein kinase (AMPK), calcium/calmodulin-dependent protein kinase II (CaMKII), protein kinase A (PKA), and protein kinase G (PKG), which phosphorylate Ser1177 (Fulton et al., 1999; Dimmeler et al., 1999; Michell et al., 1999; Chen et al., 1999; Fleming et al., 2001; Atochin et al., 2007). Phosphorylation by Akt, in particular, is essential for eNOS activation in endothelial cells in response to VEGF and shear stress (Dimmeler et al., 1999; Di

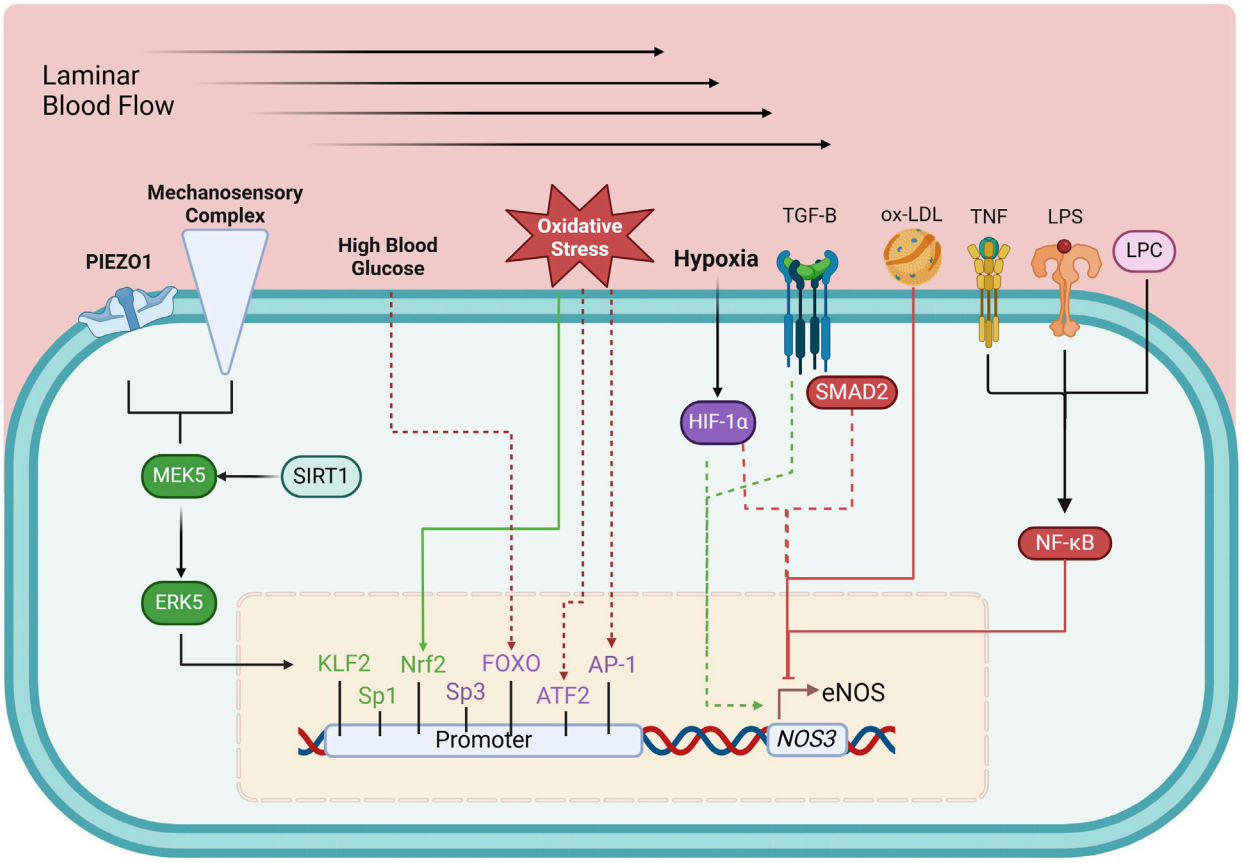

FIGURE 2
Transcriptional regulation of eNOS. Green boxes, upregulating factors; purple boxes, dual-regulating factors; red boxes, down-regulating factors; solid arrows, connection between environmental and metabolic elements to their respective regulating factors; dashed arrows, circumstantial elements that determine the effects of dual-regulating factors; AP-1, activator protein 1; ATF-2, activating transcription factor 2; ERK5, extracellular-regulated kinase 5; FOXO, forkhead box O; HIF-1α, hypoxia-inducible factor 1-α; KLF2, Krüppel-like factor 2; LPC, lysophosphatidylcholine; LPS, lipopolysaccharide; MEK5, Mitogen-activated protein kinase kinase 5; Nrf2, Nuclear factor erythroid 2-related factor; NF-κB, Nuclear Factor kappa-light-chain-enhancer of activated B cells; ox-LDL, oxidized low-density lipoprotein; SIRT1, sirtuin 1; SMAD2, mothers against decapentaplegic homolog-2; Sp1, specificity protein 1; Sp3, specificity protein 3; TGF-β, tumor growth factor β; TNF, tumor necrosis factor. See text for details.

Lorenzo et al., 2013). Ser1177 phosphorylation also increases the Ca^{2+} sensitivity of the synthase, permitting CaM binding and enzyme activation at lower intracellular Ca^{2+} levels (Tran et al., 2009; Mount et al., 2007; McCabe et al., 2000). *Serine 633* is phosphorylated in response to shear stress, exercise, and metabolic stimuli (Mount et al., 2007). Ser633 phosphorylation by PKA and AMPK during physical activity improves NO bioavailability and supports vascular homeostasis (Mount et al., 2007; Michell et al., 2002). *Serine 615* phosphorylation enhances eNOS activity, working cooperatively with Ser1177 to enhance the binding affinity of the Ca^{2+}-CaM complex to eNOS, a critical step for eNOS activation, which ensures a robust response to Ca^{2+} signals (Tran et al., 2009; Bauer et al., 2003). *Threonine 495* phosphorylation, in contrast, inhibits eNOS by suppressing CaM binding (Fleming et al., 2001). Kinases like AMPK and PKC mediate this modification, especially during oxidative stress (Chen et al., 1999). Agonists such as bradykinin promote NO release by inducing Thr495 dephosphorylation, allowing CaM to activate eNOS (Harris et al., 2001). This dephosphorylation is mediated by calcineurin and inhibited by cyclosporine A (Harris et al., 2001). The balance between Thr495 phosphorylation and dephosphorylation is crucial for regulating eNOS activity and NO production. *Serine 114* is phosphorylated in response to shear stress (Mount et al., 2007; Gallis et al., 1999). Though its role remains debatable, phosphorylation at Ser114 is considered a negative regulator of eNOS activity (Mount et al., 2007), supported by the observations that its dephosphorylation by VEGF treatment enhances eNOS function (Bauer et al., 2003) and that a phospho-null mutation here inhibits eNOS activity (Kou et al., 2002; Li et al., 2007).

Acetylation regulates eNOS interactions with other proteins, its plasma membrane localization, and overall enzymatic efficiency. Acetylation at *lysine 609* affects eNOS interaction with heat shock protein 90 (Hsp90) and CaM, both essential for eNOS activation (Taubert et al., 2004). Lysine 609 acetylation is mediated by histone deacetylase 3 and inhibits eNOS activity by preventing proper electron transfer (Jung et al., 2010). In contrast, its deacetylation by sirtuin 1 (SIRT1) restores eNOS activity, enhancing eNOS-CaM interaction (Donato et al., 2011; Arunachalam et al., 2010).

S-nitrosylation is a reversible modification that constrains NO synthesis via a product feedback mechanism (Lipton et al., 1993; Erwin et al., 2005; Lima et al., 2010). S-nitrosylation involves the covalent attachment of a NO group to cysteine thiols, specifically

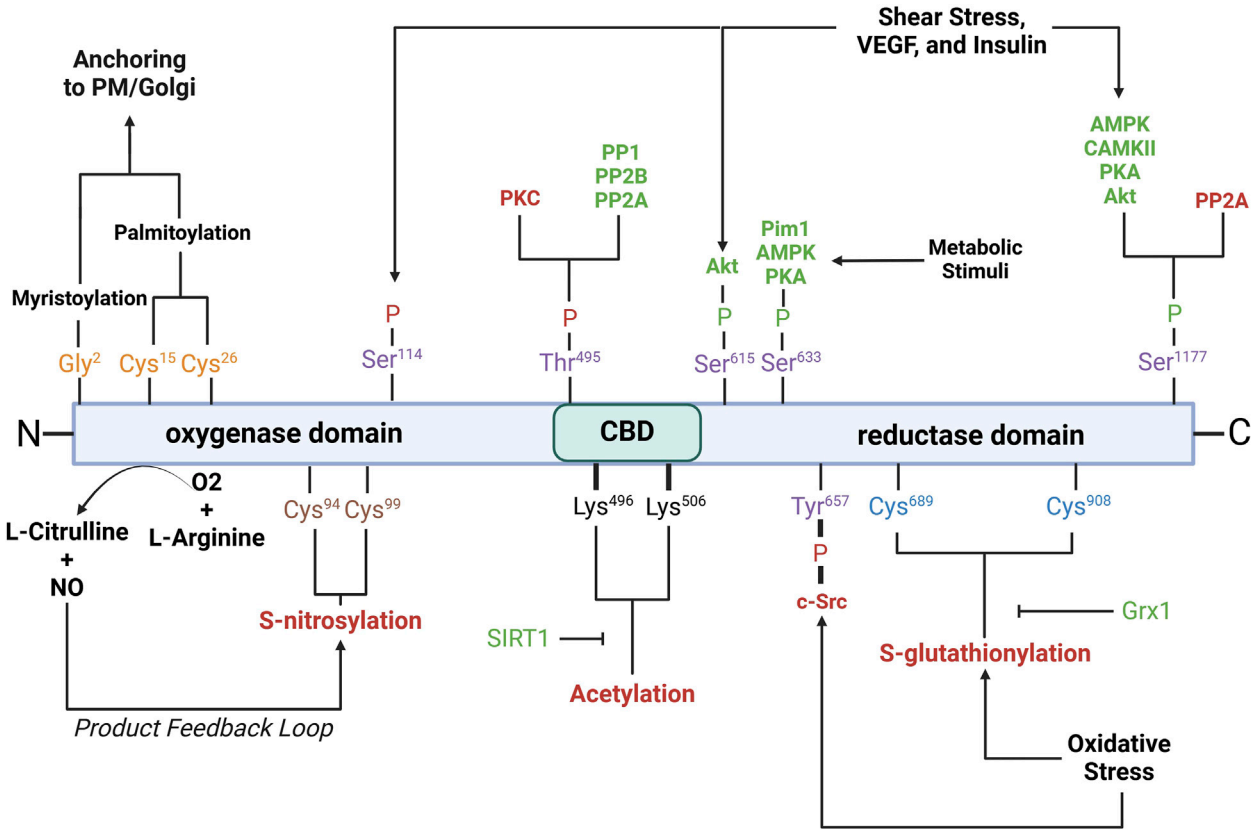

FIGURE 3
Schematic of eNOS domains with key residues involved in post-translational modifications. Purple residues, phosphorylation sites; yellow residues, myristoylation/palmitoylation sites; brown residues, S-nitrosylation sites; black residues, acetylation sites; blue residues, S-glutathionylation sites. Red- and green-letter enzymes, inhibitory and stimulatory effects on eNOS, respectively. Akt, protein kinase B; AMPK, AMP-activated protein kinase; CaMKII, calcium/calmodulin-dependent protein kinase II; c-Src, cellular sarcoma; Grx1, glutaredoxin; Pim1, proviral integration site for Moloney murine leukemia virus 1; PKA, protein kinase A; PKC, protein kinase C; PP1, protein phosphatase 1; PP2A, protein phosphatase 2a; PP2B, protein phosphatase 2b; PM, plasma membrane; SIRT1, sirtuin 1; VEGF, vascular endothelial growth factor. See text for further details.

Cys94 and Cys99 of eNOS, forming S-nitrosothiols (SNOs) (Erwin et al., 2006). Cys94 and Cys99 are located within the zinc tetrathiolate cluster (Erwin et al., 2005) that is important for the eNOS dimer interface; nevertheless, mutation of these sites does not disrupt dimer formation (Erwin et al., 2005). Paradoxically, agonist stimulation, which increases NO production, also promotes rapid denitrosylation of eNOS, in a similar timeframe as phosphorylation at Ser1177 (Erwin et al., 2005). S-nitrosylated eNOS exhibits reduced catalytic activity, which can be reversed with the release of NO. The subcellular localization of eNOS influences the degree of S-nitrosylation, with membrane-bound eNOS being more heavily nitrosylated than its cytosolic counterpart due to higher NO production at the membrane (Erwin et al., 2006).

Glutathionylation is a reversible post-translational modification in which the tripeptide glutathione attaches to cysteine residues in eNOS, notably Cys689 and Cys908, in the reductase domain (Chen et al., 2010). Glutathionylation is promoted by oxidative stress and results in decreased NO production and increased superoxide generation due to disrupted flavin-dependent electron transport (Chen et al., 2010; Crabtree et al., 2013). Fortunately, this modification is reversible through the action of glutaredoxin (Grx1), which interacts closely with eNOS (Chen et al., 2013). Loss of Grx1, either by oxidative stress or genetic silencing, increases eNOS glutathionylation and further NO synthesis (Chen et al., 2013).

Palmitoylation and myristoylation are lipid modifications that regulate the localization and activity of eNOS. Myristoylation, the irreversible attachment of myristic acid to Gly2, anchors eNOS to membranes such as the plasma membrane and Golgi apparatus (Liu et al., 1995; Sessa et al., 1995). Myristoylation is a prerequisite for palmitoylation, a reversible process where palmitic acid binds to Cys15 and Cys26, anchoring eNOS within plasmalemmal caveolae (Fernandez-Hernando et al., 2006). The reversible cycle of palmitoylation and depalmitoylation allows eNOS to dynamically shift between membrane locations in response to physiological signals (Yeh et al., 1999).

Regulation of eNOS by protein-protein interactions (PPIs)

eNOS activity is intricately regulated through its interactions with various binding partners. These interactions play essential roles in modulating its localization, dimerization, and activation, ensuring

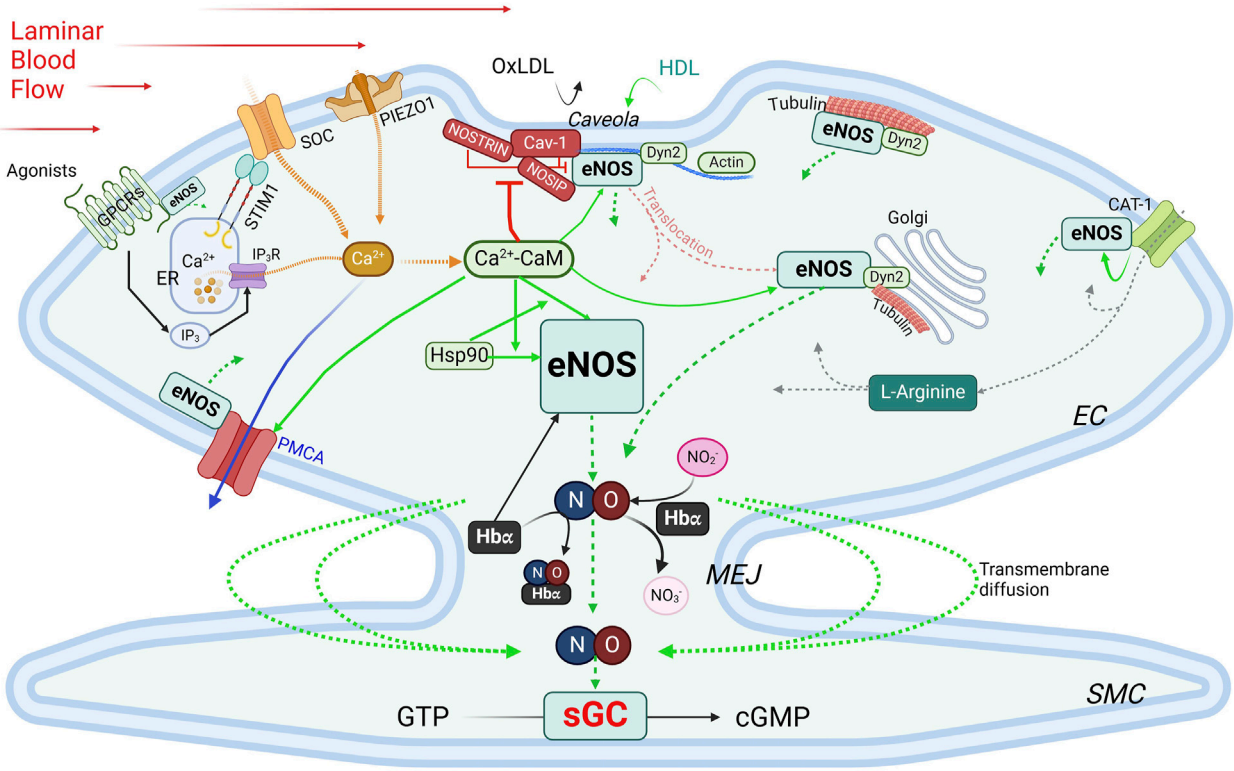

FIGURE 4
Regulation of eNOS by PPIs. Green boxes, stimulatory interacting partners; red boxes, inhibitory interacting partners. Green arrows indicate stimulatory interactions; dotted green arrows, NO production/diffusion; yellow dotted arrows, increase of intracellular Ca^{2+}; solid blue arrow, Ca^{2+} extrusion; grey dotted arrows, L-Arginine transportation. See text for details. CAT-1, cationic anion transporter 1; Cav-1, caveolin-1; Ca^{2+}-CaM, calcium-bound calmodulin; Dyn2, dynamin-2; EC, endothelial cells; ER, endoplasmic reticulum; GPCR, G protein-coupled receptor; Hbα, α subunit of hemoglobin; HDL, high-density lipoprotein; Hsp90, heat shock protein 90; IP_3, inositol trisphosphate; IP_3R, inositol trisphosphate receptor; MEJ, myoendothelial junctions; NOSIP, eNOS-interacting protein; NOSTRIN, eNOS trafficking inducer; ox-LDL, oxidized low-density lipoprotein; PMCA, plasma membrane Ca^{2+}-ATPase; SMC, smooth muscle cell; SOC, store-operated Ca^{2+} channel; STIM1, stromal interaction protein 1.

that eNOS responds appropriately to cellular and environmental signals (Figure 4).

Caveolin-1 (Cav-1) is the main caveolin of caveolae in endothelial cells (Feron et al., 1996; Garcia-Cardena et al., 1996; Ju et al., 1997). Cav-1 binds to eNOS at the caveolin-scaffolding domain (CSD, a.a. 81–101), preventing eNOS interaction with activators, thus inhibiting NO production under basal conditions (Garcia-Cardena et al., 1997; Michel et al., 1997). Physiological stimuli such as shear stress or G protein-coupled receptor (GPCR) agonists like bradykinin promote Ca^{2+} entry, leading to dissociation of the Cav-1-eNOS complex and allowing eNOS to be activated via phosphorylation by kinases such as Akt (Feron et al., 1998). Cav-1 deletion enhances endothelium-dependent relaxation and lowers blood pressure (Murata et al., 2007; Razani et al., 2001). Interaction with Cav-1, however, avoids excessive or aberrant eNOS activity, and Cav-1 deficiency can cause pulmonary hypertension and cardiomyopathy (Drab et al., 2001; Zhao et al., 2002). While plasma membrane localization is ideal for eNOS activation, this also exposes eNOS to external factors like ox-LDL and high-density lipoprotein (HDL). Ox-LDL can disrupt the cholesterol-rich environment in caveolae, thereby reducing NO production specifically from plasma membrane-bound eNOS, whereas Golgi-localized eNOS is more resistant (Zhang et al., 2006; Blair et al., 1999). HDL, on the other hand, provides cholesterol esters to maintain caveolae's cholesterol, and via palmitoylation, retain eNOS at the plasma membrane (Uittenbogaard et al., 2000).

Ca^{2+}-calmodulin eNOS activity is regulated by a complex and tightly regulated network of functionally and physically interacting proteins involved in Ca^{2+} signaling, including Ca^{2+} entry, the Ca^{2+} sensor CaM, and Ca^{2+} efflux. CaM, in its Ca^{2+}-bound form (Ca^{2+}-CaM), is required for activating eNOS by facilitating electron flow from the reductase domain to the oxygenase domain and promoting dimerization of the latter (Forstermann et al., 1991; Busse and Mulsch, 1990; Hellermann and Solomonson, 1997). The Ca^{2+} entry mechanisms in ECs play important roles in this process, as evidenced by the observations that removal of extracellular Ca^{2+} or inhibition of CaM suppresses agonist-induced NO production (Forstermann et al., 1991; Busse and Mulsch, 1990; Singer and Peach, 1982). *Two major Ca^{2+} entry pathways* are important for NO production: store-operated Ca^{2+} entry (SOCE), the main agonist-induced Ca^{2+} entry mechanism in ECs (Abdullaev et al., 2008; Tran, 2020), and mechanosensitive Ca^{2+} entry, stimulated by blood shear stress. For activation of SOCE, the stromal interaction molecule 1 (STIM1) is required (Roos et al., 2005; Soboloff et al., 2012). Vascular STIM1 plays opposing roles in the regulation of vascular tone; smooth muscle cell STIM1 is important for VSMC contractility, proliferation and the development of hypertension (Kassan et al., 2016). On the other hand, endothelial STIM1 plays a

critical role in the activation of eNOS to produce NO, such that EC-specific deletion of the *STIM1* gene impairs endothelium-dependent vasorelaxation and increases blood pressure (Nishimoto et al., 2018). Shear stress, a potent physiological stimulus of NO production, stimulates PIEZO1 mechanosensitive channel for Ca^{2+} entry (Wang et al., 2016; Ranade et al., 2014; Li J. et al., 2014). Once bound to Ca^{2+}, CaM regulates eNOS activity via *two important mechanisms*. First, the Ca^{2+}-CaM complex displaces eNOS from the inhibitory interaction with caveolin (Michel et al., 1997). Second, CaM binds eNOS at a canonical CaM-binding site encompassing amino acids 493–512 (Venema et al., 1996) with a K_d value of ~0.2 nM (Tran et al., 2005). This interaction is inhibited at low Ca^{2+} concentration by the autoinhibitory domain (residues 595–639) (Chen and Wu, 2000). Upon increases in intracellular Ca^{2+}, Ca^{2+}-bound CaM binds eNOS, displacing the autoinhibitory loop and facilitating electron transfer between the two domains (Pollock et al., 1991; Nishida and Ortiz de Montellano, 1999). Phosphorylation at Ser615 within this loop reduces the concentration of Ca^{2+} required for eNOS-CaM interaction, alleviating the autoinhibitory effect (Tran et al., 2008). CaM binding also enhances eNOS phosphorylation at Ser1177, which, in combination with Ser615 phosphorylation, further increases the Ca^{2+} sensitivity of eNOS-CaM interaction and synthase activation (Fleming et al., 2001; Tran et al., 2009; Tsukahara et al., 1994; Fleming et al., 1997). These phosphorylation events facilitate significant eNOS-CaM interaction and synthase activity at basal level of intracellular Ca^{2+} and explain the effects of factors that promote NO production without triggering significant increases in global cytoplasmic Ca^{2+}. *Interaction with Ca^{2+} efflux channel* – The plasma membrane Ca^{2+}-ATPase (PMCA) is a key Ca^{2+} extrusion mechanism in ECs (Wang et al., 2002; Tran et al., 2003). eNOS directly interacts via residues 735 – 934 in its reductase domain with residues 428–651 in the catalytic domain of PMCA (Holton et al., 2010). This interaction enhances phosphorylation of Thr495 in the CaM-binding domain of eNOS (Holton et al., 2010), which reduces eNOS-CaM interaction (Fleming et al., 2001). The Ca^{2+}/CaM-dependent phosphatase calcineurin is associated with the PMCA-eNOS complex, suggesting a potential role in the effect of PMCA expression on Thr495 phosphorylation status (Holton et al., 2010). Interestingly, PMCA activity is controlled by CaM interaction (Di Leva et al., 2008) and Ca^{2+} extrusion via PMCA moderates eNOS-CaM binding and synthase activation (Tran et al., 2016). Thus, CaM binding fine-tunes NO synthesis in response to subtle changes in the Ca^{2+} concentration surrounding eNOS and by control the activities of many of its interacting partners. With sub-nanomolar affinity for its interaction with CaM and limited abundance of CaM in ECs, eNOS expression level and activation in turn significantly influences the CaM-binding proteome in ECs (Tran et al., 2005; Tran et al., 2003). Treatment with 17β-estradiol or an agonist of the G protein-coupled estrogen receptor enhances CaM expression level substantially in ECs and promotes eNOS activity by moderating Ca^{2+} entry and efflux, enhancing eNOS-CaM interaction and associated eNOS phosphorylation (Tran, 2020; Tran et al., 2016; Fredette et al., 2017; Tran et al., 2015; Terry et al., 2017).

Interactions with components of the cytoskeleton and membrane-targeted proteins Actin interacts with an eight-amino acid motif (Jo et al., 2011; Higashi et al., 2002; Maier et al., 2000; Setoguchi et al., 2001; Fukuda et al., 2002; Holowatz and Kenney, 2011; Nystrom et al., 2004; Worthley et al., 2007) in the oxygenase domain of eNOS (Kondrikov et al., 2010). In *in vitro* assays, G-actin promotes eNOS activity more than does F actin (Su et al., 2003); however, a low G/F actin ratio appears to correlate with higher eNOS expression level (Searles et al., 2004). *Dynamin-2* (Dyn2) is a GTP-binding protein in the caveolae and the Golgi (McClure and Robinson, 1996). Dynamin-2 interacts directly with eNOS in these compartments in ECs; this interaction is enhanced by Ca^{2+} and increases eNOS activity (Cao et al., 2001). *NOSTRIN* (e*NOS t*rafficking *in*ducer), a 506-a.a. protein enriched in vascular tissues, interacts with eNOS via an SH3 domain, promotes eNOS redistribution from the membrane, and inhibits synthase activity (Zimmermann et al., 2002). It also interacts with a region spanning a.a. 1- 61 of cav-1, N-terminally from the cav-1 scaffolding domain, thus forming a ternary complex with eNOS and cav-1 (Schilling et al., 2006). NOSTRIN interacts with dynamin-2 and is required for recruitment of eNOS to dynamin-containing structures (Icking et al., 2005). *NOSIP* (e*NOS-i*nteracting *p*rotein) is another protein residing in caveolae that interacts with eNOS and promotes its translocation from the plasma membrane and inhibit NO production (Dedio et al., 2001). In addition, eNOS associates with *tubulin* (Dedio et al., 2001), which plays an important role in its trafficking to the Golgi. Acetylation of α tubulin is involved in stabilizing microtubules where eNOS is associated in the Golgi and is phosphorylated for basal activity (Giustiniani et al., 2009). *Interaction with GPCRs* – Evidence from *in vitro* studies indicates that eNOS can interact with the juxtamembranous regions of AT_1R, ET_A, ET_B and bradykinin B_2 receptor (Marrero et al., 1999). While these interactions are likely important because activation of these receptors increases intracellular Ca^{2+}, which is predicted to activate eNOS, they require further verification *in vivo*. Activity of eNOS is also regulated by its direct association with the *cationic amino acid transporter (CAT)-1*, the key transporter of L-arginine (Li et al., 2005). The promotion of eNOS activity by its interaction with CAT-1 is independent of L-arginine transport and is associated with enhanced phosphorylation at Ser1177 and Ser633 and reduced interaction with cav-1 (Li et al., 2005).

Heat shock protein 90 (Hsp90) is a molecular chaperone that stabilizes eNOS, thereby promoting its activation. The substrate-binding region of Hsp90 binds to the oxygenase domain of eNOS between a.a. 310–323 (Fontana et al., 2002; Xu H. et al., 2007). This interaction is increased by stimuli such as VEGF, histamine, estrogen, and shear stress (Garcia-Cardena et al., 1998; Russell et al., 2000; Venema et al., 1997). Hsp90 binding enhances phosphorylation at Ser1177 by recruiting kinases such as Akt, which further boosts NO production (Fontana et al., 2002). Hsp90 is critical for eNOS activity, and is involved in a *reciprocal interactive relationship with eNOS and CaM*: Hsp90 enhances both the magnitude and sensitivity of eNOS activation in response to Ca^{2+}-CaM; in turn, the effect of Hsp90 to promote eNOS activity is enhanced by Ca^{2+}-CaM complex (Takahashi and Mendelsohn,

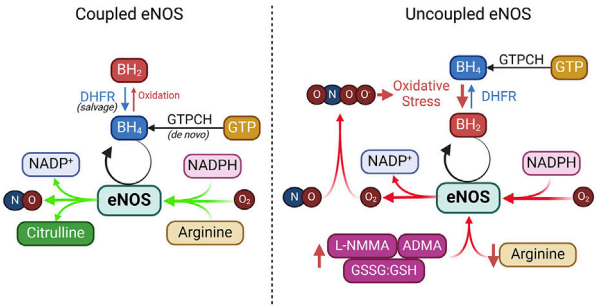

FIGURE 5
Coupled vs. uncoupled eNOS. See text for details. ADMA, asymmetric dimethylarginine; DHFR, dihydrofolate reductase; GTPCH, GTP cyclohydrolase I; GSSG, glutathione disulfide; GSH, glutathione; L-NMMA, NG-Monomethyl-L-arginine; NADPH, nicotinamide adenine dinucleotide phosphate.

2003). Hsp90 also exerts a CaM-independent effect to promote eNOS activity (Takahashi and Mendelsohn, 2003).

Hemoglobin alpha (Hbα) The α, but not β, subunit of hemoglobin is expressed in ECs in resistance blood vessels, where it is concentrated in the myoendothelial junctions (MEJs) between ECs and VSMCs (Straub et al., 2012). Hbα regulates NO availability via three mechanisms. *First*, it can bind and release NO and thus can act as both a reservoir and scavenger of NO, thereby regulating NO-mediated processes (Straub et al., 2014a; Keller et al., 2022; Straub et al., 2014b). In its ferrous (Fe^{2+}) form, Hbα binds NO with high affinity, yielding nitrate and ferric (Fe^{3+}) Hbα, which binds NO with much lower affinity (Straub et al., 2012). The reduction of Fe^{3+} Hbα to Fe^{2+} Hbα, catalyzed by cytochrome b5 reductase 3 (CytB5R3), thus enhances the scavenging action of NO by Hbα (Straub et al., 2012). *Second*, Hbα associates at its residues 34–43 with the oxygenase domain of eNOS in a macromolecular complex (Straub et al., 2014a), an interaction dictated by amino acids ^{36}SFPT^{39} in the Hbα sequence (Keller et al., 2022). However, excessive NO scavenging in conditions of elevated Hb concentrations in the MEJs can reduce NO bioavailability and induce endothelial dysfunction (Denton et al., 2021), increasing vascular resistance (Straub et al., 2014a). *Third*, endothelial Hbα can function as a nitrite reductase, which produces NO through reduction of nitrite in hypoxic condition (Keller et al., 2022). These dynamic interactions help ensure that NO is available when needed, particularly in response to conditions like hypoxia and exercise, where vasodilation and increased tissue oxygen delivery are critical (Kim-Shapiro et al., 2005; Umbrello et al., 2013). In this context, it is worth noting that myoglobin is expressed in VSMCs and contributes to nitrite-dependent generation of NO in response to hypoxia independently of eNOS or iNOS (Totzeck et al., 2012).

Regulation of eNOS by substrates, co-factors, and product recycling

The availability of substrates, co-factors, and the efficiency of product recycling are critical factors that dictate the outcome of eNOS activation. Disruptions in substrate availability, co-factor balance, or recycling processes—due to oxidative stress, metabolic disorders, or nutrient deficiencies—can impair eNOS activity and reduce NO bioavailability (Figure 5).

L-arginine is the primary substrate for eNOS and is converted into NO and L-citrulline during the enzymatic reaction. Given its high affinity for eNOS (K_m ~2–3 μM) and an intracellular concentration above 100 μM, L-arginine is considered abundant in endothelial cells (Bode-Boger et al., 2007; Hardy and May, 2002). Nevertheless, extracellular L-arginine at millimolar concentrations can stimulate NO production (McDonald et al., 1997a; McDonald et al., 1997b). This has been considered the "arginine paradox." Several mechanisms have been proposed to explain this phenomenon. One hypothesis involves the close association of eNOS with arginine transporters like CAT-1 and L-arginine recycling enzymes such as argininosuccinate lyase (ASL) (Erez et al., 2011). Other factors like competition from other amino acids, reduced uptake by cationic amino acid transporters (CATs), and elevated arginase activity—common in conditions such as hypertension and diabetes—can limit L-arginine availability to eNOS, diverting it away from NO production (McDonald et al., 1997a; McDonald et al., 1997b). Additionally, asymmetric dimethylarginine (ADMA), an endogenous inhibitor of eNOS, competes with L-arginine for binding, reducing NO synthesis (Boger et al., 1998a; Boger et al., 1998b). In addition to reducing NO synthesis, ADMA removes the suppression by NO of T-type voltage-dependent Ca^{2+} channels in VSMCs (Smith et al., 2020), triggering depolarizing Ca^{2+} spikes in VSMCs leading to vasoconstriction (Ng et al., 2024).

Tetrahydrobiopterin (BH_4) is an essential cofactor for eNOS required for efficient electron transfer during the synthase's catalytic cycle (Alp and Channon, 2004; Crabtree et al., 2009a; Bendall et al., 2014). BH_4 keeps eNOS in a "coupled" state, in which it synthesizes NO rather than harmful superoxide (Alp and Channon, 2004; Crabtree et al., 2009b). BH_4 can be produced through two pathways: *de novo synthesis*, regulated by the rate-limiting enzyme guanosine triphosphate cyclohydrolase I (GTPCH), or through *the salvage pathway*, where dihydrobiopterin (BH_2) is recycled back to BH_4 by dihydrofolate reductase (DHFR) (Crabtree et al., 2009b; Crabtree and Channon, 2011). Under oxidative stress, BH_4 is rapidly oxidized into BH_2 by superoxide anions or peroxynitrite, which is particularly strong during NO scavenging (Milstien and Katusic, 1999). This oxidative depletion of BH_4 causes uncoupling of eNOS, where it produces superoxide instead of NO.

NADPH is a critical electron donor in eNOS and facilitates electron transfer through FAD and FMN for effective NO production. It also maintains the redox state of BH_4, ensuring efficient NO synthesis (Reyes et al., 2015). Depletion of NADPH, as seen in glucose-6-phosphate dehydrogenase deficiency or due to excessive consumption by NADPH oxidases, leads to eNOS uncoupling and oxidative stress (Noreng et al., 2022). Additionally, activation of CD38 in post-ischemic heart injury can severely deplete NADPH, impairing eNOS function and disrupting NADPH-dependent BH_4 salvage and synthesis (Reyes et al., 2015).

FAD and FMN, both derived from riboflavin (vitamin B_2), are essential co-factors for eNOS's electron transfer process. These flavins facilitate the flow of electrons from NADPH to the

oxygenase domain, ensuring efficient NO production (Figure 1). Deficiency in FAD and FMN due to poor dietary intake or metabolic disorders can impair eNOS activity, resulting in reduced NO synthesis and increased oxidative stress.

eNOS uncoupling

Under certain conditions, eNOS can become "uncoupled," shifting from producing NO to generating superoxide ($O_2^{\cdot-}$), which not only reduces NO availability but also increases oxidative stress, reducing endothelial dysfunction. This section briefly explores the main causes of eNOS uncoupling and their therapeutic implications (Figure 5).

BH_4 deficiency

Suboptimal levels of BH_4, or a decreased BH_4/BH_2 ratio, are significant contributors to eNOS uncoupling observed in hypertension, diabetes, and atherosclerosis (Vasquez-Vivar et al., 1998; Wever et al., 1997; Soltis and Cassis, 1991; Hong et al., 2001; Landmesser et al., 2003; Lee et al., 2009). Studies in animal models, such as hypertensive mice and rats and apolipoprotein E-deficient mice, have demonstrated that oxidative depletion of BH_4 leads to increased eNOS-derived superoxide, which impairs vasorelaxation (Hong et al., 2001; Landmesser et al., 2003; Laursen et al., 2001). In humans, decreased BH_4 levels and eNOS uncoupling have been linked to coronary artery disease, diabetes, and hypertension (Antoniades et al., 2007; Ismaeel et al., 2020; Heitzer et al., 2000b; Stroes et al., 1997). This imbalance is further exacerbated by oxidative stress, which directly oxidizes BH_4 to BH_2, reducing BH_4 availability for NO synthesis (Vasquez-Vivar et al., 1998; Laursen et al., 2001; Guzik et al., 2002; Alp et al., 2003; Bendall et al., 2005). Additionally, reduced expression of GTP-cyclohydrolase 1, the rate-limiting enzyme in BH_4 synthesis, and dihydrofolate reductase, the enzyme that recycles BH_2 to BH_4, further contributes to eNOS uncoupling in diabetes and hypercholesterolemia (Alp and Channon, 2004; Xu et al., 2009; Xu J. et al., 2007; Whitsett et al., 2007; Munzel and Daiber, 2017; Chuaiphichai et al., 2017).

L-arginine deficiency or imbalance

L-arginine depletion is a significant contributor to eNOS uncoupling. Although intracellular L-arginine concentration typically far exceeds its K_m for eNOS, obesity, diabetes, and cardiovascular diseases can cause L-arginine deficiency. In such cases, reduced availability of L-arginine limits its ability to act as a substrate for eNOS, favoring the production of ROS over that of NO (Bode-Boger et al., 2007; Yang and Ming, 2013). A key mechanism of L-arginine depletion is upregulation of arginase, an enzyme that competes with eNOS for L-arginine and converts it into urea and L-ornithine. Arginase induction is particularly prevalent in obesity, diabetes, and atherosclerosis (Lass et al., 2002). For example, oxidized LDL significantly increases ARG2 expression levels in ECs (~20%) but increases its activity by ~80% (Ryoo et al., 2006). Many other factors can upregulate the expression level and activity of arginase, such as lipopolysaccharide, TNF-α, glucose, thrombin, hypoxia and angiotensin II [reviewed in Pernow and Jung (2013)]. Inhibiting arginase or supplementing L-arginine can restore NO production and improve endothelial function in these conditions (Chicoine et al., 2004). Furthermore, imbalance between L-arginine and ADMA, an endogenous inhibitor of eNOS, leading to reduced L-arginine/ADMA ratio, contributes to eNOS uncoupling (Closs et al., 2012; Watson et al., 2016; Peyton et al., 2018).

Oxidative stress and reactive oxygen species (ROS)

Oxidative stress plays a pivotal role in disrupting endothelial function by promoting eNOS uncoupling. Excessive ROS overwhelms the antioxidant defense system and causes oxidative stress that damages lipids, proteins, and DNA, contributing to the development of CVD (Thannickal and Fanburg, 2000; Costa et al., 2021; Sharifi-Rad et al., 2020; Li H. et al., 2013). Risk factors such as dyslipidemia, diabetes, hypertension, obesity, and smoking increase ROS levels, increasing endothelial dysfunction and CVD progression (Cai and Harrison, 2000; Xiang et al., 2021; Jurcau and Ardelean, 2022). ROS also play a key role in ischemia-reperfusion injury (Xiang et al., 2021; Jurcau and Ardelean, 2022). In the vascular wall, enzymes such as NADPH oxidase, xanthine oxidase, and uncoupled eNOS generate ROS, particularly superoxide. Superoxide reacts with NO to form peroxynitrite ($ONOO^-$), a toxic compound that depletes NO and worsens endothelial dysfunction (Li H. et al., 2014; Thomson et al., 1995; Victor et al., 2009). NADPH oxidases, particularly NOX_2, are major sources of superoxide in diabetes, hypertension, smoking, and aging (Konior et al., 2014; Gray et al., 2013; Manea et al., 2018; Fukui et al., 1997; Marchi et al., 2016; Kim et al., 2014; Jiang et al., 2011). The oxidative depletion of BH_4 by ROS, especially via NADPH oxidases, further exacerbates eNOS uncoupling (Konior et al., 2014; Zhang et al., 2020).

eNOS glutathionylation

S-glutathionylation at Cys689 and Cys908 in the reductase domain results in eNOS uncoupling (Figure 3) (Chen et al., 2010; Chen et al., 2013; Suvorava et al., 2015; Zweier et al., 2011). This modification typically occurs under oxidative stress, when the ratio of reduced glutathione (GSH) to oxidized glutathione (GSSG) decreases (Suvorava et al., 2017; Benson et al., 2013; Daiber et al., 2002). S-glutathionylation disrupts the alignment of FAD and FMN, essential cofactors for eNOS's electron transport, resulting in superoxide production instead of NO (Chen et al., 2010; Zweier et al., 2011). This mechanism of eNOS uncoupling is unique in that it occurs in the reductase domain, unlike other uncoupling mechanisms that occur in the oxygenase domain, and can be inhibited by L-NAME (Chen et al., 2010). *In vivo* studies have confirmed the association of eNOS S-glutathionylation with endothelial dysfunction in hypertension, aging, and cardiovascular diseases (Chen et al., 2010; Suvorava et al., 2015). In *ex vivo* rat aortic segments and spontaneously hypertensive rats, high levels of eNOS S-glutathionylation correspond with impaired vasodilation. S-glutathionylation can be reversed by Grx-1 (Chen et al., 2013; Shang et al., 2017).

Strategies to enhance endogenous no production

The use of exogenous NO donors is limited by the short-lived nature of their effects and the development of nitrate tolerance.

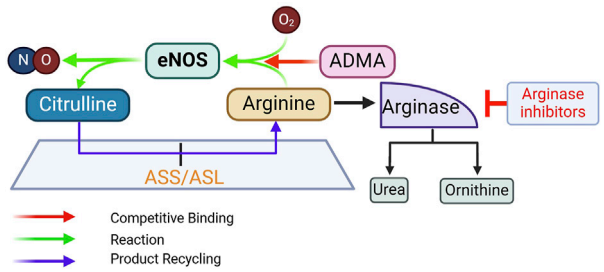

FIGURE 6
Rationale for supplementing L-arginine, inhibiting arginase, and supplementing L-citrulline to promote eNOS activity. ADMA, asymmetric dimethylarginine; ASL, argininosuccinate lyase; ASS, argininosuccinate synthase. See text for more details.

Enhancing endogenous NO production should provide physiological and more sustained effects. Current strategies involve promoting eNOS activity by providing essential substrates or cofactors or by pharmacologically upregulating eNOS expression and activity; this could also be done by preventing/reversing eNOS uncoupling. We will divide our review below of these approaches based on the level of available evidence.

Approaches with both preclinical and clinical evidence

L-arginine supplementation

Rationale

L-arginine supplementation to promote NO production is based on the premise that in conditions of endothelial dysfunction, intracellular L-arginine levels may become suboptimal. It is also based on the "arginine paradox," discussed above, that despite an intracellular L-arginine concentration much higher than its K_m for eNOS activity, high extracellular concentration of L-arginine can still promote NO production. Additionally, L-arginine also competes with ADMA, an endogenous eNOS inhibitor (Boger et al., 1998c), thereby restoring the L-arginine/ADMA ratio that is critical for eNOS activity (Dong et al., 2011) (Figure 6).

Evidence

Early preclinical studies provided evidence that oral L-arginine supplementation improves acetylcholine (ACh)-induced vasorelaxation and NO production (Girerd et al., 1990; Cooke et al., 1991; Rossitch et al., 1991; Boger et al., 1995). Clinical studies began with *intravascular injection of L-arginine* in small groups of subjects. In hypercholesterolemic patients (n = 8, mean age 51.5) with slight luminal irregularities of the left anterior descending coronary artery (LAD), ACh-induced reduction in coronary blood flow, an indication of endothelial dysfunction, is improved by intracoronary injection of L-arginine (Drexler et al., 1991). In patients with diffuse atherosclerotic LADs (n = 13, age 56 ± 7.5), direct intracoronary L-arginine injection also ameliorates the ACh-induced vasoconstriction and reduction in blood flow (Dubois-Rande et al., 1992). In patients with critical peripheral limb ischemia (n = 10, age 68.3 ± 3.1), a single intravenous dose of L-arginine significantly increases blood flow, accompanied by urinary cGMP excretion (Bode-Boger et al., 1996). *Overall, intravascular L-arginine delivery in humans offers acute improvement of endothelial function.* In young healthy subjects (n = 80, age 25.4 ± 0.2), this effect is achieved with higher doses and is correlated with L-arginine plasma concentrations (Bode-Boger et al., 1998).

From clinical trials testing the effects of oral administration of L-arginine, a picture has emerged that *short-term L-arginine administration (≤3 months) provides benefits, whereas longer supplementation (≥6 months) gives mixed results.* For example, 4-week L-arginine supplementation improves reactive hyperemia in patients with hypertension and hyperhomocysteinemia (2.4 g/d, n = 25, age 40–65) (Reule et al., 2017); and flow-mediated dilation is improved by 3-month L-arginine supplementation in hypertensive subjects (2.4 g/d, n = 40, age 40–65) (Menzel et al., 2018). In patients with a history of coronary bypass surgery, 6-month supplementation with L-arginine (6.4 g/d, n = 32, age 65 ± 10) reduces ADMA levels, increases plasma cGMP, and improves reactive hyperemia compared to placebo (n = 32, age 64 ± 11) (Lucotti et al., 2009). However, 6-month supplementation with L-arginine in patients with peripheral arterial disease (3 g/d, n = 66, age 73 ± 9) does not increase NO synthesis or improve vascular reactivity vs. placebo (3 g/d, n = 67, age 72 ± 7) (Wilson et al., 2007) or alter vascular stiffness in post-myocardial infarction (MI) patients (3 × 3 g/day, n = 75, age 60.4 ± 12.9) (Schulman et al., 2006). This has led to the "*arginine tolerance*" hypothesis (Wilson et al., 2007), akin to the common nitrate tolerance phenomenon.

Challenges

Given the state of current evidence, major cardiovascular guidelines do not include L-arginine supplementation for the prevention of CVD. Among explanations for the absence of effect of long-term L-arginine administration in some clinical trials, oxidative depletion of BH_4 can result in eNOS uncoupling even with sufficient L-arginine supply (Xiong et al., 2014; Scalera et al., 2009). L-arginine also increases arginase expression, which in turn reduces L-arginine availability (Caldwell et al., 2018; Wang et al., 2006), a mechanism that may partly explain the arginine tolerance hypothesis. Nevertheless, interpretation of results of clinical trials for oral L-arginine should include whether the treatment regimens include other drugs that also promote eNOS function and whether there is baseline L-arginine deficiency. For example, in post-MI patients (n = 78, age 60.2 ± 14.2), addition of L-arginine (3 × 3 g/d) to the post-MI treatment regimen for 6 months does not improve vascular stiffness or left ventricular function compared to patients receiving placebo (n = 75, age 60.4 ± 12.9) (Schulman et al., 2006). However, in addition to the normal baseline L-arginine levels in both groups, this treatment regimen includes aspirin, which acetylates eNOS and promotes NO production (Taubert et al., 2004); clopidogrel, which stimulates eNOS phosphorylation (Schafer et al., 2011); an ACE inhibitor, which inhibits degradation of bradykinin, thereby triggering endothelial Ca^{2+} signals and activating eNOS (Bachetti et al., 2001); and a statin, which stabilizes eNOS mRNA and activates the PI3K/Akt pathway to activate the synthase (Wang et al., 2005). Similarly, in patients with hypertension and hyperhomocysteinemia (18 males and 7 females, age 40–65), reactive hyperemia is improved by 4 weeks oral L-arginine (Reule et al., 2017), administered in a

mixture with pycnogenol, which itself activates eNOS (Fitzpatrick et al., 1998); α lipoic acid, which promotes eNOS recoupling (Sena et al., 2008); vitamin B2, which is a cofactor for eNOS; and folic acid, which activates eNOS and prevents its uncoupling (Stroes et al., 2000). The effects of co-treatment agents on eNOS may obscure or reduce the observed effect of L-arginine on endothelial function.

Inhibiting arginase

Rationale

Arginase was identified in 1904 as the enzyme that hydrolyzes L-arginine into ornithine and urea (Kossel and Dakin, 1904). Two isoforms exist – *Arg1* and *Arg2*. *Arg1* is expressed abundantly in hepatic tissue, where it plays a major role in the urea cycle, whereas *Arg2* is more predominant in extrahepatic tissues. Both isoforms are expressed in ECs (Buga et al., 1996); and many risk factors of CVD can increase the expression levels and activity of endothelial arginase (Pernow and Jung, 2013; Ryoo et al., 2008). Thus, arginase inhibition in ECs is predicted to increase L-arginine availability for NO production by eNOS (Figure 6).

Evidence

Considering a high K_m value for L-arginine as substrate for arginase (1–3 mM), it has been reasoned that the main function of arginase is to limit the intracellular accumulation of L-arginine; whereas given a low K_m value for L-arginine as substrate of NOS (10–20 μM), arginase may not affect basal NO production, unless L-arginine level falls below 10–20 μM (Buga et al., 1996). Nevertheless, the Vmax for L-arginine of arginase is ~1,000-fold higher than that of the NO synthases (Wu and Morris, 1998). So theoretically, arginase can compete with eNOS for L-arginine and affect NO synthesis. Indeed, treatment of ECs with L-arginine increases production of both urea and NO, while treatment with L-valine, which inhibits arginase [IC_{50} ~ 6.2 ± 0.4 mM (Paik et al., 1978)], increases NO production only; consistently, combined treatment with L-arginine and L-valine shifts the balance towards NO synthesis over urea formation (Chicoine et al., 2004). Additionally, overexpression of both arginase isoforms reduces L-arginine availability (Li et al., 2001). Many arginase inhibitors with high affinity have been developed over the past several decades, such as N-hydroxy-L-arginine [NOHA, K_i = 3.6 μM for human ARG1 (Di Costanzo et al., 2010), 1.6 μM for human ARG2 (Colleluori and Ash, 2001)], N-hydroxy-nor-L-arginine [nor-NOHA, K_d = 0.47 μM for human ARG1 (Di Costanzo et al., 2010), 51 nM for human ARG2 (Colleluori and Ash, 2001)] and boronic acid derivatives like 2(S)-amino-6-hexanoic acid (ABH) [IC_{50} values of derivatives range 17–1,470 nM for human ARG1, 30–2,150 nM for human ARG2 (Collet et al., 2000; Ilies et al., 2011)] and S-(2-boronoethyl)-l-cysteine (BEC) [K_i = 0.4–0.6 μM (Busnel et al., 2005)]. A comprehensive review of arginase inhibitors can be found in Pudlo et al. (2017). In *preclinical models,* arginase inhibition prevents eNOS uncoupling and atherogenesis. In hypercholesterolemic mice, deletion of *Arg2* or inhibition of arginase with BEC improves endothelial function and reduces atherosclerosis (Ryoo et al., 2008). Similarly, in diet-induced obesity models, arginase inhibition with ABH or deletion of *Arg1* or *Arg2* reverses vascular dysfunction (Bhatta et al., 2017; Atawia et al., 2019). In diabetic mice, the use of ABH effectively restores endothelial function (Pernow et al., 2015). *Clinical studies* in small groups of patients have shown effect of *intravascular* injection of nor-NOHA in several vascular beds in various conditions of EC dysfunction. Intra-arterial infusion of nor-NOHA (0.1 mg/min) improves endothelium-dependent vasorelaxation in radial artery following ischemia-reperfusion injury in male patients (average age 65) with coronary artery disease (CAD, n = 12) or CAD and type 2 diabetes (T2D, n = 12) (Kovamees et al., 2014). The same dose of nor-NOHA administration also improves endothelium-dependent vasorelaxation in forearm vessels in patients with heterozygous familial hypercholesterolemia (n = 12, age 32) and healthy controls (n = 12, age 30) (Kovamees et al., 2016a). Similarly, 0.1 mg/min infusion of nor-NOHA improves endothelium-dependent vasodilation in the forearm microvasculature in T2D patients (n = 12, age 66 ± 4), but not in age-matched healthy subjects (n = 12) (Kovamees et al., 2016b). Intracoronary infusion of nor-NOHA (0.1 mg/min) also enhances endothelium-dependent vasorelaxation in coronary arteries in patients (age 69 ± 3) with CAD (n = 16), or CAD and T2D (n = 16), but not in healthy subjects (n = 16) (Shemyakin et al., 2012). These effects appear to be more pronounced in aged than in younger subjects (n = 21, age 48–75) (Mahdi et al., 2019), and does not depend on efficacy of blood glucose-lowering therapy in T2D patients (n = 16, average age 64) (Mahdi et al., 2018). Nor-NOHA improves EC dysfunction in T2D patients (n = 26), but not in type 1 diabetes (T1D) patients (n = 13) with equal blood glucose levels (Tengbom et al., 2024).

Challenges

Clinical trials testing the effect of *oral arginase inhibitors* on endothelial function are currently not available, due perhaps to the fact that most oral formulations of arginase inhibitors have poor oral bioavailability (Pudlo et al., 2017). Some clinical trials have begun to test new oral arginase inhibitors in cancer therapy, based on the high expression level of ARG1 in immunosuppressive cells. Examples include OATD-02, a recently developed ARG1/2 dual inhibitor with ~15 nM affinity (Borek et al., 2023) and CB-1158, which has IC_{50} values of 86 nM and 296 nM for ARG1 and ARG2, respectively (Naing et al., 2024; Steggerda et al., 2017). However, using oral arginase inhibitors long-term to promote NO production may be challenged by the lack of isoform specificity, making it difficult to balance the roles of arginase isoforms in the urea cycle and NO production and potential disruption of nitrogen metabolism (Pudlo et al., 2017). While nor-NOHA is specific for ARG2, it is not available in oral formulations due to issues with stability and absorption with oral administration. Overall, due to the lack of clinical trials, arginase inhibitors are not currently recommended for the prevention or treatment of cardiovascular disease in clinical practice guidelines.

L-citrulline supplementation

Rationale

Oral L-arginine undergoes first-pass metabolism [~38% in humans (Castillo et al., 1993)], whereas L-citrulline is converted into L-arginine via the argininosuccinate pathway, in which argininosuccinate synthase (ASS) catalyzes the formation of argininosuccinate from citrulline and aspartate; argininosuccinate is subsequently cleaved to form arginine and fumarate by ASL. Citrulline conversion to arginine takes place in multiple cell types, including ECs (Hecker et al., 1990; Wu and Meininger, 1993)

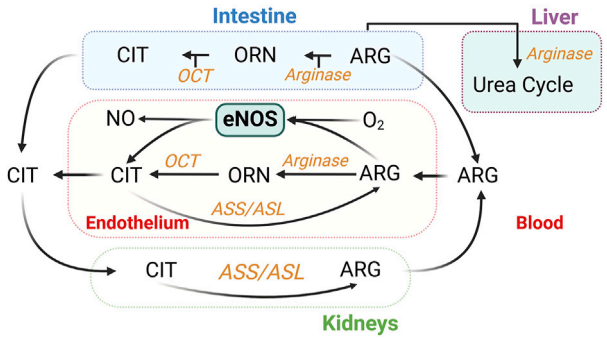

FIGURE 7
Inter-organ metabolism of L-citrulline (CIT) and L-arginine (ARG). Endothelium-derived NO synthesis takes place in all organs. Urea is also generated in the kidneys (Levillain, 2012). ASL, argininosuccinate lyase; ASS, argininosuccinate synthase; OCT, ornithine transcarbamylase; ORN, ornithine.

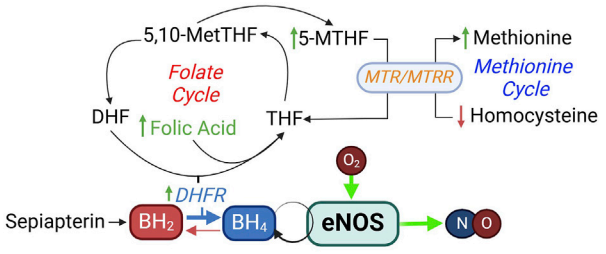

FIGURE 8
Folic acid in BH_4 synthesis and homocysteine metabolism. DHF, dihydrofolate; DHFR, dihydrofolate reductase; MTHF, methylhydrofolate; MTR, methionine synthase; MTRR, methionine synthase reductase.

(Figure 7). Oral L-citrulline has high intestinal absorption but minimal first-pass metabolism and renal reabsorption (Bahadoran et al., 2021), yielding more stable increases in plasma L-arginine levels. L-citrulline is also an inhibitor of arginase activity, as measured by the production of urea (Shearer et al., 1997). L-citrulline supplementation is thus a promising way to promote NO production (Yu et al., 1997; Agarwal et al., 2017; Osowska et al., 2004).

Evidence

L-citrulline administration as a means to promote NO production has received significant attention recently. In *cell models* such as ECs exposed to hypoxia or high glucose, L-citrulline supplementation restores NO bioavailability and reduces ARG2 expression level and activity (Douglass et al., 2023; Tsuboi et al., 2018). In *animal studies*, L-citrulline increases NO production and improves vascular function, with positive effects on glucose tolerance, exercise capacity, and placental angiogenesis (Li et al., 2023; Eshreif et al., 2020). Several *clinical studies* in the past decade have examined the effects of L-citrulline administration in small cohorts with endothelial dysfunction. In patients with vasospastic angina (n = 22, age 41–64), L-citrulline supplementation (0.8 g/d, 4–8 weeks) increases brachial artery flow-mediated dilation, plasma NOx levels, and L-arginine/ADMA ratio (Morita et al., 2013). In T2D patients (n = 25, age 25–65), consumption of 1 g L-citrulline twice a day for 4 weeks reduces the T2D-induced increase in arginase activity and increases plasma nitrites, effects corroborated by improvement of ACh-induced relaxation in *ex vivo* mouse aortic rings incubated (24-h) in low or high glucose-containing media and increases in NO production in ECs treated with high glucose (Shatanawi et al., 2020). In hypertensive postmenopausal women (n = 14, age 61 ± 6), high-dose L-citrulline (10 g/d, 4 weeks) improves flow-mediated dilatation and aortic stiffness and reduces blood pressure (Maharaj et al., 2022). Most recently, in hypertensive postmenopausal women (n = 14, age 60 ± 1), L-citrulline (10 g/d, 4 weeks) reduces the increases in systolic blood pressure and pulse pressure induced by isometric handgrip exercise and the pressures of forward and backward aortic waves during postexercise muscle ischemia (Dillon et al., 2024).

Challenges

Positive effects have been demonstrated of drastically different daily doses of L-citrulline in recent studies, from 0.8 g/d (Morita et al., 2013) to 10 g/d (Maharaj et al., 2022; Dillon et al., 2024). While side effects have not been reported, L-citrulline exerts a dose-dependent effect to activate arginase activity in a cell-based study (Douglass et al., 2023). This may limit its own effects via reduction in L-arginine availability. In addition, high doses of L-citrulline might also affect nitrogen metabolism, based on its complicated interorgan metabolism (Breuillard et al., 2015) (Figure 7). While there are promising results, more large-scale, long-term clinical trials are needed to establish the role of L-citrulline in the prevention or treatment of CVD.

Folic acid supplementation

Rationale

Folic acid cannot be synthesized by the body and can only come from diet or supplementation. In addition to important role in the folate cycle that is involved in the reduction of BH_2 to BH_4, it is an important component in homocysteine metabolism via the methionine cycle (Blom and Smulders, 2011) (Figure 8), and is critical for neural tube development. Increases in plasma homocysteine concentration is strongly associated with cardiovascular disease, and supplementation of folic acid can lower plasma homocysteine levels (Kaye et al., 2020). Folic acid supplementation appears to have a variety of beneficial cardiovascular effects. These include reducing oxidative stress and inflammation, improving plasma lipid profile, and control of blood pressure and blood glucose levels (Asbaghi et al., 2021a; Asbaghi et al., 2021b; Asbaghi et al., 2022; Asbaghi et al., 2021c; Asbaghi et al., 2023).

Evidence

Studies *in cells* and *animals* have supported a direct role of folic acid to enhance NO availability via effects on eNOS and DHFR expression and activity (Stroes et al., 2000; Gao et al., 2009). In regard to eNOS function, 5-methyltetrahydrofolate (MTHF), the active form of folic acid, does not have an effect on pterin-free eNOS, but directly interferes with BH_4-repleted, partially uncoupled eNOS, shifting it from superoxide production toward NO production (Stroes et al., 2000). Folic acid enhances DHFR expression and activity, thereby increasing BH_4 and NO availability and reducing

oxidant production in ECs and in mice (Gao et al., 2009). Some small-scale *clinical trials* (sample sizes ~16–50 participants) have indicated improvement of endothelial function with folic acid supplementation. A recent meta-analysis of 21 randomized controlled trials on the effect of folic acid supplementation on endothelial function suggests that this intervention significantly improves flow-mediated dilation percentage (FMD%) and flow-mediated dilation, but not end-diastolic diameter (EDD) or intracellular adhesion molecule 1 (ICAM-1) expression (Zamani et al., 2023).

Challenges

Due to its well-established role in neural tube development, folic acid supplementation is recommended in clinical guidelines (US Preventive Services Task Force, American College of Obstetricians and Gynecologists, American Academy of Family Physicians, American Academy of Pediatrics, and the Center for Disease Control and Prevention) for those who are planning to or could become pregnant (Force et al., 2023). However, given the lack of large-scale trials, folic acid supplementation is currently not recommended for cardiovascular disease prevention or treatment, although it may be considered in specific populations, such as those with elevated homocysteine levels (Kaye et al., 2020) or in regions with low dietary folate intake.

Increasing BH_4 supply

Rationale

As reviewed above, BH_4 deficiency is a common cause of eNOS uncoupling in many cardiovascular diseases (Figure 5) (Vasquez-Vivar et al., 1998; Wever et al., 1997; Soltis and Cassis, 1991; Hong et al., 2001; Landmesser et al., 2003; Lee et al., 2009). Sapropterin is a synthetic formulation of BH_4. Sepiapterin is a stable precursor in the salvage pathway of BH_4 biosynthesis, which converts sepiapterin to BH_4 via the activities of sepiapterin reductase and DHFR (Figure 8). It has higher cell permeability than BH_4 (Sawabe et al., 2008).

Evidence

Many *preclinical studies* have examined effects of BH_4 or sepiapterin administration on NO-dependent functions in the cardiovascular system. For example, BH_4 administration following transverse aortic constriction (TAC) for 5 weeks in mice recouples eNOS and reduces oxidative stress, reverses cardiac hypertrophy and fibrosis, and improves cardiac function (Moens et al., 2008). Similarly, oral administration of sepiapterin for 8 weeks after TAC increases NO availability, inhibits oxidative stress, and reduces cardiomyocyte hypertrophy (Yoshioka et al., 2015). Of note, in the model of myocardial infarction, iNOS expression is upregulated, and oral sepiapterin administration inhibits nitrotyrosine formation and increases in nitrite and nitrate in wildtype, $eNOS^{-/-}$, and $nNOS^{-/-}$ mice, but not $iNOS^{-/-}$ mice; these effects are associated with prevention of cardiac remodeling and dysfunction (Shimazu et al., 2011). Similar findings are observed in an MI model with streptozotocin-induced T2D (Jo et al., 2011). Multiple small-scale *clinical studies* (5–30 participants each) have shown BH_4 supplementation can improve endothelial function in various cardiovascular conditions. Most early studies tested the effects of *intravascular delivery of BH_4*. These studies showed that BH_4 injection improves forearm blood flow in patients with hypercholesterolemia (Stroes et al., 1997), hypertension (Higashi et al., 2002) and T2D (Heitzer et al., 2000b). BH_4 injection also increases coronary endothelial function in patients with CAD (Maier et al., 2000; Setoguchi et al., 2001; Fukuda et al., 2002), and increases skin blood flow responses to local heating, an indication of microvasculature EC function, in hypercholesterolemic patients (Stroes et al., 1997; Holowatz and Kenney, 2011). Nevertheless, in some studies, intraarterial infusion of BH_4 fails to improve endothelial function (Nystrom et al., 2004; Worthley et al., 2007). *Chronic oral supplementation* of BH_4 has only been examined in limited number of trials. In patients with poorly controlled hypertension (n = 16, age 57 ± 9), 400 mg/d oral BH_4 for 4 weeks significantly improves brachial flow-mediated vasodilation and reduces BP (Porkert et al., 2008). In hypercholesterolemic patients (n = 22, age 60.8 ± 9.2), oral BH_4 (400 mg bid) for 4 weeks normalizes ACh-induced vasodilation, vascular oxidative stress, and NO and superoxide production (Cosentino et al., 2008).

Challenges

Despite evidence that BH_4 and its analogs can improve endothelial function, the lack of large-scale trials and mixed outcomes of the published small-scale clinical studies have prevented their translation into current practice guidelines for CVD prevention and management (Heidenreich et al., 2022). Additionally, issues such as the oxidation of BH_4 to inactive forms like BH_2 limit its therapeutic potential (Cunnington et al., 2012). Of note, BH_4 is also a cofactor of phenylalanine hydroxylase, which converts phenylalanine to tyrosine, a precursor to catecholamines. Large-scale trials are only available for BH_4, sepiapterin or sapropterin in phenylketonuria (Muntau et al., 2024), an autosomal recessive disorder caused by deficiency of phenylalanine hydroxylase, leading to hyperphenylalaninemia, developmental delay, behavioral problems, and reduced quality of life (Blau et al., 2010).

Approaches with preclinical evidence only

Promoting transcriptional regulation of eNOS

Several compounds have been identified to enhance eNOS transcription and promote NO production. *AVE3085* is a novel synthetic agent that acts as an eNOS transcription enhancer. Oral administration of AVE3085 for 7 days increases eNOS expression and activity, reverse eNOS uncoupling, reduces oxidative stress and improve endothelial function in diabetic mice (Cheang et al., 2011). Four-week administration of AVE3085 upregulates eNOS mRNA and protein levels, enhances eNOS phosphorylation and decreases nitrotyrosine formation, leading to improved endothelium-dependent vasorelaxation in hypertensive animals (Yang et al., 2011). These effects are absent in $eNOS^{-/-}$ mice (Cheang et al., 2011; Yang et al., 2011). *AVE9488* is another eNOS transcription enhancer that has been shown to increase eNOS expression and activity, reverse eNOS uncoupling, protect against ischemia-reperfusion cardiac injury, and improve post-infarct function (Sasaki et al., 2006; Wohlfart et al., 2008; Frantz et al., 2009; Fraccarollo et al., 2008). More recently, *LEENE*, a long non-coding RNA induced downstream of KLF2/KLF4 has been shown to form proximity association with the eNOS promoter and

enhances eNOS transcription through chromatin association (Miao et al., 2018). Atorvastatin increases LEENE expression, thereby upregulating eNOS expression, while inhibition of LEENE strongly enhances ECs-monocyte adhesion induced by pulsatile shear stress (Miao et al., 2018). No clinical trials have examined the effects of these transcription enhancers on endothelial function in humans.

Modulating eNOS localization

Disrupting the inhibitory interaction between Cav-1 and eNOS (Figure 4) should promote eNOS activation and NO production. Cavnoxin, a 20-amino-acid peptide designed based on the caveolin scaffolding domain with alanine substitutions at key inhibitory residues (T90, T91, F92) (Bernatchez et al., 2005), releases eNOS from inhibition. In wild-type mice, cavnoxin administration significantly increases NO levels, reduces mean blood pressure, and improves vascular function, effects that are lost in eNOS$^{-/-}$ and Cav-1$^{-/-}$ mice (Bernatchez et al., 2011). Additionally, chronic cavnoxin treatment reduced atherosclerosis in ApoE-knockout mice and diabetic atherosclerotic models.

Targeting Hbα

Disrupting Hbα-eNOS interaction can reduce the NO-scavenging action of Hbα (Figure 4). In addition, inhibiting CytB5R3 can increase NO availability by reducing Hb from its Fe^{2+} to Fe^{3+} form, thereby releasing NO from its high-affinity interaction. *HbαX*, a peptide based of the eNOS-interacting sequence of Hbα (a.a. 34–43), tagged to an HIV TAT cell-penetration sequence, has been developed to disrupt the interaction between Hbα and eNOS, which increases NO availability, acutely reducing blood pressure (Straub et al., 2014a). HbαX lowers blood pressure in mice with angiotensin II-induced hypertension and blunts vasoconstrictive response to phenylephrine in isolated human vessels (Keller et al., 2016). Pharmacological inhibition or genetic deletion of CytB5R3 increases NO availability in blood vessels (Straub et al., 2012).

Promoting dihydrofolate reductase activity

DHFR plays a critical role in regenerating BH_4 from its oxidized form BH_2 (Figure 5). Enhancing DHFR activity will help maintain or increase BH_4 levels, thus preventing eNOS uncoupling and promoting NO production. Genetic knockdown of DHFR decreases BH_4 levels and increases BH_2 levels, uncoupling eNOS and reducing NO production (Crabtree et al., 2009b; Crabtree et al., 2011). Oxidative stress, such as that induced by angiotensin II, downregulates DHFR, exacerbating eNOS uncoupling and reducing NO availability (Chalupsky and Cai, 2005). In addition, DHFR S-nitrosylation by eNOS-derived NO stabilizes DHFR, thereby preventing its degradation and ensuring its activity in recycling BH_4 (Cai et al., 2015). This highlights the interdependence between eNOS-derived NO and DHFR stability. *Challenges*–Due to the lack of specific DHFR activators, there are no clinical studies that examined the possibility of stimulating its activity to increase NO availability. Antimetabolic drugs such as methotrexate or fluorodeoxyuridine and hydroxyurea stimulate DHFR promoter (Eastman et al., 1991); however, their actions are non-specific.

Conclusion and future perspectives

Nearly five decades have passed since NO was identified. Since eNOS was cloned (Marsden et al., 1992), our understanding of how NO availability is regulated has increased exponentially. Nevertheless, only general measures to improve eNOS function such as healthy lifestyle and physical exercise and approaches to amplify certain downstream components of NO signaling have made it to clinical practice guidelines. Among the salient indications, inhaled NO is used for acute pulmonary vasoreactivity testing and severe hypoxia in pulmonary arterial hypertension (PAH), nitrates are used extensively in ischemic heart disease and heart failure, sGC stimulators and activators are used for PAH, and PDE5 inhibitors are used for erectile dysfunction, PAH and benign prostatic hyperplasia.

This article has reviewed the basic regulatory mechanisms of eNOS activities and relevant approaches to improve endogenous NO production that have been tested to date but not yet approved clinically. We have highlighted the rationale, current evidence, and challenges that have prevented these approaches from entering the clinical armamentarium to improve endothelial function. Among the main challenges are the lack of specificity, lack of consistent efficacy of long-term treatment, and lack of large-scale clinical data.

Given this backdrop, what can be done? Obviously, *additional studies and large-scale trials* are needed in many cases. The lack of consistent outcomes of L-arginine supplementation could be due to multiple mechanisms, as discussed. Could *intermittent L-arginine delivery*, a strategy widely applied clinically to prevent nitrate tolerance to some degree, be considered and tested to reduce a potential "arginine tolerance"? In addition, because L-arginine supplementation increases arginase activity, which limits the efficacy, now that arginase inhibitors are available with better oral availability, *L-arginine supplementation could be considered in combination with arginase inhibition*. In regard to arginase inhibition, development of *ARG2-specific inhibitors* would help limit issues associated with disruption of the urea cycle in the liver, where ARG1 is more abundant. L-citrulline as a single supplementation appears to have yielded superior outcomes than L-arginine supplementation; however, large-scale trials are needed, and *identifying the minimum effective dose range for L-citrulline is necessary*, considering a potential effect of high doses on nitrogen balance. *For peptide-based interventions*, factors such as peptide stability and efficient delivery need to be addressed before clinical application can be considered.

Biochemically, it is worth noting that for NO-induced vasodilation, there does not need to be a high concentration of NO because of its picomolar affinity for sGC (Wu et al., 2022). Therefore, promoting NO production to a low level may preferentially promote vasodilation via the eNOS-NO-sGC pathway and prevent the formation of reactive nitrogen species. In addition, *targeting interventions specifically to the endothelium* is an ideal solution that is difficult to achieve but would reduce the required effective doses and limit many off-target effects. This would be particularly helpful for approaches aimed to target eNOS's essential interacting partners and

numerous transcriptional factors that are abundant also in other tissues.

Author contributions

MG: Writing–original draft, Writing–review and editing. SC: Writing–review and editing. EW: Writing–review and editing. DC: Writing–review and editing. Q-KT: Conceptualization, Funding acquisition, Writing–original draft, Writing–review and editing.

Funding

The author(s) declare that financial support was received for the research, authorship, and/or publication of this article. This work was supported by National Heart, Lung, and Blood Institute grant HL173818 (Q-KT), National Institute on Alcohol Abuse and Alcoholism grant AA031063 (DC), and Iowa Osteopathic and Educational Research grant IOER122204 (Q-KT). MG is supported by a scholarship from the PhD Program in Biomedical Sciences at Des Moines University.

Conflict of interest

The authors declare that the research was conducted in the absence of any commercial or financial relationships that could be construed as a potential conflict of interest.

The author(s) declared that they were an editorial board member of Frontiers, at the time of submission. This had no impact on the peer review process and the final decision.

Generative AI statement

The author(s) declare that no Generative AI was used in the creation of this manuscript.

Publisher's note

References

Abdullaev, I. F., Bisaillon, J. M., Potier, M., Gonzalez, J. C., Motiani, R. K., and Trebak, M. (2008). Stim1 and Orai1 mediate CRAC currents and store-operated calcium entry important for endothelial cell proliferation. *Circ. Res.* 103 (11), 1289–1299. doi:10.1161/01.RES.0000338496.95579.56

Agarwal, U., Didelija, I. C., Yuan, Y., Wang, X., and Marini, J. C. (2017). Supplemental citrulline is more efficient than arginine in increasing systemic arginine availability in mice. *J. Nutr.* 147 (4), 596–602. doi:10.3945/jn.116.240382

Alheid, U., Frolich, J. C., and Forstermann, U. (1987). Endothelium-derived relaxing factor from cultured human endothelial cells inhibits aggregation of human platelets. *Thromb. Res.* 47 (5), 561–571. doi:10.1016/0049-3848(87)90361-6

Alp, N. J., and Channon, K. M. (2004). Regulation of endothelial nitric oxide synthase by tetrahydrobiopterin in vascular disease. *Arterioscler. Thromb. Vasc. Biol.* 24 (3), 413–420. doi:10.1161/01.ATV.0000110785.96039.f6

Alp, N. J., Mussa, S., Khoo, J., Cai, S., Guzik, T., Jefferson, A., et al. (2003). Tetrahydrobiopterin-dependent preservation of nitric oxide-mediated endothelial function in diabetes by targeted transgenic GTP-cyclohydrolase I overexpression. *J. Clin. Invest.* 112 (5), 725–735. doi:10.1172/JCI17786

Antoniades, C., Shirodaria, C., Crabtree, M., Rinze, R., Alp, N., Cunnington, C., et al. (2007). Altered plasma versus vascular biopterins in human atherosclerosis reveal relationships between endothelial nitric oxide synthase coupling, endothelial function, and inflammation. *Circulation* 116 (24), 2851–2859. doi:10.1161/CIRCULATIONAHA.107.704155

Arnold, W. P., Mittal, C. K., Katsuki, S., and Murad, F. (1977). Nitric oxide activates guanylate cyclase and increases guanosine 3':5'-cyclic monophosphate levels in various tissue preparations. *Proc. Natl. Acad. Sci. U. S. A.* 74 (8), 3203–3207. doi:10.1073/pnas.74.8.3203

Arunachalam, G., Yao, H., Sundar, I. K., Caito, S., and Rahman, I. (2010). SIRT1 regulates oxidant- and cigarette smoke-induced eNOS acetylation in endothelial cells: role of resveratrol. *Biochem. Biophys. Res. Commun.* 393 (1), 66–72. doi:10.1016/j.bbrc.2010.01.080

Asbaghi, O., Ashtary-Larky, D., Bagheri, R., Moosavian, S. P., Nazarian, B., Afrisham, R., et al. (2021a). Effects of folic acid supplementation on inflammatory markers: a grade-assessed systematic review and dose-response meta-analysis of randomized controlled trials. *Nutrients* 13 (7), 2327. doi:10.3390/nu13072327

Asbaghi, O., Ashtary-Larky, D., Bagheri, R., Moosavian, S. P., Olyaei, H. P., Nazarian, B., et al. (2021b). Folic acid supplementation improves glycemic control for diabetes prevention and management: a systematic review and dose-response meta-analysis of randomized controlled trials. *Nutrients* 13 (7), 2355. doi:10.3390/nu13072355

Asbaghi, O., Ashtary-Larky, D., Bagheri, R., Nazarian, B., Pourmirzaei Olyaei, H., Rezaei Kelishadi, M., et al. (2022). Beneficial effects of folic acid supplementation on lipid markers in adults: a GRADE-assessed systematic review and dose-response meta-analysis of data from 21,787 participants in 34 randomized controlled trials. *Crit. Rev. Food Sci. Nutr.* 62 (30), 8435–8453. doi:10.1080/10408398.2021.1928598

Asbaghi, O., Ghanavati, M., Ashtary-Larky, D., Bagheri, R., Rezaei Kelishadi, M., Nazarian, B., et al. (2021c). Effects of folic acid supplementation on oxidative stress markers: a systematic review and meta-analysis of randomized controlled trials. *Antioxidants (Basel)* 10 (6), 871. doi:10.3390/antiox10060871

Asbaghi, O., Salehpour, S., Rezaei Kelishadi, M., Bagheri, R., Ashtary-Larky, D., Nazarian, B., et al. (2023). Folic acid supplementation and blood pressure: a GRADE-assessed systematic review and dose-response meta-analysis of 41,633 participants. *Crit. Rev. Food Sci. Nutr.* 63 (13), 1846–1861. doi:10.1080/10408398.2021.1968787

Atawia, R. T., Toque, H. A., Meghil, M. M., Benson, T. W., Yiew, N. K. H., Cutler, C. W., et al. (2019). Role of arginase 2 in systemic metabolic activity and adipose tissue fatty acid metabolism in diet-induced obese mice. *Int. J. Mol. Sci.* 20 (6), 1462. doi:10.3390/ijms20061462

Atochin, D. N., Wang, A., Liu, V. W., Critchlow, J. D., Dantas, A. P., Looft-Wilson, R., et al. (2007). The phosphorylation state of eNOS modulates vascular reactivity and outcome of cerebral ischemia *in vivo*. *J. Clin. Invest.* 117 (7), 1961–1967. doi:10.1172/JCI29877

Bachetti, T., Comini, L., Pasini, E., Cargnoni, A., Curello, S., and Ferrari, R. (2001). Ace-inhibition with quinapril modulates the nitric oxide pathway in normotensive rats. *J. Mol. Cell Cardiol.* 33 (3), 395–403. doi:10.1006/jmcc.2000.1311

Bahadoran, Z., Mirmiran, P., Kashfi, K., and Ghasemi, A. (2021). Endogenous flux of nitric oxide: citrulline is preferred to Arginine. *Acta Physiol. (Oxf)* 231 (3), e13572. doi:10.1111/apha.13572

Balligand, J. L., Feron, O., and Dessy, C. (2009). eNOS activation by physical forces: from short-term regulation of contraction to chronic remodeling of cardiovascular tissues. *Physiol. Rev.* 89 (2), 481–534. doi:10.1152/physrev.00042.2007

Bauer, P. M., Fulton, D., Boo, Y. C., Sorescu, G. P., Kemp, B. E., Jo, H., et al. (2003). Compensatory phosphorylation and protein-protein interactions revealed by loss of function and gain of function mutants of multiple serine phosphorylation sites in endothelial nitric-oxide synthase. *J. Biol. Chem.* 278 (17), 14841–14849. doi:10.1074/jbc.M211926200

Bendall, J. K., Alp, N. J., Warrick, N., Cai, S., Adlam, D., Rockett, K., et al. (2005). Stoichiometric relationships between endothelial tetrahydrobiopterin, endothelial NO synthase (eNOS) activity, and eNOS coupling *in vivo*: insights from transgenic mice with endothelial-targeted GTP cyclohydrolase 1 and eNOS overexpression. *Circ. Res.* 97 (9), 864–871. doi:10.1161/01.RES.0000187447.03525.72

Bendall, J. K., Douglas, G., McNeill, E., Channon, K. M., and Crabtree, M. J. (2014). Tetrahydrobiopterin in cardiovascular health and disease. *Antioxid. Redox Signal* 20 (18), 3040–3077. doi:10.1089/ars.2013.5566

Benjamin, N., O'Driscoll, F., Dougall, H., Duncan, C., Smith, L., Golden, M., et al. (1994). Stomach NO synthesis. *Nature* 368 (6471), 502. doi:10.1038/368502a0

Benson, M. A., Batchelor, H., Chuaiphichai, S., Bailey, J., Zhu, H., Stuehr, D. J., et al. (2013). A pivotal role for tryptophan 447 in enzymatic coupling of human endothelial nitric oxide synthase (eNOS): effects on tetrahydrobiopterin-dependent catalysis and eNOS dimerization. *J. Biol. Chem.* 288 (41), 29836–29845. doi:10.1074/jbc.M113.493023

Bernatchez, P., Sharma, A., Bauer, P. M., Marin, E., and Sessa, W. C. (2011). A noninhibitory mutant of the caveolin-1 scaffolding domain enhances eNOS-derived NO synthesis and vasodilation in mice. *J. Clin. Invest.* 121 (9), 3747–3755. doi:10.1172/JCI44778

Bernatchez, P. N., Bauer, P. M., Yu, J., Prendergast, J. S., He, P., and Sessa, W. C. (2005). Dissecting the molecular control of endothelial NO synthase by caveolin-1 using cell-permeable peptides. *Proc. Natl. Acad. Sci. U. S. A.* 102 (3), 761–766. doi:10.1073/pnas.0407224102

Bhatta, A., Yao, L., Xu, Z., Toque, H. A., Chen, J., Atawia, R. T., et al. (2017). Obesity-induced vascular dysfunction and arterial stiffening requires endothelial cell arginase 1. *Cardiovasc Res.* 113 (13), 1664–1676. doi:10.1093/cvr/cvx164

Black, S. M., Fineman, J. R., Steinhorn, R. H., Bristow, J., and Soifer, S. J. (1998). Increased endothelial NOS in lambs with increased pulmonary blood flow and pulmonary hypertension. *Am. J. Physiol.* 275 (5), H1643–H1651. doi:10.1152/ajpheart.1998.275.5.H1643

Blair, A., Shaul, P. W., Yuhanna, I. S., Conrad, P. A., and Smart, E. J. (1999). Oxidized low density lipoprotein displaces endothelial nitric-oxide synthase (eNOS) from plasmalemmal caveolae and impairs eNOS activation. *J. Biol. Chem.* 274 (45), 32512–32519. doi:10.1074/jbc.274.45.32512

Blau, N., van Spronsen, F. J., and Levy, H. L. (2010). Phenylketonuria. *Lancet.* 376 (9750), 1417–1427. doi:10.1016/S0140-6736(10)60961-0

Blekkenhorst, L. C., Bondonno, N. P., Liu, A. H., Ward, N. C., Prince, R. L., Lewis, J. R., et al. (2018). Nitrate, the oral microbiome, and cardiovascular health: a systematic literature review of human and animal studies. *Am. J. Clin. Nutr.* 107 (4), 504–522. doi:10.1093/ajcn/nqx046

Blom, H. J., and Smulders, Y. (2011). Overview of homocysteine and folate metabolism. With special references to cardiovascular disease and neural tube defects. *J. Inherit. Metab. Dis.* 34 (1), 75–81. doi:10.1007/s10545-010-9177-4

Bode-Boger, S. M., Boger, R. H., Alfke, H., Heinzel, D., Tsikas, D., Creutzig, A., et al. (1996). L-arginine induces nitric oxide-dependent vasodilation in patients with critical limb ischemia. A randomized, controlled study. *Circulation* 93 (1), 85–90. doi:10.1161/01.cir.93.1.85

Bode-Boger, S. M., Boger, R. H., Galland, A., Tsikas, D., and Frolich, J. C. (1998). L-arginine-induced vasodilation in healthy humans: pharmacokinetic-pharmacodynamic relationship. *Br. J. Clin. Pharmacol.* 46 (5), 489–497. doi:10.1046/j.1365-2125.1998.00803.x

Bode-Boger, S. M., Scalera, F., and Ignarro, L. J. (2007). The L-arginine paradox: importance of the L-arginine/asymmetrical dimethylarginine ratio. *Pharmacol. Ther.* 114 (3), 295–306. doi:10.1016/j.pharmthera.2007.03.002

Boger, R. H., Bode-Boger, S. M., Mugge, A., Kienke, S., Brandes, R., Dwenger, A., et al. (1995). Supplementation of hypercholesterolaemic rabbits with L-arginine reduces the vascular release of superoxide anions and restores NO production. *Atherosclerosis* 117 (2), 273–284. doi:10.1016/0021-9150(95)05582-h

Boger, R. H., Bode-Boger, S. M., Phivthong-ngam, L., Brandes, R. P., Schwedhelm, E., Mugge, A., et al. (1998b). Dietary L-arginine and alpha-tocopherol reduce vascular oxidative stress and preserve endothelial function in hypercholesterolemic rabbits via different mechanisms. *Atherosclerosis* 141 (1), 31–43. doi:10.1016/s0021-9150(98)00145-2

Boger, R. H., Bode-Boger, S. M., Szuba, A., Tsao, P. S., Chan, J. R., Tangphao, O., et al. (1998c). Asymmetric dimethylarginine (ADMA): a novel risk factor for endothelial dysfunction: its role in hypercholesterolemia. *Circulation* 98 (18), 1842–1847. doi:10.1161/01.cir.98.18.1842

Boger, R. H., Bode-Boger, S. M., Thiele, W., Creutzig, A., Alexander, K., and Frolich, J. C. (1998a). Restoring vascular nitric oxide formation by L-arginine improves the symptoms of intermittent claudication in patients with peripheral arterial occlusive disease. *J. Am. Coll. Cardiol.* 32 (5), 1336–1344. doi:10.1016/s0735-1097(98)00375-1

Bonauer, A., Carmona, G., Iwasaki, M., Mione, M., Koyanagi, M., Fischer, A., et al. (2009). MicroRNA-92a controls angiogenesis and functional recovery of ischemic tissues in mice. *Science* 324 (5935), 1710–1713. doi:10.1126/science.1174381

Bonderman, D., Pretsch, I., Steringer-Mascherbauer, R., Jansa, P., Rosenkranz, S., Tufaro, C., et al. (2014). Acute hemodynamic effects of riociguat in patients with pulmonary hypertension associated with diastolic heart failure (DILATE-1): a randomized, double-blind, placebo-controlled, single-dose study. *Chest* 146 (5), 1274–1285. doi:10.1378/chest.14-0106

Borek, B., Nowicka, J., Gzik, A., Dziegielewski, M., Jedrzejczak, K., Brzezinska, J., et al. (2023). Arginase 1/2 inhibitor OATD-02: from discovery to first-in-man setup in cancer immunotherapy. *Mol. Cancer Ther.* 22 (7), 807–817. doi:10.1158/1535-7163.MCT-22-0721

Bredt, D. S., Hwang, P. M., Glatt, C. E., Lowenstein, C., Reed, R. R., and Snyder, S. H. (1991). Cloned and expressed nitric oxide synthase structurally resembles cytochrome P-450 reductase. *Nature* 351 (6329), 714–718. doi:10.1038/351714a0

Bredt, D. S., and Snyder, S. H. (1990). Isolation of nitric oxide synthetase, a calmodulin-requiring enzyme. *Proc. Natl. Acad. Sci. U. S. A.* 87 (2), 682–685. doi:10.1073/pnas.87.2.682

Breuillard, C., Cynober, L., and Moinard, C. (2015). Citrulline and nitrogen homeostasis: an overview. *Amino Acids* 47 (4), 685–691. doi:10.1007/s00726-015-1932-2

Buga, G. M., Singh, R., Pervin, S., Rogers, N. E., Schmitz, D. A., Jenkinson, C. P., et al. (1996). Arginase activity in endothelial cells: inhibition by NG-hydroxy-L-arginine during high-output NO production. *Am. J. Physiol.* 271 (5 Pt 2), H1988–H1998. doi:10.1152/ajpheart.1996.271.5.H1988

Busnel, O., Carreaux, F., Carboni, B., Pethe, S., Goff, S. V., Mansuy, D., et al. (2005). Synthesis and evaluation of new omega-borono-alpha-amino acids as rat liver arginase inhibitors. *Bioorg Med. Chem.* 13 (7), 2373–2379. doi:10.1016/j.bmc.2005.01.053

Busse, R., and Mulsch, A. (1990). Calcium-dependent nitric oxide synthesis in endothelial cytosol is mediated by calmodulin. *FEBS Lett.* 265 (1-2), 133–136. doi:10.1016/0014-5793(90)80902-u

Cai, H., and Harrison, D. G. (2000). Endothelial dysfunction in cardiovascular diseases: the role of oxidant stress. *Circ. Res.* 87 (10), 840–844. doi:10.1161/01.res.87.10.840

Cai, Z., Lu, Q., Ding, Y., Wang, Q., Xiao, L., Song, P., et al. (2015). Endothelial nitric oxide synthase-derived nitric oxide prevents dihydrofolate reductase degradation via promoting S-nitrosylation. *Arterioscler. Thromb. Vasc. Biol.* 35 (11), 2366–2373. doi:10.1161/ATVBAHA.115.305796

Caldwell, R. W., Rodriguez, P. C., Toque, H. A., Narayanan, S. P., and Caldwell, R. B. (2018). Arginase: a multifaceted enzyme important in health and disease. *Physiol. Rev.* 98 (2), 641–665. doi:10.1152/physrev.00037.2016

Cao, S., Yao, J., McCabe, T. J., Yao, Q., Katusic, Z. S., Sessa, W. C., et al. (2001). Direct interaction between endothelial nitric-oxide synthase and dynamin-2. Implications for nitric-oxide synthase function. *J. Biol. Chem.* 276 (17), 14249–14256. doi:10.1074/jbc.M006258200

Castillo, L., Chapman, T. E., Yu, Y. M., Ajami, A., Burke, J. F., and Young, V. R. (1993). Dietary arginine uptake by the splanchnic region in adult humans. *Am. J. Physiol.* 265 (4 Pt 1), E532–E539. doi:10.1152/ajpendo.1993.265.4.E532

Chalupsky, K., and Cai, H. (2005). Endothelial dihydrofolate reductase: critical for nitric oxide bioavailability and role in angiotensin II uncoupling of endothelial nitric oxide synthase. *Proc. Natl. Acad. Sci. U. S. A.* 102 (25), 9056–9061. doi:10.1073/pnas.0409594102

Cheang, W. S., Wong, W. T., Tian, X. Y., Yang, Q., Lee, H. K., He, G. W., et al. (2011). Endothelial nitric oxide synthase enhancer reduces oxidative stress and restores endothelial function in db/db mice. *Cardiovasc Res.* 92 (2), 267–275. doi:10.1093/cvr/cvr233

Chen, C. A., De Pascali, F., Basye, A., Hemann, C., and Zweier, J. L. (2013). Redox modulation of endothelial nitric oxide synthase by glutaredoxin-1 through reversible oxidative post-translational modification. *Biochemistry* 52 (38), 6712–6723. doi:10.1021/bi400404s

Chen, C. A., Wang, T. Y., Varadharaj, S., Reyes, L. A., Hemann, C., Talukder, M. A., et al. (2010). S-glutathionylation uncouples eNOS and regulates its cellular and vascular function. *Nature* 468 (7327), 1115–1118. doi:10.1038/nature09599

Chen, P. F., and Wu, K. K. (2000). Characterization of the roles of the 594-645 region in human endothelial nitric-oxide synthase in regulating calmodulin binding and electron transfer. *J. Biol. Chem.* 275 (17), 13155–13163. doi:10.1074/jbc.275.17.13155

Chen, Z., Zhang, J., and Stamler, J. S. (2002). Identification of the enzymatic mechanism of nitroglycerin bioactivation. *Proc. Natl. Acad. Sci. U. S. A.* 99 (12), 8306–8311. doi:10.1073/pnas.122225199

Chen, Z. P., Mitchelhill, K. I., Michell, B. J., Stapleton, D., Rodriguez-Crespo, I., Witters, L. A., et al. (1999). AMP-activated protein kinase phosphorylation of endothelial NO synthase. *FEBS Lett.* 443 (3), 285–289. doi:10.1016/s0014-5793(98)01705-0

Chicoine, L. G., Paffett, M. L., Young, T. L., and Nelin, L. D. (2004). Arginase inhibition increases nitric oxide production in bovine pulmonary arterial endothelial cells. *Am. J. Physiol. Lung Cell Mol. Physiol.* 287 (1), L60–L68. doi:10.1152/ajplung.00194.2003

Chuaiphichai, S., Crabtree, M. J., McNeill, E., Hale, A. B., Trelfa, L., Channon, K. M., et al. (2017). A key role for tetrahydrobiopterin-dependent endothelial NOS regulation in resistance arteries: studies in endothelial cell tetrahydrobiopterin-deficient mice. *Br. J. Pharmacol.* 174 (8), 657–671. doi:10.1111/bph.13728

Closs, E. I., Ostad, M. A., Simon, A., Warnholtz, A., Jabs, A., Habermeier, A., et al. (2012). Impairment of the extrusion transporter for asymmetric dimethyl-L-arginine: a novel mechanism underlying vasospastic angina. *Biochem. Biophys. Res. Commun.* 423 (2), 218–223. doi:10.1016/j.bbrc.2012.05.044

Colleluori, D. M., and Ash, D. E. (2001). Classical and slow-binding inhibitors of human type II arginase. *Biochemistry* 40 (31), 9356–9362. doi:10.1021/bi010783g

Collet, S., Carreau, F., Boucher, J. L., Pethe, S., Lepoivre, M., Danion-Bougot, R., et al. (2000). Synthesis and evaluation of -borono- -amino acids † as active-site probes of arginase and nitric oxide synthases. *J. Chem. Soc. Perkin Trans.* 1 (2), 177–182. doi:10.1039/A908140B

Cooke, J. P., Andon, N. A., Girerd, X. J., Hirsch, A. T., and Creager, M. A. (1991). Arginine restores cholinergic relaxation of hypercholesterolemic rabbit thoracic aorta. *Circulation* 83 (3), 1057–1062. doi:10.1161/01.cir.83.3.1057

Cosentino, F., Hurlimann, D., Delli Gatti, C., Chenevard, R., Blau, N., Alp, N. J., et al. (2008). Chronic treatment with tetrahydrobiopterin reverses endothelial dysfunction and oxidative stress in hypercholesterolaemia. *Heart* 94 (4), 487–492. doi:10.1136/hrt.2007.122184

Costa, T. J., Barros, P. R., Arce, C., Santos, J. D., da Silva-Neto, J., Egea, G., et al. (2021). The homeostatic role of hydrogen peroxide, superoxide anion and nitric oxide in the vasculature. *Free Radic. Biol. Med.* 162, 615–635. doi:10.1016/j.freeradbiomed.2020.11.021

Crabtree, M. J., Brixey, R., Batchelor, H., Hale, A. B., and Channon, K. M. (2013). Integrated redox sensor and effector functions for tetrahydrobiopterin- and glutathionylation-dependent endothelial nitric-oxide synthase uncoupling. *J. Biol. Chem.* 288 (1), 561–569. doi:10.1074/jbc.M112.415992

Crabtree, M. J., and Channon, K. M. (2011). Synthesis and recycling of tetrahydrobiopterin in endothelial function and vascular disease. *Nitric Oxide* 25 (2), 81–88. doi:10.1016/j.niox.2011.04.004

Crabtree, M. J., Hale, A. B., and Channon, K. M. (2011). Dihydrofolate reductase protects endothelial nitric oxide synthase from uncoupling in tetrahydrobiopterin deficiency. *Free Radic. Biol. Med.* 50 (11), 1639–1646. doi:10.1016/j.freeradbiomed.2011.03.010

Crabtree, M. J., Tatham, A. L., Al-Wakeel, Y., Warrick, N., Hale, A. B., Cai, S., et al. (2009a). Quantitative regulation of intracellular endothelial nitric-oxide synthase (eNOS) coupling by both tetrahydrobiopterin-eNOS stoichiometry and biopterin redox status: insights from cells with tet-regulated GTP cyclohydrolase I expression. *J. Biol. Chem.* 284 (2), 1136–1144. doi:10.1074/jbc.M805403200

Crabtree, M. J., Tatham, A. L., Hale, A. B., Alp, N. J., and Channon, K. M. (2009b). Critical role for tetrahydrobiopterin recycling by dihydrofolate reductase in regulation of endothelial nitric-oxide synthase coupling: relative importance of the *de novo* biopterin synthesis versus salvage pathways. *J. Biol. Chem.* 284 (41), 28128–28136. doi:10.1074/jbc.M109.041483

Cunnington, C., Van Assche, T., Shirodaria, C., Kylintireas, I., Lindsay, A. C., Lee, J. M., et al. (2012). Systemic and vascular oxidation limits the efficacy of oral tetrahydrobiopterin treatment in patients with coronary artery disease. *Circulation* 125 (11), 1356–1366. doi:10.1161/CIRCULATIONAHA.111.038919

Daiber, A., Frein, D., Namgaladze, D., and Ullrich, V. (2002). Oxidation and nitrosation in the nitrogen monoxide/superoxide system. *J. Biol. Chem.* 277 (14), 11882–11888. doi:10.1074/jbc.M111988200

Dedio, J., Konig, P., Wohlfart, P., Schroeder, C., Kummer, W., and Muller-Esterl, W. (2001). NOSIP, a novel modulator of endothelial nitric oxide synthase activity. *Faseb J.* 15 (1), 79–89. doi:10.1096/fj.00-0078com

Denton, C. C., Shah, P., Suriany, S., Liu, H., Thuptimdang, W., Sunwoo, J., et al. (2021). Loss of alpha-globin genes in human subjects is associated with improved nitric oxide-mediated vascular perfusion. *Am. J. Hematol.* 96 (3), 277–281. doi:10.1002/ajh.26058

Di Costanzo, L., Ilies, M., Thorn, K. J., and Christianson, D. W. (2010). Inhibition of human arginase I by substrate and product analogues. *Arch. Biochem. Biophys.* 496 (2), 101–108. doi:10.1016/j.abb.2010.02.004

Di Leva, F., Domi, T., Fedrizzi, L., Lim, D., and Carafoli, E. (2008). The plasma membrane Ca2+ ATPase of animal cells: structure, function and regulation. *Arch. Biochem. Biophys.* 476 (1), 65–74. doi:10.1016/j.abb.2008.02.026

Dillon, K. N., Kang, Y., Maharaj, A., Martinez, M. A., Fischer, S. M., and Figueroa, A. (2024). L-Citrulline supplementation attenuates aortic pressure and pressure waves during metaboreflex activation in postmenopausal women. *Br. J. Nutr.* 131 (3), 474–481. doi:10.1017/S000711452300199X

Di Lorenzo, A., Lin, M. I., Murata, T., Landskroner-Eiger, S., Schleicher, M., Kothiya, M., et al. (2013). eNOS-derived nitric oxide regulates endothelial barrier function through VE-cadherin and Rho GTPases. *J. Cell Sci.* 126 (Pt 24), 5541–5552. doi:10.1242/jcs.115972

Dimmeler, S., Fleming, I., Fisslthaler, B., Hermann, C., Busse, R., and Zeiher, A. M. (1999). Activation of nitric oxide synthase in endothelial cells by Akt-dependent phosphorylation. *Nature* 399 (6736), 601–605. doi:10.1038/21224

Donato, A. J., Magerko, K. A., Lawson, B. R., Durrant, J. R., Lesniewski, L. A., and Seals, D. R. (2011). SIRT-1 and vascular endothelial dysfunction with ageing in mice and humans. *J. Physiol.* 589 (Pt 18), 4545–4554. doi:10.1113/jphysiol.2011.211219

Dong, J. Y., Qin, L. Q., Zhang, Z., Zhao, Y., Wang, J., Arigoni, F., et al. (2011). Effect of oral L-arginine supplementation on blood pressure: a meta-analysis of randomized, double-blind, placebo-controlled trials. *Am. Heart J.* 162 (6), 959–965. doi:10.1016/j.ahj.2011.09.012

Douglass, M. S., Kaplowitz, M. R., Zhang, Y., and Fike, C. D. (2023). Impact of l-citrulline on nitric oxide signaling and arginase activity in hypoxic human pulmonary artery endothelial cells. *Pulm. Circ.* 13 (2), e12221. doi:10.1002/pul2.12221

Drab, M., Verkade, P., Elger, M., Kasper, M., Lohn, M., Lauterbach, B., et al. (2001). Loss of caveolae, vascular dysfunction, and pulmonary defects in caveolin-1 gene-disrupted mice. *Science* 293 (5539), 2449–2452. doi:10.1126/science.1062688

Drexler, H., Zeiher, A. M., Meinzer, K., and Just, H. (1991). Correction of endothelial dysfunction in coronary microcirculation of hypercholesterolaemic patients by L-arginine. *Lancet* 338 (8782-8783), 1546–1550. doi:10.1016/0140-6736(91)92372-9

Dubois-Rande, J. L., Zelinsky, R., Roudot, F., Chabrier, P. E., Castaigne, A., Geschwind, H., et al. (1992). Effects of infusion of L-arginine into the left anterior descending coronary artery on acetylcholine-induced vasoconstriction of human atheromatous coronary arteries. *Am. J. Cardiol.* 70 (15), 1269–1275. doi:10.1016/0002-9149(92)90760-v

Eastman, H. B., Swick, A. G., Schmitt, M. C., and Azizkhan, J. C. (1991). Stimulation of dihydrofolate reductase promoter activity by antimetabolic drugs. *Proc. Natl. Acad. Sci. U. S. A.* 88 (19), 8572–8576. doi:10.1073/pnas.88.19.8572

Erdmann, E., Semigran, M. J., Nieminen, M. S., Gheorghiade, M., Agrawal, R., Mitrovic, V., et al. (2013). Cinaciguat, a soluble guanylate cyclase activator, unloads the heart but also causes hypotension in acute decompensated heart failure. *Eur. Heart J.* 34 (1), 57–67. doi:10.1093/eurheartj/ehs196

Erez, A., Nagamani, S. C., Shchelochkov, O. A., Premkumar, M. H., Campeau, P. M., Chen, Y., et al. (2011). Requirement of argininosuccinate lyase for systemic nitric oxide production. *Nat. Med.* 17 (12), 1619–1626. doi:10.1038/nm.2544

Erwin, P. A., Lin, A. J., Golan, D. E., and Michel, T. (2005). Receptor-regulated dynamic S-nitrosylation of endothelial nitric-oxide synthase in vascular endothelial cells. *J. Biol. Chem.* 280 (20), 19888–19894. doi:10.1074/jbc.M413058200

Erwin, P. A., Mitchell, D. A., Sartoretto, J., Marletta, M. A., and Michel, T. (2006). Subcellular targeting and differential S-nitrosylation of endothelial nitric-oxide synthase. *J. Biol. Chem.* 281 (1), 151–157. doi:10.1074/jbc.M510421200

Eshreif, A., Al Batran, R., Jamieson, K. L., Darwesh, A. M., Gopal, K., Greenwell, A. A., et al. (2020). l-Citrulline supplementation improves glucose and exercise tolerance in obese male mice. *Exp. Physiol.* 105 (2), 270–281. doi:10.1113/EP088109

Fernandez-Hernando, C., Fukata, M., Bernatchez, P. N., Fukata, Y., Lin, M. I., Bredt, D. S., et al. (2006). Identification of Golgi-localized acyl transferases that palmitoylate and regulate endothelial nitric oxide synthase. *J. Cell Biol.* 174 (3), 369–377. doi:10.1083/jcb.200601051

Feron, O., Belhassen, L., Kobzik, L., Smith, T. W., Kelly, R. A., and Michel, T. (1996). Endothelial nitric oxide synthase targeting to caveolae. Specific interactions with caveolin isoforms in cardiac myocytes and endothelial cells. *J. Biol. Chem.* 271 (37), 22810–22814. doi:10.1074/jbc.271.37.22810

Feron, O., Saldana, F., Michel, J. B., and Michel, T. (1998). The endothelial nitric-oxide synthase-caveolin regulatory cycle. *J. Biol. Chem.* 273 (6), 3125–3128. doi:10.1074/jbc.273.6.3125

Fish, J. E., and Marsden, P. A. (2006). Endothelial nitric oxide synthase: insight into cell-specific gene regulation in the vascular endothelium. *Cell Mol. Life Sci.* 63 (2), 144–162. doi:10.1007/s00018-005-5421-8

Fish, J. E., Yan, M. S., Matouk, C. C., St Bernard, R., Ho, J. J., Gavryushova, A., et al. (2010). Hypoxic repression of endothelial nitric-oxide synthase transcription is coupled with eviction of promoter histones. *J. Biol. Chem.* 285 (2), 810–826. doi:10.1074/jbc.M109.067868

Fitzpatrick, D. F., Bing, B., and Rohdewald, P. (1998). Endothelium-dependent vascular effects of Pycnogenol. *J. Cardiovasc Pharmacol.* 32 (4), 509–515. doi:10.1097/00005344-199810000-00001

Fleming, I., Bauersachs, J., and Busse, R. (1997). Calcium-dependent and calcium-independent activation of the endothelial NO synthase. *J. Vasc. Res.* 34 (3), 165–174. doi:10.1159/000159220

Fleming, I., Fisslthaler, B., Dimmeler, S., Kemp, B. E., and Busse, R. (2001). Phosphorylation of Thr(495) regulates Ca(2+)/calmodulin-dependent endothelial nitric oxide synthase activity. *Circ. Res.* 88 (11), E68–E75. doi:10.1161/hh1101.092677

Fontana, J., Fulton, D., Chen, Y., Fairchild, T. A., McCabe, T. J., Fujita, N., et al. (2002). Domain mapping studies reveal that the M domain of hsp90 serves as a molecular scaffold to regulate Akt-dependent phosphorylation of endothelial nitric oxide synthase and NO release. *Circ. Res.* 90 (8), 866–873. doi:10.1161/01.res.0000016837.26733.be

Force, USPST, Barry, M. J., Nicholson, W. K., Silverstein, M., Chelmow, D., Coker, T. R., et al. (2023). Folic acid supplementation to prevent neural tube defects: US preventive Services Task force reaffirmation recommendation statement. *JAMA* 330 (5), 454–459. doi:10.1001/jama.2023.12876

Forstermann, U., Closs, E. I., Pollock, J. S., Nakane, M., Schwarz, P., Gath, I., et al. (1994). Nitric oxide synthase isozymes. Characterization, purification, molecular cloning, and functions. *Hypertension* 23 (6 Pt 2), 1121–1131. doi:10.1161/01.hyp.23.6.1121

Forstermann, U., Mugge, A., Alheid, U., Bode, S. M., and Frolich, J. C. (1989). Endothelium-derived relaxing factor (EDRF): a defence mechanism against platelet aggregation and vasospasm in human coronary arteries. *Eur. Heart J.* 10 (Suppl. F), 36–43. doi:10.1093/eurheartj/10.suppl_f.36

Forstermann, U., Pollock, J. S., Schmidt, H. H., Heller, M., and Murad, F. (1991). Calmodulin-dependent endothelium-derived relaxing factor/nitric oxide synthase activity is present in the particulate and cytosolic fractions of bovine aortic endothelial cells. *Proc. Natl. Acad. Sci. U. S. A.* 88 (5), 1788–1792. doi:10.1073/pnas.88.5.1788

Fraccarollo, D., Widder, J. D., Galuppo, P., Thum, T., Tsikas, D., Hoffmann, M., et al. (2008). Improvement in left ventricular remodeling by the endothelial nitric oxide synthase enhancer AVE9488 after experimental myocardial infarction. *Circulation* 118 (8), 818–827. doi:10.1161/CIRCULATIONAHA.107.717702

Frantz, S., Adamek, A., Fraccarollo, D., Tillmanns, J., Widder, J. D., Dienesch, C., et al. (2009). The eNOS enhancer AVE 9488: a novel cardioprotectant against ischemia reperfusion injury. *Basic Res. Cardiol.* 104 (6), 773–779. doi:10.1007/s00395-009-0041-3

Fredette, N. C., Meyer, M. R., and Prossnitz, E. R. (2017). Role of GPER in estrogen-dependent nitric oxide formation and vasodilation. *J. steroid Biochem. Mol. Biol.* 176, 65–72. doi:10.1016/j.jsbmb.2017.05.006

Fukuda, Y., Teragawa, H., Matsuda, K., Yamagata, T., Matsuura, H., and Chayama, K. (2002). Tetrahydrobiopterin improves coronary endothelial function, but does not prevent coronary spasm in patients with vasospastic angina. *Circ. J.* 66 (1), 58–62. doi:10.1253/circj.66.58

Fukui, T., Ishizaka, N., Rajagopalan, S., Laursen, J. B., Capers, Qt, Taylor, W. R., et al. (1997). p22phox mRNA expression and NADPH oxidase activity are increased in aortas from hypertensive rats. *Circ. Res.* 80 (1), 45–51. doi:10.1161/01.res.80.1.45

Fulton, D., Gratton, J. P., McCabe, T. J., Fontana, J., Fujio, Y., Walsh, K., et al. (1999). Regulation of endothelium-derived nitric oxide production by the protein kinase Akt. *Nature* 399 (6736), 597–601. doi:10.1038/21218

Furchgott, R. F., and Zawadzki, J. V. (1980). The obligatory role of endothelial cells in the relaxation of arterial smooth muscle by acetylcholine. *Nature* 288 (5789), 373–376. doi:10.1038/288373a0

Gallis, B., Corthals, G. L., Goodlett, D. R., Ueba, H., Kim, F., Presnell, S. R., et al. (1999). Identification of flow-dependent endothelial nitric-oxide synthase phosphorylation sites by mass spectrometry and regulation of phosphorylation and nitric oxide production by the phosphatidylinositol 3-kinase inhibitor LY294002. *J. Biol. Chem.* 274 (42), 30101–30108. doi:10.1074/jbc.274.42.30101

Gao, L., Chalupsky, K., Stefani, E., and Cai, H. (2009). Mechanistic insights into folic acid-dependent vascular protection: dihydrofolate reductase (DHFR)-mediated reduction in oxidant stress in endothelial cells and angiotensin II-infused mice: a novel HPLC-based fluorescent assay for DHFR activity. *J. Mol. Cell Cardiol.* 47 (6), 752–760. doi:10.1016/j.yjmcc.2009.07.025

Garcia-Cardena, G., Fan, R., Shah, V., Sorrentino, R., Cirino, G., Papapetropoulos, A., et al. (1998). Dynamic activation of endothelial nitric oxide synthase by Hsp90. *Nature* 392 (6678), 821–824. doi:10.1038/33934

Garcia-Cardena, G., Fan, R., Stern, D. F., Liu, J., and Sessa, W. C. (1996). Endothelial nitric oxide synthase is regulated by tyrosine phosphorylation and interacts with caveolin-1. *J. Biol. Chem.* 271 (44), 27237–27240. doi:10.1074/jbc.271.44.27237

Garcia-Cardena, G., Martasek, P., Masters, B. S., Skidd, P. M., Couet, J., Li, S., et al. (1997). Dissecting the interaction between nitric oxide synthase (NOS) and caveolin. Functional significance of the nos caveolin binding domain *in vivo*. *J. Biol. Chem.* 272 (41), 25437–25440. doi:10.1074/jbc.272.41.25437

Geller, D. A., Lowenstein, C. J., Shapiro, R. A., Nussler, A. K., Di Silvio, M., Wang, S. C., et al. (1993). Molecular cloning and expression of inducible nitric oxide synthase from human hepatocytes. *Proc. Natl. Acad. Sci. U. S. A.* 90 (8), 3491–3495. doi:10.1073/pnas.90.8.3491

Girerd, X. J., Hirsch, A. T., Cooke, J. P., Dzau, V. J., and Creager, M. A. (1990). L-arginine augments endothelium-dependent vasodilation in cholesterol-fed rabbits. *Circ. Res.* 67 (6), 1301–1308. doi:10.1161/01.res.67.6.1301

Giustiniani, J., Couloubaly, S., Baillet, A., Pourci, M. L., Cantaloube, I., Fourniat, C., et al. (2009). Basal endothelial nitric oxide synthase (eNOS) phosphorylation on Ser(1177) occurs in a stable microtubule- and tubulin acetylation-dependent manner. *Exp. Cell Res.* 315 (20), 3509–3520. doi:10.1016/j.yexcr.2009.07.018

Gray, S. P., Di Marco, E., Okabe, J., Szyndralewiez, C., Heitz, F., Montezano, A. C., et al. (2013). NADPH oxidase 1 plays a key role in diabetes mellitus-accelerated atherosclerosis. *Circulation* 127 (18), 1888–1902. doi:10.1161/CIRCULATIONAHA.112.132159

Guzik, T. J., Mussa, S., Gastaldi, D., Sadowski, J., Ratnatunga, C., Pillai, R., et al. (2002). Mechanisms of increased vascular superoxide production in human diabetes mellitus: role of NAD(P)H oxidase and endothelial nitric oxide synthase. *Circulation* 105 (14), 1656–1662. doi:10.1161/01.cir.0000012748.58444.08

Hardy, T. A., and May, J. M. (2002). Coordinate regulation of L-arginine uptake and nitric oxide synthase activity in cultured endothelial cells. *Free Radic. Biol. Med.* 32 (2), 122–131. doi:10.1016/s0891-5849(01)00781-x

Harris, M. B., Ju, H., Venema, V. J., Liang, H., Zou, R., Michell, B. J., et al. (2001). Reciprocal phosphorylation and regulation of endothelial nitric-oxide synthase in response to bradykinin stimulation. *J. Biol. Chem.* 276 (19), 16587–16591. doi:10.1074/jbc.M100229200

Hecker, M., Sessa, W. C., Harris, H. J., Anggard, E. E., and Vane, J. R. (1990). The metabolism of L-arginine and its significance for the biosynthesis of endothelium-derived relaxing factor: cultured endothelial cells recycle L-citrulline to L-arginine. *Proc. Natl. Acad. Sci. U. S. A.* 87 (21), 8612–8616. doi:10.1073/pnas.87.21.8612

Heidenreich, P. A., Bozkurt, B., Aguilar, D., Allen, L. A., Byun, J. J., Colvin, M. M., et al. (2022). 2022 AHA/ACC/HFSA guideline for the management of heart failure: executive summary: a report of the American College of cardiology/American heart association joint committee on clinical practice guidelines. *J. Am. Coll. Cardiol.* 79 (17), 1757–1780. doi:10.1016/j.jacc.2021.12.011

Heitzer, T., Brockhoff, C., Mayer, B., Warnholtz, A., Mollnau, H., Henne, S., et al. (2000a). Tetrahydrobiopterin improves endothelium-dependent vasodilation in chronic smokers: evidence for a dysfunctional nitric oxide synthase. *Circ. Res.* 86 (2), E36–E41. doi:10.1161/01.res.86.2.e36

Heitzer, T., Krohn, K., Albers, S., and Meinertz, T. (2000b). Tetrahydrobiopterin improves endothelium-dependent vasodilation by increasing nitric oxide activity in patients with Type II diabetes mellitus. *Diabetologia* 43 (11), 1435–1438. doi:10.1007/s001250051551

Hellermann, G. R., and Solomonson, L. P. (1997). Calmodulin promotes dimerization of the oxygenase domain of human endothelial nitric-oxide synthase. *J. Biol. Chem.* 272 (18), 12030–12034. doi:10.1074/jbc.272.18.12030

Higashi, Y., Sasaki, S., Nakagawa, K., Fukuda, Y., Matsuura, H., Oshima, T., et al. (2002). Tetrahydrobiopterin enhances forearm vascular response to acetylcholine in both normotensive and hypertensive individuals. *Am. J. Hypertens.* 15 (4 Pt 1), 326–332. doi:10.1016/s0895-7061(01)02317-2

Holowatz, L. A., and Kenney, W. L. (2011). Acute localized administration of tetrahydrobiopterin and chronic systemic atorvastatin treatment restore cutaneous microvascular function in hypercholesterolaemic humans. *J. Physiol.* 589 (Pt 19), 4787–4797. doi:10.1113/jphysiol.2011.212100

Holton, M., Mohamed, T. M., Oceandy, D., Wang, W., Lamas, S., Emerson, M., et al. (2010). Endothelial nitric oxide synthase activity is inhibited by the plasma membrane calcium ATPase in human endothelial cells. *Cardiovasc Res.* 87 (3), 440–448. doi:10.1093/cvr/cvq077

Hong, H. J., Hsiao, G., Cheng, T. H., and Yen, M. H. (2001). Supplemention with tetrahydrobiopterin suppresses the development of hypertension in spontaneously hypertensive rats. *Hypertension* 38 (5), 1044–1048. doi:10.1161/hy1101.095331

Huang, P. L., Huang, Z., Mashimo, H., Bloch, K. D., Moskowitz, M. A., Bevan, J. A., et al. (1995). Hypertension in mice lacking the gene for endothelial nitric oxide synthase. *Nature* 377 (6546), 239–242. doi:10.1038/377239a0

Icking, A., Matt, S., Opitz, N., Wiesenthal, A., Muller-Esterl, W., and Schilling, K. (2005). NOSTRIN functions as a homotrimeric adaptor protein facilitating internalization of eNOS. *J. Cell Sci.* 118 (Pt 21), 5059–5069. doi:10.1242/jcs.02620

Ignarro, L. J., Adams, J. B., Horwitz, P. M., and Wood, K. S. (1986a). Activation of soluble guanylate cyclase by NO-hemoproteins involves NO-heme exchange. Comparison of heme-containing and heme-deficient enzyme forms. *J. Biol. Chem.* 261 (11), 4997–5002. doi:10.1016/s0021-9258(19)89205-0

Ignarro, L. J., Buga, G. M., Wood, K. S., Byrns, R. E., and Chaudhuri, G. (1987). Endothelium-derived relaxing factor produced and released from artery and vein is nitric oxide. *Proc. Natl. Acad. Sci. U. S. A.* 84 (24), 9265–9269. doi:10.1073/pnas.84.24.9265

Ignarro, L. J., Harbison, R. G., Wood, K. S., and Kadowitz, P. J. (1986b). Activation of purified soluble guanylate cyclase by endothelium-derived relaxing factor from intrapulmonary artery and vein: stimulation by acetylcholine, bradykinin and arachidonic acid. *J. Pharmacol. Exp. Ther.* 237 (3), 893–900.

Ignarro, L. J., Wood, K. S., and Wolin, M. S. (1982). Activation of purified soluble guanylate cyclase by protoporphyrin IX. *Proc. Natl. Acad. Sci. U. S. A.* 79 (9), 2870–2873. doi:10.1073/pnas.79.9.2870

Ilies, M., Di Costanzo, L., Dowling, D. P., Thorn, K. J., and Christianson, D. W. (2011). Binding of α,α-disubstituted amino acids to arginase suggests new avenues for inhibitor design. *J. Med. Chem.* 54 (15), 5432–5443. doi:10.1021/jm200443b

Ismaeel, A., Papoutsi, E., Miserlis, D., Lavado, R., Haynatzki, G., Casale, G. P., et al. (2020). The nitric oxide system in peripheral artery disease: connection with oxidative stress and biopterins. *Antioxidants (Basel)* 9 (7), 590. doi:10.3390/antiox9070590

Janaszak-Jasiecka, A., Ploska, A., Wieronska, J. M., Dobrucki, L. W., and Kalinowski, L. (2023). Endothelial dysfunction due to eNOS uncoupling: molecular mechanisms as potential therapeutic targets. *Cell Mol. Biol. Lett.* 28 (1), 21. doi:10.1186/s11658-023-00423-2

Janssens, S. P., Simouchi, A., Quertermous, T., Bloch, D. B., and Bloch, K. D. (1992). Cloning and expression of a cDNA encoding human endothelium-derived relating factor/nitric oxide synthase. *J. Biol. Chem.* 267 (31), 22694. doi:10.1016/s0021-9258(18)41728-0

Jiang, F., Lim, H. K., Morris, M. J., Prior, L., Velkoska, E., Wu, X., et al. (2011). Systemic upregulation of NADPH oxidase in diet-induced obesity in rats. *Redox Rep.* 16 (6), 223–229. doi:10.1179/174329211X13049558293713

Jo, H., Otani, H., Jo, F., Shimazu, T., Okazaki, T., Yoshioka, K., et al. (2011). Inhibition of nitric oxide synthase uncoupling by sepiapterin improves left ventricular function in streptozotocin-induced diabetic mice. *Clin. Exp. Pharmacol. Physiol.* 38 (8), 485–493. doi:10.1111/j.1440-1681.2011.05535.x

Ju, H., Zou, R., Venema, V. J., and Venema, R. C. (1997). Direct interaction of endothelial nitric-oxide synthase and caveolin-1 inhibits synthase activity. *J. Biol. Chem.* 272 (30), 18522–18525. doi:10.1074/jbc.272.30.18522

Jung, S. B., Kim, C. S., Naqvi, A., Yamamori, T., Mattagajasingh, I., Hoffman, T. A., et al. (2010). Histone deacetylase 3 antagonizes aspirin-stimulated endothelial nitric

oxide production by reversing aspirin-induced lysine acetylation of endothelial nitric oxide synthase. *Circ. Res.* 107 (7), 877–887. doi:10.1161/CIRCRESAHA.110.222968

Jurcau, A., and Ardelean, A. I. (2022). Oxidative stress in ischemia/reperfusion injuries following acute ischemic stroke. *Biomedicines* 10 (3), 574. doi:10.3390/biomedicines10030574

Karantzoulis-Fegaras, F., Antoniou, H., Lai, S. L., Kulkarni, G., D'Abreo, C., Wong, G. K., et al. (1999). Characterization of the human endothelial nitric-oxide synthase promoter. *J. Biol. Chem.* 274 (5), 3076–3093. doi:10.1074/jbc.274.5.3076

Kashiwagi, S., Atochin, D. N., Li, Q., Schleicher, M., Pong, T., Sessa, W. C., et al. (2013). eNOS phosphorylation on serine 1176 affects insulin sensitivity and adiposity. *Biochem. Biophys. Res. Commun.* 431 (2), 284–290. doi:10.1016/j.bbrc.2012.12.110

Kassan, M., Ait-Aissa, K., Radwan, E., Mali, V., Haddox, S., Gabani, M., et al. (2016). Essential role of smooth muscle STIM1 in hypertension and cardiovascular dysfunction. *Arterioscler. Thromb. Vasc. Biol.* 36 (9), 1900–1909. doi:10.1161/ATVBAHA.116.307869

Katsuki, S., Arnold, W., Mittal, C., and Murad, F. (1977). Stimulation of guanylate cyclase by sodium nitroprusside, nitroglycerin and nitric oxide in various tissue preparations and comparison to the effects of sodium azide and hydroxylamine. *J. Cycl. Nucleotide Res.* 3 (1), 23–35.

Kaye, A. D., Jeha, G. M., Pham, A. D., Fuller, M. C., Lerner, Z. I., Sibley, G. T., et al. (2020). Folic acid supplementation in patients with elevated homocysteine levels. *Adv. Ther.* 37 (10), 4149–4164. doi:10.1007/s12325-020-01474-z

Keller, T. C. S, Lechauve, C., Keller, A. S., Broseghini-Filho, G. B., Butcher, J. T., Askew Page, H. R., et al. (2022). Endothelial alpha globin is a nitrite reductase. *Nat. Commun.* 13 (1), 6405. doi:10.1038/s41467-022-34154-3

Keller, T. C. S., Butcher, J. T., Broseghini-Filho, G. B., Marziano, C., DeLalio, L. J., Rogers, S., et al. (2016). Modulating vascular hemodynamics with an alpha globin mimetic peptide (HbαX). *Hypertension* 68 (6), 1494–1503. doi:10.1161/HYPERTENSIONAHA.116.08171

Kim, M., Han, C. H., and Lee, M. Y. (2014). NADPH oxidase and the cardiovascular toxicity associated with smoking. *Toxicol. Res.* 30 (3), 149–157. doi:10.5487/TR.2014.30.3.149

Kim-Shapiro, D. B., Gladwin, M. T., Patel, R. P., and Hogg, N. (2005). The reaction between nitrite and hemoglobin: the role of nitrite in hemoglobin-mediated hypoxic vasodilation. *J. Inorg. Biochem.* 99 (1), 237–246. doi:10.1016/j.jinorgbio.2004.10.034

Knorr, M., Hausding, M., Kroller-Schuhmacher, S., Steven, S., Oelze, M., Heeren, T., et al. (2011). Nitroglycerin-induced endothelial dysfunction and tolerance involve adverse phosphorylation and S-Glutathionylation of endothelial nitric oxide synthase: beneficial effects of therapy with the AT1 receptor blocker telmisartan. *Arterioscler. Thromb. Vasc. Biol.* 31 (10), 2223–2231. doi:10.1161/ATVBAHA.111.232058

Kondrikov, D., Fonseca, F. V., Elms, S., Fulton, D., Black, S. M., Block, E. R., et al. (2010). Beta-actin association with endothelial nitric-oxide synthase modulates nitric oxide and superoxide generation from the enzyme. *J. Biol. Chem.* 285 (7), 4319–4327. doi:10.1074/jbc.M109.063172

Konior, A., Schramm, A., Czesnikiewicz-Guzik, M., and Guzik, T. J. (2014). NADPH oxidases in vascular pathology. *Antioxid. Redox Signal* 20 (17), 2794–2814. doi:10.1089/ars.2013.5607

Kossel, A., and Dakin, H. D. (1904). Uber die Arginase. *Z Physiol. Chem.* 41, 321–331. doi:10.1515/bchm2.1904.41.4.321

Kou, R., Greif, D., and Michel, T. (2002). Dephosphorylation of endothelial nitric-oxide synthase by vascular endothelial growth factor. Implications for the vascular responses to cyclosporin A. *J. Biol. Chem.* 277 (33), 29669–29673. doi:10.1074/jbc.M204519200

Kovamees, O., Shemyakin, A., Checa, A., Wheelock, C. E., Lundberg, J. O., Ostenson, C. G., et al. (2016b). Arginase inhibition improves microvascular endothelial function in patients with type 2 diabetes mellitus. *J. Clin. Endocrinol. Metab.* 101 (11), 3952–3958. doi:10.1210/jc.2016-2007

Kovamees, O., Shemyakin, A., Eriksson, M., Angelin, B., and Pernow, J. (2016a). Arginase inhibition improves endothelial function in patients with familial hypercholesterolaemia irrespective of their cholesterol levels. *J. Intern Med.* 279 (5), 477–484. doi:10.1111/joim.12461

Kovamees, O., Shemyakin, A., and Pernow, J. (2014). Effect of arginase inhibition on ischemia-reperfusion injury in patients with coronary artery disease with and without diabetes mellitus. *PLoS One* 9 (7), e103260. doi:10.1371/journal.pone.0103260

Kraehling, J. R., and Sessa, W. C. (2017). Contemporary approaches to modulating the nitric oxide-cGMP pathway in cardiovascular disease. *Circ. Res.* 120 (7), 1174–1182. doi:10.1161/CIRCRESAHA.117.303776

Landmesser, U., Dikalov, S., Price, S. R., McCann, L., Fukai, T., Holland, S. M., et al. (2003). Oxidation of tetrahydrobiopterin leads to uncoupling of endothelial cell nitric oxide synthase in hypertension. *J. Clin. Invest.* 111 (8), 1201–1209. doi:10.1172/JCI14172

Lass, A., Suessenbacher, A., Wolkart, G., Mayer, B., and Brunner, F. (2002). Functional and analytical evidence for scavenging of oxygen radicals by L-arginine. *Mol. Pharmacol.* 61 (5), 1081–1088. doi:10.1124/mol.61.5.1081

Laumonnier, Y., Nadaud, S., Agrapart, M., and Soubrier, F. (2000). Characterization of an upstream enhancer region in the promoter of the human endothelial nitric-oxide synthase gene. *J. Biol. Chem.* 275 (52), 40732–40741. doi:10.1074/jbc.M004696200

Laursen, J. B., Somers, M., Kurz, S., McCann, L., Warnholtz, A., Freeman, B. A., et al. (2001). Endothelial regulation of vasomotion in apoE-deficient mice: implications for interactions between peroxynitrite and tetrahydrobiopterin. *Circulation* 103 (9), 1282–1288. doi:10.1161/01.cir.103.9.1282

Lee, C. K., Han, J. S., Won, K. J., Jung, S. H., Park, H. J., Lee, H. M., et al. (2009). Diminished expression of dihydropteridine reductase is a potent biomarker for hypertensive vessels. *Proteomics* 9 (21), 4851–4858. doi:10.1002/pmic.200800973

Levillain, O. (2012). Expression and function of arginine-producing and consuming-enzymes in the kidney. *Amino Acids* 42 (4), 1237–1252. doi:10.1007/s00726-011-0897-z

Li, C., Huang, W., Harris, M. B., Goolsby, J. M., and Venema, R. C. (2005). Interaction of the endothelial nitric oxide synthase with the CAT-1 arginine transporter enhances NO release by a mechanism not involving arginine transport. *Biochem. J.* 386 (Pt 3), 567–574. doi:10.1042/BJ20041005

Li, C., Ruan, L., Sood, S. G., Papapetropoulos, A., Fulton, D., and Venema, R. C. (2007). Role of eNOS phosphorylation at Ser-116 in regulation of eNOS activity in endothelial cells. *Vasc. Pharmacol.* 47 (5-6), 257–264. doi:10.1016/j.vph.2007.07.001

Li, H., Horke, S., and Forstermann, U. (2013). Oxidative stress in vascular disease and its pharmacological prevention. *Trends Pharmacol. Sci.* 34 (6), 313–319. doi:10.1016/j.tips.2013.03.007

Li, H., Horke, S., and Forstermann, U. (2014). Vascular oxidative stress, nitric oxide and atherosclerosis. *Atherosclerosis* 237 (1), 208–219. doi:10.1016/j.atherosclerosis.2014.09.001

Li, H., Meininger, C. J., Hawker, J. R., Jr., Haynes, T. E., Kepka-Lenhart, D., Mistry, S. K., et al. (2001). Regulatory role of arginase I and II in nitric oxide, polyamine, and proline syntheses in endothelial cells. *Am. J. Physiol. Endocrinol. Metab.* 280 (1), E75–E82. doi:10.1152/ajpendo.2001.280.1.E75

Li, H., Witte, K., August, M., Brausch, I., Godtel-Armbrust, U., Habermeier, A., et al. (2006). Reversal of endothelial nitric oxide synthase uncoupling and up-regulation of endothelial nitric oxide synthase expression lowers blood pressure in hypertensive rats. *J. Am. Coll. Cardiol.* 47 (12), 2536–2544. doi:10.1016/j.jacc.2006.01.071

Li, J., Hou, B., Tumova, S., Muraki, K., Bruns, A., Ludlow, M. J., et al. (2014). Piezo1 integration of vascular architecture with physiological force. *Nature* 515 (7526), 279–282. doi:10.1038/nature13701

Li, Q., Atochin, D., Kashiwagi, S., Earle, J., Wang, A., Mandeville, E., et al. (2013). Deficient eNOS phosphorylation is a mechanism for diabetic vascular dysfunction contributing to increased stroke size. *Stroke* 44 (11), 3183–3188. doi:10.1161/STROKEAHA.113.002073

Li, X., Bazer, F. W., Johnson, G. A., Burghardt, R. C., and Wu, G. (2023). Dietary supplementation with L-citrulline improves placental angiogenesis and embryonic survival in gilts. *Exp. Biol. Med. (Maywood)* 248 (8), 702–711. doi:10.1177/15353702231157943

Liao, J. K., Shin, W. S., Lee, W. Y., and Clark, S. L. (1995). Oxidized low-density lipoprotein decreases the expression of endothelial nitric oxide synthase. *J. Biol. Chem.* 270 (1), 319–324. doi:10.1074/jbc.270.1.319

Lima, B., Forrester, M. T., Hess, D. T., and Stamler, J. S. (2010). S-nitrosylation in cardiovascular signaling. *Circ. Res.* 106 (4), 633–646. doi:10.1161/CIRCRESAHA.109.207381

Lin, Z., Kumar, A., SenBanerjee, S., Staniszewski, K., Parmar, K., Vaughan, D. E., et al. (2005). Kruppel-like factor 2 (KLF2) regulates endothelial thrombotic function. *Circ. Res.* 96 (5), e48–e57. doi:10.1161/01.RES.0000159707.05637.a1

Lipton, S. A., Choi, Y. B., Pan, Z. H., Lei, S. Z., Chen, H. S., Sucher, N. J., et al. (1993). A redox-based mechanism for the neuroprotective and neurodestructive effects of nitric oxide and related nitroso-compounds. *Nature* 364 (6438), 626–632. doi:10.1038/364626a0

List, B. M., Klosch, B., Volker, C., Gorren, A. C., Sessa, W. C., Werner, E. R., et al. (1997). Characterization of bovine endothelial nitric oxide synthase as a homodimer with down-regulated uncoupled NADPH oxidase activity: tetrahydrobiopterin binding kinetics and role of haem in dimerization. *Biochem. J.* 323 (Pt 1), 159–165. doi:10.1042/bj3230159

Liu, J., Garcia-Cardena, G., and Sessa, W. C. (1995). Biosynthesis and palmitoylation of endothelial nitric oxide synthase: mutagenesis of palmitoylation sites, cysteines-15 and/or -26, argues against depalmitoylation-induced translocation of the enzyme. *Biochemistry* 34 (38), 12333–12340. doi:10.1021/bi00038a029

Lu, J. L., Schmiege, L. M., 3rd, Kuo, L., and Liao, J. C. (1996). Downregulation of endothelial constitutive nitric oxide synthase expression by lipopolysaccharide. *Biochem. Biophys. Res. Commun.* 225 (1), 1–5. doi:10.1006/bbrc.1996.1121

Lucotti, P., Monti, L., Setola, E., La Canna, G., Castiglioni, A., Rossodivita, A., et al. (2009). Oral L-arginine supplementation improves endothelial function and ameliorates insulin sensitivity and inflammation in cardiopathic nondiabetic patients after an aortocoronary bypass. *Metabolism* 58 (9), 1270–1276. doi:10.1016/j.metabol.2009.03.029

Lundberg, J. O., Gladwin, M. T., and Weitzberg, E. (2015). Strategies to increase nitric oxide signalling in cardiovascular disease. *Nat. Rev. Drug Discov.* 14 (9), 623–641. doi:10.1038/nrd4623

Lundberg, J. O., Weitzberg, E., Lundberg, J. M., and Alving, K. (1994). Intragastric nitric oxide production in humans: measurements in expelled air. *Gut* 35 (11), 1543–1546. doi:10.1136/gut.35.11.1543

Maharaj, A., Fischer, S. M., Dillon, K. N., Kang, Y., Martinez, M. A., and Figueroa, A. (2022). Effects of L-citrulline supplementation on endothelial function and blood pressure in hypertensive postmenopausal women. *Nutrients* 14 (20), 4396. doi:10.3390/nu14204396

Mahdi, A., Kovamees, O., Checa, A., Wheelock, C. E., von Heijne, M., Alvarsson, M., et al. (2018). Arginase inhibition improves endothelial function in patients with type 2 diabetes mellitus despite intensive glucose-lowering therapy. *J. Intern Med.* 284 (4), 388–398. doi:10.1111/joim.12785

Mahdi, A., Pernow, J., and Kovamees, O. (2019). Arginase inhibition improves endothelial function in an age-dependent manner in healthy elderly humans. *Rejuvenation Res.* 22 (5), 385–389. doi:10.1089/rej.2018.2135

Maier, W., Cosentino, F., Lutolf, R. B., Fleisch, M., Seiler, C., Hess, O. M., et al. (2000). Tetrahydrobiopterin improves endothelial function in patients with coronary artery disease. *J. Cardiovasc Pharmacol.* 35 (2), 173–178. doi:10.1097/00005344-200002000-00001

Man, H. S. J., Sukumar, A. N., Lam, G. C., Turgeon, P. J., Yan, M. S., Ku, K. H., et al. (2018). Angiogenic patterning by STEEL, an endothelial-enriched long noncoding RNA. *Proc. Natl. Acad. Sci. U. S. A.* 115 (10), 2401–2406. doi:10.1073/pnas.1715182115

Manea, S. A., Antonescu, M. L., Fenyo, I. M., Raicu, M., Simionescu, M., and Manea, A. (2018). Epigenetic regulation of vascular NADPH oxidase expression and reactive oxygen species production by histone deacetylase-dependent mechanisms in experimental diabetes. *Redox Biol.* 16, 332–343. doi:10.1016/j.redox.2018.03.011

Marchi, K. C., Ceron, C. S., Muniz, J. J., De Martinis, B. S., Tanus-Santos, J. E., and Tirapelli, C. R. (2016). NADPH oxidase plays a role on ethanol-induced hypertension and reactive oxygen species generation in the vasculature. *Alcohol Alcohol* 51 (5), 522–534. doi:10.1093/alcalc/agw043

Marrero, M. B., Venema, V. J., Ju, H., He, H., Liang, H., Caldwell, R. B., et al. (1999). Endothelial nitric oxide synthase interactions with G-protein-coupled receptors. *Biochem. J.* 343 (Pt 2), 335–340. doi:10.1042/0264-6021:3430335

Marsden, P. A., Schappert, K. T., Chen, H. S., Flowers, M., Sundell, C. L., Wilcox, J. N., et al. (1992). Molecular cloning and characterization of human endothelial nitric oxide synthase. *FEBS Lett.* 307 (3), 287–293. doi:10.1016/0014-5793(92)80697-f

Mattsson, E. J., Kohler, T. R., Vergel, S. M., and Clowes, A. W. (1997). Increased blood flow induces regression of intimal hyperplasia. *Arterioscler. Thromb. Vasc. Biol.* 17 (10), 2245–2249. doi:10.1161/01.atv.17.10.2245

McCabe, T. J., Fulton, D., Roman, L. J., and Sessa, W. C. (2000). Enhanced electron flux and reduced calmodulin dissociation may explain "calcium-independent" eNOS activation by phosphorylation. *J. Biol. Chem.* 275 (9), 6123–6128. doi:10.1074/jbc.275.9.6123

McClure, S. J., and Robinson, P. J. (1996). Dynamin, endocytosis and intracellular signalling (review). *Mol. Membr. Biol.* 13 (4), 189–215. doi:10.3109/09687689609160598

McDonald, K. K., Rouhani, R., Handlogten, M. E., Block, E. R., Griffith, O. W., Allison, R. D., et al. (1997a). Inhibition of endothelial cell amino acid transport System y+ by arginine analogs that inhibit nitric oxide synthase. *Biochim. Biophys. Acta* 1324 (1), 133–141. doi:10.1016/s0005-2736(96)00226-x

McDonald, K. K., Zharikov, S., Block, E. R., and Kilberg, M. S. (1997b). A caveolar complex between the cationic amino acid transporter 1 and endothelial nitric-oxide synthase may explain the arginine paradox. *J. Biol. Chem.* 272 (50), 31213–31216. doi:10.1074/jbc.272.50.31213

McQuillan, L. P., Leung, G. K., Marsden, P. A., Kostyk, S. K., and Kourembanas, S. (1994). Hypoxia inhibits expression of eNOS via transcriptional and posttranscriptional mechanisms. *Am. J. Physiol.* 267 (5 Pt 2), H1921–H1927. doi:10.1152/ajpheart.1994.267.5.H1921

Menzel, D., Haller, H., Wilhelm, M., and Robenek, H. (2018). L-Arginine and B vitamins improve endothelial function in subjects with mild to moderate blood pressure elevation. *Eur. J. Nutr.* 57 (2), 557–568. doi:10.1007/s00394-016-1342-6

Miao, Y., Ajami, N. E., Huang, T. S., Lin, F. M., Lou, C. H., Wang, Y. T., et al. (2018). Enhancer-associated long non-coding RNA LEENE regulates endothelial nitric oxide synthase and endothelial function. *Nat. Commun.* 9 (1), 292. doi:10.1038/s41467-017-02113-y

Michel, J. B., Feron, O., Sase, K., Prabhakar, P., and Michel, T. (1997). Caveolin versus calmodulin. Counterbalancing allosteric modulators of endothelial nitric oxide synthase. *J. Biol. Chem.* 272 (41), 25907–25912. doi:10.1074/jbc.272.41.25907

Michell, B. J., Griffiths, J. E., Mitchelhill, K. I., Rodriguez-Crespo, I., Tiganis, T., Bozinovski, S., et al. (1999). The Akt kinase signals directly to endothelial nitric oxide synthase. *Curr. Biol.* 9 (15), 845–848. doi:10.1016/s0960-9822(99)80371-6

Michell, B. J., Harris, M. B., Chen, Z. P., Ju, H., Venema, V. J., Blackstone, M. A., et al. (2002). Identification of regulatory sites of phosphorylation of the bovine endothelial nitric-oxide synthase at serine 617 and serine 635. *J. Biol. Chem.* 277 (44), 42344–42351. doi:10.1074/jbc.M205144200

Milstien, S., and Katusic, Z. (1999). Oxidation of tetrahydrobiopterin by peroxynitrite: implications for vascular endothelial function. *Biochem. Biophys. Res. Commun.* 263 (3), 681–684. doi:10.1006/bbrc.1999.1422

Mitchell, J. A., Forstermann, U., Warner, T. D., Pollock, J. S., Schmidt, H. H., Heller, M., et al. (1991). Endothelial cells have a particulate enzyme system responsible for EDRF formation: measurement by vascular relaxation. *Biochem. Biophys. Res. Commun.* 176 (3), 1417–1423. doi:10.1016/0006-291x(91)90444-c

Moens, A. L., Takimoto, E., Tocchetti, C. G., Chakir, K., Bedja, D., Cormaci, G., et al. (2008). Reversal of cardiac hypertrophy and fibrosis from pressure overload by tetrahydrobiopterin: efficacy of recoupling nitric oxide synthase as a therapeutic strategy. *Circulation* 117 (20), 2626–2636. doi:10.1161/CIRCULATIONAHA.107.737031

Morita, M., Sakurada, M., Watanabe, F., Yamasaki, T., Doi, H., Ezaki, H., et al. (2013). Effects of oral L-citrulline supplementation on lipoprotein oxidation and endothelial dysfunction in humans with vasospastic angina. *Immunol. Endocr. Metab. Agents Med. Chem.* 13 (3), 214–220. doi:10.2174/18715222113139990008

Mount, P. F., Kemp, B. E., and Power, D. A. (2007). Regulation of endothelial and myocardial NO synthesis by multi-site eNOS phosphorylation. *J. Mol. Cell Cardiol.* 42 (2), 271–279. doi:10.1016/j.yjmcc.2006.05.023

Muntau, A. C., Longo, N., Ezgu, F., Schwartz, I. V. D., Lah, M., Bratkovic, D., et al. (2024). Effects of oral sepiapterin on blood Phe concentration in a broad range of patients with phenylketonuria (APHENITY): results of an international, phase 3, randomised, double-blind, placebo-controlled trial. *Lancet* 404 (10460), 1333–1345. doi:10.1016/S0140-6736(24)01556-3

Munzel, T., and Daiber, A. (2017). Does endothelial tetrahydrobiopterin control the endothelial NO synthase coupling state in arterial resistance arteries? *Br. J. Pharmacol.* 174 (14), 2422–2424. doi:10.1111/bph.13827

Munzel, T., Daiber, A., and Gori, T. (2013). More answers to the still unresolved question of nitrate tolerance. *Eur. Heart J.* 34 (34), 2666–2673. doi:10.1093/eurheartj/eht249

Munzel, T., Daiber, A., Ullrich, V., and Mulsch, A. (2005). Vascular consequences of endothelial nitric oxide synthase uncoupling for the activity and expression of the soluble guanylyl cyclase and the cGMP-dependent protein kinase. *Arterioscler. Thromb. Vasc. Biol.* 25 (8), 1551–1557. doi:10.1161/01.ATV.0000168896.64927.bb

Munzel, T., Giaid, A., Kurz, S., Stewart, D. J., and Harrison, D. G. (1995b). Evidence for a role of endothelin 1 and protein kinase C in nitroglycerin tolerance. *Proc. Natl. Acad. Sci. U. S. A.* 92 (11), 5244–5248. doi:10.1073/pnas.92.11.5244

Munzel, T., Meinertz, T., Tebbe, U., Schneider, H. T., Stalleicken, D., Wargenau, M., et al. (2014). Efficacy of the long-acting nitro vasodilator pentaerithrityl tetranitrate in patients with chronic stable angina pectoris receiving anti-anginal background therapy with beta-blockers: a 12-week, randomized, double-blind, placebo-controlled trial. *Eur. Heart J.* 35 (14), 895–903. doi:10.1093/eurheartj/eht384

Munzel, T., Sayegh, H., Freeman, B. A., Tarpey, M. M., and Harrison, D. G. (1995a). Evidence for enhanced vascular superoxide anion production in nitrate tolerance. A novel mechanism underlying tolerance and cross-tolerance. *J. Clin. Invest.* 95 (1), 187–194. doi:10.1172/JCI117637

Murata, T., Lin, M. I., Huang, Y., Yu, J., Bauer, P. M., Giordano, F. J., et al. (2007). Reexpression of caveolin-1 in endothelium rescues the vascular, cardiac, and pulmonary defects in global caveolin-1 knockout mice. *J. Exp. Med.* 204 (10), 2373–2382. doi:10.1084/jem.20062340

Nadaud, S., Philippe, M., Arnal, J. F., Michel, J. B., and Soubrier, F. (1996). Sustained increase in aortic endothelial nitric oxide synthase expression *in vivo* in a model of chronic high blood flow. *Circ. Res.* 79 (4), 857–863. doi:10.1161/01.res.79.4.857

Naing, A., Papadopoulos, K. P., Pishvaian, M. J., Rahma, O., Hanna, G. J., Garralda, E., et al. (2024). First-in-human phase 1 study of the arginase inhibitor INCB001158 alone or combined with pembrolizumab in patients with advanced or metastatic solid tumours. *BMJ Oncol.* 3, e000249. doi:10.1136/bmjonc-2023-000249

Neumann, P., Gertzberg, N., and Johnson, A. (2004). TNF-alpha induces a decrease in eNOS promoter activity. *Am. J. Physiol. Lung Cell Mol. Physiol.* 286 (2), L452–L459. doi:10.1152/ajplung.00378.2002

Ng, Y. Y. H., Dora, K. A., Lemmey, H. A. L., Lin, J., Alden, J., Wallis, L., et al. (2024). Asymmetric dimethylarginine enables depolarizing spikes and vasospasm in mesenteric and coronary resistance arteries. *Hypertension* 81 (4), 764–775. doi:10.1161/HYPERTENSIONAHA.123.22454

Nishida, C. R., and Ortiz de Montellano, P. R. (1999). Autoinhibition of endothelial nitric-oxide synthase. Identification of an electron transfer control element. *J. Biol. Chem.* 274 (21), 14692–14698. doi:10.1074/jbc.274.21.14692

Nishida, K., Harrison, D. G., Navas, J. P., Fisher, A. A., Dockery, S. P., Uematsu, M., et al. (1992). Molecular cloning and characterization of the constitutive bovine aortic endothelial cell nitric oxide synthase. *J. Clin. Invest.* 90 (5), 2092–2096. doi:10.1172/JCI116092

Nishimoto, M., Mizuno, R., Fujita, T., and Isshiki, M. (2018). Stromal interaction molecule 1 modulates blood pressure via NO production in vascular endothelial cells. *Hypertens. Res.* 41 (7), 506–514. doi:10.1038/s41440-018-0045-1

Noreng, S., Ota, N., Sun, Y., Ho, H., Johnson, M., Arthur, C. P., et al. (2022). Structure of the core human NADPH oxidase NOX2. *Nat. Commun.* 13 (1), 6079. doi:10.1038/s41467-022-33711-0

Nystrom, T., Nygren, A., and Sjoholm, A. (2004). Tetrahydrobiopterin increases insulin sensitivity in patients with type 2 diabetes and coronary heart disease. *Am. J. Physiol. Endocrinol. Metab.* 287 (5), E919–E925. doi:10.1152/ajpendo.00046.2004

Oelze, M., Knorr, M., Kroller-Schon, S., Kossmann, S., Gottschlich, A., Rummler, R., et al. (2013). Chronic therapy with isosorbide-5-mononitrate causes endothelial dysfunction, oxidative stress, and a marked increase in vascular endothelin-1 expression. *Eur. Heart J.* 34 (41), 3206–3216. doi:10.1093/eurheartj/ehs100

Osowska, S., Moinard, C., Neveux, N., Loi, C., and Cynober, L. (2004). Citrulline increases arginine pools and restores nitrogen balance after massive intestinal resection. *Gut* 53 (12), 1781–1786. doi:10.1136/gut.2004.042317

Ou, H., Shen, Y. H., Utama, B., Wang, J., Wang, X., Coselli, J., et al. (2005). Effect of nuclear actin on endothelial nitric oxide synthase expression. *Arterioscler. Thromb. Vasc. Biol.* 25 (12), 2509–2514. doi:10.1161/01.ATV.0000189306.99112.4c

Paik, W. K., Nochumson, S., and Kim, S. (1978). Effect of modification on inhibitory amino acids on arginase activity. *Biochem. Med.* 19 (1), 39–46. doi:10.1016/0006-2944(78)90005-4

Palmer, R. M., Ashton, D. S., and Moncada, S. (1988). Vascular endothelial cells synthesize nitric oxide from L-arginine. *Nature* 333 (6174), 664–666. doi:10.1038/333664a0

Palmer, R. M., Ferrige, A. G., and Moncada, S. (1987). Nitric oxide release accounts for the biological activity of endothelium-derived relaxing factor. *Nature* 327 (6122), 524–526. doi:10.1038/327524a0

Park, K., Mima, A., Li, Q., Rask-Madsen, C., He, P., Mizutani, K., et al. (2016). Insulin decreases atherosclerosis by inducing endothelin receptor B expression. *JCI Insight* 1 (6), e86574. doi:10.1172/jci.insight.86574

Pernow, J., and Jung, C. (2013). Arginase as a potential target in the treatment of cardiovascular disease: reversal of arginine steal? *Cardiovasc Res.* 98 (3), 334–343. doi:10.1093/cvr/cvt036

Pernow, J., Kiss, A., Tratsiakovich, Y., and Climent, B. (2015). Tissue-specific up-regulation of arginase I and II induced by p38 MAPK mediates endothelial dysfunction in type 1 diabetes mellitus. *Br. J. Pharmacol.* 172 (19), 4684–4698. doi:10.1111/bph.13242

Peyton, K. J., Liu, X. M., Shebib, A. R., Johnson, F. K., Johnson, R. A., and Durante, W. (2018). Arginase inhibition prevents the development of hypertension and improves insulin resistance in obese rats. *Amino Acids* 50 (6), 747–754. doi:10.1007/s00726-018-2567-x

Pollock, J. S., Forstermann, U., Mitchell, J. A., Warner, T. D., Schmidt, H. H., Nakane, M., et al. (1991). Purification and characterization of particulate endothelium-derived relaxing factor synthase from cultured and native bovine aortic endothelial cells. *Proc. Natl. Acad. Sci. U. S. A.* 88 (23), 10480–10484. doi:10.1073/pnas.88.23.10480

Porkert, M., Sher, S., Reddy, U., Cheema, F., Niessner, C., Kolm, P., et al. (2008). Tetrahydrobiopterin: a novel antihypertensive therapy. *J. Hum. Hypertens.* 22 (6), 401–407. doi:10.1038/sj.jhh.1002329

Pudlo, M., Demougeot, C., and Girard-Thernier, C. (2017). Arginase inhibitors: a rational approach over one century. *Med. Res. Rev.* 37 (3), 475–513. doi:10.1002/med.21419

Ranade, S. S., Qiu, Z., Woo, S. H., Hur, S. S., Murthy, S. E., Cahalan, S. M., et al. (2014). Piezo1, a mechanically activated ion channel, is required for vascular development in mice. *Proc. Natl. Acad. Sci. U. S. A.* 111 (28), 10347–10352. doi:10.1073/pnas.1409233111

Rapoport, R. M., Waldman, S. A., Ginsburg, R., Molina, C. R., and Murad, F. (1987). Effects of glyceryl trinitrate on endothelium-dependent and -independent relaxation and cyclic GMP levels in rat aorta and human coronary artery. *J. Cardiovasc Pharmacol.* 10 (1), 82–89. doi:10.1097/00005344-198707000-00012

Razani, B., Engelman, J. A., Wang, X. B., Schubert, W., Zhang, X. L., Marks, C. B., et al. (2001). Caveolin-1 null mice are viable but show evidence of hyperproliferative and vascular abnormalities. *J. Biol. Chem.* 276 (41), 38121–38138. doi:10.1074/jbc.M105408200

Rees, D. D., Palmer, R. M., and Moncada, S. (1989). Role of endothelium-derived nitric oxide in the regulation of blood pressure. *Proc. Natl. Acad. Sci. U. S. A.* 86 (9), 3375–3378. doi:10.1073/pnas.86.9.3375

Reule, C. A., Goyvaerts, B., and Schoen, C. (2017). Effects of an L-arginine-based multi ingredient product on endothelial function in subjects with mild to moderate hypertension and hyperhomocysteinemia - a randomized, double-blind, placebo-controlled, cross-over trial. *BMC Complement. Altern. Med.* 17 (1), 92. doi:10.1186/s12906-017-1603-9

Reyes, L. A., Boslett, J., Varadharaj, S., De Pascali, F., Hemann, C., Druhan, L. J., et al. (2015). Depletion of NADP(H) due to CD38 activation triggers endothelial dysfunction in the postischemic heart. *Proc. Natl. Acad. Sci. U. S. A.* 112 (37), 11648–11653. doi:10.1073/pnas.1505556112

Roos, J., DiGregorio, P. J., Yeromin, A. V., Ohlsen, K., Lioudyno, M., Zhang, S., et al. (2005). STIM1, an essential and conserved component of store-operated Ca2+ channel function. *J. Cell Biol.* 169 (3), 435–445. doi:10.1083/jcb.200502019

Rossitch, E., Jr., Alexander, E., 3rd, Black, P. M., and Cooke, J. P. (1991). L-arginine normalizes endothelial function in cerebral vessels from hypercholesterolemic rabbits. *J. Clin. Invest.* 87 (4), 1295–1299. doi:10.1172/JCI115132

Russell, K. S., Haynes, M. P., Caulin-Glaser, T., Rosneck, J., Sessa, W. C., and Bender, J. R. (2000). Estrogen stimulates heat shock protein 90 binding to endothelial nitric oxide synthase in human vascular endothelial cells. Effects on calcium sensitivity and NO release. *J. Biol. Chem.* 275 (7), 5026–5030. doi:10.1074/jbc.275.7.5026

Ryoo, S., Gupta, G., Benjo, A., Lim, H. K., Camara, A., Sikka, G., et al. (2008). Endothelial arginase II: a novel target for the treatment of atherosclerosis. *Circ. Res.* 102 (8), 923–932. doi:10.1161/CIRCRESAHA.107.169573

Ryoo, S., Lemmon, C. A., Soucy, K. G., Gupta, G., White, A. R., Nyhan, D., et al. (2006). Oxidized low-density lipoprotein-dependent endothelial arginase II activation contributes to impaired nitric oxide signaling. *Circ. Res.* 99 (9), 951–960. doi:10.1161/01.RES.0000247034.24662.b4

Sasaki, K., Heeschen, C., Aicher, A., Ziebart, T., Honold, J., Urbich, C., et al. (2006). *Ex vivo* pretreatment of bone marrow mononuclear cells with endothelial NO synthase enhancer AVE9488 enhances their functional activity for cell therapy. *Proc. Natl. Acad. Sci. U. S. A.* 103 (39), 14537–14541. doi:10.1073/pnas.0604144103

Saura, M., Zaragoza, C., Cao, W., Bao, C., Rodriguez-Puyol, M., Rodriguez-Puyol, D., et al. (2002). Smad2 mediates transforming growth factor-beta induction of endothelial nitric oxide synthase expression. *Circ. Res.* 91 (9), 806–813. doi:10.1161/01.res.0000040397.23817.e5

Sawabe, K., Yamamoto, K., Harada, Y., Ohashi, A., Sugawara, Y., Matsuoka, H., et al. (2008). Cellular uptake of sepiapterin and push-pull accumulation of tetrahydrobiopterin. *Mol. Genet. Metab.* 94 (4), 410–416. doi:10.1016/j.ymgme.2008.04.007

Scalera, F., Closs, E. I., Flick, E., Martens-Lobenhoffer, J., Boissel, J. P., Lendeckel, U., et al. (2009). Paradoxical effect of L-arginine: acceleration of endothelial cell senescence. *Biochem. Biophys. Res. Commun.* 386 (4), 650–655. doi:10.1016/j.bbrc.2009.06.091

Schafer, A., Fraccarollo, D., Pfortsch, S., Loch, E., Neuser, J., Vogt, C., et al. (2011). Clopidogrel improves endothelial function and NO bioavailability by sensitizing adenylyl cyclase in rats with congestive heart failure. *Basic Res. Cardiol.* 106 (3), 485–494. doi:10.1007/s00395-011-0153-4

Schilling, K., Opitz, N., Wiesenthal, A., Oess, S., Tikkanen, R., Muller-Esterl, W., et al. (2006). Translocation of endothelial nitric-oxide synthase involves a ternary complex with caveolin-1 and NOSTRIN. *Mol. Biol. Cell* 17 (9), 3870–3880. doi:10.1091/mbc.e05-08-0709

Schulman, S. P., Becker, L. C., Kass, D. A., Champion, H. C., Terrin, M. L., Forman, S., et al. (2006). L-arginine therapy in acute myocardial infarction: the Vascular Interaction with Age in Myocardial Infarction (VINTAGE MI) randomized clinical trial. *JAMA* 295 (1), 58–64. doi:10.1001/jama.295.1.58

Scotland, R. S., Morales-Ruiz, M., Chen, Y., Yu, J., Rudic, R. D., Fulton, D., et al. (2002). Functional reconstitution of endothelial nitric oxide synthase reveals the importance of serine 1179 in endothelium-dependent vasomotion. *Circ. Res.* 90 (8), 904–910. doi:10.1161/01.res.0000016506.04193.96

Searles, C. D. (2006). Transcriptional and posttranscriptional regulation of endothelial nitric oxide synthase expression. *Am. J. Physiol. Cell Physiol.* 291 (5), C803–C816. doi:10.1152/ajpcell.00457.2005

Searles, C. D., Ide, L., Davis, M. E., Cai, H., and Weber, M. (2004). Actin cytoskeleton organization and posttranscriptional regulation of endothelial nitric oxide synthase during cell growth. *Circ. Res.* 95 (5), 488–495. doi:10.1161/01.RES.0000138953.21377.80

Sena, C. M., Nunes, E., Louro, T., Proenca, T., Fernandes, R., Boarder, M. R., et al. (2008). Effects of alpha-lipoic acid on endothelial function in aged diabetic and high-fat fed rats. *Br. J. Pharmacol.* 153 (5), 894–906. doi:10.1038/sj.bjp.0707474

Sessa, W. C., Garcia-Cardena, G., Liu, J., Keh, A., Pollock, J. S., Bradley, J., et al. (1995). The Golgi association of endothelial nitric oxide synthase is necessary for the efficient synthesis of nitric oxide. *J. Biol. Chem.* 270 (30), 17641–17644. doi:10.1074/jbc.270.30.17641

Setoguchi, S., Mohri, M., Shimokawa, H., and Takeshita, A. (2001). Tetrahydrobiopterin improves endothelial dysfunction in coronary microcirculation in patients without epicardial coronary artery disease. *J. Am. Coll. Cardiol.* 38 (2), 493–498. doi:10.1016/s0735-1097(01)01382-1

Shang, Q., Bao, L., Guo, H., Hao, F., Luo, Q., Chen, J., et al. (2017). Contribution of glutaredoxin-1 to S-glutathionylation of endothelial nitric oxide synthase for mesenteric nitric oxide generation in experimental necrotizing enterocolitis. *Transl. Res.* 188, 92–105. doi:10.1016/j.trsl.2016.01.004

Sharifi-Rad, M., Anil Kumar, N. V., Zucca, P., Varoni, E. M., Dini, L., Panzarini, E., et al. (2020). Lifestyle, oxidative stress, and antioxidants: back and forth in the pathophysiology of chronic diseases. *Front. Physiol.* 11, 694. doi:10.3389/fphys.2020.00694

Shatanawi, A., Momani, M. S., Al-Aqtash, R., Hamdan, M. H., and Gharaibeh, M. N. (2020). L-citrulline supplementation increases plasma nitric oxide levels and reduces arginase activity in patients with type 2 diabetes. *Front. Pharmacol.* 11, 584669. doi:10.3389/fphar.2020.584669

Shearer, J. D., Richards, J. R., Mills, C. D., and Caldwell, M. D. (1997). Differential regulation of macrophage arginine metabolism: a proposed role in wound healing. *Am. J. Physiol.* 272 (2 Pt 1), E181–E190. doi:10.1152/ajpendo.1997.272.2.E181

Shemyakin, A., Kovamees, O., Rafnsson, A., Bohm, F., Svenarud, P., Settergren, M., et al. (2012). Arginase inhibition improves endothelial function in patients with coronary artery disease and type 2 diabetes mellitus. *Circulation* 126 (25), 2943–2950. doi:10.1161/CIRCULATIONAHA.112.140335

Shimazu, T., Otani, H., Yoshioka, K., Fujita, M., Okazaki, T., and Iwasaka, T. (2011). Sepiapterin enhances angiogenesis and functional recovery in mice after myocardial infarction. *Am. J. Physiol. Heart Circ. Physiol.* 301 (5), H2061–H2072. doi:10.1152/ajpheart.00525.2011

Singer, H. A., and Peach, M. J. (1982). Calcium- and endothelial-mediated vascular smooth muscle relaxation in rabbit aorta. *Hypertension* 4 (3 Pt 2), 19–25. doi:10.1161/01.hyp.4.3.19

Smith, J. F., Lemmey, H. A. L., Borysova, L., Hiley, C. R., Dora, K. A., and Garland, C. J. (2020). Endothelial nitric oxide suppresses action-potential-like transient spikes and vasospasm in small resistance arteries. *Hypertension* 76 (3), 785–794. doi:10.1161/HYPERTENSIONAHA.120.15491

Soboloff, J., Rothberg, B. S., Madesh, M., and Gill, D. L. (2012). STIM proteins: dynamic calcium signal transducers. *Nat. Rev. Mol. cell Biol.* 13 (9), 549–565. doi:10.1038/nrm3414

Soltis, E. E., and Cassis, L. A. (1991). Influence of perivascular adipose tissue on rat aortic smooth muscle responsiveness. *Clin. Exp. Hypertens. A* 13 (2), 277–296. doi:10.3109/10641969109042063

Steggerda, S. M., Bennett, M. K., Chen, J., Emberley, E., Huang, T., Janes, J. R., et al. (2017). Inhibition of arginase by CB-1158 blocks myeloid cell-mediated immune suppression in the tumor microenvironment. *J. Immunother. Cancer* 5 (1), 101. doi:10.1186/s40425-017-0308-4

Straub, A. C., Butcher, J. T., Billaud, M., Mutchler, S. M., Artamonov, M. V., Nguyen, A. T., et al. (2014a). Hemoglobin α/eNOS coupling at myoendothelial junctions is required for nitric oxide scavenging during vasoconstriction. *Arterioscler. Thromb. Vasc. Biol.* 34 (12), 2594–2600. doi:10.1161/ATVBAHA.114.303974

Straub, A. C., Lohman, A. W., Billaud, M., Johnstone, S. R., Dwyer, S. T., Lee, M. Y., et al. (2012). Endothelial cell expression of haemoglobin α regulates nitric oxide signalling. *Nature* 491 (7424), 473–477. doi:10.1038/nature11626

Straub, A. C., Zeigler, A. C., and Isakson, B. E. (2014b). The myoendothelial junction: connections that deliver the message. *Physiol. (Bethesda)* 29 (4), 242–249. doi:10.1152/physiol.00042.2013

Stroes, E., Kastelein, J., Cosentino, F., Erkelens, W., Wever, R., Koomans, H., et al. (1997). Tetrahydrobiopterin restores endothelial function in hypercholesterolemia. *J. Clin. Invest.* 99 (1), 41–46. doi:10.1172/JCI119131

Stroes, E. S., van Faassen, E. E., Yo, M., Martasek, P., Boer, P., Govers, R., et al. (2000). Folic acid reverts dysfunction of endothelial nitric oxide synthase. *Circ. Res.* 86 (11), 1129–1134. doi:10.1161/01.res.86.11.1129

Stuehr, D. J. (1997). Structure-function aspects in the nitric oxide synthases. *Annu. Rev. Pharmacol. Toxicol.* 37, 339–359. doi:10.1146/annurev.pharmtox.37.1.339

Stuehr, D. J., Wei, C. C., Wang, Z., and Hille, R. (2005). Exploring the redox reactions between heme and tetrahydrobiopterin in the nitric oxide synthases. *Dalton Trans.* (21), 3427–3435. doi:10.1039/b506355h

Su, Y., Edwards-Bennett, S., Bubb, M. R., and Block, E. R. (2003). Regulation of endothelial nitric oxide synthase by the actin cytoskeleton. *Am. J. Physiol. Cell Physiol.* 284 (6), C1542–C1549. doi:10.1152/ajpcell.00248.2002

Suarez, Y., Fernandez-Hernando, C., Pober, J. S., and Sessa, W. C. (2007). Dicer dependent microRNAs regulate gene expression and functions in human endothelial cells. *Circ. Res.* 100 (8), 1164–1173. doi:10.1161/01.RES.0000265065.26744.17

Suvorava, T., Nagy, N., Pick, S., Lieven, O., Ruther, U., Dao, V. T., et al. (2015). Impact of eNOS-dependent oxidative stress on endothelial function and neointima formation. *Antioxid. Redox Signal* 23 (9), 711–723. doi:10.1089/ars.2014.6059

Suvorava, T., Pick, S., and Kojda, G. (2017). Selective impairment of blood pressure reduction by endothelial nitric oxide synthase dimer destabilization in mice. *J. Hypertens.* 35 (1), 76–88. doi:10.1097/HJH.0000000000001127

Takahashi, S., and Mendelsohn, M. E. (2003). Calmodulin-dependent and -independent activation of endothelial nitric-oxide synthase by heat shock protein 90. *J. Biol. Chem.* 278 (11), 9339–9344. doi:10.1074/jbc.M212651200

Tang, J. L., Zembowicz, A., Xu, X. M., and Wu, K. K. (1995). Role of Sp1 in transcriptional activation of human nitric oxide synthase type III gene. *Biochem. Biophys. Res. Commun.* 213 (2), 673–680. doi:10.1006/bbrc.1995.2184

Taubert, D., Berkels, R., Grosser, N., Schroder, H., Grundemann, D., and Schomig, E. (2004). Aspirin induces nitric oxide release from vascular endothelium: a novel mechanism of action. *Br. J. Pharmacol.* 143 (1), 159–165. doi:10.1038/sj.bjp.0705907

Tengbom, J., Kontidou, E., Collado, A., Yang, J., Alvarsson, M., Brinck, J., et al. (2024). Differences in endothelial function between patients with Type 1 and Type 2 diabetes: effects of red blood cells and arginase. *Clin. Sci. (Lond).* 138 (15), 975–985. doi:10.1042/CS20240447

Terry, L. E., VerMeer, M., Giles, J., and Tran, Q. K. (2017). Suppression of store-operated Ca2+ entry by activation of GPER: contribution to a clamping effect on endothelial Ca2+ signaling. *Biochem. J.* 474, 3627–3642. doi:10.1042/BCJ20170630

Thannickal, V. J., and Fanburg, B. L. (2000). Reactive oxygen species in cell signaling. *Am. J. Physiol. Lung Cell Mol. Physiol.* 279 (6), L1005–L1028. doi:10.1152/ajplung.2000.279.6.L1005

Thomson, L., Trujillo, M., Telleri, R., and Radi, R. (1995). Kinetics of cytochrome c2+ oxidation by peroxynitrite: implications for superoxide measurements in nitric oxide-producing biological systems. *Arch. Biochem. Biophys.* 319 (2), 491–497. doi:10.1006/abbi.1995.1321

Tomada, I., Negrao, R., Almeida, H., and Neves, D. (2014). Long-term high-fat consumption leads to downregulation of Akt phosphorylation of eNOS at Ser1177 and upregulation of Sirtuin-1 expression in rat cavernous tissue. *Age (Dordr).* 36 (2), 597–611. doi:10.1007/s11357-013-9591-2

Totzeck, M., Hendgen-Cotta, U. B., Luedike, P., Berenbrink, M., Klare, J. P., Steinhoff, H. J., et al. (2012). Nitrite regulates hypoxic vasodilation via myoglobin-dependent nitric oxide generation. *Circulation* 126 (3), 325–334. doi:10.1161/CIRCULATIONAHA.111.087155

Tran, Q. K. (2020). Reciprocality between estrogen biology and calcium signaling in the cardiovascular system. *Front. Endocrinol. (Lausanne)* 11, 568203. doi:10.3389/fendo.2020.568203

Tran, Q. K., Black, D. J., and Persechini, A. (2003). Intracellular coupling via limiting calmodulin. *J. Biol. Chem.* 278 (27), 24247–24250. doi:10.1074/jbc.C300165200

Tran, Q. K., Black, D. J., and Persechini, A. (2005). Dominant affectors in the calmodulin network shape the time courses of target responses in the cell. *Cell Calcium* 37 (6), 541–553. doi:10.1016/j.ceca.2005.02.001

Tran, Q. K., Firkins, R., Giles, J., Francis, S., Matnishian, V., Tran, P., et al. (2016). Estrogen enhances linkage in the vascular endothelial calmodulin network via a feedforward mechanism at the G protein-coupled estrogen receptor 1. *J. Biol. Chem.* 291 (20), 10805–10823. doi:10.1074/jbc.M115.697334

Tran, Q. K., Leonard, J., Black, D. J., Nadeau, O. W., Boulatnikov, I. G., and Persechini, A. (2009). Effects of combined phosphorylation at Ser-617 and Ser-1179 in endothelial nitric-oxide synthase on EC50(Ca2+) values for calmodulin binding and enzyme activation. *J. Biol. Chem.* 284 (18), 11892–11899. doi:10.1074/jbc.M806205200

Tran, Q. K., Leonard, J., Black, D. J., and Persechini, A. (2008). Phosphorylation within an autoinhibitory domain in endothelial nitric oxide synthase reduces the Ca(2+) concentrations required for calmodulin to bind and activate the enzyme. *Biochemistry* 47 (28), 7557–7566. doi:10.1021/bi8003186

Tran, Q. K., VerMeer, M., Burgard, M. A., Hassan, A. B., and Giles, J. (2015). Hetero-oligomeric complex between the G protein-coupled estrogen receptor 1 and the plasma membrane Ca2+-ATPase 4b. *J. Biol. Chem.* 290 (21), 13293–13307. doi:10.1074/jbc.M114.628743

Tsuboi, T., Maeda, M., and Hayashi, T. (2018). Administration of L-arginine plus L-citrulline or L-citrulline alone successfully retarded endothelial senescence. *PLoS One* 13 (2), e0192252. doi:10.1371/journal.pone.0192252

Tsukahara, H., Gordienko, D. V., Tonshoff, B., Gelato, M. C., and Goligorsky, M. S. (1994). Direct demonstration of insulin-like growth factor-I-induced nitric oxide production by endothelial cells. *Kidney Int.* 45 (2), 598–604. doi:10.1038/ki.1994.78

Uittenbogaard, A., Shaul, P. W., Yuhanna, I. S., Blair, A., and Smart, E. J. (2000). High density lipoprotein prevents oxidized low density lipoprotein-induced inhibition of endothelial nitric-oxide synthase localization and activation in caveolae. *J. Biol. Chem.* 275 (15), 11278–11283. doi:10.1074/jbc.275.15.11278

Umbrello, M., Dyson, A., Feelisch, M., and Singer, M. (2013). The key role of nitric oxide in hypoxia: hypoxic vasodilation and energy supply-demand matching. *Antioxid. Redox Signal* 19 (14), 1690–1710. doi:10.1089/ars.2012.4979

Varadharaj, S., Kelly, O. J., Khayat, R. N., Kumar, P. S., Ahmed, N., and Zweier, J. L. (2017). Role of dietary antioxidants in the preservation of vascular function and the modulation of health and disease. *Front. Cardiovasc Med.* 4, 64. doi:10.3389/fcvm.2017.00064

Vasquez-Vivar, J., Kalyanaraman, B., Martasek, P., Hogg, N., Masters, B. S., Karoui, H., et al. (1998). Superoxide generation by endothelial nitric oxide synthase: the influence of cofactors. *Proc. Natl. Acad. Sci. U. S. A.* 95 (16), 9220–9225. doi:10.1073/pnas.95.16.9220

Venema, R. C., Sayegh, H. S., Kent, J. D., and Harrison, D. G. (1996). Identification, characterization, and comparison of the calmodulin-binding domains of the endothelial and inducible nitric oxide synthases. *J. Biol. Chem.* 271 (11), 6435–6440. doi:10.1074/jbc.271.11.6435

Venema, V. J., Zou, R., Ju, H., Marrero, M. B., and Venema, R. C. (1997). Caveolin-1 detergent solubility and association with endothelial nitric oxide synthase is modulated by tyrosine phosphorylation. *Biochem. Biophys. Res. Commun.* 236 (1), 155–161. doi:10.1006/bbrc.1997.6921

Victor, V. M., Rocha, M., Sola, E., Banuls, C., Garcia-Malpartida, K., and Hernandez-Mijares, A. (2009). Oxidative stress, endothelial dysfunction and atherosclerosis. *Curr. Pharm. Des.* 15 (26), 2988–3002. doi:10.2174/138161209789058093

Wang, J., Sim, A. S., Wang, X. L., and Wilcken, D. E. (2006). L-arginine regulates asymmetric dimethylarginine metabolism by inhibiting dimethylarginine dimethylaminohydrolase activity in hepatic (HepG2) cells. *Cell Mol. Life Sci.* 63 (23), 2838–2846. doi:10.1007/s00018-006-6271-8

Wang, J., Tokoro, T., Matsui, K., Higa, S., and Kitajima, I. (2005). Pitavastatin at low dose activates endothelial nitric oxide synthase through PI3K-AKT pathway in endothelial cells. *Life Sci.* 76 (19), 2257–2268. doi:10.1016/j.lfs.2004.12.003

Wang, S., Chennupati, R., Kaur, H., Iring, A., Wettschureck, N., and Offermanns, S. (2016). Endothelial cation channel PIEZO1 controls blood pressure by mediating flow-induced ATP release. *J. Clin. Invest.* 126 (12), 4527–4536. doi:10.1172/JCI87343

Wang, W., Ha, C. H., Jhun, B. S., Wong, C., Jain, M. K., and Jin, Z. G. (2010). Fluid shear stress stimulates phosphorylation-dependent nuclear export of HDAC5 and mediates expression of KLF2 and eNOS. *Blood* 115 (14), 2971–2979. doi:10.1182/blood-2009-05-224824

Wang, X., Reznick, S., Li, P., Liang, W., and van Breemen, C. (2002). Ca(2+) removal mechanisms in freshly isolated rabbit aortic endothelial cells. *Cell Calcium* 31 (6), 265–277. doi:10.1016/s0143-4160(02)00075-1

Wariishi, S., Miyahara, K., Toda, K., Ogoshi, S., Doi, Y., Ohnishi, S., et al. (1995). A SP1 binding site in the GC-rich region is essential for a core promoter activity of the

human endothelial nitric oxide synthase gene. *Biochem. Biophys. Res. Commun.* 216 (2), 729–735. doi:10.1006/bbrc.1995.2682

Watson, C. P., Pazarentzos, E., Fidanboylu, M., Padilla, B., Brown, R., and Thomas, S. A. (2016). The transporter and permeability interactions of asymmetric dimethylarginine (ADMA) and L-arginine with the human blood-brain barrier *in vitro*. *Brain Res.* 1648 (Pt A)), 232–242. doi:10.1016/j.brainres.2016.07.026

Wever, R. M., van Dam, T., van Rijn, H. J., de Groot, F., and Rabelink, T. J. (1997). Tetrahydrobiopterin regulates superoxide and nitric oxide generation by recombinant endothelial nitric oxide synthase. *Biochem. Biophys. Res. Commun.* 237 (2), 340–344. doi:10.1006/bbrc.1997.7069

Whitsett, J., Picklo, M. J., and Vasquez-Vivar, J. (2007). 4-Hydroxy-2-nonenal increases superoxide anion radical in endothelial cells via stimulated GTP cyclohydrolase proteasomal degradation. *Arterioscler. Thromb. Vasc. Biol.* 27 (11), 2340–2347. doi:10.1161/ATVBAHA.107.153742

Wilson, A. M., Harada, R., Nair, N., Balasubramanian, N., and Cooke, J. P. (2007). L-arginine supplementation in peripheral arterial disease: no benefit and possible harm. *Circulation* 116 (2), 188–195. doi:10.1161/CIRCULATIONAHA.106.683656

Wohlfart, P., Xu, H., Endlich, A., Habermeier, A., Closs, E. I., Hubschle, T., et al. (2008). Antiatherosclerotic effects of small-molecular-weight compounds enhancing endothelial nitric-oxide synthase (eNOS) expression and preventing eNOS uncoupling. *J. Pharmacol. Exp. Ther.* 325 (2), 370–379. doi:10.1124/jpet.107.128009

Worthley, M. I., Kanani, R. S., Sun, Y. H., Sun, Y., Goodhart, D. M., Curtis, M. J., et al. (2007). Effects of tetrahydrobiopterin on coronary vascular reactivity in atherosclerotic human coronary arteries. *Cardiovasc Res.* 76 (3), 539–546. doi:10.1016/j.cardiores.2007.07.009

Wu, G., and Meininger, C. J. (1993). Regulation of L-arginine synthesis from L-citrulline by L-glutamine in endothelial cells. *Am. J. Physiol.* 265 (6 Pt 2), H1965–H1971. doi:10.1152/ajpheart.1993.265.6.H1965

Wu, G., and Morris, S. M., Jr (1998). Arginine metabolism: nitric oxide and beyond. *Biochem. J.* 336 (Pt 1), 1–17. doi:10.1042/bj3360001

Wu, G., Sharina, I., and Martin, E. (2022). Soluble guanylyl cyclase: molecular basis for ligand selectivity and action *in vitro* and *in vivo*. *Front. Mol. Biosci.* 9, 1007768. doi:10.3389/fmolb.2022.1007768

Wu, W., Geng, P., Zhu, J., Li, J., Zhang, L., Chen, W., et al. (2019). KLF2 regulates eNOS uncoupling via Nrf2/HO-1 in endothelial cells under hypoxia and reoxygenation. *Chem. Biol. Interact.* 305, 105–111. doi:10.1016/j.cbi.2019.03.010

Xia, Y., Roman, L. J., Masters, B. S., and Zweier, J. L. (1998b). Inducible nitric-oxide synthase generates superoxide from the reductase domain. *J. Biol. Chem.* 273 (35), 22635–22639. doi:10.1074/jbc.273.35.22635

Xia, Y., Tsai, A. L., Berka, V., and Zweier, J. L. (1998a). Superoxide generation from endothelial nitric-oxide synthase. A Ca2+/calmodulin-dependent and tetrahydrobiopterin regulatory process. *J. Biol. Chem.* 273 (40), 25804–25808. doi:10.1074/jbc.273.40.25804

Xiang, M., Lu, Y., Xin, L., Gao, J., Shang, C., Jiang, Z., et al. (2021). Role of oxidative stress in reperfusion following myocardial ischemia and its treatments. *Oxid. Med. Cell Longev.* 2021, 6614009. doi:10.1155/2021/6614009

Xiong, Y., Fru, M. F., Yu, Y., Montani, J. P., Ming, X. F., and Yang, Z. (2014). Long term exposure to L-arginine accelerates endothelial cell senescence through arginase-II and S6K1 signaling. *Aging (Albany NY)* 6 (5), 369–379. doi:10.18632/aging.100663

Xu, H., Shi, Y., Wang, J., Jones, D., Weilrauch, D., Ying, R., et al. (2007). A heat shock protein 90 binding domain in endothelial nitric-oxide synthase influences enzyme function. *J. Biol. Chem.* 282 (52), 37567–37574. doi:10.1074/jbc.M706464200

Xu, J., Wang, S., Wu, Y., Song, P., and Zou, M. H. (2009). Tyrosine nitration of PA700 activates the 26S proteasome to induce endothelial dysfunction in mice with angiotensin II-induced hypertension. *Hypertension* 54 (3), 625–632. doi:10.1161/HYPERTENSIONAHA.109.133736

Xu, J., Wu, Y., Song, P., Zhang, M., Wang, S., and Zou, M. H. (2007). Proteasome-dependent degradation of guanosine 5'-triphosphate cyclohydrolase I causes tetrahydrobiopterin deficiency in diabetes mellitus. *Circulation* 116 (8), 944–953. doi:10.1161/CIRCULATIONAHA.106.684795

Yang, F., Zhang, L., Huo, X. S., Yuan, J. H., Xu, D., Yuan, S. X., et al. (2011). Long noncoding RNA high expression in hepatocellular carcinoma facilitates tumor growth through enhancer of zeste homolog 2 in humans. *Hepatology* 54 (5), 1679–1689. doi:10.1002/hep.24563

Yang, Z., and Ming, X. F. (2013). Arginase: the emerging therapeutic target for vascular oxidative stress and inflammation. *Front. Immunol.* 4, 149. doi:10.3389/fimmu.2013.00149

Yeh, D. C., Duncan, J. A., Yamashita, S., and Michel, T. (1999). Depalmitoylation of endothelial nitric-oxide synthase by acyl-protein thioesterase 1 is potentiated by Ca(2+)-calmodulin. *J. Biol. Chem.* 274 (46), 33148–33154. doi:10.1074/jbc.274.46.33148

Yoshioka, K., Otani, H., Shimazu, T., Fujita, M., Iwasaka, T., and Shiojima, I. (2015). Sepiapterin prevents left ventricular hypertrophy and dilatory remodeling induced by pressure overload in rats. *Am. J. Physiol. Heart Circ. Physiol.* 309 (10), H1782–H1791. doi:10.1152/ajpheart.00417.2015

Yu, J. G., O'Brien, W. E., and Lee, T. J. (1997). Morphologic evidence for L-citrulline conversion to L-arginine via the argininosuccinate pathway in porcine cerebral perivascular nerves. *J. Cereb. Blood Flow. Metab.* 17 (8), 884–893. doi:10.1097/00004647-199708000-00007

Zamani, M., Rezaiian, F., Saadati, S., Naseri, K., Ashtary-Larky, D., Yousefi, M., et al. (2023). The effects of folic acid supplementation on endothelial function in adults: a systematic review and dose-response meta-analysis of randomized controlled trials. *Nutr. J.* 22 (1), 12. doi:10.1186/s12937-023-00843-y

Zhang, Q., Church, J. E., Jagnandan, D., Catravas, J. D., Sessa, W. C., and Fulton, D. (2006). Functional relevance of Golgi- and plasma membrane-localized endothelial NO synthase in reconstituted endothelial cells. *Arterioscler. Thromb. Vasc. Biol.* 26 (5), 1015–1021. doi:10.1161/01.ATV.0000216044.49494.c4

Zhang, Y., Murugesan, P., Huang, K., and Cai, H. (2020). NADPH oxidases and oxidase crosstalk in cardiovascular diseases: novel therapeutic targets. *Nat. Rev. Cardiol.* 17 (3), 170–194. doi:10.1038/s41569-019-0260-8

Zhao, Y. Y., Liu, Y., Stan, R. V., Fan, L., Gu, Y., Dalton, N., et al. (2002). Defects in caveolin-1 cause dilated cardiomyopathy and pulmonary hypertension in knockout mice. *Proc. Natl. Acad. Sci. U. S. A.* 99 (17), 11375–11380. doi:10.1073/pnas.172360799

Zimmermann, K., Opitz, N., Dedio, J., Renne, C., Muller-Esterl, W., and Oess, S. (2002). NOSTRIN: a protein modulating nitric oxide release and subcellular distribution of endothelial nitric oxide synthase. *Proc. Natl. Acad. Sci. U. S. A.* 99 (26), 17167–17172. doi:10.1073/pnas.252345399

Zweier, J. L., Chen, C. A., and Druhan, L. J. (2011). S-glutathionylation reshapes our understanding of endothelial nitric oxide synthase uncoupling and nitric oxide/reactive oxygen species-mediated signaling. *Antioxid. Redox Signal* 14 (10), 1769–1775. doi:10.1089/ars.2011.3904

Glossary

ABH	2(S)-amino-6-hexanoic acid
ACh	acetylcholine
ADMA	asymmetric dimethylarginine
Akt	protein kinase B
AMPK	AMP-activated protein kinase
ASL	argininosuccinate lyase
ASS	argininosuccinate synthase
BEC	S-(2-boronoethyl)-l-cysteine
BH_2	dihydrobiopterin
BH_4	tetrahydrobiopterin
CAD	Coronary Artery Disease
CaM	calmodulin
CaMKII	calcium/calmodulin-dependent protein kinase II
CAT-1	cationic amino acid transporter-1
Cav-1	caveolin-1
cGMP	cyclic GMP
CSD	caveolin-scaffolding domain
CVD	cardiovascular disease
CytB5R3	cytochrome b5 reductase 3
DHFR	dihydrofolate reductase
Dyn2	dynamin-2
ECs	endothelial cells
EDD	end-diastolic diameter
eNOS	endothelial nitric oxide synthase
FAD	flavin adenine dinucleotide
FMD%	flow-mediated dilation percentage
FMN	flavin mononucleotide
GPCR	G-protein coupled receptor
Grx1	glutaredoxin
GSH	reduced glutathione
GSSG	oxidized glutathione
GTPCH	guanosine triphosphate cyclohydrolase I
Hbα	alpha subunit of hemoglobin
HDL	high-density lipoprotein
HIF-1α	hypoxia-inducible factor-1 alpha
Hsp90	heat shock protein 90
ICAM-1	intracellular adhesion molecule 1
iNOS	inducible NOS
KLF2/KLF4	Krüppel-like factor 2/Krüppel-like factor 4
LAD	left anterior descending coronary artery
lncRNAs	long non-coding RNAs
LPS	lipopolysaccharide
MEJ	myoendothelial junctions
MI	myocardial infarction
METHF	5-methyltetrahydrofolate
NADPH	nicotinamide adenine dinucleotide phosphate
NF-κB	nuclear factor kappa-light-chain-enhancer of activated B cells
nNOS	neuronal NOS
NO	nitric oxide
NOHA	N-hydroxy-L-arginine
nor-NOHA	N-hydroxy-nor-L-arginine
NOS	NO synthases
NOSIP	eNOS interacting protein
NOSTRIN	eNOS trafficking inducer
NOX_2	NADPH oxidase 2
Nrf2	nuclear factor erythroid 2-related factor
ox-LDL	oxidized low-density lipoprotein
PAH	pulmonary arterial hypertension
PDE	phosphodiesterase
PKA	protein kinase A
PKG	protein kinase G
PMCA	plasma membrane Ca^{2+}-ATPase
PPIs	protein-protein interactions
PTMs	post-translational modifications
ROS	reactive oxygen species
sGC	soluble guanylate cyclase
SIRT1	sirtuin 1
SMAD2	mothers against decapentaplegic homolog-2
SNOs	s-nitrosothiols
SOCE	store-operated Ca^{2+} entry
Sp1	specificity protein 1
Sp3	specificity protein 3
STIM1	stromal interaction molecule 1
T1D	type 1 diabetes
T2D	type 2 diabetes
TAC	transverse aortic constriction
TGF-β	tumor growth factor-beta
TNF-α	tumor necrosis factor-alpha
VEGF	vascular endothelial growth factor
VSMCs	vascular smooth muscle cells

frontiers | Frontiers in Physiology

TYPE Perspective
PUBLISHED 10 February 2025
DOI 10.3389/fphys.2025.1548242

OPEN ACCESS

EDITED BY
Luis A. Martinez-Lemus,
University of Missouri, United States

REVIEWED BY
Yongsoo Kim,
Penn State Milton S. Hershey Medical Center, United States

*CORRESPONDENCE
Guy Malkinson,
guy.malkinson@inserm.fr
Catarina M. Henriques,
c.m.henriques@sheffield.ac.uk

†PRESENT ADDRESS
Guy Malkinson,
Université de Lorraine, Inserm, DCAC, Nancy, France

RECEIVED 19 December 2024
ACCEPTED 21 January 2025
PUBLISHED 10 February 2025

CITATION
Malkinson G and Henriques CM (2025) Cerebrovascular ageing: how zebrafish can contribute to solving the puzzle.
Front. Physiol. 16:1548242.
doi: 10.3389/fphys.2025.1548242

Cerebrovascular ageing: how zebrafish can contribute to solving the puzzle

Guy Malkinson[1,2*†] and Catarina M. Henriques[3,4*]

[1]Université de Lorraine, Inserm, DCAC, Nancy, France, [2]Center for Interdisciplinary Research in Biology (CIRB), College de France, CNRS, INSERM, Université PSL, Paris, France, [3]Department of Oncology and Metabolism, Healthy Lifespan Institute and MRC-Arthritis Research UK Centre for Integrated Research into Musculoskeletal Ageing, University of Sheffield, Sheffield, United Kingdom, [4]Bateson Centre, University of Sheffield, Sheffield, United Kingdom

The mean life expectancy continues to increase world-wide. However, this extended lifespan trend is not accompanied by health span, or years of healthy life. Understanding the fundamental mechanisms responsible for the switch from health to morbidity with ageing are key to identifying potential therapeutic targets to decrease age-associated morbidity and increase years spent in good health. The leading cause of morbidity in Europe are diseases of the circulatory system and diseases of the nervous system and cognitive disorders are among the top-ten. Cerebrovascular ageing is therefore of particular importance as it links circulatory disease to brain functions, cognition, and behavior. Despite major progress in brain research and related technologies, little is known on how the cerebrovascular network changes its properties as ageing proceeds. Importantly, we do not understand why this is different in different individuals in what concerns rate of dysfunction and its downstream impact on brain function. Here we explore how the zebrafish has evolved as an attractive complementary ageing model and how it could provide key insights to understanding the mechanisms underlying cerebrovascular ageing and downstream consequences.

KEYWORDS

zebrafish, brain, telomere, telomerase, cerebrovascular, ageing

1 Introduction

The mean life expectancy has and continues to increase world-wide. However, this extended lifespan trend is not accompanied by health span or years of healthy life. Data from Eurostat reveals that whereas the average life-expectancy at birth was 83.3 and 77.9 years for women and men, respectively, only an average of ~63 of those years is spent in health. This means that, with increased numbers of elderly and decreased birth rates, there is an increasing burden of morbidity and healthcare costs in society which are predicted to become unsustainable within the next 50 years, according to the European Commission's Ageing Reports (Commission, 2015; Commission, 2018). Understanding the fundamental mechanisms behind the switch from health to morbidity with ageing are key to identifying potential therapeutic targets to decrease age-associated morbidity and increase years spent in good health.

A fundamental feature of ageing is its temporal dimension, as it is a process that unfolds over time. Depending on the lifespan of the organism, this process can take weeks, months or years, and current ageing models depict it as a series of gradual changes, rather than rapid

abrupt variations, whereby ageing reflects the number of changes that accumulate up to a given time point (Meyer and Schumacher, 2024). While there is an on-going debate on how to describe biological ageing with respect to either calendar or chronological ageing (Ikram, 2024), it is accepted that ageing *per se* entails functional and structural changes that affect the physiology of our tissues, organs and body, and much attention is devoted, in fundamental research and medicine, to understanding these changes with the aim of promoting healthy ageing and treating ageing-related pathologies. Different people age differently, at different rates, and are impacted differently by the process. Moreover, evidence suggests a more heterogenous nature of ageing than previously thought, where different organs in the same individual may exhibit different ageing rates (Oh et al., 2023). Our ability to describe the ageing process by observing any changes in the molecular, structural and functional properties, as they occur, would contribute greatly to our understanding of this process.

The leading cause of morbidity in Europe are diseases of the circulatory system and diseases of the nervous system and cognitive disorders are among the top ten. Cerebrovascular ageing is therefore of particular importance as it links circulatory disease to brain functions, cognition, and behavior. The anatomical and physiological changes that are hallmarks of ageing of the cardiovascular network are a risk factor for cardiovascular (CV) diseases (CVD), with a huge impact on health (Laina et al., 2018). Much of what we know about CV ageing comes from epidemiological studies, showing that ageing is a major non-reversible risk factor for CVD. A major hallmark of vascular ageing is the gradual change of vascular structure and function, resulting in increased arterial stiffening, affecting arterial hemodynamics. Molecular mechanisms that may serve as potential targets to delay this phenomenon include telomere shortening and endothelial ubiquitin proteasome system (Laina et al., 2018). CVD is the leading cause of mortality and morbidity in western societies (Townsend et al., 2015), thus the question of how the cardiovascular network ages is of high relevance for aged people. Of particular concern to CV ageing is understanding the changes that happen in the cerebrovascular network, since alterations in this network may result in substantial impact on neural functions and behavior (Zimmerman et al., 2021). Any reduction in the efficacy of the cerebrovascular system will influence hemodynamics and tissue irrigation, with a significant consequent impact on neural functions, cognitive functions and behavior. Vascular calcification, extracellular matrix alterations and synaptic protein shedding were found to be linked to early cognitive decline (Oh et al., 2023). At the morphological level, ageing of the brain itself is associated with loss of brain volume, thinning of the cortex, degradation of white matter, loss of gyrification and enlarged ventricles. At the histological level, this may be accompanied by shrinking and degeneration of neurons, dendrites and synapses, demyelination, white matter lesions, glial cell activation and small vessel disease (Blinkouskaya et al., 2021). Cerebrovascular ageing may also entail loss of arterial elasticity (arteriosclerosis) and plaque buildup (atherosclerosis), impacting tissue perfusion and hemodynamics and leading to inflammation and consequent ischemia. Some vessels increase their tortuosity, resulting in perturbed hemodynamics, and weakening of the endothelial wall of small vessels can in turn lead to aneurysms and hemorrhages, while capillary density itself may decrease. Importantly, the properties of the brain-unique barrier, the blood-brain-barrier (BBB), may be impacted during ageing. The BBB can become leakier, leading to impaired delivery of nutrients and energy to brain tissue, or impaired clearance of cellular waste, and also via altered and dysfunctional neural-vascular-glial signaling, leading to perturbed cerebrovascular reactivity (Zimmerman et al., 2021).

While ageing has vascular correlates that are apparent at the anatomical and mechanical levels, how exactly these different manifestations appear over time is mostly unknown. Some of the open fundamental questions that need to be addressed are whether there is a typical temporal order to the observed changes, if the time of the onset of ageing is similar across different tissues and organs, what are the molecular and cellular signals that underlie ageing, what are their sources and what triggers their release, (activation or deactivation?) Also, how are neural degradation and vascular stiffening linked in time and space, and whether there are reciprocal signals that serve as feedback in the degradation of these systems? Contemporary research into ageing is hampered to a large extent by the difficulty to study this long process at different biological levels, from the molecular level all the way up to physiology and behaviour. This is furthermore complicated in the case of the brain, which is a complex organ that is difficult to access and to repeatedly measure. The field would benefit from a model that enables the observation of the gradual molecular, structural and physiological changes over- time to help build a more holistic picture of ageing in the brain.

2 Zebrafish: from a developmental to adult and disease model

Due to the optical transparency of the zebrafish embryo, and the relatively quick and robust development in its first days of life, zebrafish is mostly used as a model for embryonic development. Seventy percent of human genes have at least one zebrafish orthologue, and vice versa (Howe et al., 2013), highlighting the genetic pertinence of this model. Over the years, zebrafish mutant lines and genetically-stable fluorescent reporter lines have contributed greatly to the understanding of early embryonic development of vertebrates, and specifically of various tissues and organs, including the cardiovascular, nervous and immune systems (Martins et al., 2019), to name a few. Zebrafish is a relevant and useful model for studying human diseases, including osteoporosis, atrial fibrillation, leukemia and autism spectrum disorders (Adhish and Manjubala, 2023). Over the last few years, efforts are devoted to using more advanced developmental stages, namely, juvenile and adult fish. While these efforts are confronted with technical challenges, they are also fruitful, and zebrafish adult fish are successfully being used as disease models in several cases. The ability to induce cell or tissue specific genetic modifications in adult-stage fish, for example with recently developed state-of-the-art UFLIP technologies (Liu et al., 2022), enables to model gene-environment interactions, and to study with greater precision pathologies such as cancer, cardiovascular diseases, infectious conditions, toxicology and social behaviors (White and Patton, 2023).

2.1 The zebrafish brain and cerebrovascular network as models

The zebrafish brain possesses different vascular features that confer to it a high degree of similarity to the mammalian brain. It is covered and protected by the cranial bones of the skull, and a recent study demonstrates the existence of a functional lymphatic system that runs in the ventral aspect of the skull, above the brain, similar to mammals (Castranova et al., 2020). Anatomically, the zebrafish brain is composed of the forebrain, midbrain and hindbrain regions. It contains conserved specialized regions such as the olfactory bulb, hypothalamus and cerebellum (Jurisch-Yaksi et al., 2020) as well as ventricles, choroid-plexus and cerebrospinal-fluid (CSF) (Korzh, 2023; Jeong et al., 2024). Its significantly smaller size compared to brains of other models, such as rodents, is an important advantage that facilitates high-resolution anatomical studies of entire intact brains (Kirst et al., 2020a; Ji et al., 2021a; Wu et al., 2022) and high-throughput molecular studies such as spatial transcriptomics. While the anatomy of the arterial anastomotic system that supplies blood to the zebrafish brain, namely, the Circle of Willis, seems to resemble that of mammals (Cheng et al., 2024), it is still not clear how the mature vascular network is organized inside the adult fish brain, and a detailed description of the vascular system of the zebrafish adult brain is still not available. For example, how superficial and penetrating arteries and veins are spatially organized, and whether the branching patterns that are hallmark of the mammalian cerebrovascular network are paralleled in zebrafish. Nevertheless, data from several studies suggest that this cerebrovascular system is still developing in juvenile stages and forms an elaborate network of blood vessels (BV) in the adult fish (Bower et al., 2017; Venero Galanternik et al., 2017; Chen et al., 2024a; van Lessen et al., 2017). At the vascular level, BV of the zebrafish brain display a striking similarity to mammalian ones. Genetically stable transgenic fish lines that express fluorescent tissue-specific reporters have confirmed the presence of various populations of perivascular cells, i.e., those that are found around the endothelium. Perivascular macrophages and mural cells, comprising Vascular Smooth Muscle Cells (VSMC) and pericytes, all have been visualized around BV in zebrafish brains (Cheng et al., 2024; Bower et al., 2017; Venero Galanternik et al., 2017; van Lessen et al., 2017; Ando et al., 2021). One of the most striking features of the mammalian brain is the presence of the BBB, that provides an isolated environment for parenchymal neural tissue. In this respect, zebrafish brains display barrier properties from three days-post-fertilization (dpf) onwards (Xie et al., 2010; Quiñonez-Silvero et al., 2020), further supported by the presence of hallmark cellular and molecular elements that comprise the BBB (O'Brown et al., 2018).

3 Zebrafish as an ageing model

Zebrafish have emerged in the past c.10 years as a valuable complementary model to study human-relevant ageing mechanisms, such as telomerase-dependencies (Henriques et al., 2013; Carneiro et al., 2016a). The zebrafish value as an ageing model and fundamental guidelines on how to use both wild type and premature ageing models such as the telomerase (*tert*$^{-/-}$) mutant have been extensively reviewed elsewhere (Henriques and Ferreira, 2024; Carneiro et al., 2016b; Pam et al., 2024; Kishi et al., 2003). Briefly, zebrafish display a time-dependent accumulation of age-associated phenotypes reminiscent of human ageing (Carneiro et al., 2016b; Pam et al., 2024; Kishi et al., 2003; Kishi et al., 2009). Zebrafish lifespan is 3 years on average and over 5 years in laboratory conditions (Kishi et al., 2009). Different tissues were shown to age at different rates, with highly proliferative tissues such as the testis and gut displaying age-associated dysfunction in WT fish from as early as 18 and 24 months, respectively. Specifically, zebrafish male fertility declines from 18 months onwards and the gut displays significantly increased DNA damage, senescence and inflammation by 24 months of age, which precedes increased gut leakiness in older ages (>30 months) (Ellis et al., 2022). Importantly, telomere shortening was shown to precede increased DNA damage response activation and a variety of phenotypes of old age (Carneiro et al., 2016a). Examples of these are: retina degeneration (Carneiro et al., 2016a), spine curvature, infections, loss of body mass and cancer (Carneiro et al., 2016a; Gerhard et al., 2002; Anchelin et al., 2013). Importantly, the cachectic/frail phenotype is underpinned by a significant decrease in subcutaneous adipose tissue and muscle fiber thickness (Carneiro et al., 2016a), as has been described in human frailty (Trueland, 2013; Takahashi et al., 2017). For simplicity, and to align with human phenotypes, we would normally consider zebrafish "old" at the age at which most of the fish present age-associated phenotypes, such as cachexia, loss of body mass and curvature of the spine. These phenotypes develop close to the time of death and are observed at >30 months of age in WT, which can be considered late stages of ageing (Figure 1), and at >12 months in *tert*$^{-/-}$[31, 41]. Telomerase deficiency in zebrafish is therefore reminiscent of the human scenario, where telomerase loss-of-function mutations or mutations affecting telomere stability lead to premature ageing syndromes (Alter et al., 2012; Hofer et al., 2005). Zebrafish also display altered behavior with ageing and show signs of neurodegeneration (Espigares et al., 2021; Van Houcke et al., 2015; Kishi et al., 2008; Hudock and Kenney, 2024; Kacprzak et al., 2017; Zambusi et al., 2020; Yu et al., 2006) (Figure 1), including telomerase-dependent neuroinflammation, senescence markers and increased blood brain barrier permeability with ageing (Raquel et al., 2024). How cerebrovasculature may change with ageing and the mechanisms involved remain, however, largely unexplored in zebrafish. Below we highlight some properties that we believe make zebrafish a valuable and exciting to study cerebrovascular ageing.

3.1 Using zebrafish in cerebrovascular ageing research

The zebrafish brain could be a valuable and useful model for studying cerebrovascular ageing for at least two main reasons. The first is that, as mentioned above, its cerebrovascular network displays important elementary similarities to the mammalian brain, at multiple levels. The second is related to the practical advantages that this model offers. Zebrafish start displaying age-associated phenotypes from c.18 months onwards, depending on the tissue, which can be considered an early stage of ageing (Figure 1). Recent advances in *in-vivo* optical microscopy of live adult fish (Castranova et al., 2022), including non-invasive imaging of the

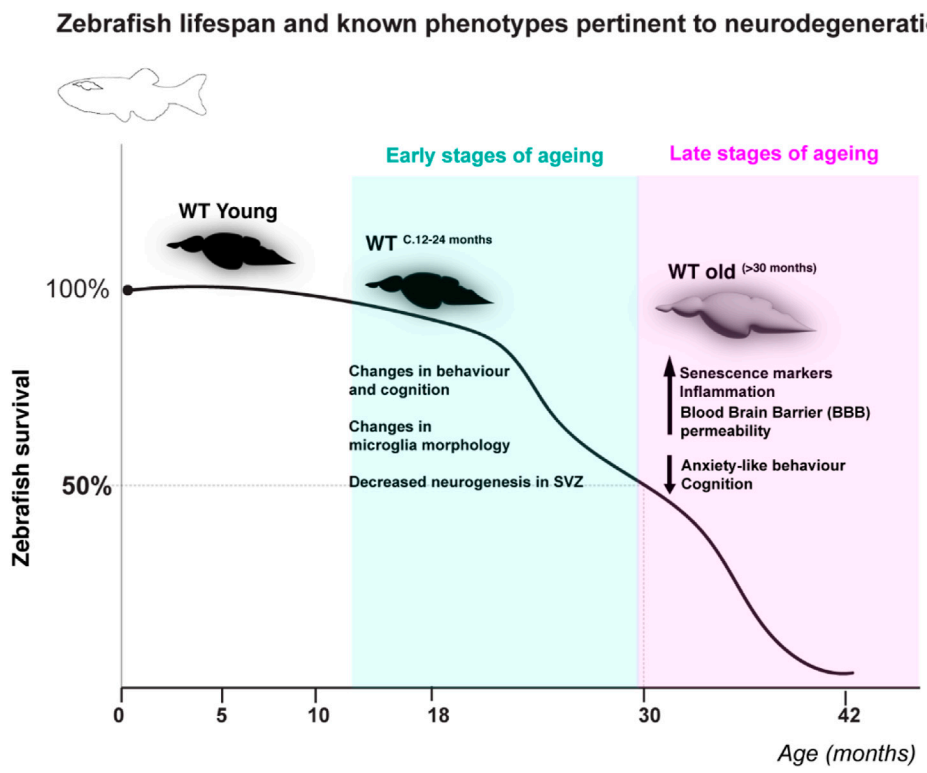

FIGURE 1
Zebrafish lifespan and known phenotypes pertinent to neurodegeneration. WT zebrafish have been shown to live up to at c.42 months in the lab and have a half-life of c. 30–31 months (cartoon depiction of lifespan based on (Carneiro et al., 2016a; Carneiro et al., 2016b). Despite many mechanisms and phenotypes pertinent to neurodegeneration remaining unknown, changes in behaviour, microglia morphology and neurogenesis have been described at early stages of zebrafish ageing (c.12–24 months), and ageing hallmarks such as senescence and inflammation, as well as increased blood brain barrier permeability have been suggested to occur at later stages of ageing (Espigares et al., 2021; Van Houcke et al., 2015; Raquel et al., 2024; Kishi et al., 2008; Hudock and Kenney, 2024; Kacprzak et al., 2017; Zambusi et al., 2020; Yu et al., 2006).

brain (Mizoguchi et al., 2023; Hamilton et al., 2022), now make it feasible to sample, at regular intervals, cerebral vessels of single fish as they age. This would enable to compare the structure of the vascular network over time, and to understand when and how it changes, for example, to detect changes in vascular density or vessel calibers throughout the lifecourse, all the way until old age. This can be further complemented by imaging of the blood flow in real time, adding a crucial functional aspect, thus linking structural and hemodynamic changes. Indeed, such a study recently reported on structural and functional changes in the ageing zebrafish telencephalon (Mizoguchi et al., 2023), in-line with results obtained in mice (Bennett et al., 2024). It will be interesting to examine whether reconstructing the zebrafish cerebrovasculature, using high-resolution three-dimensional imaging methods, will reveal heterogeneities in vascular densities across different brain regions as were found in the mouse brain (Kirst et al., 2020b; Ji et al., 2021b; Wu et al., 2022). This is likely to be easier to achieve in zebrafish due to their small size. Moreover, the wealth of available vascular-specific fluorescent transgenic lines and mutants (Ando et al., 2021; Choe et al., 2021) offers the possibility to examine what happens also to the different vascular components, and especially the BBB, throughout life and into ageing. Other advantages of zebrafish that could be used in the context of ageing are generation of novel transgenic reporter or mutant lines that target specific age-related genes. In zebrafish this is now performed more efficiently with Crispr/Cas9, and can be corroborated with high-throughput screens for potential drugs or molecules. Finally, a unique property of zebrafish is that even at adult stages, damaged tissue or organs can regenerate following injury (Marques et al., 2019). This is also the case for the zebrafish brain, where damaged tissue regenerates with minimal or absent scarring (Chen et al., 2024b). Little is currently known on how the vascular system regenerates in the brain, and this property of zebrafish can be used to examine if and how the regenerative efficacy is affected by age. Importantly, regeneration studies so far have relied on several damage paradigms, including phototoxic (Ranski et al., 2018) and ouabain-induced lesions (Mitchell et al., 2019), which induce rapid cell death post-insult. While high-intensity acute damage models are suitable for exploring the cellular and molecular mechanisms underpinning tissue regenerative potential, they do not test whether this regenerative response is also occurring with natural ageing, and so the use of a suitable ageing model is essential. In fact, previous work highlights how natural ageing does not elicit the same regenerative response as high-intensity acute damage in the zebrafish retina (Martins et al., 2022).

Zebrafish is therefore a unique model in that it allows the identification of age-associated mechanisms underpinning degeneration and regeneration in the same tissue, using different techniques (Figure 2).

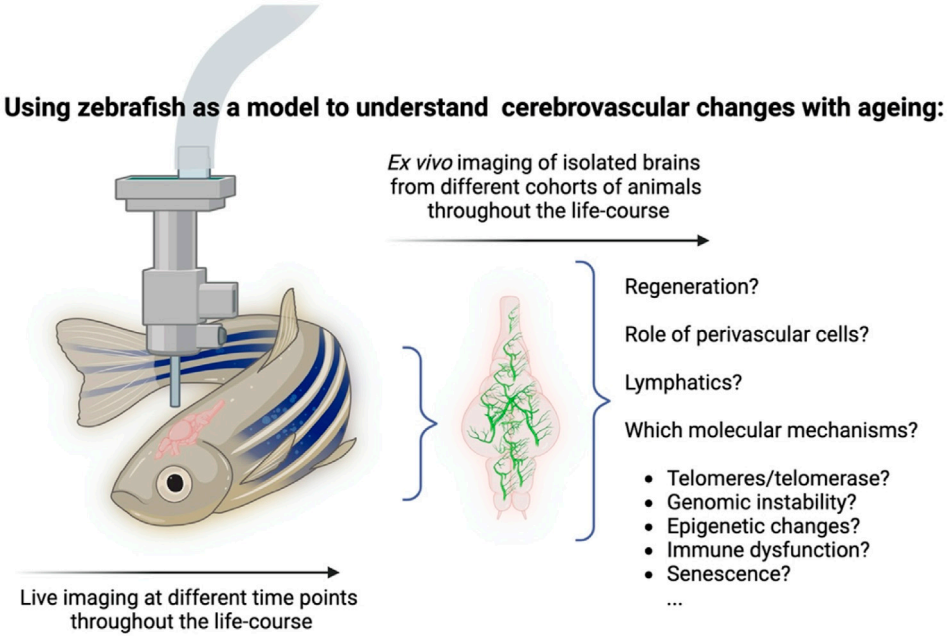

FIGURE 2
Using zebrafish as a model to understand cerebrovascular changes with ageing. The zebrafish offers unique characteristics that make it amenable to study cerebrovascular ageing throughout life. Either using live imaging techniques or via *ex-vivo* imaging of isolated brains from cohorts of animals throughout the life-course. Combinations of cell-specific fluorescent reporter lines combined with premature models of ageing should allow the identification of key mechanisms underpinning degeneration. Created in BioRender. Henriques, C. (2025) https://BioRender.com/w52z573. Image not to scale and cerebrovascular network depiction is not anatomically representative- for illustration purposes only.

4 Conclusion

A number of studies in recent years highlight the inter- and intra-heterogenic nature of ageing, i.e., the differences between individuals and within the same individual. This would suggest that there are elements such as genetic variations, environmental factors and inherent physiological determinants that come into play in this lengthy process, and that a variety of interactions must be considered in order to describe ageing and its underlying mechanisms. This may seem surprising given that hallmark molecular and cellular signatures to ageing have been identified, which were suggested to underpin age-associated degeneration and disease (López-Otín et al., 2023). Nevertheless, it is recognised that an important hurdle in ageing research is the ability to link what is known to occur at molecular and cellular levels to the tissue, organ and entire organism levels. In the specific context of vascular ageing, it will be important to understand some of the following questions, such as if and how molecular and genomic-level events (instabilities, epigenetic and telomeric changes) and cellular-level events (mitochondrial dysfunction, senescence, exhaustion of stem cells) lead over time to changes in the structure and function of the vascular system; what are the pathways that are involved; and do all vascular beds and tissues age in the same manner, across different organs. In order to tackle such questions, it is necessary to use an appropriate model. What makes any model a suitable one for studying ageing in general, and cerebrovascular ageing in particular? The most basic requisite is that it has to display signatures of ageing, where a gradual deterioration in the function and structure of tissues and organs is the most obvious phenotypical change. Ideally, it should also display a large set of common features with other models, which would enable to draw conclusions across species. Finally, pertaining to inherent features of the model itself, it should enable to study ageing over time, at a relevant and meaningful temporal resolution, which would enable to construct a chronological "atlas" of the process, in the same animal. In this respect, the zebrafish cerebrovascular network may be well suited to examine the changes that are associated with ageing throughout the lifecourse, over time, and to link molecular and cellular changes to an overall structural and functional vascular decline (Figure 2). Using the advantages of this model to complement existing models could open new research paths and greatly enhance our understanding, at a higher temporal resolution, of how the vascular network evolves over time, what are the molecular and cellular that underlie these events, and if and how these series of events can be modified or manipulated to induce a beneficial outcome.

Data availability statement

The original contributions presented in the study are included in the article/supplementary material, further inquiries can be directed to the corresponding authors.

Author contributions

GM: Writing–original draft, Writing–review and editing. CH: Writing–original draft, Writing–review and editing.

Funding

The author(s) declare that financial support was received for the research, authorship, and/or publication of this article. GM and CH received funding from Inserm FirstStep Tremplin International. CH is funded by a Sir Henry Dale Fellowship by the Wellcome Trust and The Royal Society (grant no: 206224/Z/17/Z/WT_/Welcome Trust/United Kingdom) and the Dunhill Medical Trust grant AISRPG2305\32.

Conflict of interest

The authors declare that the research was conducted in the absence of any commercial or financial relationships that could be construed as a potential conflict of interest.

Generative AI statement

The author(s) declare that no Generative AI was used in the creation of this manuscript.

Publisher's note

All claims expressed in this article are solely those of the authors and do not necessarily represent those of their affiliated organizations, or those of the publisher, the editors and the reviewers. Any product that may be evaluated in this article, or claim that may be made by its manufacturer, is not guaranteed or endorsed by the publisher.

References

Adhish, M., and Manjubala, I. (2023). Effectiveness of zebrafish models in understanding human diseases-A review of models. *Heliyon* 9 (3), e14557. doi:10.1016/j.heliyon.2023.e14557

Alter, B. P., Rosenberg, P. S., Giri, N., Baerlocher, G. M., Lansdorp, P. M., and Savage, S. A. (2012). Telomere length is associated with disease severity and declines with age in dyskeratosis congenita. *Haematologica* 97 (3), 353–359. doi:10.3324/haematol.2011.055269

Anchelin, M., Alcaraz-Perez, F., Martinez, C. M., Bernabe-Garcia, M., Mulero, V., and Cayuela, M. L. (2013). Premature aging in telomerase-deficient zebrafish. *Dis. Model Mech.* 6 (5), 1101–1112. doi:10.1242/dmm.011635

Ando, K., Ishii, T., and Fukuhara, S. (2021). Zebrafish vascular mural cell biology: recent advances, development, and functions. *Life (Basel)* 11 (10), 1041. doi:10.3390/life11101041

Bennett, H. C., Zhang, Q., Wu, Y. T., Manjila, S. B., Chon, U., Shin, D., et al. (2024). Aging drives cerebrovascular network remodeling and functional changes in the mouse brain. *Nat. Commun.* 15 (1), 6398. doi:10.1038/s41467-024-50559-8

Blinkouskaya, Y., Caçoilo, A., Gollamudi, T., Jalalian, S., and Weickenmeier, J. (2021). Brain aging mechanisms with mechanical manifestations. *Mech. Ageing Dev.* 200, 111575. doi:10.1016/j.mad.2021.111575

Bower, N. I., Koltowska, K., Pichol-Thievend, C., Virshup, I., Paterson, S., Lagendijk, A. K., et al. (2017). Mural lymphatic endothelial cells regulate meningeal angiogenesis in the zebrafish. *Nat. Neurosci.* 20 (6), 774–783. doi:10.1038/nn.4558

Carneiro, M. C., de Castro, I. P., and Ferreira, M. G. (2016b). Telomeres in aging and disease: lessons from zebrafish. *Dis. Model Mech.* 9 (7), 737–748. doi:10.1242/dmm.025130

Carneiro, M. C., Henriques, C. M., Nabais, J., Ferreira, T., Carvalho, T., and Ferreira, M. G. (2016a). Short telomeres in key tissues initiate local and systemic aging in zebrafish. *PLoS Genet.* 12, e1005798. doi:10.1371/journal.pgen.1005798

Castranova, D., Samasa, B., Venero Galanternik, M., Gore, A. V., Goldstein, A. E., Park, J. S., et al. (2022). Long-term imaging of living adult zebrafish. *Development* 149 (4), dev199667. doi:10.1242/dev.199667

Castranova, D., Samasa, B., Venero Galanternik, M., Jung, H. M., Pham, V. N., and Weinstein, B. M. (2020). Live imaging of intracranial lymphatics in the zebrafish. *Circ. Res.* 128, 42–58. doi:10.1161/CIRCRESAHA.120.317372

Chen, J., Ding, J., Li, Y., Feng, F., Xu, Y., Wang, T., et al. (2024a). Epidermal growth factor-like domain 7 drives brain lymphatic endothelial cell development through integrin αvβ3. *Nat. Commun.* 15 (1), 5986. doi:10.1038/s41467-024-50389-8

Chen, J., Sanchez-Iranzo, H., Diotel, N., and Rastegar, S. (2024b). Comparative insight into the regenerative mechanisms of the adult brain in zebrafish and mouse: highlighting the importance of the immune system and inflammation in successful regeneration. *FEBS J.* 291 (19), 4193–4205. doi:10.1111/febs.17231

Cheng, S., Xia, I. F., Wanner, R., Abello, J., Stratman, A. N., and Nicoli, S. (2024). Hemodynamics regulate spatiotemporal artery muscularization in the developing circle of Willis. *Elife* 13. doi:10.7554/eLife.94094

Choe, C. P., Choi, S. Y., Kee, Y., Kim, M. J., Kim, S. H., Lee, Y., et al. (2021). Transgenic fluorescent zebrafish lines that have revolutionized biomedical research. *Lab. Anim. Res.* 37 (1), 26. doi:10.1186/s42826-021-00103-2

Commission, D. (2018). *Ageing report: underlying assumptions and projection methodologies*. EU publications. doi:10.2765/286359 https://economy-finance.ec.europa.eu/publications/2018-ageing-report-underlying-assumptions-and-projection-methodologies_en

Commission, E. (2015). *The 2015 ageing report: economic and budgetary projections for the 28 EU member states (2013-2060)*, 3. European Commission Report: EUROPEAN ECONOMY.

Ellis, P. S., Martins, R. R., Thompson, E. J., Farhat, A., Renshaw, S. A., and Henriques, C. M. (2022). A subset of gut leukocytes has telomerase-dependent "hyper-long" telomeres and require telomerase for function in zebrafish. *Immun. Ageing* 19 (1), 31. doi:10.1186/s12979-022-00287-8

Espigares, F., Abad-Tortosa, D., Varela, S. A. M., Ferreira, M. G., and Oliveira, R. F. (2021). Short telomeres drive pessimistic judgement bias in zebrafish. *Biol. Lett.* 17 (3), 20200745. doi:10.1098/rsbl.2020.0745

Gerhard, G. S., Kauffman, E. J., Wang, X., Stewart, R., Moore, J. L., Kasales, C. J., et al. (2002). Life spans and senescent phenotypes in two strains of Zebrafish (*Danio rerio*). *Exp. Gerontol.* 37 (8-9), 1055–1068. doi:10.1016/s0531-5565(02)00088-8

Hamilton, N., Allen, C., and Reynolds, S. (2022). Longitudinal MRI brain studies in live adult zebrafish. *NMR in Biomed.* 36 (7), e4891. doi:10.1002/nbm.4891

Henriques, C. M., and Ferreira, M. G. (2024). Telomere length is an epigenetic trait - implications for the use of telomerase-deficient organisms to model human disease. *Dis. Model Mech.* 17 (3), dmm050581. doi:10.1242/dmm.050581

Henriques, C. M., Carneiro, M. C., Tenente, I. M., Jacinto, A., and Ferreira, M. G. (2013). Telomerase is required for zebrafish lifespan. *PLoS Genet.* 9 (1), e1003214. doi:10.1371/journal.pgen.1003214

Hofer, A. C., Tran, R. T., Aziz, O. Z., Wright, W., Novelli, G., Shay, J., et al. (2005). Shared phenotypes among segmental progeroid syndromes suggest underlying pathways of aging. *J. Gerontol. A Biol. Sci. Med. Sci.* 60 (1), 10–20. doi:10.1093/gerona/60.1.10

Howe, K., Clark, M. D., Torroja, C. F., Torrance, J., Berthelot, C., Muffato, M., et al. (2013). The zebrafish reference genome sequence and its relationship to the human genome. *Nature* 496 (7446), 498–503. doi:10.1038/nature12111

Hudock, J., and Kenney, J. W. (2024). Aging in zebrafish is associated with reduced locomotor activity and strain dependent changes in bottom dwelling and thigmotaxis. *PLoS One* 19 (5), e0300227. doi:10.1371/journal.pone.0300227

Ikram, M. A. (2024). The use and misuse of 'biological aging' in health research. *Nat. Med.* 30 (11), 3045. doi:10.1038/s41591-024-03297-9

Jeong, I., Andreassen, S. N., Hoang, L., Poulain, M., Seo, Y., Park, H. C., et al. (2024). The evolutionarily conserved choroid plexus contributes to the homeostasis of brain ventricles in zebrafish. *Cell Rep.* 43 (6), 114331. doi:10.1016/j.celrep.2024.114331

Ji, X., Ferreira, T., Friedman, B., Liu, R., Liechty, H., Bas, E., et al. (2021a). Brain microvasculature has a common topology with local differences in geometry that match metabolic load. *Neuron* 109 (7), 1168–1187.e13. doi:10.1016/j.neuron.2021.02.006

Ji, X., Ferreira, T., Friedman, B., Liu, R., Liechty, H., Bas, E., et al. (2021b). Brain microvasculature has a common topology with local differences in geometry that match metabolic load. *Neuron* 109 (7), 1168–1187.e13. doi:10.1016/j.neuron.2021.02.006

Jurisch-Yaksi, N., Yaksi, E., and Kizil, C. (2020). Radial glia in the zebrafish brain: functional, structural, and physiological comparison with the mammalian glia. *Glia* 68 (12), 2451–2470. doi:10.1002/glia.23849

Kacprzak, V., Patel, N. A., Riley, E., Yu, L., Yeh, J. J., and Zhdanova, I. V. (2017). Dopaminergic control of anxiety in young and aged zebrafish. *Pharmacol. Biochem. Behav.* 157, 1–8. doi:10.1016/j.pbb.2017.01.005

Kirst, C., Skriabine, S., Vieites-Prado, A., Topilko, T., Bertin, P., Gerschenfeld, G., et al. (2020a). Mapping the fine-scale organization and plasticity of the brain vasculature. *Cell* 180 (4), 780–795. doi:10.1016/j.cell.2020.01.028

Kirst, C., Skriabine, S., Vieites-Prado, A., Topilko, T., Bertin, P., Gerschenfeld, G., et al. (2020b). Mapping the fine-scale organization and plasticity of the brain vasculature. *Cell* 180 (4), 780–795. doi:10.1016/j.cell.2020.01.028

Kishi, S., Bayliss, P. E., Uchiyama, J., Koshimizu, E., Qi, J., Nanjappa, P., et al. (2008). The identification of zebrafish mutants showing alterations in senescence-associated biomarkers. *PLoS Genet.* 4 (8), e1000152. doi:10.1371/journal.pgen.1000152

Kishi, S., Slack, B. E., Uchiyama, J., and Zhdanova, I. V. (2009). Zebrafish as a genetic model in biological and behavioral gerontology: where development meets aging in vertebrates--a mini-review. *Gerontology* 55 (4), 430–441. doi:10.1159/000228892

Kishi, S., Uchiyama, J., Baughman, A. M., Goto, T., Lin, M. C., and Tsai, S. B. (2003). The zebrafish as a vertebrate model of functional aging and very gradual senescence. *Exp. Gerontol.* 38 (7), 777–786. doi:10.1016/s0531-5565(03)00108-6

Korzh, V. (2023). Development of the brain ventricular system from a comparative perspective. *Clin. Anat.* 36 (2), 320–334. doi:10.1002/ca.23994

Laina, A., Stellos, K., and Stamatelopoulos, K. (2018). Vascular ageing: underlying mechanisms and clinical implications. *Exp. Gerontol.* 109, 16–30. doi:10.1016/j.exger.2017.06.007

Liu, F., Kambakam, S., Almeida, M. P., Ming, Z., Welker, J. M., Wierson, W. A., et al. (2022). Cre/lox regulated conditional rescue and inactivation with zebrafish UFlip alleles generated by CRISPR-Cas9 targeted integration. *Elife* 11, e71478. doi:10.7554/eLife.71478

López-Otín, C., Blasco, M. A., Partridge, L., Serrano, M., and Kroemer, G. (2021). Hallmarks of aging: an expanding universe. *Cell* 186 (2), 243–278. doi:10.1016/j.cell.2022.11.001

Marques, I. J., Lupi, E., and Mercader, N. (2019). Model systems for regeneration: zebrafish. *Development* 146 (18), dev167692. doi:10.1242/dev.167692

Martins, R. R., Ellis, P. S., MacDonald, R. B., Richardson, R. J., and Henriques, C. M. (2019). Resident immunity in tissue repair and maintenance: the zebrafish model coming of age. *Front. Cell Dev. Biol.* 7, 12. doi:10.3389/fcell.2019.00012

Martins, R. R., Zamzam, M., Tracey-White, D., Moosajee, M., Thummel, R., Henriques, C. M., et al. (2022). Müller Glia maintain theirregenerative potential despite degeneration in the aged zebrafish retina. *Aging cell* 21, e13597. doi:10.1111/acel.13597

Meyer, D. H., and Schumacher, B. (2024). Aging clocks based on accumulating stochastic variation. *Nat. Aging* 4 (6), 871–885. doi:10.1038/s43587-024-00619-x

Mitchell, D. M., Sun, C., Hunter, S. S., New, D. D., and Stenkamp, D. L. (2019). Regeneration associated transcriptional signature of retinal microglia and macrophages. *Sci. Rep.* 9 (1), 4768. doi:10.1038/s41598-019-41298-8

Mizoguchi, T., Okita, M., Minami, Y., Fukunaga, M., Maki, A., and Itoh, M. (2023). Age-dependent dysfunction of the cerebrovascular system in the zebrafish telencephalon. *Exp. Gerontol.* 178, 112206. doi:10.1016/j.exger.2023.112206

O'Brown, N. M., Pfau, S. J., and Gu, C. (2018). Bridging barriers: a comparative look at the blood-brain barrier across organisms. *Genes Dev.* 32 (7-8), 466–478. doi:10.1101/gad.309823.117

Oh, H. S., Rutledge, J., Nachun, D., Pálovics, R., Abiose, O., Moran-Losada, P., et al. (2023). Organ aging signatures in the plasma proteome track health and disease. *Nature* 624 (7990), 164–172. doi:10.1038/s41586-023-06802-1

Pam, S., and Ellis, R. R. M. a. C. M. H. (2024). "Adult zebrafish as a vertebrate model of ageing," in *Zebrafish: a practical guide to husbandry, welfare and research methodology*. Editor C. A. a. J.-P. Mocho (CABI), 159–181. doi:10.1079/9781800629431.0000

Quiñonez-Silvero, C., Hübner, K., and Herzog, W. (2020). Development of the brain vasculature and the blood-brain barrier in zebrafish. *Dev. Biol.* 457 (2), 181–190. doi:10.1016/j.ydbio.2019.03.005

Ranski, A. H., Kramer, A. C., Morgan, G. W., Perez, J. L., and Thummel, R. (2018). Characterization of retinal regeneration in adult zebrafish following multiple rounds of phototoxic lesion. *PeerJ* 6, e5646. doi:10.7717/peerj.5646

Raquel, R., Martins, S. B., Ellis, P., Hartopp, N., Mughal, N., Evans, O., et al. (2024). Telomerase-dependent ageing. *Zebrafish Brain BioRxiv*. doi:10.1101/2022.05.24.493215

Takahashi, T., Sugie, M., Nara, M., Koyama, T., Obuchi, S. P., Harada, K., et al. (2017). Femoral muscle mass relates to physical frailty components in community-dwelling older people. *Geriatr. Gerontol. Int.* 17, 1636–1641. doi:10.1111/ggi.12945

Townsend, N., Nichols, M., Scarborough, P., and Rayner, M. (2015). Cardiovascular disease in Europe 2015: epidemiological update. *Eur. Heart J.* 36 (40), 2673–2674. doi:10.1093/eurheartj/ehv428

Trueland, J. (2013). Older people: an index of frailty. *Health Serv. J.* 123 (6376), Suppl 6–7.

Van Houcke, J., De Groef, L., Dekeyster, E., and Moons, L. (2015). The zebrafish as a gerontology model in nervous system aging, disease, and repair. *Ageing Res. Rev.* 24 (Pt B), 358–368. doi:10.1016/j.arr.2015.10.004

van Lessen, M., Shibata-Germanos, S., van Impel, A., Hawkins, T. A., Rihel, J., and Schulte-Merker, S. (2017). Intracellular uptake of macromolecules by brain lymphatic endothelial cells during zebrafish embryonic development. *Elife* 6, e25932. doi:10.7554/eLife.25932

Venero Galanternik, M., Castranova, D., Gore, A. V., Blewett, N. H., Jung, H. M., Stratman, A. N., et al. (2017). A novel perivascular cell population in the zebrafish brain. *Elife* 6, e24369. doi:10.7554/eLife.24369

White, R. M., and Patton, E. E. (2023). Adult zebrafish as advanced models of human disease. *Dis. Model Mech.* 16 (8), dmm050351. doi:10.1242/dmm.050351

Wu, Y. T., Bennett, H. C., Chon, U., Vanselow, D. J., Zhang, Q., Munoz-Castaneda, R., et al. (2022). Quantitative relationship between cerebrovascular network and neuronal cell types in mice. *Cell Rep.* 39 (12), 110978. doi:10.1016/j.celrep.2022.110978

Xie, J., Farage, E., Sugimoto, M., and Anand-Apte, B. (2010). A novel transgenic zebrafish model for blood-brain and blood-retinal barrier development. *BMC Dev. Biol.* 10, 76. doi:10.1186/1471-213X-10-76

Yu, L., Tucci, V., Kishi, S., and Zhdanova, I. V. (2006). Cognitive aging in zebrafish. *PLoS One* 1, e14. doi:10.1371/journal.pone.0000014

Zambusi, A., Pelin Burhan, O., Di Giaimo, R., Schmid, B., and Ninkovic, J. (2020). Granulins regulate aging kinetics in the adult zebrafish telencephalon. *Cells* 9 (2), 350. doi:10.3390/cells9020350

Zimmerman, B., Rypma, B., Gratton, G., and Fabiani, M. (2021). Age-related changes in cerebrovascular health and their effects on neural function and cognition: a comprehensive review. *Psychophysiology* 58 (7), e13796. doi:10.1111/psyp.13796

frontiers | Frontiers in Physiology

TYPE Original Research
PUBLISHED 19 February 2025
DOI 10.3389/fphys.2025.1536437

OPEN ACCESS

EDITED BY
Luis A. Martinez-Lemus,
University of Missouri, United States

REVIEWED BY
Kedra Wallace,
University of Mississippi Medical Center, United States
Nirupama Ramadas,
University of North Carolina at Chapel Hill, United States

*CORRESPONDENCE
Ricardo Carvalho Cavalli,
rcavalli@fmrp.usp.br
Valeria Cristina Sandrim,
valeria.sandrim@unesp.br

†These authors have contributed equally to this work and share first authorship

‡These authors have contributed equally to this work and share senior authorship

RECEIVED 28 November 2024
ACCEPTED 28 January 2025
PUBLISHED 19 February 2025

CITATION
Kaihara JNS, Grepi Okano HC, Veiga ECA, Tallarico GM, Dias-Junior CA, Cavalli RC and Sandrim VC (2025) Differences between macrovascular and microvascular functions in pregnant women with chronic hypertension or preeclampsia: new insights into maternal vascular health.
Front. Physiol. 16:1536437.
doi: 10.3389/fphys.2025.1536437

Differences between macrovascular and microvascular functions in pregnant women with chronic hypertension or preeclampsia: new insights into maternal vascular health

Julyane N. S. Kaihara[1†], Hellen Cristiane Grepi Okano[2†], Eduardo Carvalho de Arruda Veiga[2], Gustavo Moleiro Tallarico[2], Carlos Alan Dias-Junior[1], Ricardo Carvalho Cavalli[2*‡] and Valeria Cristina Sandrim[1*‡]

[1]Department of Biophysics and Pharmacology, Institute of Biosciences, Sao Paulo State University (UNESP), Botucatu, Brazil, [2]Department of Gynecology and Obstetrics, Ribeirao Preto Medical School, University of Sao Paulo (USP), Ribeirao Preto, Brazil

Introduction: Hypertensive disorders of pregnancy, including chronic hypertension (CH) and preeclampsia (PE), stand as prominent global contributors to maternal and perinatal morbidity and mortality. Endothelial dysfunction plays a central role in the pathophysiology of these conditions. This dysfunction impacts blood flow and the regulation of vascular response, potentially leading to alterations in the remodeling of blood vessels. Nitric oxide bioavailability, a key regulator of vascular tone, is often diminished in endothelial dysfunction, with nitrite levels serving as a surrogate marker. Methods such as pulse wave velocity (PWV) and peripheral arterial tonometry provide valuable insights into vascular health in large and small vessels, respectively, in hypertensive pregnancies. Among these, peripheral arterial tonometry stands out as a less explored technique in research. This study aimed to evaluate potential alterations in the macrovascular arterial stiffness and the microvascular endothelial function among pregnant women diagnosed with CH or PE compared to healthy pregnant (HP) women. Additionally, we aimed to correlate these vascular parameters with demographic and clinical data.

Methods: The study enrolled 24 HP women, 24 with CH during pregnancy, and 24 with PE who underwent evaluations of large-artery stiffness via PWV assessments and peripheral arterial tonometry via natural logarithm of the reactive hyperemia index (lnRHI) assessments.

Results: Patients with CH and PE exhibited higher large-artery stiffness than HP, although the lnRHI values remained comparable across all groups. Furthermore, PWV values demonstrated a direct correlation or tendency toward a positive correlation with systolic and diastolic blood pressures (SBP and DBP) in all groups. However, PWV and nitrite concentrations were not correlated. Notably, microvascular function was positively correlated with SBP and DBP in PE, but not in CH or HP. The correlation between lnRHI and nitrite concentrations was observed in the PE group.

Conclusion: Thus, our findings indicate that, while HDPs have demonstrated increased large-artery stiffness in comparison to HP, the microvasculature analyzed by peripheral arterial tonometry was similar among all three groups. Interestingly, the correlation patterns in the nitrite levels, blood pressure, and microvascular function differed in the PE and CH groups.

KEYWORDS

arterial stiffness, chronic hypertension in pregnancy, endothelial dysfunction, preeclampsia, pulse wave velocity, peripheral arterial tonometry

1 Introduction

Hypertensive disorders of pregnancy (HDPs), including chronic hypertension (CH) and preeclampsia (PE), stand as prominent contributors to maternal and perinatal morbidity and mortality on a global scale (American College of Obstetricians and Gynecologists ACOG, 2020). CH affects 1%–2% of pregnancies and stands as the primary risk factor for the development of PE (Panaitescu et al., 2017), among other maternal characteristics.

One of the key factors in the development of both PE and CH is endothelial dysfunction. In PE, abnormal placentation and imbalanced placental factors in the maternal circulation cause endothelial injury, leading to impaired endothelial function (Tomimatsu et al., 2019; Powe et al., 2011), which is evidenced by a reduced flow-mediated dilation (FMD) in the vasculature (Cockell and Poston, 1997; Weissgerber et al., 2016). As a result of a decrease in vasodilator factors and an increase in vasoconstrictors (Tomimatsu et al., 2019), endothelial dysfunction significantly impacts blood flow and regulation of vascular response. This dysfunction can result in alterations in the remodeling of blood vessels, leading to arterial stiffening, impaired arterial compliance, and/or contractility in response to changes in blood pressure (Safar, 2018), and increased pulse wave velocity (PWV) propagation through the aorta and large arteries (Chirinos et al., 2019). Therefore, arterial stiffness can contribute to end-organ damage (Chirinos et al., 2019) and has a recognized prognostic value in assessing cardiovascular disease risk (Boutouyrie et al., 2021).

Nitric oxide (NO) is synthesized by nitric oxide synthase (NOS) through the catalysis of L-arginine. In endothelial cells, NO mediates smooth muscle relaxation in blood vessels by activating cyclic guanosine monophosphate (cGMP), which lowers intracellular calcium levels (Lowe, 2000). Accordingly, a decrease in NO bioavailability is recognized as a contributing factor to endothelial dysfunction, a condition associated with various cardiovascular disorders. As NO is a gaseous molecule with a relatively short half-life in biological systems, direct quantification of NO is challenging. Nitrite, a stable metabolite of NO, serves as a reliable surrogate marker for evaluating NO bioavailability in plasma.

Endothelial dysfunction can be evaluated by analyzing the vascular tone subsequent to the induction of reactive hyperemia through the temporary occlusion of the blood vessel. When the occlusion is released, the shear stress induced by the blood flow stimulates the endothelium. If the endothelial function is preserved, its cells will increase the NO production, resulting in a relative augmentation in blood vessel diameter (vasodilation) (Korkmaz and Onalan, 2008). The ultrasound assessment of FMD in the brachial artery is considered the gold standard for evaluating large-artery endothelial function (Stoner et al., 2013). In this context, peripheral arterial tonometry emerges as a novel and semi-automated method for assessing endothelial health, particularly regarding small-diameter blood vessels. However, the utilization of this methodology in research has been explored to a minor extent.

There are significant advancements in evaluating endothelial dysfunction using peripheral arterial tonometry, and most studies employing this method have focused on the detection of endothelial dysfunction in various pathological conditions, including PE (Meeme et al., 2017; Yinon et al., 2006; Carty et al., 2012). However, an important gap remains in the literature, as these studies have largely overlooked the specific group of pregnant women with CH and have not simultaneously evaluated arterial stiffness in these populations. Consequently, our study stands out by providing new insights into the vascular health of pregnant women with CH, contributing to a more comprehensive understanding of vascular complications in CH during pregnancy compared to PE. Therefore, we aimed to investigate potential variations in peripheral vascular endothelium and large-artery stiffness in women with CH and PE in comparison to normotensive women, by means of PWV and reactive hyperemia index (RHI) measurements. Additionally, we analyzed the correlations between these vascular parameters with demographic and clinical data, including plasma nitrite concentrations.

2 Methods

2.1 Study population

This case-control study was approved by the Ethics Committee of the University Hospital, Ribeirao Preto Medical School, University of São Paulo, Brazil (HCFMRP-USP) under protocol number 1.974.303 on 21 March 2017. The research was conducted in accordance with the institutional guidelines and regulations for research involving human subjects and in alignment with the Declaration of Helsinki. Participants recruited voluntarily provided written informed consent during clinical attendance. In the case of pregnant women under 18, consent was obtained from their parents or legal guardians. The study population enrolled a total of 72 women. It included 24 women with CH and 24 PE between 26 and 42 weeks of gestation who were followed up at the high-risk pregnancy outpatient clinic of the HCFMRP-USP. Moreover, 24 healthy pregnant women (HP, without HDPs or other complications) who attended the Reference Center for

Women's Health of Ribeirao Preto (MATER) were also included. CH in pregnancy was defined as sustained hypertension (systolic blood pressure, SBP ≥140 mmHg and/or diastolic blood pressure, DBP ≥90 mmHg) diagnosed before pregnancy or before 20 weeks of gestation, or if hypertension persisted for more than 12 weeks *postpartum*, in the absence of gestational trophoblastic disease (Vidaeff et al., 2019; Brown et al., 2018). PE was defined as new-onset hypertension diagnosed after 20 weeks of gestation associated with proteinuria (qualitatively identified via dipstick reading of 2+) or other end-organ damage, such as thrombocytopenia, renal insufficiency, impaired liver function, pulmonary edema, and visual symptoms (American College of Obstetricians and Gynecologists ACOG, 2020). Clinical data analysis and laboratory tests were conducted for the diagnosis of CH and PE, while ultrasound analysis was performed to identify a single fetus and determine corrected gestational age. All HDPs patients were receiving anti-hypertensive medications, including methyldopa and nifedipine, either as monotherapy or in combination. Data on delivery and newborn information were collected from medical records. Participants with multiple pregnancies or a history of fetal distress diagnosis, as well as those with positive serology for diseases such as human immunodeficiency virus (HIV), hepatitis B (HBsAg), hepatitis C (HCV), syphilis (VDRL), toxoplasmosis, or rubella, were excluded from the study. Additionally, participants with positive parasitological stool tests or urine cultures, type 1 diabetes, liver, heart, or kidney diseases that affect blood pressure, superimposed PE (when a CH patient develops any of the end-organ dysfunctions after 20 weeks of gestation consistent with PE) (Vidaeff et al., 2019; Brown et al., 2018), abnormal fetal ultrasound findings, those who developed hemolysis, elevated liver enzymes, and low platelet count (HELLP) syndrome, or those who withdrew during large-artery stiffness and peripheral arterial tonometry examinations were also excluded.

2.2 Large-artery stiffness assessment

Large-artery stiffness was evaluated using PWV measurement, which is a non-invasive method and the gold standard for assessing the stiffness of central muscular arteries. PWV data were recorded and analyzed via Sphygmocor Software version 9.0 (AtCor Medical, Sydney, Australia). Following a 5 min rest in an air-conditioned room, the participant was placed in a supine position. The external transducer was then placed directly on the skin over the right carotid artery and right femoral artery, and pulse wave velocities were recorded for a minimum of 10 s. The PWV was automatically computed as the ratio of carotid-femoral distance and the time interval between the two pulses (Hale et al., 2013).

2.3 Peripheral arterial tonometry

Endothelial function was assessed using the EndoPAT 2000 device (Itamar Medical Ltd., Caesarea, Israel) at the time of diagnosis, following the manufacturer's instructions. This pneumatic plethysmograph identifies variations in the digital pulse waveforms known as peripheral arterial tone (PAT) signals by positioning probes on the distal phalanx of the fourth finger of both arms. The patients were placed in an air-conditioned room with a neutral temperature for the examinations. All objects that could interfere with the examination, such as restrictive clothing, jewelry, and accessories, were removed. Patients were made comfortable and allowed to sit or lie down in a relaxed position for a minimum of 15 min to ensure cardiovascular stability and acclimation to room temperature. Initially, a standard blood pressure cuff on the brachial artery of the non-dominant arm is set to induce a 5 min blood flow occlusion (Kuvin et al., 2003). Upon cuff release, blood flow increases (hyperemia), leading to endothelial-dependent flow-mediated vasodilation. The device detects this reactive hyperemia as an increase in the amplitude of the PAT signal. Subsequently, the device's software calculates the RHI by comparing the ratio of the post- and pre-occlusion PAT signal in the occluded arm to that in the control (dominant) arm. The natural logarithm of the RHI (lnRHI) after vascular occlusion was used as it closely approximates a Gaussian distribution, with lnRHI ≤0.51 indicating abnormal microvascular function.

2.4 Plasma nitrite assay

The plasma nitrite concentrations were quantified using the Griess Reagent System (#G2930; Promega Corporation, Madison, United States), following the manufacturer's instructions. Briefly, this assay involves incubations with sulfanilamide solution (1% sulfanilamide in 5% phosphoric acid) and NED solution (0.1% N-1-naphthyl ethylenediamine dihydrochloride in water) at room temperature. The absorbance of the colored compound formed by the reaction was then measured. Nitrite concentrations were determined by comparing the absorbance to a sodium nitrite standard reference curve.

2.5 Statistical analysis

The demographic and clinical variables as well as the PWV and lnRHI values of the subjects enrolled in this study underwent normality tests. For qualitative variables, One-Way ANOVA, Welch's ANOVA, or Kruskal–Wallis test, followed by *post hoc* tests such as Tukey's, Dunnett's, or Dunn's were applied as appropriate. The statistical analysis of categorical variables was conducted using Chi-square (χ^2) or Fisher's exact tests. A p-value ≤0.05 was considered significant. Pearson's and Spearman's correlation tests were performed to measure the linear relationships between the PWV and lnRHI data with the clinical characteristics of the subjects. A p-value <0.05 was considered significant for the correlations. All analyses were conducted via GraphPad Prism version 9.5 (GraphPad Software Inc., San Diego, United States).

3 Results

Table 1 provides an overview of the demographic and clinical characteristics of the 72 pregnant women included in this study. The HP and PE groups had similar ages, while CH patients were older than both. At the time of enrollment, CH and PE patients had higher

10.3389/fphys.2025.1536437

TABLE 1 Demographic and clinical characteristics of all the subjects enrolled in this study.

Parameter	HP	CH	PE	*p*-value
Age (years)	27.2 ± 6.0	32.7 ± 5.4*	28.5 ± 5.8#	0.0038
BMI (kg/m^2)	27.8 ± 4.2	36.1 ± 4.2*	31.8 ± 5.0*#	<0.0001
SBP (mmHg)	111.1 ± 12.2	135.3 ± 21.7*	147.0 ± 18.6*	<0.0001
DBP (mmHg)	74.5 ± 8.1	84.6 ± 11.0*	95.8 ± 13.5*#	<0.0001
Heart Rate (bpm)	76.0 ± 13.0	82.2 ± 15.0	78.6 ± 13.5	0.3081
GAS (weeks)	35.3 ± 2.3	36.5 ± 3.1	33.8 ± 4.0#	0.0184
GAD (weeks)	40.0 [37.0–41.0]	38.0 [34.0–42.0]*	36.0 [26.0–40.0]*#	<0.0001
Newborn Weight (g)	3,355.0 ± 324.6	3,236.0 ± 528.1	2020.0 ± 933.4*#	<0.0001
APGAR Score 1 (1 min) < 7	1.0 (4.2)	0.0 (0.0)	7.0 (33.3)*#	0.0010
APGAR Score 2 (5 min) < 7	0.0 (0.0)	0.0 (0.0)	1.0 (4.8)	0.4281

BMI, body mass index; CH, chronic hypertension in pregnancy; DBP, diastolic blood pressure; GAD, gestational age at delivery; GAS, gestational age at sampling; HP, healthy pregnant; PE, preeclampsia; SBP, systolic blood pressure. Data are expressed as mean ± SD, median [minimum-maximum], or absolute number (% of total). *$p < 0.05$ versus HP, #$p < 0.05$ versus CH.

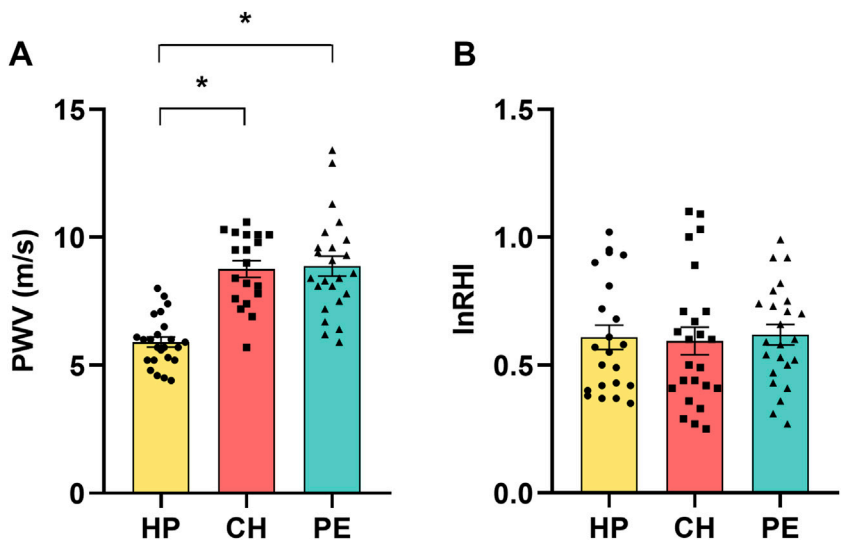

FIGURE 1
(A) Pulse wave velocity (PWV) and **(B)** natural logarithm of the reactive hyperemia index (lnRHI) in healthy pregnant women (HP), those with chronic hypertension during pregnancy (CH), and those with preeclampsia (PE). Data presented as mean ± SEM. *$p \leq 0.05$ compared to HP.

body mass indexes (BMI) than HP women, and CH patients presented higher BMI values than PE patients. As expected, CH and PE patients presented higher SBP and DBP in comparison to the HP group, and the PE group also exhibited higher DBP than the CH group, despite both groups receiving anti-hypertensive therapy. Resting heart rates were similar across all groups. A comparison of the gestational age at sampling (GAS) revealed a similarity between the groups. However, the PE group exhibited an earlier GAS compared to the CH group. In terms of gestational age at delivery (GAD) and newborn weight, PE women delivered earlier and gave birth to smaller newborns compared to those in the HP and CH groups, as anticipated. The women with CH also delivered earlier than HP. Furthermore, newborns of PE women had a higher incidence of APGAR scores below 7 at the 1 min assessment after delivery, but no significant differences were observed during the 5 min assessment. Plasma nitrite concentrations were similar across all groups and are presented in Supplementary Figure 1.

Figure 1 displays the assessments of large-artery stiffness via PWV assessment (Figure 1A) and endothelial dysfunction in the microvasculature via peripheral arterial tonometry (Figure 1B). Compared to HP women, patients with CH and PE exhibited higher PWV values, indicative of large-arterial stiffness in those groups. The mean values of lnRHI among the HP, CH, and PE groups were similar. This suggests that the endothelial function in the microvasculature was comparable across all groups.

All patients enrolled in the CH and PE groups initiated anti-hypertensive therapy with pregnancy-specific medications following their respective diagnoses until delivery, including the day of sampling. Subsequently, a comparative analysis of PWV and lnRHI values was conducted based on the administered

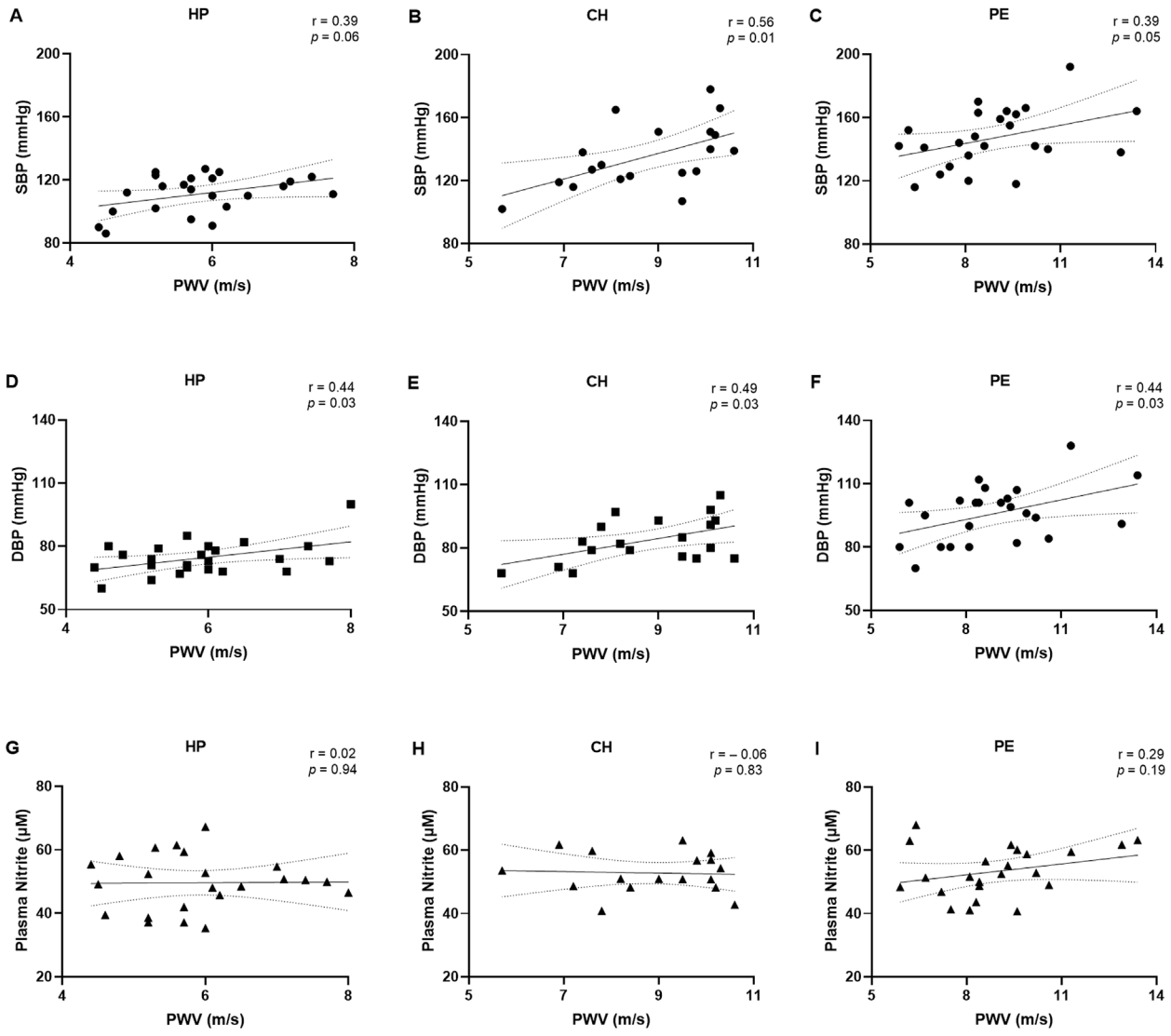

FIGURE 2
Correlations between pulse wave velocity (PWV) with systolic blood pressure **(A–C)**, diastolic blood pressure **(D–F)**, and plasma nitrite concentrations **(G–I)** in the healthy pregnant (HP), chronic hypertension during pregnancy (CH), and preeclampsia (PE) groups. Data presented as Pearson's or Spearman's correlation. r, Pearson's or Spearman's correlation coefficient.

medication (methyldopa, nifedipine, or a combination of both). The results of this analysis are presented in Supplementary Figure 2. The findings revealed that both PWV and lnRHI demonstrated comparable outcomes across all subgroups, suggesting that these parameters remained unaffected by the anti-hypertensive medication.

Figure 2 and the Supplementary Table display the correlations between demographic and clinical data and PWV values. SBP tended to be positively correlated with PWV values in the HP (r = 0.39, Figure 2A), while this correlation was statistically significant in the CH group (r = 0.56, Figure 2B) and PE group (r = 0.39, Figure 2C). Similarly, DBP was positively correlated with PWV values in the HP group (r = 0.44, Figure 2D), CH group (r = 0.49, Figure 2E), and PE group (r = 0.44, Figure 2F). There was no correlation between PWV values and plasma nitrite concentrations among all groups (Figures 2G–I). Moreover, PWV values showed a tendency towards a positive correlation with BMI in the HP group, but no significant correlations were observed with other demographic or clinical parameters, including age, GAD, and newborn weight (Supplementary Table).

The correlations between demographic and clinical data with the lnRHI values are presented in Figure 3 and the Supplementary Table. No correlations were observed when considering lnRHI with SBP and DBP in the HP (Figures 3A,B) or CH groups (Figures 3D,E). Nevertheless, in the PE group, a moderate positive correlation was observed between lnRHI with SBP (r = 0.55, Figure 3C) and between lnRHI with DBP (r = 0.50, Figure 3F), indicating that the higher the blood pressure, the higher the lnRHI. This is a notable finding, as greater values of lnRHI are associated with physiological

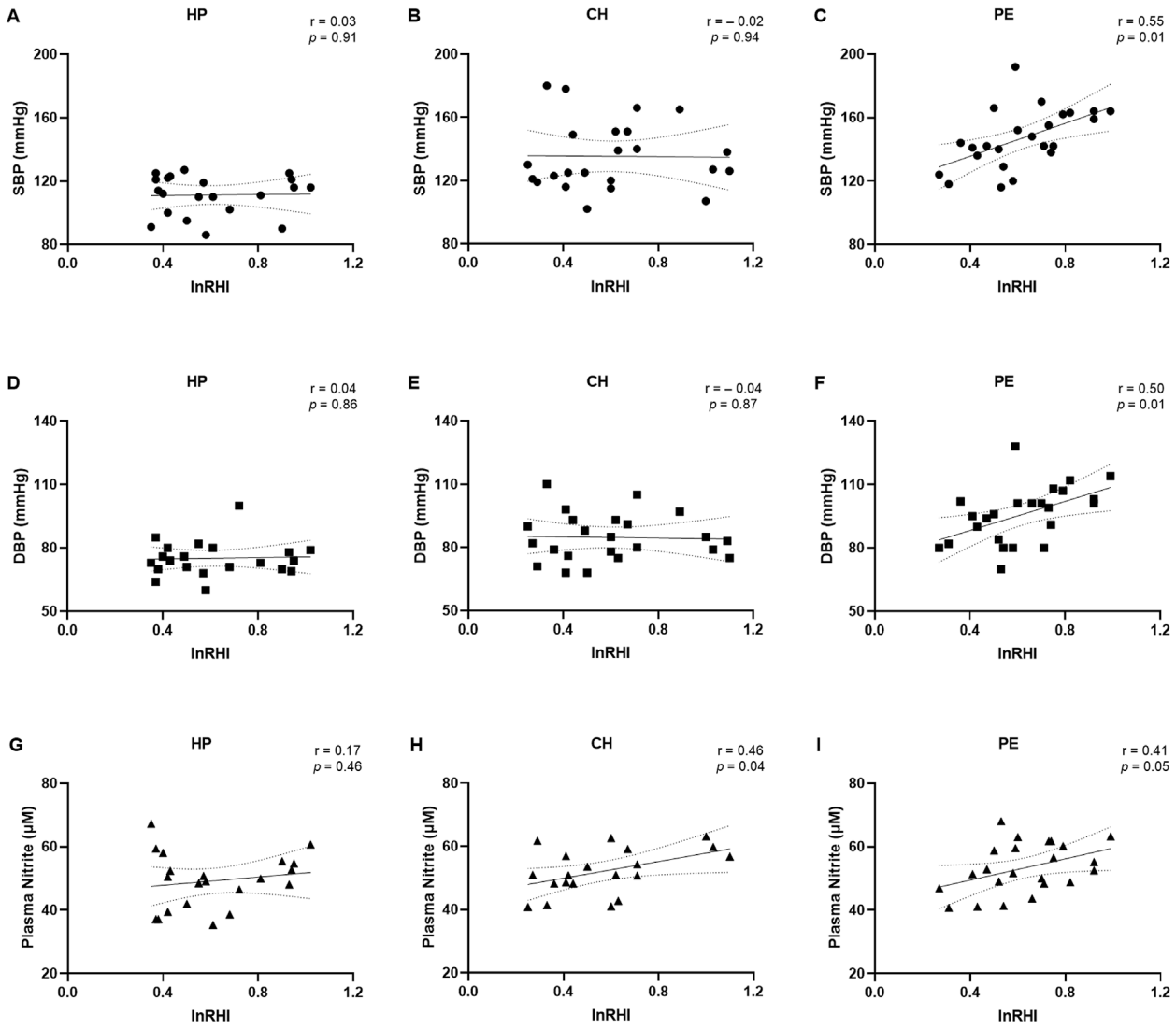

FIGURE 3
Correlations between the natural logarithm of the reactive hyperemia index (lnRHI) with systolic blood pressure **(A–C)**, diastolic blood pressure **(D–F)**, and plasma nitrite concentrations **(G–I)** in the healthy pregnant (HP), chronic hypertension during pregnancy (CH), and preeclampsia (PE) groups. Data presented as Pearson's or Spearman's correlation. r, Pearson's or Spearman's correlation coefficient.

endothelial-dependent vasodilation and normal endothelial function. In contrast to the findings observed in the macrovasculature, lnRHI was positively correlated with plasma nitrite concentrations in the CH group (r = 0.46, Figure 3H) and in the PE group (r = 0.41, Figure 3I). However, no such correlation was evident in the HP group (Figure 3G). It is worth noting that after excluding the three overt outliers in the correlation graph between lnRHI and plasma nitrite, the correlation became non-significant. There was no correlation between age, BMI, GAD, and newborn weight with lnRHI values across the three experimental groups (Supplementary Table), which suggests that the endothelial function may be independent of these demographic and clinical parameters in this study population.

Figure 4 presents an overview of the study design, methodologies, and key findings. This graphical abstract summarizes the analyses of macro- and microvascular functions in the HP, CH, and PE groups.

4 Discussion

In this study, we investigated the macrovascular arterial stiffness and microvascular endothelial function in the context of two HDPs–CH and PE–in comparison to normotensive HP women. Pregnant women with CH and PE showed significant large-artery stiffness compared to those with HP. In all groups, SBP showed a positive correlation or a tendency towards a positive correlation with arterial stiffness, with a similar association observed for DBP. Nevertheless, plasma nitrite concentrations were not correlated with arterial stiffness. Endothelial function in the microvasculature was comparable across all groups. However, our findings indicated that higher values of lnRHI in the PE group were associated with higher SBP and DBP, whereas no such correlations were observed between SBP and DBP in HP and CH. Additionally, there was a positive correlation between lnRHI and higher plasma nitrite concentrations in the CH and PE.

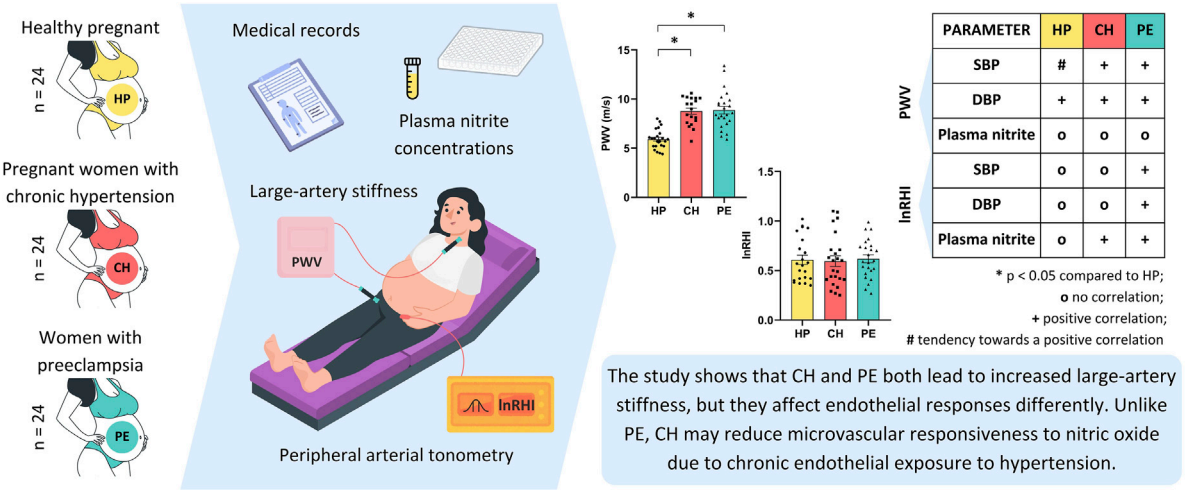

FIGURE 4
Graphical abstract.

Our analysis revealed that large-artery stiffness was altered in the groups with HDPs, as evidenced by higher values of PWV. This finding is supported by other recent studies in other populations of patients with PE compared to healthy controls (Kaihura et al., 2009; Namugowa et al., 2017). Furthermore, women with a previous history of early-onset PE (Orabona et al., 2017a), and those with a previous history of PE with or without HELLP syndrome (Orabona et al., 2017b), continued to present altered arterial stiffness after delivery. Also, Hale et al. longitudinally evaluated the PWV of women during pre-pregnancy, early, and late pregnancy periods (Hale et al., 2013). The study found a difference in the pre-pregnant PWV between normotensive and hypertensive women, suggesting subclinical altered arterial stiffness in those with a predisposition to PE. Thus, our study not only provides additional information beyond the findings of Hale et al. (2013) indicating altered arterial stiffness in women with PE but also extends this understanding by revealing comparable alterations in women with CH in a larger cohort. The direct correlation between SBP, DBP, and PWV in the PE group may be attributable to the close association between arterial stiffness and its contribution to the development of hypertension. This association is further influenced by the high force of the blood against the artery walls, which leads to increased collagen production and elastin degradation (Mitchell, 2014) and influences the premature aging of the blood vessels (Shimokawa, 1998).

The physiological shear stress created by the blood flow over the endothelial cells activates mechanoreceptors and leads to a cascade of intracellular signaling pathways that result in the production of vasodilatory and growth factors to help maintain vascular tone (Davies, 2009). However, in hypertensive disorders, the impaired blood flow leads to abnormal shear stress, disrupting the hemodynamics and contributing to endothelial dysfunction by promoting a proinflammatory and prothrombotic state that further exacerbates vascular injury and stiffness (Davies, 2009). Our findings indicated that the endothelial state of women with HDPs and those with HP as assessed through peripheral arterial tonometry were similar. Limited research has been conducted on this topic, and previous reports have yielded conflicting results regarding the RHI of PE patients, even when using the same equipment. Differences in recruitment methodology relative to inclusion and exclusion criteria, or differences in the preparatory steps for the examinations could be reasons for this discrepancy. Yinon et al. reported that women with PE (n = 17 and mean GAS = 32.0 ± 4.0 weeks) exhibited lower RHI values than normotensive controls (Yinon et al., 2006). Similarly, Meeme et al. obtained the same result in a larger cohort (case group: n = 105 and mean GAS = 30.8 ± 0.4 weeks), but it is worth noting that it included HIV-positive patients (Meeme et al., 2017). When classified into subgroups of HIV-positive and HIV-negative patients, the difference in RHI between normotensive HIV-negative women and those preeclamptic HIV-negative lost significance, which is consistent with our findings.

Furthermore, the moderate positive correlation found between SBP and DBP with lnRHI in the PE group was noteworthy, as higher lnRHI values indicated a more responsive microvascular endothelial state. This may be attributed to the direct correlation between plasma nitrite and lnRHI, as well as the endothelial response to shear stress following cuff release, which stimulates the NO production in the microvasculature. Previous reports have indicated that the circulating nitrite levels were either increased (Noorbakhsh et al., 2013; Bartha et al., 1999) in PE or similar (Acauan Filho et al., 2016; Elmas et al., 2016) compared to healthy controls. Additionally, it has been demonstrated that serum nitrite levels were decreased in CH women in comparison to healthy controls (Bartha et al., 1999). As a response to the hypertensive state, the elevated nitrite levels, a biomarker of NO, observed in the PE group may indicate that NO plays a role in the response of the microvascular endothelium in PE, improving endothelial function. However, this does not appear to be the case in macrovasculature, as evidenced by the lack of correlation between PWV and plasma nitrite concentrations. Conversely, the same correlation of lnRHI with SBP and DBP was not observed in the CH group. This may be caused by established

vascular structural and epigenetic remodeling (Davies, 2009; Mengozzi et al., 2023) as a result of the chronic changes in the hemodynamic state in these hypertensive patients, which impairs the endothelial response to shear stress. Therefore, these findings suggest that the differential correlation patterns between blood pressure and lnRHI in PE and CH are associated with the chronic nature of hypertension in CH. The blood pressure of this group was consistently elevated prior to the pregnancy. In contrast, the endothelial alterations observed in PE are less pronounced due to the new onset of hypertension during pregnancy, allowing for peripheral vasodilation. Further investigation is necessary to ascertain this hypothesis, as, to the best of our knowledge, there are no studies regarding the impact of the altered shear stress in the systemic vessels in conditions such as CH in pregnancy and PE.

This study has limitations. As this was a non-longitudinal study, our results elucidated associations between the variables under investigation and it was not possible to identify causal relationships, as the large-artery stiffness and peripheral endothelial function of the patients before and after pregnancy were unexplored. The observed discrepancies in BMI measurements among the study groups may be due to the inherent association between higher BMI values and an increased risk for CH and PE development. Although previous studies have shown a relationship between aging and vascular changes (Reference Values for Arterial Stiffness Collaboration, 2010; Mitchell et al., 2010), the age range in our study was relatively narrow. While we observed statistical differences in age between our groups, these age ranges are smaller compared to those evaluated in previous studies, which often include a broader spectrum of ages. Furthermore, our study revealed no correlation between endothelial function and age, or between arterial stiffness and age. Therefore, the impact of age on vascular changes in our study may be limited. Moreover, other biomarkers of vascular health that would provide a more complete understanding of vascular changes were not evaluated.

5 Conclusion

Our findings indicate that, while HDPs have demonstrated increased large-artery stiffness in comparison to HP, the microvasculature analyzed by peripheral arterial tonometry was similar among all three groups. Interestingly, the correlation patterns in the nitrite levels, blood pressure, and microvascular function differed in the PE and CH groups. These results bring new perspectives on endothelial function in macro- and microvasculature in HDPs and open new possibilities for diagnoses and treatments.

Data availability statement

The original contributions presented in the study are included in the article/supplementary material, further inquiries can be directed to the corresponding authors.

Ethics statement

The studies involving humans were approved by Ethics Committee of the University Hospital, Ribeirao Preto Medical School, University of São Paulo, Brazil. The studies were conducted in accordance with the local legislation and institutional requirements. The participants provided their written informed consent to participate in this study.

Author contributions

JK: Funding acquisition, Visualization, Writing–original draft, Writing–review and editing, Data curation, Formal Analysis, Methodology, Validation. HG: Data curation, Formal Analysis, Methodology, Validation, Writing–original draft, Writing–review and editing, Conceptualization, Investigation, Project administration. EC: Data curation, Formal Analysis, Writing–original draft, Writing–review and editing. GT: Writing–review and editing. CD-J: Writing–review and editing. RC: Data curation, Formal Analysis, Project administration, Resources, Supervision, Writing–original draft, Writing–review and editing. VS: Funding acquisition, Supervision, Visualization, Writing–original draft, Writing–review and editing.

Funding

The author(s) declare that financial support was received for the research, authorship, and/or publication of this article. This work was supported by the *Conselho Nacional de Desenvolvimento Científico e Tecnológico* (CNPq) [grant number 308504/2021-6] and the *Fundação de Amparo à Pesquisa do Estado de São Paulo* (FAPESP) [grant numbers 2021/12010-7 and 2023/08897-1]. The funding sources had no role in study design, in the collection, analysis and interpretation of data, in the writing of the manuscript, or in the decision to submit the article for publication.

Acknowledgments

The graphical abstract was generated using Canva (www.canva.com) and icons created by Storyset from www.storyset.com; irasutoya, Elionas, and Vik_Y from www.canva.com; IYIKON and Freepik from www.flaticon.com.

Conflict of interest

The authors declare that the research was conducted in the absence of any commercial or financial relationships that could be construed as a potential conflict of interest.

The author(s) declared that they were an editorial board member of Frontiers, at the time of submission. This had no impact on the peer review process and the final decision.

Generative AI statement

The author(s) declare that no Generative AI was used in the creation of this manuscript.

Publisher's note

All claims expressed in this article are solely those of the authors and do not necessarily represent those of their affiliated organizations, or those of the publisher, the editors and the reviewers. Any product that may be evaluated in this article, or claim that may be made by its manufacturer, is not guaranteed or endorsed by the publisher.

Supplementary material

The Supplementary Material for this article can be found online at: https://www.frontiersin.org/articles/10.3389/fphys.2025.1536437/full#supplementary-material

References

Acauan Filho, B. J., Pinheiro da Costa, B. E., Ogando, P. B., Vieira, M. C., Antonello, I. C., and Poli-de-Figueiredo, C. E. (2016). Serum nitrate and NOx levels in preeclampsia are higher than in normal pregnancy. *Hypertens. Pregnancy* 35 (2), 226–233. doi:10.3109/10641955.2016.1139718

American College of Obstetricians and Gynecologists (ACOG) (2020). Gestational Hypertension and Preeclampsia: ACOG practice bulletin number 222. *Obstetrics and Gynecol.* 135 (6), e237–e260. doi:10.1097/AOG.0000000000003891

Bartha, J. L., Comino-Delgado, R., Bedoya, F. J., Barahona, M., Lubian, D., and Garcia-Benasach, F. (1999). Maternal serum nitric oxide levels associated with biochemical and clinical parameters in hypertension in pregnancy. *Eur. J. Obstetrics and Gynecol. Reproductive Biol.* 82 (2), 201–207. doi:10.1016/s0301-2115(98)00234-6

Boutouyrie, P., Chowienczyk, P., Humphrey, J. D., and Mitchell, G. F. (2021). Arterial stiffness and cardiovascular risk in hypertension. *Circ. Res.* 128 (7), 864–886. doi:10.1161/CIRCRESAHA.121.318061

Brown, M. A., Magee, L. A., Kenny, L. C., Karumanchi, S. A., McCarthy, F. P., Saito, S., et al. (2018). Hypertensive disorders of pregnancy: ISSHP classification, diagnosis, and management recommendations for international practice. *Hypertension* 72 (1), 24–43. doi:10.1161/HYPERTENSIONAHA.117.10803

Carty, D. M., Anderson, L. A., Duncan, C. N., Baird, D. P., Rooney, L. K., Dominiczak, A. F., et al. (2012). Peripheral arterial tone: assessment of microcirculatory function in pregnancy. *J. Hypertens.* 30 (1), 117–123. doi:10.1097/HJH.0b013e32834d76fb

Chirinos, J. A., Segers, P., Hughes, T., and Townsend, R. (2019). Large-artery stiffness in health and Disease: JACC state-of-the-art review. *J. Am. Coll. Cardiol.* 74 (9), 1237–1263. doi:10.1016/j.jacc.2019.07.012

Cockell, A. P., and Poston, L. (1997). Flow-mediated vasodilatation is enhanced in normal pregnancy but reduced in preeclampsia. *Hypertension* 30 (2), 247–251. doi:10.1161/01.hyp.30.2.247

Davies, P. F. (2009). Hemodynamic shear stress and the endothelium in cardiovascular pathophysiology. *Nat. Clin. Pract. Cardiovasc Med.* 6 (1), 16–26. doi:10.1038/ncpcardio1397

Elmas, O., Elmas, O., Aliciguzel, Y., and Simsek, T. (2016). The relationship between hypertension and plasma allantoin, uric acid, xanthine oxidase activity and nitrite, and their predictive capacity in severe preeclampsia. *J. Obstet. Gynaecol. (Lahore)* 36 (1), 34–38. doi:10.3109/01443615.2015.1030608

Hale, S. A., Badger, G. J., McBride, C., Magness, R., and Bernstein, I. M. (2013). Prepregnancy vascular dysfunction in women who subsequently develop hypertension during pregnancy. *Pregnancy Hypertens. Int. J. Women's Cardiovasc. Health* 3 (2), 140–145. doi:10.1016/j.preghy.2013.01.006

Kaihura, C., Savvidou, M. D., Anderson, J. M., McEniery, C. M., and Nicolaides, K. H. (2009). Maternal arterial stiffness in pregnancies affected by preeclampsia. *Am. J. Physiology-Heart Circulatory Physiology* 297 (2), H759–H764. doi:10.1152/ajpheart.01106.2008

Korkmaz, H., and Onalan, O. (2008). Evaluation of endothelial dysfunction: flow-mediated dilation. *Endothelium* 15 (4), 157–163. doi:10.1080/10623320802228872

Kuvin, J. T., Patel, A. R., Sliney, K. A., Pandian, N. G., Sheffy, J., Schnall, R. P., et al. (2003). Assessment of peripheral vascular endothelial function with finger arterial pulse wave amplitude. *Am. Heart J.* 146 (1), 168–174. doi:10.1016/S0002-8703(03)00094-2

Lowe, D. T. (2000). Nitric oxide dysfunction in the pathophysiology of preeclampsia. *Nitric Oxide* 4 (4), 441–458. doi:10.1006/niox.2000.0296

Meeme, A., Buga, G., Mammen, M., and Namugowa, A. (2017). Endothelial dysfunction and arterial stiffness in pre-eclampsia demonstrated by the EndoPAT method. *Cardiovasc J. Afr.* 28 (1), 23–29. doi:10.5830/CVJA-2016-047

Mengozzi, A., Costantino, S., Mongelli, A., Mohammed, S. A., Gorica, E., Delfine, V., et al. (2023). Epigenetic signatures in arterial hypertension: focus on the microvasculature. *Int. J. Mol. Sci.* 24 (5), 4854. doi:10.3390/ijms24054854

Mitchell, G. F. (2014). Arterial stiffness and hypertension: chicken or egg? *Hypertension* 64 (2), 210–214. doi:10.1161/HYPERTENSIONAHA.114.03449

Mitchell, G. F., Wang, N., Palmisano, J. N., Larson, M. G., Hamburg, N. M., Vita, J. A., et al. (2010). Hemodynamic correlates of blood pressure across the adult age spectrum: noninvasive evaluation in the Framingham Heart Study. *Circulation* 122 (14), 1379–1386. doi:10.1161/CIRCULATIONAHA.109.914507

Namugowa, A., Iputo, J., Wandabwa, J., Meeme, A., and Buga, G. A. B. (2017). Comparison of arterial stiffness in preeclamptic and normotensive pregnant women from a semi-rural region of South Africa. *Clin. Exp. Hypertens.* 39 (3), 277–283. doi:10.1080/10641963.2016.1254227

Noorbakhsh, M., Kianpour, M., and Nematbakhsh, M. (2013). Serum levels of asymmetric dimethylarginine, vascular endothelial growth factor, and nitric oxide metabolite levels in preeclampsia patients. *ISRN Obstet. Gynecol.* 2013, 104213–104215. doi:10.1155/2013/104213

Orabona, R., Sciatti, E., Vizzardi, E., Bonadei, I., Prefumo, F., Valcamonico, A., et al. (2017b). Maternal endothelial function and vascular stiffness after HELLP syndrome: a case–control study. *Ultrasound Obstetrics and Gynecol.* 50 (5), 596–602. doi:10.1002/uog.17394

Orabona, R., Sciatti, E., Vizzardi, E., Bonadei, I., Valcamonico, A., Metra, M., et al. (2017a). Endothelial dysfunction and vascular stiffness in women with previous pregnancy complicated by early or late pre-eclampsia. *Ultrasound Obstetrics and Gynecol.* 49 (1), 116–123. doi:10.1002/uog.15893

Panaitescu, A. M., Syngelaki, A., Prodan, N., Akolekar, R., and Nicolaides, K. H. (2017). Chronic hypertension and adverse pregnancy outcome: a cohort study. *Ultrasound Obstetrics and Gynecol.* 50 (2), 228–235. doi:10.1002/uog.17493

Powe, C. E., Levine, R. J., and Karumanchi, S. A. (2011). Preeclampsia, a disease of the maternal endothelium: the role of antiangiogenic factors and implications for later cardiovascular disease. *Circulation* 123 (24), 2856–2869. doi:10.1161/CIRCULATIONAHA.109.853127

Reference Values for Arterial Stiffness Collaboration (2010). Determinants of pulse wave velocity in healthy people and in the presence of cardiovascular risk factors: 'establishing normal and reference values. ' *Eur. Heart J.* 31 (19), 2338–2350. doi:10.1093/eurheartj/ehq165

Safar, M. E. (2018). Arterial stiffness as a risk factor for clinical hypertension. *Nat. Rev. Cardiol.* 15 (2), 97–105. doi:10.1038/nrcardio.2017.155

Shimokawa, H. (1998). Endothelial dysfunction in hypertension. *J. Atheroscler. Thromb.* 4 (3), 118–127. doi:10.5551/jat1994.4.118

Stoner, L., Tarrant, M. A., Fryer, S., and Faulkner, J. (2013). How should flow-mediated dilation be normalized to its stimulus? *Clin. Physiol. Funct. Imaging* 33 (1), 75–78. doi:10.1111/j.1475-097X.2012.01154.x

Tomimatsu, T., Mimura, K., Matsuzaki, S., Endo, M., Kumasawa, K., and Kimura, T. (2019). Preeclampsia: maternal systemic vascular disorder caused by generalized endothelial dysfunction due to placental antiangiogenic factors. *Int. J. Mol. Sci.* 20 (17), 4246. doi:10.3390/ijms20174246

Vidaeff, A., Espinoza, J., Simhan, H., and Pettker, C. M. (2019). ACOG practice bulletin No. 203: chronic hypertension in pregnancy. *Obstetrics Gynecol.* 133 (1), E26–E50. doi:10.1097/AOG.0000000000003020

Weissgerber, T. L., Milic, N. M., Milin-Lazovic, J. S., and Garovic, V. D. (2016). Impaired flow-mediated dilation before, during, and after preeclampsia: a systematic review and meta-analysis. *Hypertension* 67 (2), 415–423. doi:10.1161/HYPERTENSIONAHA.115.06554

Yinon, D., Lowenstein, L., Suraya, S., Beloosesky, R., Zmora, O., Malhotra, A., et al. (2006). Pre-eclampsia is associated with sleep-disordered breathing and endothelial dysfunction. *Eur. Respir. J.* 27 (2), 328–333. doi:10.1183/09031936.06.00010905

frontiers | Frontiers in Physiology

TYPE Original Research
PUBLISHED 18 March 2025
DOI 10.3389/fphys.2025.1561867

OPEN ACCESS

EDITED BY
Luis A. Martinez-Lemus,
University of Missouri, United States

REVIEWED BY
Zhongkui Hong,
Texas Tech University, United States
Camilla Ferreira Wenceslau,
University of South Carolina, United States
Erik Josef Behringer,
Loma Linda University, United States

*CORRESPONDENCE
Aaron J. Trask,
aaron.trask@nationwidechildrens.org

RECEIVED 16 January 2025
ACCEPTED 19 February 2025
PUBLISHED 18 March 2025

CITATION
McCallinhart PE, Stone KR, Lucchesi PA and Trask AJ (2025) Coronary cytoskeletal modulation of coronary blood flow in the presence and absence of type 2 diabetes: the role of cofilin.
Front. Physiol. 16:1561867.
doi: 10.3389/fphys.2025.1561867

Coronary cytoskeletal modulation of coronary blood flow in the presence and absence of type 2 diabetes: the role of cofilin

Patricia E. McCallinhart[1], Kathlyene R. Stone[1], Pamela A. Lucchesi[2] and Aaron J. Trask[1,3]*

[1]Center for Cardiovascular Research, The Heart Center, The Abigail Wexner Research Institute at Nationwide Children's Hospital, Columbus, OH, United States, [2]Department of Undergraduate Medical Education, University of Texas Tyler School of Medicine, Tyler, TX, United States, [3]Department of Pediatrics, The Ohio State University College of Medicine, Columbus, OH, United States

Background: Coronary resistance microvessels (CRMs) from type 2 diabetic (T2DM) mice and pigs are less stiff compared to normal, a finding that is dictated by less stiff coronary vascular smooth muscle cells (VSMCs). Cofilin is an endogenous actin regulatory protein that depolymerizes filamentous (F)-actin, and portions of F-actin bound to cofilin are less stiff compared to their unbound F-actin counterparts. In this study, we hypothesized that altering the actin cytoskeleton modifies VSMC stiffness, which contributes to changes in coronary blood flow in normal and T2DM conditions.

Methods and results: Utilizing phalloidin staining, we found that F-actin was significantly reduced in T2DM CRM VSMCs, and we showed cofilin expression was increased in T2DM by proteomics and Western blot analysis. Cofilin knockdown in both human and mouse coronary VSMCs using siRNA significantly increased F/G actin ratio. Cofilin knockdown also caused a significant increase in elastic modulus by atomic force microscopy of coronary VSMCs. Treatment with Latrunculin B, an actin disruptor, significantly decreased VSMC elastic modulus. Acute Latrunculin B infusion into the coronary circulation of *ex vivo* isolated Langendorff mouse hearts increased peak coronary blood flow.

Conclusion: Together, we demonstrated that the CRM VSMC actin cytoskeleton is altered in T2DM to favor less stiff cells, and pharmacological manipulation of the actin cytoskeleton alters VSMC biomechanics. This study is also the first to demonstrate that coronary cellular modulation of mechanics can acutely modulate coronary blood flow.

KEYWORDS

coronary microcirculation, vascular smooth muscle cells, diabetes, cofilin, actin remodeling, coronary blood flow

1 Introduction

Type 2 diabetes mellitus (T2DM) is a metabolic disorder characterized by hyperglycemia and insulin resistance and is recognized as a cardiovascular disease due

to the high associated prevalence of myocardial infarction (MI), atherosclerosis, and coronary artery disease (CAD) in T2DM patients (Gil-Ortega and Carlos Kaski, 2006; Mozaffarian et al., 2015). Over 500 million adults between the ages 20–79 are living with diabetes and it is projected to reach 643 million by 2030 and 783 million by 2045 (IDF Diabetes Atlas, 2023). Despite several decades of research and therapy targeting these conditions, cardiovascular complications, including MI, remain the number one cause of death in T2DM patients (Tsao et al., 2023; Grundy et al., 1999). Coronary blood flow (CBF) is crucial for supplying the heart cells with the nutrients they need to meet their metabolic demands, and any reduction in CBF can lead to severe conditions like heart failure. Coronary microvascular disease (CMD) is increasingly recognized as an early subclinical contributor to perturbations in CBF and ultimately, heart disease (McCallinhart et al., 2024). Previous data from our laboratory demonstrated that adverse structural remodeling of coronary resistance microvessels (CRMs) and impaired CBF occur in T2DM (Katz et al., 2011; Trask et al., 2012a; Trask et al., 2012b; Husarek et al., 2016a; Trask et al., 2012a). We previously reported that the process of T2DM CRM remodeling occurs early, equivalent to premature aging (McCallinhart et al., 2018). Diabetic macrovessels such as the aorta and carotid arteries increase in stiffness (Reddy, 2004). However, previous anti-dogmatic data from our laboratory revealed that CRMs are less stiff in both T2DM and metabolic syndrome (MetS) (Katz et al., 2011; Trask et al., 2012b) – a finding that does not appear to be due to the extracellular matrix (ECM) (Anghelescu et al., 2015; Katz et al., 2011; Trask et al., 2012a). Rather, utilizing atomic force microscopy (AFM), we showed that primary CRM vascular smooth muscle cells (VSMCs) isolated from db/db mice and T2DM humans were less stiff relative to normal, indicating that overall CRM tissue stiffness is driven by coronary VSMCs (McCallinhart et al., 2020). This observation raised the intriguing possibility that the molecular mechanisms that regulate cellular stiffness may play a central role in the pathophysiology of CMD.

The VSMC actin cytoskeleton is an integral component that not only contributes to the structural integrity of the cell, but also allows for cell movement and contraction. The connection of cytoskeletal components to the basement membrane and the surrounding ECM is dictated by focal adhesion (FA) complexes and together they contribute to cellular mechanics (Lacolley et al., 2017). Actin's structural and biomechanical roles also arise from the ability to dynamically polymerize and depolymerize, forming polymers and filaments of varying lengths (Serebryannyy et al., 2016). Filamentous actin (F-actin) is a thin flexible fiber-type microfilament made up of monomeric globular actin (G-actin). It is widely accepted that actin filaments provide mechanical stability by regulating cell elastic modulus (Fels et al., 2014; Grimm et al., 2014; Sehgel et al., 2013) and that disruption of the cytoskeleton via pharmacological agents causes a striking reduction in cell stiffness (Petersen et al., 1982; Wakatsuki et al., 2001). Conversely, actin stabilizers/polymerizers, including jasplakinolide, enhance myogenic tone via smooth muscle contraction and increased F-actin to G actin-ratio (Cipolla et al., 2002).

Cofilin is an endogenous actin regulatory protein that depolymerizes F-actin and severs the actin filaments. Interestingly, portions of F-actin bound to cofilin have decreased stiffness compared to their unbound F-actin counterparts (McCullough et al., 2008; Schramm et al., 2017). Interestingly, there are reports that arterial stiffening adversely affects coronary flow and flow reserve, but those data are taken from large conduit arteries outside of the coronary circulation (Fukuda et al., 2006; Leung et al., 2006; Tritakis et al., 2016). However, little is known about the role of altering the actin cytoskeleton in coronary VSMCs and how that contributes to CBF. The goal of this present study was to test the hypothesis that modulating coronary cellular stiffness inversely affects coronary blood flow in normal and T2DM mice and that cofilin plays a role. To test this hypothesis, we used a combination of siRNA knockdown experiments, AFM, pharmacological modulation of the actin cytoskeleton, and Langendorff isolated hearts in mice.

2 Methods and materials

2.1 Materials

Antibodies: Total cofilin (D3F9) #5175 (concentration 1:1000) was acquired from Cell Signaling Technology for Western blot analysis. Beta actin (8226) (concentration 1:1000) was obtained from Abcam for Western blot analysis. Cofilin (PA5-27627) for staining (concentration 1:200), deoxyribonuclease 1 Alexa Fluor 488 for G-actin staining (concentration 1:200), and phalloidin Alexa Fluro 568 for F-actin staining (concentration 1:400), were all purchased from Invitrogen (Waltham, MA). 4′,6-Diamidino-2-phenylindole dihydrochloride (DAPI) from MP Biomedicals (Solon, OH) was used for nuclear staining (1:500).

Mouse cofilin siRNA and scramble siRNA were purchased from Invitrogen (Waltham, MA). Human cofilin siRNA and scramble were purchased from Dharmacon (Lafayette, CO). Deidentified normal and T2DM human primary coronary VSMCs were obtained from both Lonza (Morristown, NJ) and ATCC (Manassas, VA). All other reagents were purchase from Fisher Scientific (Pittsburgh, PA) unless otherwise noted.

2.2 Animals

Male T2DM homozygous *db*/*db* and control nondiabetic heterozygous *Db*/*db* mice were acquired from The Jackson Laboratories. By 4 weeks of age, *db*/*db* mice are leptin receptor deficient and develop hyperglycemia, obesity, insulin resistance, and dyslipidemia. They were housed under a 12 h light,12 h dark cycle at 22°C and 60% humidity and were allowed *ad libitum* access to standard low-fat laboratory chow and water. All experiments were conducted at 16–17 weeks of age. This study was conducted in accordance with National Institutes of Health guidelines, and it was approved by the Institutional Animal Care and Use Committee at Nationwide Children's Hospital.

Abbreviations: AFM, atomic force microscopy; CAD, coronary artery disease; CBF, coronary blood flow; CMD, coronary microvascular disease; CRM, coronary resistance microvessel; ECM, extracellular matrix; LatB, latrunculin B; MetS, metabolic syndrome; MI, myocardial infarction; T2DM, type 2 diabetes mellitusv; VSMC, vascular smooth muscle cell.

2.3 Blood glucose measurements

Blood was drawn from the mouse tail vein and glucose levels were determined with the AlphaTrak glucometer (Abbott Laboratories, Alameda, CA).

2.4 Proteomics

Septal CRMs were isolated from both normal heterozygous Db/db and diabetic homozygous db/db mice and were pooled (n = 4-5 pools of 4 CRMs per biological replicate) for proteomic data collection/analysis. CRMs were lysed by repeated sonication in 110 µL tissue lysis buffer + protease and phosphatase inhibitors + antifoaming agent. Lysates were kept cold and centrifuged briefly at 4°C between sonications to bring unlysed material to the bottom of the tube. All lysates were centrifuged 10 min, 4°C, 14,000 RPM and supernatants were removed to fresh tubes. 16 µg protein of each sample were methanol/chloroform precipitated. Dried samples were resuspended in SDS loading buffer, heated to 70°C for 5 min, and then separated on a 10% SDS-PAGE gel. The Sypro-stained gel was analyzed by LC-MS/MS (LTQ mass spec followed by 2D LC chromatography–MudPIT; Mascot sequence identification) at the Ohio State University Mass Spec & Proteomics Facility.

2.5 Mouse coronary VSMC isolation

Normal Db/db and T2DM db/db mouse CRM VSMCs were isolated as previously described by our laboratory (Husarek et al., 2016b; McCallinhart et al., 2020). In short, hearts were isolated from anesthetized mice (3% isoflurane until lack of toe pinch response) and gently perfused via retrograde Langendorff with digestion solution having ~300 U/mL of collagenase type II (Worthington), 0.1 mg/mL soybean trypsin inhibitor, and 1 mM $CaCl_2$. Every 15 min, the perfusates were collected, centrifuged, resuspended in growth medium, and placed in a 37°C incubator. After coronary perfusate collections were finished for a total of 90 min of digestion, all the resuspended cells were combined into one tube, pelleted by centrifugation, resuspended in plating medium, and plated on 35-mm tissue culture dishes. Diabetic VSMCs were cultured in high-glucose (25 mM) DMEM, whereas nondiabetic VSMCs were cultured in normal-glucose (15 mM) DMEM. All experiments were performed with passage 2 or lower coronary microvascular VSMCs. To obtain adequate numbers of cells for experiments, cells from n = 2 mice were pooled into one 35-mm dish for each biological replicate.

2.6 Western blot

Human coronary VSMCs were washed twice with ice-cold PBS and then lysed with 90 µL of ice-cold lysate buffer (modified Hunter buffer freshly supplemented with 0.5 mM PMSF, 10 µg/mL aprotinin, 1 mM Na_3VO_4). Following sonication at 4°C for 10 s, lysates were spun at 15,000 rpm at 4°C for 15 min. Protein levels were quantified following the specified protocol in the BCA kit (Pierce). Ten micrograms of VSMC protein lysates (n = 4-5 per group) were separated on 8%–12% SDS-PAGE gels that were transferred to PVDF membranes for 1 h on ice. The membranes were then blocked in 5% milk in PBS with 0.5% Tween 20 (PBST) at room temperature for 1 h. Antibodies were diluted in 2.5% milk with PBST and then membranes incubated overnight at 4°C. Membranes were washed three times in PBST and then incubated in the appropriate horseradish peroxidase (HRP) secondary antibody for 1 h at room temperature. Membranes were washed again three times in PBST and then imaged and analyzed with Bio-Rad Image Lab.

2.7 siRNA and latrunculin B VSMC treatments

Human: Human primary coronary VSMCs (passage 5–7) were plated at 0.4×10^4 cells per well onto an 8-well chamber slide. 24 h later at approximately 60%–80% confluency, cells were then treated for 48 h prior to experiments with either cofilin siRNA (10 µM) or scramble transfection control from Cell Signaling Technology in antibiotic free, low serum DMEM, utilizing Lipofectamine RNAiMAX Transfection protocol following manufacturer's instructions (Invitrogen/ThermoFisher). Transfection efficiency was confirmed 48 h post transfection by immunofluorescent staining. For Latrunculin B (LatB), cells were incubated in low serum media for 24 h. LatB (1 µM) was added 2 h prior to AFM or fixation.

Mouse: Experiments were performed on passage 1 mouse primary coronary VSMCs. Cells were plated at 0.4×10^4 cells per well onto an 8-well chamber slide. Following 24 h in culture, cells (60%–80% confluency) were treated with antibiotic free, low serum medium containing DharmaFECT 1 transfection reagent and either 100 nmol of nontargeting siRNA or siRNA specifically targeting cofilin (Dharmacon SMARTpool) for 48 h prior to experiments. Transfection efficiency was confirmed 48 h post transfection by immunofluorescent staining. For LatB, cells were incubated in low serum media for 24 h. LatB (1 µM) was added 2 h prior to AFM or fixation.

2.8 Atomic force microscopy

For mouse VSMC (n = 5 for all groups) and human VSMC (n = 4-5 for all groups) AFM experiments, cells were treated as described above. Using an Asylum MFP-3D-Infinity-BIO atomic force microscope (AFM) with probes (Bruker MLCT) coated with 0.5 mg/mL fibronectin (FN, Gibco), a nano-indentation protocol (Costa, 2003; Hong et al., 2015) was used to measure elastic modulus, an indicator of cellular stiffness, and adhesion to FN. The following parameters were set for each experiment: Force Distance was set to 1.6 µm, sample rate was set to 625 Hz, and set point was set to 0.3 V. For each experiment, we collected 25–35 curves per cell and 8–12 cells per dish. The AFM data were collected and analyzed using Igor Pro software (WaveMetrics). Elastic modulus was calculated using the Oliver-Pharr method, a modified Hertz model (Akhtar et al., 2009).

2.9 Immunofluorescence

Cells were gently rinsed cells with cold phosphate buffer saline (PBS) twice and then fixed on ice with cold 2% paraformaldehyde

(PFA) for 30min. After fixation, the cells were rinsed with PBS twice and then treated with PBS-Tween-Triton for a 20-min permeabilization. Next the cells were incubated in fish skin gelatin blocking solution for 30 min at room temperature. Next, for assessing F/G actin, the cells were then incubated for 30 min with DNAse (488) and phalloidin (567), and DAPI to stain for G-actin, F-actin, and the nuclei, respectively. To assess cofilin expression, cells were incubated primary cofilin antibody overnight at 4°. The following morning, cells were washed with PBS three times, then incubated with secondary antibody for 1 h at room temperature. Next, all cells were washed with PBS three times and then fresh PBS was added to cover cells. Cells were then imaged using an Olympus IX51 and intensity per cell was measured using the NIH ImageJ software.

2.10 Heart isolation and langendorff perfusion

Isolated mouse whole hearts were rapidly excised and perfused at a constant pressure (80 mmHg) with Kreb's solution (in mM: NaCl 118, KCl 4.7, $MgSO_4$ 1.64, KH_2PO_4 1.18, $CaCl_2$ 2.52, $NaHCO_3$ 25, Glucose 5.55, Na-pyruvate 2) on a Langendorff apparatus (Model IH-SR, Harvard Apparatus) as previously described by us (Trask et al., 2007; Trask et al., 2008). Flow was continuously monitored using a flow meter (Model TS420, Transonic Flow Systems) connected to a PowerLab 16/30 (AD Instruments), and data were acquired and analyzed using LabChart 8 (AD Instruments). Following a 15-min equilibration, ML-7 (myosin light chain kinase inhibitor to remove basal active tone) was infused directly into the coronary circulation via a custom dual PE-10 catheter using a custom modification to the system's infusion port that allows for the direct infusion into the coronary circulation. ML-7 was infused toward a target concentration of 50 μM to inhibit MLCK in cells. After 15 min of ML-7, LatB was added to the infusion toward a concentration target of 1 μM, which was shown to effectively inhibit acting polymerization and reduce cellular stiffness (Embry et al., 2016). Infusion rates were controlled using syringe pump (Model 11 Plus, Harvard Apparatus) and were adjusted every 5 min during infusion to account for changes in CBF. The infusion rate was adjusted based on the coronary flow, e.g., at 50 μL/min per coronary flow mL/min (e.g., 50 μL/min when coronary flow was 1 mL/min) for both ML-7 pre-treatment and LatB/ML-7 infusion. Data are reported at 3 timepoints; baseline (after 15-min equilibration/before ML-7 infusion), ML-7 (at the end of 15-min ML-7 pre-treatment), and LatB (at the end of ~15-min ML-7/LatB infusion).

2.11 Statistical analysis

All data are expressed as means ± SEM, with a probability of $p < 0.05$ used to denote statistical significance with GraphPad Prism 8 (GraphPad Software, La Jolla, CA). A power calculation (90% power, $\alpha < 0.05$), based on mean differences in coronary VSMC stiffness, indicated that $n = 3$ were needed per group. Either ANOVA or Student's t-test were performed. Data values that were beyond ±2 standard deviations of the mean were excluded from analysis.

3 Results

3.1 CRM VSCM actin cytoskeleton favors less stiff cell in diabetes

Since actin can dynamically polymerize and depolymerize to contribute to the structure and biomechanics of the cell (Serebryannyy et al., 2016), and diabetes can lead to dysregulation of actin polymerization and depolymerization dynamics in other cell types (Romanelli et al., 2020), we aimed to determine whether endogenous F-actin and G-actin content were altered in diabetic db/db mice CRM VSMCs to favor a less stiff cytoskeleton. In mouse primary CRM VSMCs, F-actin content was significantly decreased in db/db CRM VSMCs (normal 2485 ± 206 vs. T2DM 560 ± 149, $p = 0.0016$, n = 3) (Figure 1). There was an insignificant trend for a decreased F/G actin ratio in the diabetic cells (Figure 1). There was no significant difference in G-actin levels between control and T2DM coronary VSMCs (Figure 1).

3.2 Cofilin expression is increased in T2DM mouse CRMs and human coronary VSMCs

Given the well-established role cofilin plays in actin dynamics, we next investigated whether cofilin may account for observed differences in actin cytoskeleton (decreased F-actin) in both diabetic animals and human cells since (Figure 1). Utilizing proteomics analysis, we obtained zero cofilin spectral hits in normal mouse CRMs and 3-4 spectral hits in each db/db CRM pooled sample set (0.00 ± 0.0 vs. 3.40 ± 0.25, $p < 0.0001$) (Figure 2). In human coronary VSMCs, cofilin protein was increased in the coronary VSMCs of diabetic patients compared to normal (normal 1.00 ± 0.16 vs. T2DM 1.837 ± 0.35, $p < 0.05$) (Figure 2).

3.3 Cofilin knockdown changes F/G actin and stiffness to favor a less stiff cell in human coronary VSMCs

Since we observed an increase in cofilin protein in T2DM CRMs and VSMCs, we next interrogated the role of cofilin in VSMC stiffness. We utilized cofilin siRNA to significantly reduce expression (34% reduction in normal, $p = 0.0190$ and 45% reduction in diabetic, $p = 0.0055$) (Figure 3) in our coronary VSMCs. We further tested the contribution of cofilin to the F/G actin ratio of coronary VSMCs by utilizing cofilin siRNA. Cofilin knockdown caused a significant increase in the F/G actin ratio when normal and diabetic data were pooled (scramble 3.029 ± 0.49 vs. siRNA 4.029 ± 0.68, $p = 0.018$, n = 8) (Figure 4). This increased F/G ratio was significant in the diabetic coronary VSMCs (scramble 2.636 ± 0.46 vs. siRNA 3.685 ± 0.41, $p = 0.049$, n = 4), and trended in the normal cells but did not reach statistical significance (scramble 3.423 ± 0.89 vs. cofilin siRNA 4.373 ± 1.37, $p = 0.22$, n = 4) (Figure 4). We next determined how cofilin impacts cellular elastic modulus, an indicator of cell stiffness. Cofilin knockdown by siRNA caused a significant increase in stiffness when normal and diabetic VSMC data were pooled (scramble 1.814 ± 0.25 vs. siRNA 3.074 ± 0.35, $p = 0.0057$, n = 8) (Figure 4) and in normal VMSCs (scramble 2.038 ± 0.31 vs. siRNA 3.445 ± 0.30, $p < 0.05$, n = 4). The trend

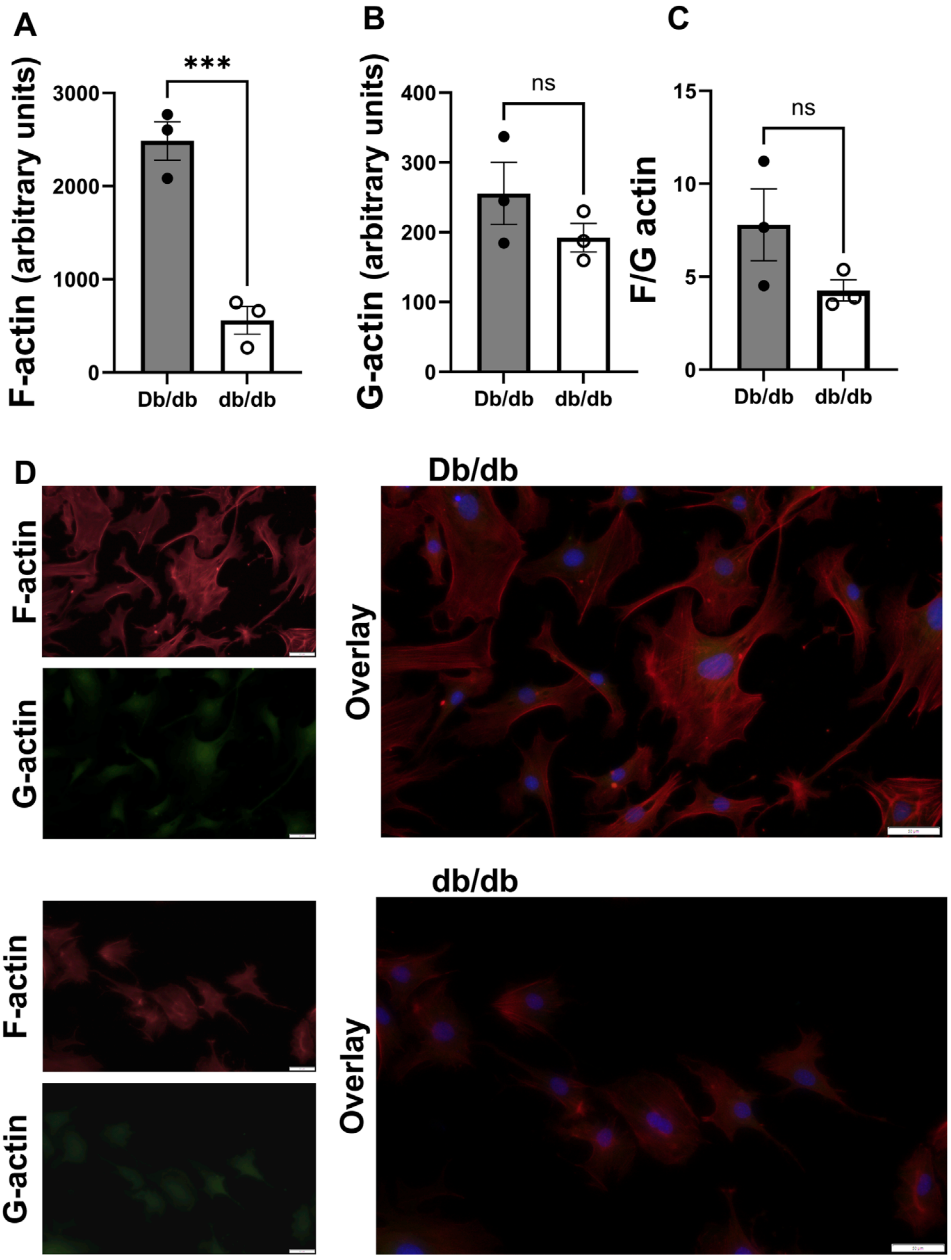

FIGURE 1
F actin is reduced in diabetic CRMs: **(A)** F actin content in control and diabetic mouse coronary VSMCs obtained via staining with phalloidin. **(B)** G actin levels in control and T2DM mouse coronary VSMCs attained through staining with DNase. **(C)** F/G actin ratio of mouse normal and diabetic coronary VSMCs. **(D)** Representative images from Db/db (top) and db/db (bottom). Data are mean ± SEM.**p ≤ 0.005. n = 3 per group.

in the diabetic VSMCs did not achieve statistical significance (scramble 1.589 ± 0.40 vs. siRNA 2.702 ± 0.62, $p = 0.18$, n = 4) (Figure 4).

3.4 F/G actin and stiffness are modified via cofilin siRNA in mouse coronary VSMCs

Cofilin siRNA treatment triggered a significant increase in the F/G actin ratio when control and diabetic data were pooled (scramble 6.838 ± 0.60 vs. siRNA 10.53 ± 1.15, $p = 0.005$, n = 5) (Figure 5). This increased F/G ratio trended in the diabetic coronary VSMCs (scramble 7.549 ± 0.74 vs. siRNA 11.35 ± 1.87, $p = 0.08$, n = 3), and trended in the control cells but did not reach statistical significance (scramble 5.772 ± 0.19 vs. cofilin siRNA 9.284 ± 0.34, $p = 0.09$, n = 2) (Figure 5). Cofilin knockdown caused a significant increase in stiffness when normal and diabetic VSMC data were pooled (scramble 1.994 ± 0.38 vs. siRNA 6.303 ± 0.32, $p < 0.0001$, n = 10) (Figure 5). Cofilin siRNA treatment significantly increased control VMSC stiffness (scramble 4.316 ± 0.37 vs. siRNA 6.613 ± 0.40, $p = 0.003$, n = 5) and significantly increased stiffness of the diabetic VSMCs (scramble 2.402 ± 0.23 vs. siRNA 5.993 ± 0.51, $p = 0.0002$, n = 5) (Figure 5).

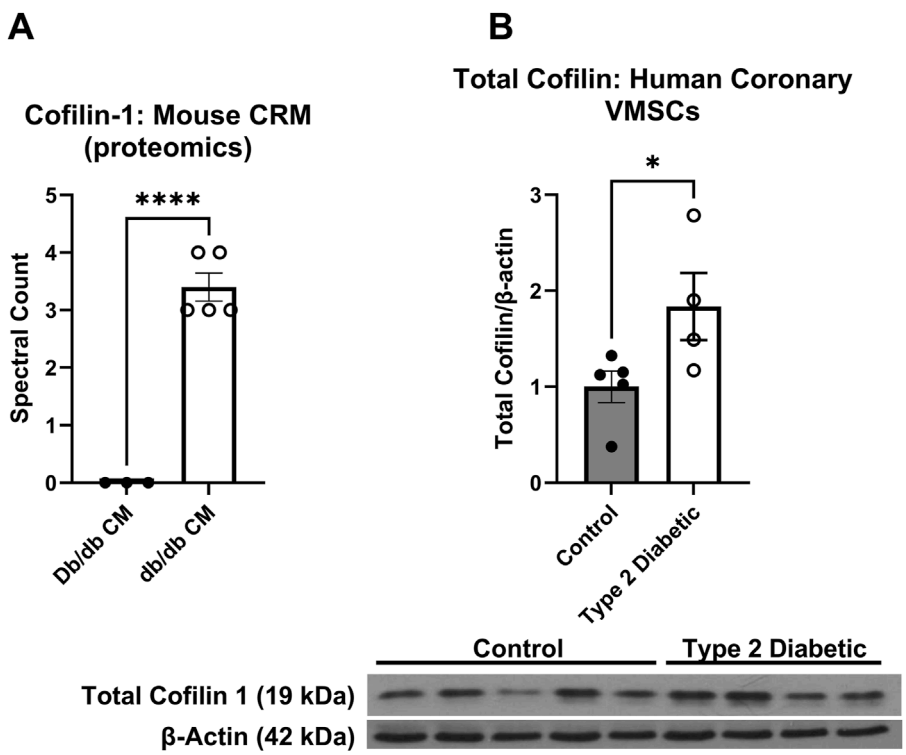

FIGURE 2
Cofilin is increased in T2DM coronary microvessels: **(A)** Proteomics analysis of cofilin spectral hits in the normal CRMs db/db CRMs. **(B)** Cofilin protein expression obtained via western blot analysis in the coronary VSMCs of normal and diabetic human patients. Data are mean ± SEM. p-values are presented on the graph and*p < 0.05 and****p ≤ 0.0001. n = 3-5 per group.

3.5 Latrunculin B significantly reduced VSMC stiffness

Next, we investigated how altering actin with a direct actin-disturbing agent alters elastic modulus. We utilized LatB is a well-known actin depolymerizing agent to disrupt the actin cytoskeleton in coronary VSMCs. In both mouse and human coronary VSMCs, LatB significantly reduced elastic modulus in the normal/control (mouse control vehicle 4.303 ± 1.12 vs. mouse LatB 1.365 ± 0.31, $p < 0.0001$, n = 5 and human normal vehicle 2.357 ± 0.50 vs. normal LatB: 0.3369 ± 0.17, $p = 0.0003$, n = 2–3) (Figure 6) groups as well as in the diabetic groups (mouse T2DM vehicle 3.208 ± 1.13 vs. mouse T2DM LatB: 1.623 ± 0.44, $p = 0.0048$, n = 5 and human T2DM vehicle: 2.030 ± 0.88 vs. human T2DM LatB: 0.4465 ± 0.04, $p = 0.0200$, n = 2–3) (Figure 6).

3.6 Latrunculin B normalizes CBF in isolated hearts

To assess whether modulating coronary cell stiffness can affect CBF, we directly infused LatB into the coronary circulation of Langendorff isolated hearts. As we have demonstrated *in vivo* (Katz et al., 2011), baseline CBF in was lower in hearts isolated from T2DM db/db mice (Figure 7A; Db/db: 0.70 ± 0.12 mL/min vs. db/db: 0.32 ± 0.04 mL/min, $p < 0.01$). After baseline measurements, the myosin light chain kinase inhibitor, ML-7, was infused first to remove active coronary tone. ML-7 resulted in a significant increase in CBF in db/db mice (Figure 7B; $p < 0.05$). LatB further augmented CBF in both normal and T2DM hearts (Figure 7B; Db/db: $p < 0.05$ and db/db: $p < 0.01$ vs. respective baselines).

4 Discussion

The actin cytoskeleton plays a crucial role in shaping and maintaining the mechanical properties of cells. Its dynamic cycle of polymerization and depolymerization allows cells to adapt to changing conditions in an attempt to maintain their biomechanical functionality. Our laboratory has previously demonstrated that T2DM or MetS coronary resistance microvessels are less stiff compared to normal CRMs, and that coronary VSMCs from T2DM humans and mice have a reduced elastic modulus, the primary indicator of stiffness (Katz et al., 2011; McCallinhart et al., 2020; McCallinhart, Scandling, and Trask, 2021; Trask et al., 2012b). In our current study, we examined how T2DM impacts the actin cytoskeleton, as well as the contribution of the altered cytoskeleton to stiffness and coronary blood flow. We observed significant reduction in F-actin in coronary VSMCs from T2DM mice. Cofilin, an actin depolymerizing protein, was significantly increased in T2DM as validated by both proteomic data from mice and Western Blot data from human coronary VSMCs. The F/G actin ratio was increased when we knocked down cofilin via siRNA treatment, which also led to a concomitant significant increase in VSMC stiffness in both mouse and human coronary VSMCs. We

10.3389/fphys.2025.1561867

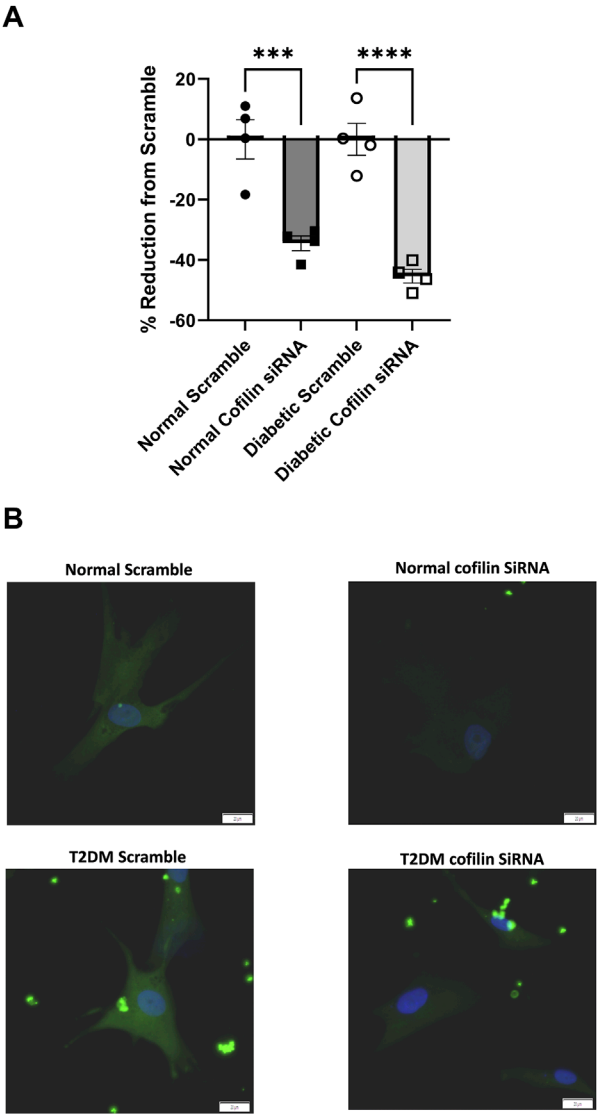

FIGURE 3
Cofilin siRNA reduces protein expression: **(A)** Percent reduction of cofilin expression after treatment with cofilin siRNA. **(B)** Representative images. Data are mean ± SEM. p-values are presented on the graph;***p ≤ 0.001 and****p ≤ 0.0001 vs. respective scramble. n = 4 per group. Scalebar: 20 μm.

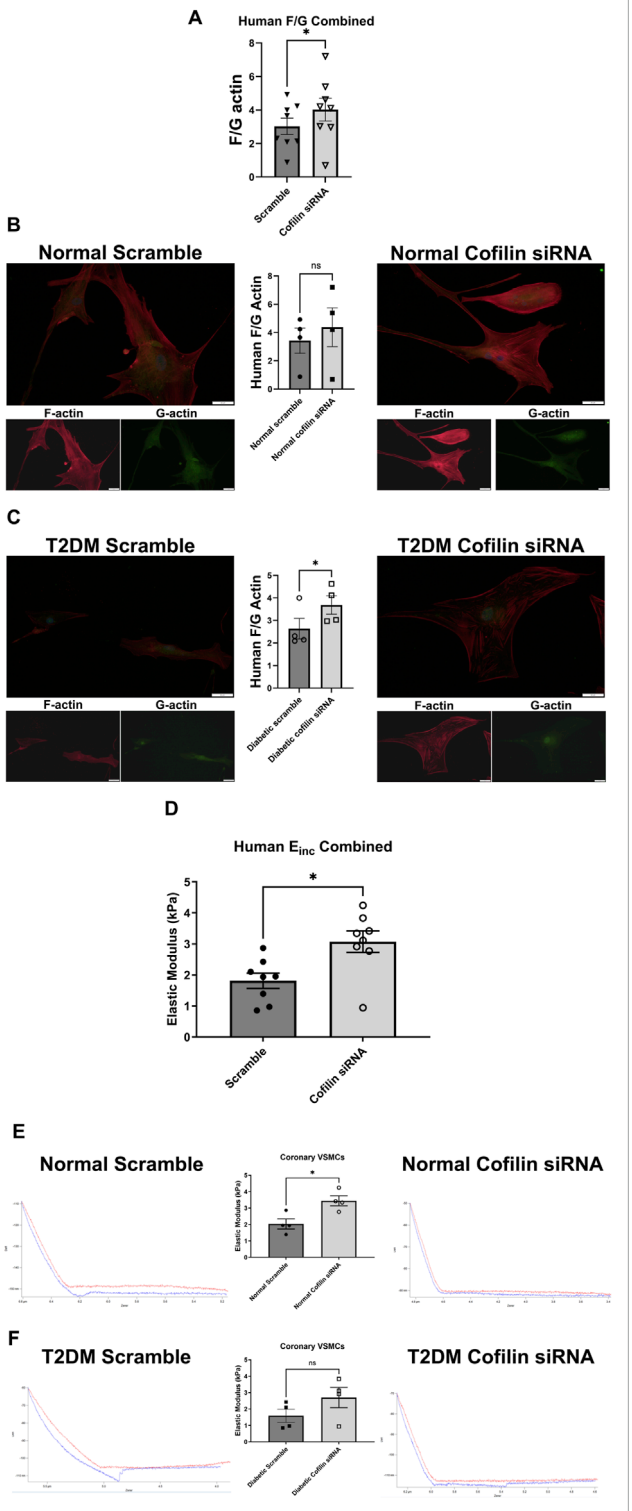

FIGURE 4
Cofilin knockdown causes altered F/G actin ratio and a significant increase in stiffness in human coronary VSMCs: **(A)** F/G actin ratio of normal and diabetic combined human coronary VSMCs treated with cofilin siRNA obtained via staining F actin (phalloidin) and G actin (DNase). **(B)** F/G actin ratio of cofilin siRNA treated normal coronary VSMCs. **(C)** F/G actin ratio of human diabetic coronary VSMCs treated with cofilin siRNA. **(D)** Elastic modulus (E_{inc}) of normal and diabetic combined human coronary VSMCs treated with cofilin siRNA acquired via atomic force microscopy. **(E)** Elastic modulus of cofilin siRNA treated human normal coronary VSMCs. **(F)** Elastic modulus of human diabetic coronary VSMCs treated with cofilin siRNA. Data are mean ± SEM.*p < 0.05. n = 4-8 per group.

also directly modified the coronary cell actin cytoskeleton utilizing LatB treatment that significantly decreased both mouse and human coronary VSMC stiffness and increased CBF when *ex vivo* hearts were treated with ML-7 (to remove tone) and LatB. These data clearly demonstrate a novel role for cofilin in governing CRM VSMC actin cytoskeleton regulation and further suggest that it may play a role in the regulation of CBF.

T2DM triggers a cascade of biochemical changes that adversely affect the VSMCs cytoskeleton. Actin is most recognized for its role as a key component of the cytoskeleton, where it significantly influences cell shape, movement, and signaling. Diabetes can lead to dysregulation of actin polymerization and depolymerization dynamics (Romanelli et al., 2020). F-actin, the filamentous form, is a major

10.3389/fphys.2025.1561867

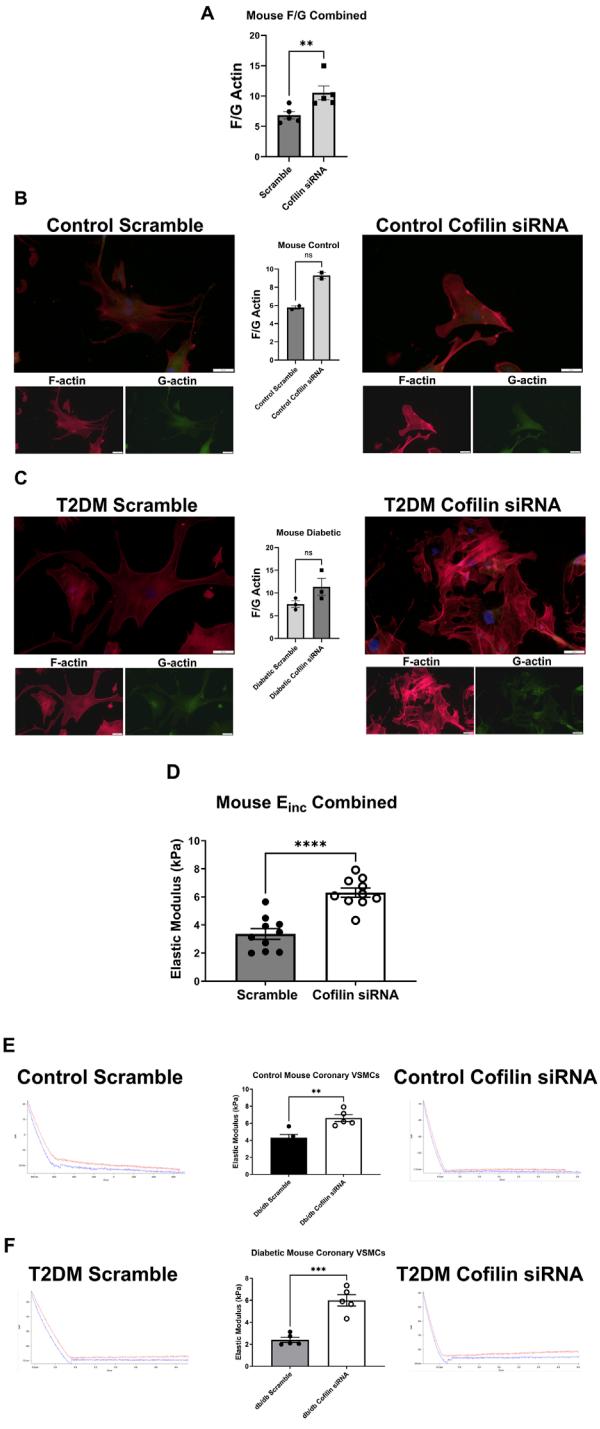

FIGURE 5
Cofilin siRNA disrupts the F/G actin ratio and increases stiffness in mouse coronary VMSCs: **(A)** F/G actin ratio of mouse normal and diabetic combined coronary VSMCs treated with cofilin siRNA obtained via staining F actin (phalloidin) and G actin (DNase). **(B)** Normal control mouse coronary VSMC F/G actin ratio after cofilin siRNA treatment. **(C)** F/G actin ratio of mouse diabetic coronary VSMCs treated with cofilin siRNA. **(D)** Normal and diabetic combined mouse coronary VSMCs treated with cofilin siRNA elastic modulus (E_{inc}) data obtained using atomic force microscopy. **(E)** Elastic modulus of cofilin siRNA treated normal control mouse coronary VSMCs. **(F)** Elastic modulus of mouse diabetic coronary VSMCs treated with cofilin siRNA. Data are mean ± SEM.**p < 0.005,***p < 0.0005, and****p < 0.0001 vs. respective scramble control. n = 2–10 per group.

component of the cytoskeleton and is essential for the formation and maintenance of focal adhesions. It is well-documented that the actin cytoskeleton bestows mechanical stability by regulating cell stiffness (Fels et al., 2014; Grimm et al., 2014; Sehgel et al., 2013). We have previously reported that T2DM decreases coronary VMSC stiffness (McCallinhart et al., 2020); as such, we aimed to investigate how the actin cytoskeleton contributes to altered stiffness in coronary VMSCs in the presence and absence of T2DM. Studies have reported that diabetes leads to cytoskeleton disorganization in cardiac and skeletal muscle via measured F-actin fluorescence in muscles of diabetic animals (Romanelli et al., 2020). Similarly, multiple studies have reported decreased F-actin content in diabetic myocardial tissue leading to cytoskeleton disorganization (Kawaguchi et al., 1999; Nemoto et al., 2006; Zhang et al., 2008). Benech et al. (2014) reported that diabetic cardiomyocytes displayed a more diffuse and irregular actin arrangement compared to control isolated cardiomyocytes that exhibited a regular and well-defined actin organization. In the same study, the authors utilized AFM to reveal that both aging and diabetic cardiomyocytes are stiffer compared to controls. Similarly to these studies, we found that control coronary VSMCs have significantly higher F-actin content compared to T2DM coronary VSMCs (Figure 1), which may account for higher stiffness in normal CRMs compared to T2DM CRMs (Katz et al., 2011; McCallinhart et al., 2020; Trask et al., 2012a).

To interrogate a possible mechanism that may be responsible for reduced F-actin content in the diabetic coronary VSMCs, we focused on cofilin initially based on a proteomic screen (Figure 2). Cofilin is an endogenous actin regulatory protein that depolymerizes F-actin and severs the actin filaments. While very little is known about cofilin in the coronary VSMCs, actin dynamics are crucial in many organs and tissues in T2DM, including a role for cytoskeletal remodeling in maintaining neuronal morphology and long-term memory (Lacolley et al., 2017). Interestingly, diabetic mice exhibited cognitive impairment at 17 weeks of age and cofilin and G-actin were highly expressed in the CA1 region of hippocampus, while phosphorylated (P)-cofilin and F-actin expression decreased (Li et al., 2023). Other recent studies have highlighted the role of cofilin in actin dynamics in diabetic conditions. Hyperglycemic conditions stimulated actin polymerization measured via F/G actin ratio and induced mRNA and protein expression of contractile smooth muscle markers in cultured mouse aortic VSMCs (Hien et al., 2016). In that same study, cofilin phosphorylation was significantly increased via high glucose treatment (Hien et al., 2016). In this study, we showed that total cofilin levels were significantly increased in T2DM human coronary VSMCs, as well as in the CRMs of db/db T2DM mice (Figure 2). These studies implicate a role for glucose levels impacting functionality and cofilin and the actin cytoskeleton.

Given the well-established relationship between cofilin and its regulation of actin remodeling, we next examined how knocking down cofilin would impact the F-actin to G-actin ratio in coronary vascular smooth muscle cells. In both human and mouse coronary VSMCs, cofilin siRNA significantly increased the F/G actin ratio when normal and diabetic data are combined (Figures 4, 5). This trend persisted when normal and diabetic are separated but only reached significance in the human coronary diabetic VSMCs (Figure 4). Interestingly, recent studies have shown that portions of F-actin bound to cofilin have a decreased stiffness compared to their unbound F-actin counterparts

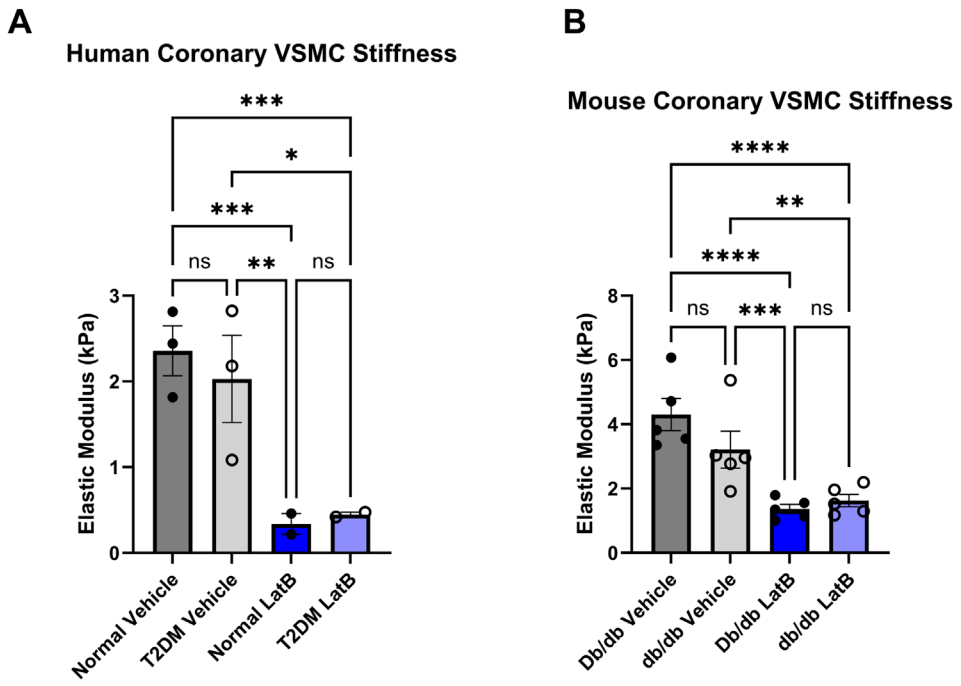

FIGURE 6
Latrunculin B treatment of coronary VSMCs significantly reduces cellular stiffness: **(A)** Elastic modulus acquired via atomic force microscopy of LatB treated normal and diabetic human coronary VSMCs. **(B)** LatB treated mouse normal and diabetic coronary VSMC elastic modulus. Data are mean ± SEM.*p < 0.05,**p < 0.005,***p < 0.0005, and****p < 0.0001. n = 2-5 per group.

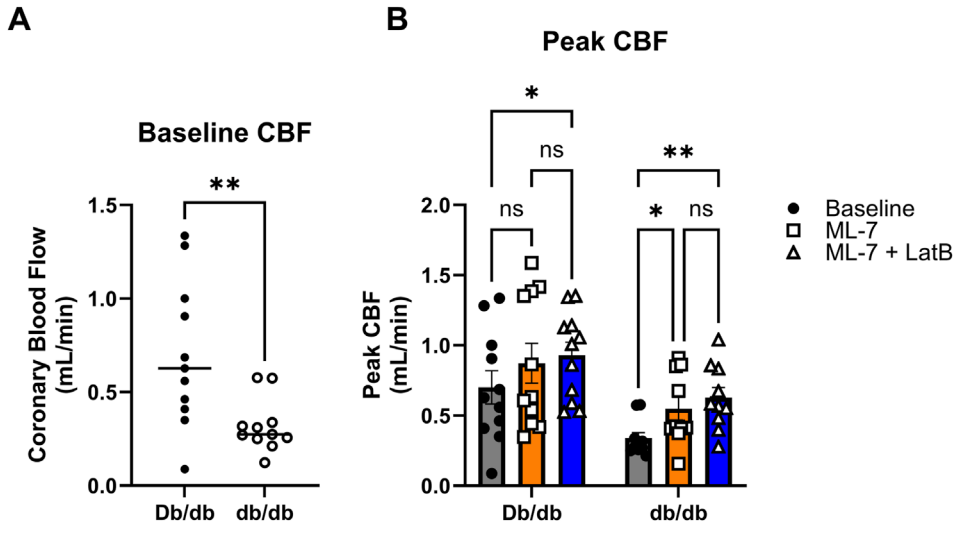

FIGURE 7
Latrunculin B increases CBF: **(A)** Baseline CBF obtained from normal and T2DM hearts *ex vivo* on the Langendorff perfusion system. **(B)** Peak responses to ML-7 and ML-7 + LatB of *ex vivo* heart on Langendorff perfusion system. Data are mean ± SEM.*p < 0.05,**p < 0.005. n = 11 per group.

(McCullough et al., 2008; Schramm et al., 2017). These data are quite intriguing given our previous data of decreased elastic modulus in primary diabetic coronary VSMCs and increased cofilin protein expression in human coronary VSMCs and mouse CRM tissue (Figure 2) (Katz et al., 2011; McCallinhart et al., 2020; Trask et al., 2012b). To investigate the role of cofilin in the stiffness of coronary VSMCs, we utilized AFM to measure elastic modulus, an indicator of cellular stiffness. Both cofilin siRNA treated mouse and human coronary VSMCs showed a significant increase in elastic modulus, likely due to the increased F/G actin ratio (Figures 4, 5). In the mouse coronary VSMCs, both normal and diabetic elastic modulus was significantly increased when the cells were treated with cofilin

siRNA (Figure 5). Other studies have implicated a role for cofilin in vascular mechanics in disease. For example, LIM Kinase (LIMK) is an enzyme that inactivates cofilin via phosphorylation. Intriguingly, inhibiting LIMK prevented small arteriolar agonist-induced inward remodeling implicating cofilin and actin polymerization play a role in microvascular remodeling (Foote et al., 2016). Morales-Quinones et al. reported that localized LIM kinase inhibition prevents arteriolar inward remodeling in hypertensive mice suggesting that hypertension may be correlated with phosphorylation of VSMC cofilin and actin stress fiber formation leading to heightened arterial stiffness (Morales-Quinones et al., 2020). In this study, we observed increased cofilin in T2DM CRM VSMCs (Figure 2), and cofilin knockdown significantly increased coronary VSMC stiffness (Figures 4, 5). We postulate this is due to cofilin's role in transforming the actin cytoskeleton (Figures 4, 5). Collectively, these data warrant further investigation into the role for LIMK and cofilin in coronary vascular mechanics.

Altering the cytoskeleton via pharmacological agents such as cytochalasin B and LatB causes a striking reduction in cell stiffness in mouse 3T3 fibroblasts and chicken embryo fibroblasts, respectively (Petersen et al., 1982; Wakatsuki et al., 2001). In isolated adult cardiomyocytes, Wu and colleagues showed that cytochalasin D and 2,3-Butanedione monoxime (BDM) treatments decreased cell stiffness by 70%–85% supporting that cardiomyocyte stiffness is dependent on the actin-myosin cytoskeleton (Wu et al., 2010). In our study, LatB treatment drastically reduced normal and diabetic coronary VSMC stiffness in both human and mouse cells (Figure 6). Utilizing AFM and fluorescent actin imaging, Gavara et al. (Gavara and Chadwick, 2016) determined that increasing amounts of actin in stress fibers caused increase in cell stiffness. Altering the actin cytoskeleton in the cells of vessels also impacts whole vessel tension. Treatment of the pulmonary artery and aorta *ex vivo* with cytochalasin D to depolymerize actin profoundly inhibited vessel tension development (Adler et al., 1983; Wright and Hurn, 1994). Conversely, actin stabilizers/polymerizers, including jasplakinolide, enhance myogenic tone via smooth muscle contraction and decreased globular- (G) to filamentous- (F) actin ratio (Cipolla et al., 2002). These actin-altering drugs are great tools to explore the balance between the filamentous and globular forms of actin and their role in cytoskeletal balance and function.

Given their roles in regulating the actin cytoskeleton, several reports have explored the potential mechanistic association of Latrunculin A, and B, and cofilin. Cofilin 1 contributes to fast, rapid actin dynamics by depolymerizing actin filaments. Interestingly after a 5-min Latrunculin A treatment, in B16F1 cells pre-treated with cofilin 1 siRNA, only ~10% of the cells had lost their stress fibers and after 30-min Latrunculin A treatment a substantial amount of these cells (roughly 80%) were morphologically approximately normal (Hotulainen et al., 2005). This implicates a competing mechanism of cofilin and Latrunculin-A on the alteration of the actin cytoskeleton. Jovceva et al. (Jovceva et al., 2007) utilized LatB to sequester G-actin in S2R + cells, leading to a continuous increase in the phosphorylation of cofilin in a short 30–60-min period and caused the rapid loss of cortical F-actin. Conversely, treatment with jasplakinolide, a drug that promotes actin filament formation, generated the rapid loss of P-cofilin and was also able to block the accumulation of P-cofilin in insulin-treated cells (Jovceva et al., 2007). Interestingly, in that same study, they reported that in S2R + cells, slingshot (ssh) RNAi suppressed both jasplakinolide- and Latrunculin-induced changes in P-cofilin rather than LIMK RNAi, a well-known regulator of cofilin. Short term treatment of myoblasts with insulin led to rapid cofilin dephosphorylation, however, this dephosphorylation was prevented with LatB treatment (Chiu et al., 2010). Similarly, treatment of MCF-7 cells with Latrunculin A suppressed SSH1L-induced cofilin dephosphorylation (Nagata-Ohashi et al., 2004). In STHdh cells, a specific cell generated to study Huntington disease, LatB treatment initiated co-localization of cofilin-labeled rods and phalloidin (F-actin) (Serebryannyy et al., 2016). In peritoneal mast cells, LatB treatment increased g-actin levels and caused translocation of both actin and cofilin into the nuclei (Pendleton et al., 2003). Further, utilizing anti-cofilin antibody on permeabilized cells reduced nuclear actin accumulation, demonstrating the dependence on cofilin for actin nuclear translocation (Pendleton et al., 2003). Collectively, these studies implicate a competing mechanism for cofilin and LatB.

Coronary blood flow (CBF) delivers essential nutrients to cardiac tissue, supporting its metabolic need. The coronary vessels are responsible for carrying blood to and from the cells of the heart, so any disruption in CBF can result in significant health issues, including heart failure. Previously, our group demonstrated that inward hypertrophic remodeling of CRMs was an early contributor to CAD and was associated with reduced coronary flow in both the db/db mouse model of T2DM and a Ossabaw swine model of MetS (Katz et al., 2011; Trask et al., 2012a). We believe this reduced T2DM stiffness is a compensatory mechanism to maintain blood flow to the myocardium; however, the association of coronary microvascular stiffness as it relates to coronary blood flow has never been explored. There is evidence that arterial stiffening adversely affects coronary flow and flow reserve, but those data are taken from large conduit arteries outside of the coronary circulation (Fukuda et al., 2006; Leung et al., 2006; Tritakis et al., 2016). We have previously reported that in keeping with Poiseuille's Law (flow is proportional to radius to the 4^{th} power), we observed that decreased CRM diameter was associated with reduced coronary blood flow (Katz et al., 2011; McCallinhart et al., 2021; Trask et al., 2012b). We have also previously reported reduced stiffness, however, it is plausible that in the absence of a reduction in CRM VSMC stiffness that coronary blood flow would be further reduced (McCallinhart et al., 2021). Therefore, the reduction in CRM VSMC stiffness may be a compensatory mechanism to limit reduction in coronary blood flow in T2DM. To assess this possibility, we aimed to uncover the regulation of the cytoskeleton and cell stiffness in CRM VSMCs, and ultimately, how it impacts CBF. The treatment of *ex vivo* vessels with pharmacological actin-targeting agents impacts vessel tension and stiffness. Cytochalasin D, an inhibitor of actin polymerization, was reported to inhibit pulmonary artery and aorta vessel tension development (Adler et al., 1983; Wright and Hurn, 1994). On the contrary, the actin polymerizer jasplakinolide enhanced myogenic tone via smooth muscle contraction and decreased G-actin content (Cipolla et al., 2002). In this study, we treated coronary VSMCs with LatB to depolymerize the actin cytoskeleton and drastically decreased elastic modulus (Figure 6). To test whether these observations held true in an intact heart and to further determine their impact on CBF, we employed the classical Langendorff isolated heart technique. This technique allows for the direct assessment of isolated CBF without significant confounding variables that accompany *in vivo* assessments. We directly infused *ex vivo* hearts with ML-7 and LatB on a Langendorff perfusion system to determine how altering cellular stiffness impacts CBF. ML-7 is a well-documented myosin

light chain kinase inhibitor. Myogenic tone and vascular stiffness both contribute to vascular biomechanics and function but have different origins. Myogenic tone is partial constriction of a blood vessel that is triggered by changes in blood pressure via calcium-induced contraction of the actin-myosin myofilament apparatus in VSMCs. Previous studies have documented an augmented myogenic response in the coronary circulation of diabetic animals (Belmadani et al., 2008; Moien-Afshari et al., 2008; Trask et al., 2012a). These dilations and constrictions of the actin-myosin apparatus during myogenic tone alter CBF in a short-term dynamic manner whereas vascular stiffness alters CBF in a long-term manner. To eliminate these short-term changes and the role of myogenic tone, and to solely focus on how changes in the actin cytoskeleton (cellular stiffness) impact CBF, we pretreated the *ex vivo* hearts with ML-7. Interestingly, upon treatment with ML-7 alone, the peak CBF response of diabetic hearts over baseline increased significantly (Figure 7). It is tempting to speculate that this finding could be due to the aforementioned enhanced basal myogenic responsiveness in T2DM CRMs relative to control. Concomitant treatment of ML-7 and LatB resulted in significant increases in peak CBF of both control and diabetic hearts over baseline (Figure 7). These data demonstrate that the reduction of the F/G actin ratio and cell stiffness via treatment with LatB results in an inversely related increase in CBF (Figure 7). This further supports our notion that in the T2DM hearts, the reduced CRM stiffness is a compensating mechanism to attempt to maintain functional CBF in the heart. This is the first study to investigate the relationship between actin cytoskeleton altering drugs and CBF *ex vivo*.

5 Conclusion

In this study, we confirm in both mouse and human coronary vascular smooth muscle a reduction in F-actin in diabetic cells, corresponding to lower stiffnesses. We also demonstrate that the actin regulatory protein, cofilin, is upregulated in diabetic coronary microvascular tissues and smooth muscle cells and knocking it down using siRNA increases the F/G actin ratio and incremental modulus. We also show that pharmacological depolymerization of the actin cytoskeleton using latrunculin B reduces primary coronary VSMC stiffness *in vitro* and that LatB infused directly into the coronary circulation of isolated hearts increased coronary blood flow. These data are the first demonstration in any vascular bed that direct modulation of vascular cell stiffness in the absence of tone can inversely modulate blood flow, and it provides a novel mechanism of blood flow regulation. In summary, this study demonstrates a novel role for cofilin in the cytoskeletal and mechanical regulation of coronary VSMCs, and we further demonstrate a novel inverse relationship between coronary cell stiffness and CBF that has the potential to be exploited for the development of novel therapeutic targets.

Data availability statement

The original contributions presented in the study are included in the article/supplementary material, further inquiries can be directed to the corresponding author.

Ethics statement

Ethical approval was not required for the studies on humans in accordance with the local legislation and institutional requirements because only commercially available established cell lines were used. The animal study was approved by Institutional Animal Care and Use Committee. The study was conducted in accordance with the local legislation and institutional requirements.

Author contributions

PM: Conceptualization, Data curation, Formal Analysis, Investigation, Methodology, Supervision, Validation, Visualization, Writing–original draft, Writing–review and editing. KS: Data curation, Formal Analysis, Investigation, Methodology, Writing–review and editing. PL: Conceptualization, Data curation, Formal Analysis, Investigation, Methodology, Resources, Supervision, Writing–review and editing. AT: Conceptualization, Data curation, Formal Analysis, Investigation, Methodology, Project administration, Resources, Supervision, Validation, Visualization, Writing–original draft, Writing–review and editing.

Funding

The author(s) declare that financial support was received for the research, authorship, and/or publication of this article. This work was supported by NIH R00HL116760, S10OD023438, R21EB026518, R01HL165124, and Nationwide Children's Hospital (to AJT).

Acknowledgments

The authors acknowledge and thank Michael R. McDermott for his contributions to this study.

Conflict of interest

The authors declare that the research was conducted in the absence of any commercial or financial relationships that could be construed as a potential conflict of interest.

The author(s) declared that they were an editorial board member of Frontiers, at the time of submission. This had no impact on the peer review process and the final decision.

Generative AI statement

The author(s) declare that no Generative AI was used in the creation of this manuscript.

Publisher's note

References

Adler, K. B., Krill, J., Alberghini, T. V., and Evans, J. N. (1983). Effect of cytochalasin D on smooth muscle contraction. *Cell. Motil.* 3, 545–551. doi:10.1002/cm.970030521

Akhtar, R., Schwarzer, N., Sherratt, M. J., Watson, R. E., Graham, H. K., Trafford, A. W., et al. (2009). Nanoindentation of histological specimens: mapping the elastic properties of soft tissues. *J. Mater Res.* 24, 638–646. doi:10.1557/JMR.2009.0130

Anghelescu, M., Tonniges, J. R., Calomeni, E., Shamhart, P. E., Agarwal, G., Gooch, K. J., et al. (2015). 'Vascular mechanics in decellularized aortas and coronary resistance microvessels in type 2 diabetic db/db mice. *Ann. Biomed. Eng.* 43, 2760–2770. doi:10.1007/s10439-015-1333-4

Belmadani, S., Palen, D. I., Gonzalez-Villalobos, R. A., Boulares, H. A., and Matrougui, K. (2008). Elevated epidermal growth factor receptor phosphorylation induces resistance artery dysfunction in diabetic db/db mice. *Diabetes* 57, 1629–1637. doi:10.2337/db07-0739

Benech, J. C., Benech, N., Zambrana, A. I., Rauschert, I., Bervejillo, V., Oddone, N., et al. (2014). 'Diabetes increases stiffness of live cardiomyocytes measured by atomic force microscopy nanoindentation. *Am. J. Physiol. Cell. Physiol.* 307, C910–C919. doi:10.1152/ajpcell.00192.2013

Chiu, T. T., Patel, N., Shaw, A. E., Bamburg, J. R., and Klip, A. (2010). 'Arp2/3- and cofilin-coordinated actin dynamics is required for insulin-mediated GLUT4 translocation to the surface of muscle cells. *Mol. Biol. Cell.* 21, 3529–3539. doi:10.1091/mbc.E10-04-0316

Cipolla, M. J., Gokina, N. I., and Osol, G. (2002). 'Pressure-induced actin polymerization in vascular smooth muscle as a mechanism underlying myogenic behavior. *Faseb J.* 16, 72–76. doi:10.1096/cj.01-0104hyp

Costa, K. D. (2003). Single-cell elastography: probing for disease with the atomic force microscope. *Dis. Markers* 19, 139–154. doi:10.1155/2004/482680

Embry, A. E., Mohammadi, H., Niu, X., Liu, L., Moe, B., Miller-Little, W. A., et al. (2016). Biochemical and cellular determinants of renal glomerular elasticity. *PLoS One* 11, e0167924. doi:10.1371/journal.pone.0167924

Fels, J., Jeggle, P., Liashkovich, I., Peters, W., and Oberleithner, H. (2014). Nanomechanics of vascular endothelium. *Cell. Tissue Res.* 355, 727–737. doi:10.1007/s00441-014-1853-5

Foote, C. A., Castorena-Gonzalez, J. A., Staiculescu, M. C., Clifford, P. S., Hill, M. A., Meininger, G. A., et al. (2016). 'Brief serotonin exposure initiates arteriolar inward remodeling processes *in vivo* that involve transglutaminase activation and actin cytoskeleton reorganization. *Am. J. Physiol. Heart Circ. Physiol.* 310, H188–H198. doi:10.1152/ajpheart.00666.2015

Fukuda, D., Yoshiyama, M., Shimada, K., Yamashita, H., Ehara, S., Nakamura, Y., et al. (2006). Relation between aortic stiffness and coronary flow reserve in patients with coronary artery disease. *Heart* 92, 759–762. doi:10.1136/hrt.2005.067934

Gavara, N., and Chadwick, R. S. (2016). Relationship between cell stiffness and stress fiber amount, assessed by simultaneous atomic force microscopy and live-cell fluorescence imaging. *Biomech. Model. Mechanobiol.* 15, 511–523. doi:10.1007/s10237-015-0706-9

Gil-Ortega, I., and Carlos Kaski, J. (2006). Diabetic miocardiopathy. *Med. Clin. Barc.* 127, 584–594. doi:10.1157/13094003

Grimm, K. B., Oberleithner, H., and Fels, J. (2014). Fixed endothelial cells exhibit physiologically relevant nanomechanics of the cortical actin web. *Nanotechnology* 25, 215101. doi:10.1088/0957-4484/25/21/215101

Grundy, S. M., Benjamin, I. J., Burke, G. L., Chait, A., Eckel, R. H., Howard, B. V., et al. (1999). 'Diabetes and cardiovascular disease: a statement for healthcare professionals from the American Heart Association. *Circulation* 100, 1134–1146. doi:10.1161/01.cir.100.10.1134

Hien, T. T., Turczyńska, K. M., Dahan, D., Ekman, M., Grossi, M., Sjögren, J., et al. (2016). 'Elevated glucose levels promote contractile and cytoskeletal gene expression in vascular smooth muscle via rho/protein kinase C and actin polymerization. *J. Biol. Chem.* 291, 3552–3568. doi:10.1074/jbc.M115.654384

Hong, Z., Reeves, K. J., Sun, Z., Li, Z., Brown, N. J., and Meininger, G. A. (2015). 'Vascular smooth muscle cell stiffness and adhesion to collagen I modified by vasoactive agonists. *PLoS One* 10, e0119533. doi:10.1371/journal.pone.0119533

Hotulainen, P., Paunola, E., Vartiainen, M. K., and Lappalainen, P. (2005). Actin-depolymerizing factor and cofilin-1 play overlapping roles in promoting rapid F-actin depolymerization in mammalian nonmuscle cells. *Mol. Biol. Cell.* 16, 649–664. doi:10.1091/mbc.e04-07-0555

Husarek, K. E., Katz, P. S., Trask, A. J., Galantowicz, M. L., Cismowski, M. J., and Lucchesi, P. A. (2016a). The angiotensin receptor blocker losartan reduces coronary arteriole remodeling in type 2 diabetic mice. *Vasc. Pharmacol.* 76, 28–36. doi:10.1016/j.vph.2015.06.013

Husarek, K. E., Zhang, X., McCallinhart, P. E., Lucchesi, P. A., and Trask, A. J. (2016b). 'Isolation of murine coronary vascular smooth muscle cells. *J. Vis. Exp.*, 53983. doi:10.3791/53983

IDF Diabetes Atlas (2023). *IDF diabetes Atlas*. International Diabetes Federation. Available at: https://diabetesatlas.org/.

Jovceva, E., Larsen, M. R., Waterfield, M. D., Baum, B., and Timms, J. F. (2007). Dynamic cofilin phosphorylation in the control of lamellipodial actin homeostasis. *J. Cell. Sci.* 120, 1888–1897. doi:10.1242/jcs.004366

Katz, P. S., Trask, A. J., Souza-Smith, F. M., Hutchinson, K. R., Galantowicz, M. L., Lord, K. C., et al. (2011). 'Coronary arterioles in type 2 diabetic (db/db) mice undergo a distinct pattern of remodeling associated with decreased vessel stiffness. *Basic Res. Cardiol.* 106, 1123–1134. doi:10.1007/s00395-011-0201-0

Kawaguchi, M., Asakura, T., Saito, F., Nemoto, O., Maehara, K., Miyake, K., et al. (1999). Changes in diameter size and F-actin expression in the myocytes of patients with diabetes and streptozotocin-induced diabetes model rats. *J. Cardiol.* 34, 333–339.

Lacolley, P., Regnault, V., Segers, P., and Laurent, S. (2017). 'Vascular smooth muscle cells and arterial stiffening: relevance in development, aging, and disease. *Physiol. Rev.* 97, 1555–1617. doi:10.1152/physrev.00003.2017

Leung, M. C., Meredith, I. T., and Cameron, J. D. (2006). Aortic stiffness affects the coronary blood flow response to percutaneous coronary intervention. *Am. J. Physiol. Heart Circ. Physiol.* 290, H624–H630. doi:10.1152/ajpheart.00380.2005

Li, H., Li, J., Wang, P., Yuan, F., and Zhang, S. (2023). Improvement of actin dynamics and cognitive impairment in diabetes through troxerutin-mediated downregulation of TRPM7/CaN/cofilin. *Neuropeptides* 102, 102381. doi:10.1016/j.npep.2023.102381

McCallinhart, P. E., Chade, A. R., Bender, S. B., and Trask, A. J. (2024). Expanding landscape of coronary microvascular disease in co-morbid conditions: metabolic disease and beyond. *J. Mol. Cell. Cardiol.* 192, 26–35. doi:10.1016/j.yjmcc.2024.05.004

McCallinhart, P. E., Cho, Y., Sun, Z., Ghadiali, S., Meininger, G. A., and Trask, A. J. (2020). 'Reduced stiffness and augmented traction force in type 2 diabetic coronary microvascular smooth muscle. *Am. J. Physiol. Heart Circ. Physiol.* 318, H1410-H1419–h19. doi:10.1152/ajpheart.00542.2019

McCallinhart, P. E., Scandling, B. W., and Trask, A. J. (2021). Coronary remodeling and biomechanics: are we going with the flow in 2020? *Am. J. Physiol. Heart Circ. Physiol.* 320, H584–H592. doi:10.1152/ajpheart.00634.2020

McCallinhart, P. E., Sunyecz, I. L., and Trask, A. J. (2018). Coronary microvascular remodeling in type 2 diabetes: synonymous with early aging? *Front. Physiol.* 9, 1463. doi:10.3389/fphys.2018.01463

McCullough, B. R., Blanchoin, L., Martiel, J. L., and De la Cruz, E. M. (2008). Cofilin increases the bending flexibility of actin filaments: implications for severing and cell mechanics. *J. Mol. Biol.* 381, 550–558. doi:10.1016/j.jmb.2008.05.055

Moien-Afshari, F., Ghosh, S., Elmi, S., Khazaei, M., Rahman, M. M., Sallam, N., et al. (2008). 'Exercise restores coronary vascular function independent of myogenic tone or hyperglycemic status in db/db mice. *Am. J. Physiol. Heart Circ. Physiol.* 295, H1470–H1480. doi:10.1152/ajpheart.00016.2008

Morales-Quinones, M., Ramirez-Perez, F. I., Foote, C. A., Ghiarone, T., Ferreira-Santos, L., Bloksgaard, M., et al. (2020). 'LIMK (LIM kinase) inhibition prevents vasoconstriction- and hypertension-induced arterial stiffening and remodeling. *Hypertension* 76, 393–403. doi:10.1161/HYPERTENSIONAHA.120.15203

Mozaffarian, D., Benjamin, E. J., Go, A. S., Arnett, D. K., Blaha, M. J., Cushman, M., et al. (2015). 'Heart disease and stroke statistics–2015 update: a report from the American Heart Association. *Circulation* 131, e29–e322. doi:10.1161/CIR.0000000000000152

Nagata-Ohashi, K., Ohta, Y., Goto, K., Chiba, S., Mori, R., Nishita, M., et al. (2004). A pathway of neuregulin-induced activation of cofilin-phosphatase Slingshot and cofilin in lamellipodia. *J. Cell. Biol.* 165, 465–471. doi:10.1083/jcb.200401136

Nemoto, O., Kawaguchi, M., Yaoita, H., Miyake, K., Maehara, K., and Maruyama, Y. (2006). Left ventricular dysfunction and remodeling in streptozotocin-induced diabetic rats. *Circ. J.* 70, 327–334. doi:10.1253/circj.70.327

Pendleton, A., Pope, B., Weeds, A., and Koffer, A. (2003). Latrunculin B or ATP depletion induces cofilin-dependent translocation of actin into nuclei of mast cells. *J. Biol. Chem.* 278, 14394–14400. doi:10.1074/jbc.M206393200

Petersen, N. O., McConnaughey, W. B., and Elson, E. L. (1982). Dependence of locally measured cellular deformability on position on the cell, temperature, and cytochalasin B. *Proc. Natl. Acad. Sci. U. S. A.* 79, 5327–5331. doi:10.1073/pnas.79.17.5327

Reddy, G. K. (2004). AGE-related cross-linking of collagen is associated with aortic wall matrix stiffness in the pathogenesis of drug-induced diabetes in rats. *Microvasc. Res.* 68, 132–142. doi:10.1016/j.mvr.2004.04.002

Romanelli, G., Varela, R., and Benech, J. C. (2020). Diabetes induces differences in the F-actin spatial organization of striated muscles. *Cytoskelet. Hob.* 77, 202–213. doi:10.1002/cm.21600

Schramm, A. C., Hocky, G. M., Voth, G. A., Blanchoin, L., Martiel, J. L., and De La Cruz, E. M. (2017). Actin filament strain promotes severing and cofilin dissociation. *Biophys. J.* 112, 2624–2633. doi:10.1016/j.bpj.2017.05.016

Sehgel, N. L., Zhu, Y., Sun, Z., Trzeciakowski, J. P., Hong, Z., Hunter, W. C., et al. (2013). Increased vascular smooth muscle cell stiffness: a novel mechanism for aortic stiffness in hypertension. *Am. J. Physiol. Heart Circ. Physiol.* 305, H1281–H1287. doi:10.1152/ajpheart.00232.2013

Serebryannyy, L. A., Yuen, M., Parilla, M., Cooper, S. T., and de Lanerolle, P. (2016). The effects of disease models of nuclear actin polymerization on the nucleus. *Front. Physiol.* 7, 454. doi:10.3389/fphys.2016.00454

Trask, A. J., Averill, D. B., Ganten, D., Chappell, M. C., and Ferrario, C. M. (2007). Primary role of angiotensin-converting enzyme-2 in cardiac production of angiotensin-(1-7) in transgenic Ren-2 hypertensive rats. *Am. J. Physiol. Heart Circ. Physiol.* 292, H3019–H3024. doi:10.1152/ajpheart.01198.2006

Trask, A. J., Delbin, M. A., Katz, P. S., Zanesco, A., and Lucchesi, P. A. (2012a). 'Differential coronary resistance microvessel remodeling between type 1 and type 2 diabetic mice: impact of exercise training. *Vasc. Pharmacol.* 57, 187–193. doi:10.1016/j.vph.2012.07.007

Trask, A. J., Jessup, J. A., Chappell, M. C., and Ferrario, C. M. (2008). 'Angiotensin-(1-12) is an alternate substrate for angiotensin peptide production in the heart. *Am. J. Physiol. Heart Circ. Physiol.* 294, H2242–H2247. doi:10.1152/ajpheart.00175.2008

Trask, A. J., Katz, P. S., Kelly, A. P., Galantowicz, M. L., Cismowski, M. J., West, T. A., et al. (2012b). Dynamic micro- and macrovascular remodeling in coronary circulation of obese Ossabaw pigs with metabolic syndrome. *J. Appl. Physiol.* 113, 1128–1140. doi:10.1152/japplphysiol.00604.2012

Tritakis, V., Tzortzis, S., Ikonomidis, I., Dima, K., Pavlidis, G., Trivilou, P., et al. (2016). Association of arterial stiffness with coronary flow reserve in revascularized coronary artery disease patients. *World J. Cardiol.* 8, 231–239. doi:10.4330/wjc.v8.i2.231

Tsao, C. W., Aday, A. W., Almarzooq, Z. I., Anderson, C. A. M., Arora, P., Avery, C. L., et al. (2023). Heart disease and stroke statistics-2023 update: a report from the American heart association. *Circulation* 147, e93–e621. doi:10.1161/CIR.0000000000001123

Wakatsuki, T., Schwab, B., Thompson, N. C., and Elson, E. L. (2001). Effects of cytochalasin D and latrunculin B on mechanical properties of cells. *J. Cell. Sci.* 114, 1025–1036. doi:10.1242/jcs.114.5.1025

Wright, G., and Hurn, E. (1994). Cytochalasin inhibition of slow tension increase in rat aortic rings. *Am. J. Physiol.* 267, H1437–H1446. doi:10.1152/ajpheart.1994.267.4.H1437

Wu, X., Sun, Z., Foskett, A., Trzeciakowski, J. P., Meininger, G. A., and Muthuchamy, M. (2010). Cardiomyocyte contractile status is associated with differences in fibronectin and integrin interactions. *Am. J. Physiol. Heart Circ. Physiol.* 298, H2071–H2081. doi:10.1152/ajpheart.01156.2009

Zhang, L., Cannell, M. B., Phillips, A. R., Cooper, G. J., and Ward, M. L. (2008). Altered calcium homeostasis does not explain the contractile deficit of diabetic cardiomyopathy. *Diabetes* 57, 2158–2166. doi:10.2337/db08-0140

frontiers | Frontiers in Physiology

TYPE Brief Research Report
PUBLISHED 27 March 2025
DOI 10.3389/fphys.2025.1563014

OPEN ACCESS

EDITED BY
Christopher Garland,
University of Oxford, United Kingdom

REVIEWED BY
William F. Jackson,
Michigan State University, United States
Erika M. Boerman,
University of Missouri, United States

*CORRESPONDENCE
Rudolf Schubert,
✉ rudolf.schubert@med.uni-augsburg.de

†These authors share first authorship

RECEIVED 18 January 2025
ACCEPTED 28 February 2025
PUBLISHED 27 March 2025

CITATION
Shvetsova AA, Gaynullina DK, Schmid J, Winkler P, Sonsala I and Schubert R (2025) Dual role of calcium-activated potassium channels of high conductance: facilitator or limiter of NO-induced arterial relaxation? *Front. Physiol.* 16:1563014. doi: 10.3389/fphys.2025.1563014

Dual role of calcium-activated potassium channels of high conductance: facilitator or limiter of NO-induced arterial relaxation?

Anastasia A. Shvetsova[1†], Dina K. Gaynullina[1,2†], Johannes Schmid[3,4], Peter Winkler[3,4], Isabella Sonsala[3,4] and Rudolf Schubert[3,4*]

[1]Faculty of Biology, M.V. Lomonosov Moscow State University, Moscow, Russia, [2]Insitute of Physiology, Russian National Research Medical University, Moscow, Russia, [3]Physiology, Faculty of Medicine, Institute of Theoretical Medicine, University of Augsburg, Augsburg, Germany, [4]Research Division Cardiovascular Physiology, Medical Faculty Mannheim, European Center of Angioscience (ECAS), Heidelberg University, Mannheim, Germany

Aim: Calcium-activated potassium channels of high conductance (BK_{Ca} channels) are important contributors to vascular smooth muscle membrane potential and thus to vascular tone. BK_{Ca} channels can promote vasodilation by facilitating vessel responses to NO. BK_{Ca} channels may also serve as limiters of the anticontractile effect of NO. However, it is unclear whether BK_{Ca} channels act simultaneously as facilitators and limiters in different vascular regions. Therefore, this study tested the hypothesis that BK_{Ca} channels both facilitate and limit NO-induced vasorelaxation in multiple vessels.

Methods: Contractile responses of rat tail, saphenous, and left and right coronary arteries were studied using wire myography.

Results: The NO-donor SNP reduced contractile responses induced by low concentrations of methoxamine or serotonin, respectively, in all arteries tested, both in the absence and in the presence of iberiotoxin. This anticontractile effect of SNP was larger in the presence of iberiotoxin than in its absence, i.e., functionally active BK_{Ca} channels limit the anticontractile effect of SNP. In contrast, the anticontractile effect of SNP at high concentrations of methoxamine or serotonin, respectively, in all arteries tested was smaller in the presence of iberiotoxin than in its absence, i.e., functionally active BK_{Ca} channels facilitate the anticontractile effect of SNP.

Conclusion: BK_{Ca} channels simultaneously limit NO-induced vasodilation at lower levels of contractility but facilitate it at higher levels of contractility in multiple vascular beds. Therefore, BK_{Ca} channels may play a dual role as

facilitators and as limiters of the effect of NO, depending on the level of contractility.

KEYWORDS

vasodilation, arterial smooth muscle, BK channel, nitric oxide, tail artery, saphenous artery, coronary arteries

1 Introduction

The regulation of blood pressure and organ perfusion is largely determined by the diameter of the arteries in the circulatory system. Arterial diameter is substantially governed by the membrane potential of vascular smooth muscle cells. Potassium channels, in particular the calcium-activated potassium channels of high conductance (BK_{Ca} channels), make an important contribution to the membrane potential. Under physiological conditions, these channels have been observed to serve as negative feedback for vasocontraction and to contribute to vasodilation (Tykocki et al., 2017). They have also been reported to be involved in several diseases such as hypertension and diabetes (Lu et al., 2005; McGahon et al., 2007; Kyle and Braun, 2014). Thus, vascular smooth muscle BK_{Ca} channels are important contributors to physiological regulation as well as pathophysiological dysregulation in the circulatory system.

Regarding the contribution of BK_{Ca} channels to vasodilation, they have been shown to facilitate vessel responses to NO (Williams et al., 1988; Khan et al., 1993; Robertson et al., 1993) in many vascular beds; sometimes BK_{Ca} channels have been reported to be resistant to NO-induced regulation (Tykocki et al., 2017). In addition, a recent study presented data showing that BK_{Ca} channels can also serve as limiters of the anticontractile effect of NO; this has been described for rat and mouse tail and rat saphenous arteries (Schmid et al., 2018). Mechanistically, this role of the BK_{Ca} channel has been explained by the existence of two simultaneous effects of NO on BK_{Ca} channels: channel activation mediated by PKG (already established for some time by a number of studies (Alioua et al., 1995; Schubert and Nelson, 2001; Kyle et al., 2013)) and channel deactivation mediated by a decrease in the intracellular calcium concentration. It has been suggested that, particularly at lower levels of vessel contractility, NO-induced PKG-mediated activation of the BK_{Ca} channel is weaker than NO-induced $[Ca^{2+}]_i$ decrease–mediated deactivation of the BK_{Ca} channel and that the overall decrease in BK_{Ca} channel activity determines the role of BK_{Ca} channels as limiters of the effect of NO. Of note, this mechanistic framework could also explain the previously described role of the BK_{Ca} channel as a facilitator of the effect of NO. It was suggested that at higher levels of vessel contractility, NO-induced PKG-mediated activation of the BK_{Ca} channel is stronger than NO-induced $[Ca^{2+}]_i$ decrease–mediated deactivation of the BK_{Ca} channel and that the overall increase in BK_{Ca} channel activity determines the role of BK_{Ca} channels as facilitators of the effect of NO. BK_{Ca} channels may therefore play a dual role, namely, as facilitators and as limiters of the effect of NO. However, it is unclear whether a simultaneous presence of the facilitator and limiter role of the BK_{Ca} channel is a more general phenomenon in the circulatory system, i.e., can be observed in different vascular regions. Therefore, this study tested the hypothesis that BK_{Ca} channels both facilitate and limit NO-induced vasorelaxation in multiple vessels.

2 Materials and methods

2.1 Animals

All experimental procedures in this study complied with the European Convention on the protection of animals used for scientific purposes (EU Directive 2010/63/EU) and were approved by German institutional committees on animal welfare (I-17/17). Male Wistar rats were used in this study. Animals were obtained from Janvier (France), aged 2–3 months and weighted 250–350 g. Rats were housed in a room with a controlled temperature and a 12/12 h light/dark cycle with free access to water and food *ad libitum*. At the day of the experiment animals were anesthetized by CO_2 and decapitated.

2.2 Wire myograph experiments

The tail, saphenous, right and left coronary arteries were utilized in this study. Arteries were carefully isolated from the surrounding tissue, each type of artery was cut into four segments and mounted in a wire myograph (620M, DMT A/S, Denmark). The endothelium was carefully removed using a rat whisker. All preparation procedures were carried out in the preparation solution containing (mmol L^{-1}): NaCl 145; KCl 4.5; $CaCl_2$ 0.1; $MgSO_4$ 1.0; NaH_2PO_4 1.2; EDTA 0.025; HEPES 5.0 (pH = 7.4).

Data from our previous study describing that BK_{Ca} channels may also serve as limiters of the anticontractile effect of NO (Schmid et al., 2018), which provide a mechanistic background for the present study, were obtained using only male rats. Because the present study is closely related to our previous study, especially in terms of mechanistic background, this study is also limited to male rats. However, we are planning such experiments for the future.

The tail artery was used because the data from our previous study describing that BK_{Ca} channels may also serve as limiters of the anticontractile effect of NO (Schmid et al., 2018) were obtained from this vessel, providing a mechanistic background for the present study. The saphenous artery was used because in several previous studies we were able to characterize the functional role of smooth muscle potassium channels, including their participation in SNP-induced vasodilation in detail (Shvetsova et al., 2019; 2025; Ma et al., 2020). The coronary arteries were used as vessels of a more "specialized" vascular bed in which NO plays an important role both under physiological (blood flow regulation)

as well as pathophysiological (therapeutic use of nitrovasodilators) conditions. There are several additional vascular beds of interest (e.g., mesenteric, cerebral, renal) that should be investigated in future studies. After mounting of the vessels, the solution was replaced by experimental solution containing (mmol L^{-1}): NaCl 120; $NaHCO_3$ 26; KCl 4.5; $CaCl_2$ 1.6; $MgSO_4$ 1.0; NaH_2PO_4 1.2; D-glucose 5.5; EDTA 0.025; HEPES 5.0 (pH = 7.4). The temperature in the chambers was heated up to 37.0°C and was maintained at this level throughout the experiment. To maintain pH = 7.4 the chambers were continuously aerated with a mixture of 5% CO_2 + 95% O_2. Data were recorded at 1 kHz using the PowerLab 4/30 system (ADInstruments, United States) and the LabChart software (ADInstruments, United States). All arterial segments were stretched to $0.9d_{100}$ (90% of the inner diameter it would have at a transmural pressure of 100 mmHg), corresponding to maximum active force development (Mulvany and Halpern, 1977).

The experimental protocol consisted of the standard activation procedure followed by three concentration-response relationships to vasoactive agonists (Figure 1). For tail and saphenous arteries the following activation procedure was performed: (1) methoxamine (α_1-adrenoceptor agonist, 10 μmol L^{-1}) for 5 min; (2) acetylcholine (10 μmol L^{-1}, 2 min) on top of methoxamine-induced pre-contraction (1 μmol L^{-1}, 5 min) - the absence of a dilatory response confirmed successful endothelium denudation; (3) methoxamine (10 μmol L^{-1}) for 5 min. 20 min after the end of the activation procedure the first concentration-response relationship to methoxamine was obtained (concentration range from 0.01 μmol L^{-1}–10 μmol L^{-1}, each concentration for 3 min). This concentration-response relationship was used to ensure similar initial sensitivity to agonist in preparations further treated with a blocker and/or NO-donor. After washout of methoxamine two of four preparations were treated with the BK_{Ca} channel blocker iberiotoxin (0.1 μmol L^{-1}) for 20 min, the other two preparations were treated with the same volume of water (solvent of iberiotoxin). Thereafter, the second concentration-response relationship to methoxamine was obtained in the same manner as the first one. The second concentration-response relationship was used to ensure similar responses in the groups treated with iberiotoxin and solvent, respectively. After washout of methoxamine, the preparations were treated for 20 min with either (1) iberiotoxin (0.1 μmol L^{-1}); (2) sodium nitroprusside (SNP, 0.1 μmol L^{-1}); (3) iberiotoxin (0.1 μmol L^{-1}) + SNP (0.1 μmol L^{-1}); (4) the same volume of water (solvent of iberiotoxin and SNP, labeled as Control in the graphs). Importantly, at this stage, the application of iberiotoxin was carried out only to those segments to which iberiotoxin had been added previously. Thereafter, the third concentration-response relationship to methoxamine was obtained in the same manner as previously. The third concentration-response relationships are presented in the graphs. The right and left coronary arteries were activated by application of (1) serotonin (10 μmol L-1, 5 min) followed by acetylcholine (10 μmol L^{-1}, 2 min); (2) high-potassium solution containing (mmol L^{-1}): NaCl 6; $NaHCO_3$ 26; KCl 118.5; $CaCl_2$ 1.6; $MgSO_4$ 1.0; NaH_2PO_4 1.2; D-glucose 5.5; EDTA 0.025; HEPES 5.0 (pH = 7.4) for 5 min; (3) serotonin (10 μmol L^{-1}, 5 min). Thereafter, a similar to tail and saphenous arteries protocol was applied except serotonin was used instead of methoxamine.

Vessel reactivity was expressed as active force. To calculate active force values at each time point of interest, the force value of the fully relaxed state was subtracted from all recorded data. Further, all active force values were expressed as the percentage of the active force developed during the last step of the activation procedure (i.e., the response to 10 μmol L^{-1} of methoxamine for tail and saphenous arteries or to 10 μmol L^{-1} of serotonin for right and left coronary arteries, Table 1). Areas under the curve (AUC) values were calculated for the third concentration-response relationships in GraphPad Prizm 9.5.1 (La Jolla, CA, United States). To obtain the values of the anticontractile effect of SNP in the absence and in the presence of iberiotoxin, the AUC values in the presence of SNP alone or together with iberiotoxin were subtracted from control or iberiotoxin groups, respectively.

2.3 Drugs

Methoxamine, serotonin, acetylcholine, SNP (all dissolved in H_2O), as well as all salts were obtained from Sigma. Iberiotoxin (dissolved in H_2O) was obtained from Alomone Labs.

2.4 Statistical analysis

Statistical analysis was performed using GraphPad Prism 9.5.1. The normality of the data distribution was tested using the Shapiro-Wilk test. Data are presented as mean and SEM (if data distribution was normal) or as median and interquartile range (if data distribution was different from normal); *n* represents the number of animals, i.e., biological replicates (only one vessel from one animal was used in each group). Concentration-response relationships between groups were compared using repeated measures ANOVA followed by two-stage linear step-up procedure of Benjamini, Krieger and Yekutieli controlling for false discovery rate. Statistical analyses of SNP's anticontractile effect in the absence and in the presence of iberiotoxin was carried out using unpaired t-test with Welch's correction or Mann-Whitney U-test, depending on the type of data distribution. Differences were accepted as statistically significant if the P-value was less than 0.05.

3 Results

3.1 Tail artery

To determine the role of BK_{Ca} channels in the anticontractile effect of NO, a detailed analysis was performed to search for those levels of contractility where BK_{Ca} channels either facilitate or limit the effect of NO. The so found levels of contractility are marked with different colors in Figure 2. In the methoxamine-concentration range between 0.01 μM and 1 μM, treatment of rat tail arteries with the BK_{Ca} channel blocker iberiotoxin increased contractile responses to methoxamine (Figure 2A). The NO-donor SNP reduced methoxamine-induced contractile responses both in the absence and in the presence of iberiotoxin (Figure 2A). The anticontractile effect of SNP was larger in the presence of iberiotoxin than in its absence (Figure 2B), i.e., functionally active BK_{Ca} channels limit the anticontractile effect of SNP. In contrast, in the methoxamine-concentration range between 1 μM and 3 μM,

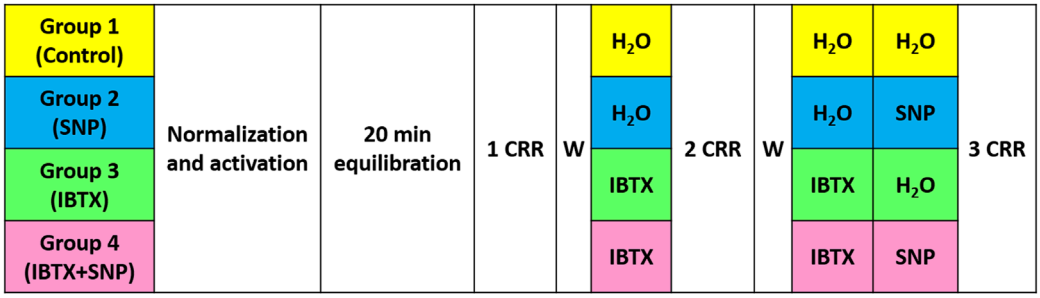

FIGURE 1
Schematic representation of the experimental protocol used in this study, see text for details. CRR–concentration response relationship, W–washout, IBTX–iberiotoxin, SNP–sodium nitroprusside.

TABLE 1 Vessel tension obtained during the last step of the activation procedure in response to 10 μmol L^{-1} of methoxamine or serotonin.

	Tension (mN/mm)			
Experimental group	Tail artery	Saphenous artery	Left coronary artery	Right coronary artery
Control	36.3 ± 4.6	32.6 ± 3.9	2.8 ± 0.6	3.8 (2.9; 6.2)
IBTX	43.3 ± 3.4	36.6 ± 2.4	4.3 ± 0.7	4.0 (3.3; 8.3)
SNP	42.2 ± 3.6	35.9 ± 3.1	3.1 ± 0.3	4.5 (3.0; 5.5)
IBTX + SNP	40.9 ± 3.6	37.4 ± 3.8	3.9 ± 0.3	4.1 (3.2; 5.3)
Statistical analysis	n = 10; p = 0.59 one-way ANOVA	n = 8; p = 0.75 one-way ANOVA	n = 10; p = 0.14 one-way ANOVA	n = 9; p = 0.95 Kruskal–Wallis

we did not detect an effect of the BK_{Ca} channel blocker iberiotoxin on contractile responses to methoxamine (Figure 2C). The NO-donor SNP reduced methoxamine-induced contractile responses both in the absence and in the presence of iberiotoxin (Figure 2C). The anticontractile effect of SNP was smaller in the presence of iberiotoxin than in its absence (Figure 2D), i.e., functionally active BK_{Ca} channels facilitate the anticontractile effect of SNP. Finally, in the methoxamine-concentration range between 3 μM and 10 μM, we did not detect an effect of the BK_{Ca} channel blocker iberiotoxin on contractile responses to methoxamine (Figure 2E). The NO-donor SNP reduced methoxamine-induced contractile responses both in the absence and in the presence of iberiotoxin (Figure 2F). We did not detect a difference of the anticontractile effect of SNP in the presence and absence of iberiotoxin (Figure 2F), i.e., functionally active BK_{Ca} channels do not contribute to the anticontractile effect of SNP.

3.2 Saphenous artery

To determine the role of BK_{Ca} channels in the anticontractile effect of NO in saphenous arteries, a detailed analysis was performed to search for those levels of contractility where BK_{Ca} channels either facilitate or limit the effect of NO. The levels of contractility found in this way are marked with different colors in Figure 3. In the methoxamine-concentration range between 0.01 μM and 1 μM treatment of rat saphenous arteries with the BK_{Ca} channel blocker iberiotoxin increased contractile responses to methoxamine (Figure 3A). The NO-donor SNP reduced methoxamine-induced contractile responses both in the absence and in the presence of iberiotoxin (Figure 3A). The anticontractile effect of SNP was larger in the presence of iberiotoxin than in its absence (Figure 3B), i.e., functionally active BK_{Ca} channels limit the anticontractile effect of SNP. In the methoxamine-concentration range between 1 μM and 10 μM, the BK_{Ca} channel blocker iberiotoxin also increased contractile responses to methoxamine (Figure 3C). The NO-donor SNP reduced methoxamine-induced contractile responses both in the absence and in the presence of iberiotoxin (Figure 3C). The anticontractile effect of SNP was smaller in the presence of iberiotoxin than in its absence (Figure 3D), i.e., functionally active BK_{Ca} channels facilitate the anticontractile effect of SNP.

3.3 Left coronary artery

To determine the role of BK_{Ca} channels in the anticontractile effect of NO in the left coronary artery, a detailed analysis was performed to search for those levels of contractility where BK_{Ca} channels either facilitate or limit the effect of NO. The so found levels of contractility are marked with different colors in

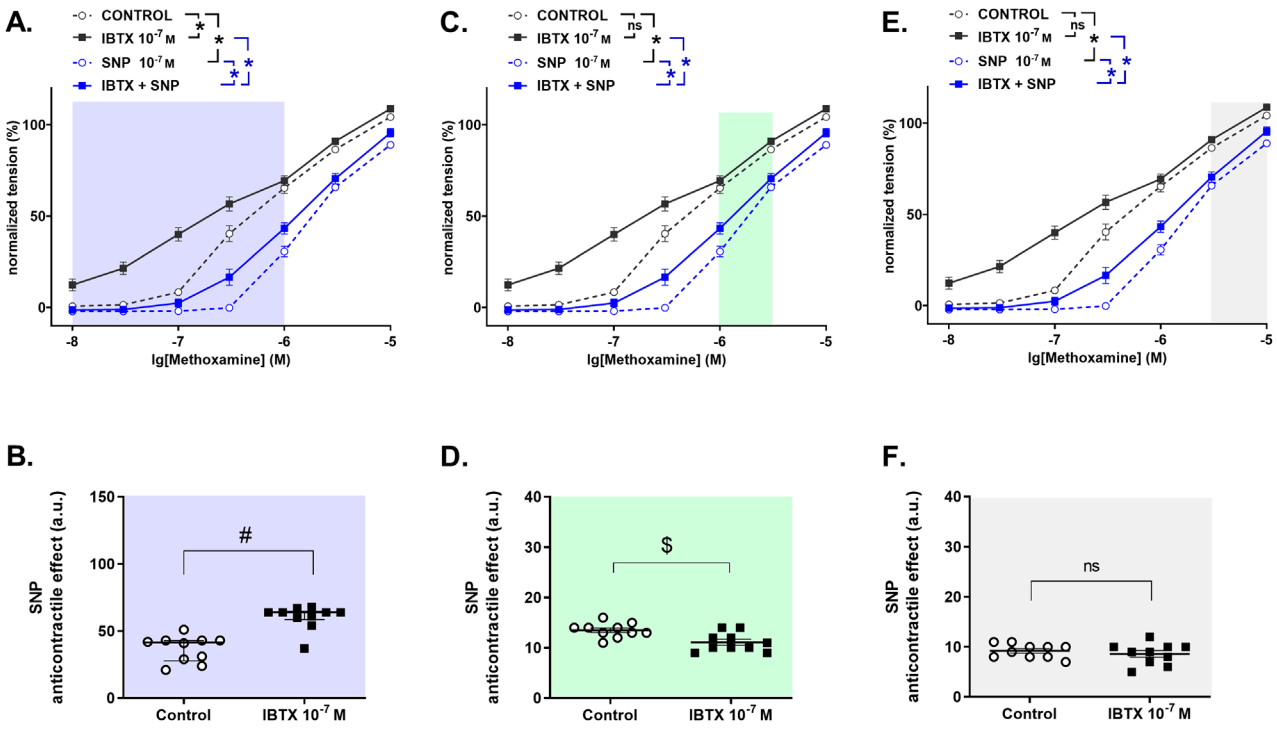

FIGURE 2
Anticontractile effect of SNP in the absence and presence of BK_{Ca} channel blockade at different levels of contractility in rat tail arteries. **(A, C, E)** Concentration–response relationships for methoxamine in the absence of any additional substances (control), in the presence of iberiotoxin (0.1 μM, IBTX), sodium nitroprusside (0.1 μM, SNP) or iberiotoxin together with sodium nitroprusside (IBTX + SNP). Data analysis was limited to the respective highlighted areas corresponding to low **(A)**, middle **(C)** and high **(E)** levels of contractility. n = 10;*- $p < 0.05$ (repeated measures ANOVA with two-stage linear step-up procedure of Benjamini, Krieger and Yekutieli). **(B, D, F)** Anticontractile effect of SNP in the absence (circles, Control) and in the presence of IBTX (squares, IBTX), presented as the difference between the area under the concentration-response relationships in the control and the SNP groups as well as in the IBTX and the IBTX + SNP groups. n = 10; # - $p < 0.05$ (Mann-Whitney test), $ - $p < 0.05$ (Welch's t-test), n.s. – non-significant.

Figure 4. In the serotonin-concentration range between 0.01 μM and 0.3 μM treatment of rat left coronary arteries with the BK_{Ca} channel blocker iberiotoxin increased contractile responses to serotonin (Figure 4A). The NO-donor SNP reduced serotonin-induced contractile responses both in the absence and in the presence of iberiotoxin (Figure 4A). The anticontractile effect of SNP was larger in the presence of iberiotoxin than in its absence (Figure 4B), i.e., functionally active BK_{Ca} channels limit the anticontractile effect of SNP. In contrast, in the serotonin-concentration range between 0.3 μM and 10 μM, we did not detect an effect of the BK_{Ca} channel blocker iberiotoxin on contractile responses to serotonin (Figure 4C). The NO-donor SNP reduced serotonin-induced contractile responses both in the absence and in the presence of iberiotoxin (Figure 4C). The anticontractile effect of SNP was smaller in the presence of iberiotoxin than in its absence (Figure 4D), i.e., functionally active BK_{Ca} channels facilitate the anticontractile effect of SNP.

3.4 Right coronary artery

To determine the role of BK_{Ca} channels in the anticontractile effect of NO in the right coronary artery, a detailed analysis was performed to search for those levels of contractility where BK_{Ca} channels either facilitate or limit the effect of NO. The so found levels of contractility are marked with different colors in Figure 5. In the serotonin-concentration range between 0.01 μM and 0.3 μM treatment of rat right coronary arteries with the BK_{Ca} channel blocker iberiotoxin increased contractile responses to serotonin (Figure 5A). The NO-donor SNP reduced serotonin-induced contractile responses both in the absence and in the presence of iberiotoxin (Figure 5A). The anticontractile effect of SNP was larger in the presence of iberiotoxin than in its absence (Figure 5B), i.e., functionally active BK_{Ca} channels limit the anticontractile effect of SNP. In contrast, in the serotonin-concentration range between 0.3 μM and 10 μM, we did not detect an effect of the BK_{Ca} channel blocker iberiotoxin on contractile responses to serotonin (Figure 5C). The NO-donor SNP reduced serotonin-induced contractile responses both in the absence and in the presence of iberiotoxin (Figure 5C). The anticontractile effect of SNP was smaller in the presence of iberiotoxin than in its absence (Figure 5D), i.e., functionally active BK_{Ca} channels facilitate the anticontractile effect of SNP.

4 Discussion

This study analyzed the differential contribution of BK_{Ca} channels to the anticontractile effect of NO at various levels of contractility in detail. The data obtained show that in rat tail arteries

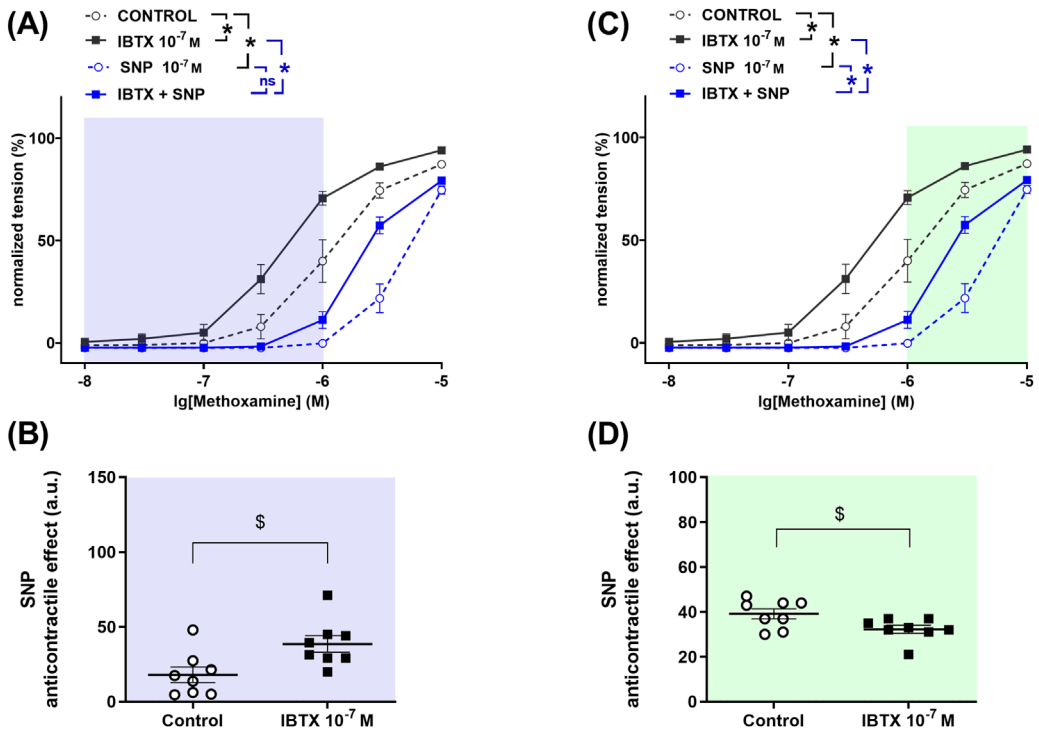

FIGURE 3
Anticontractile effect of SNP in the absence and presence of BK_{Ca} channel blockade at different levels of contractility in rat saphenous arteries. **(A, C)** Concentration–response relationships for methoxamine in the absence of any additional substances (control), in the presence of iberiotoxin (0.1 μM, IBTX), sodium nitroprusside (0.1 μM, SNP) or iberiotoxin together with sodium nitroprusside (IBTX + SNP). Data analysis was limited to the respective highlighted areas corresponding to low **(A)** and high **(C)** levels of contractility. n = 8;* - $p < 0.05$ (repeated measures ANOVA with two-stage linear step-up procedure of Benjamini, Krieger and Yekutieli). **(B, D)** Anticontractile effect of SNP in the absence (circles, Control) and in the presence of IBTX (squares, IBTX), presented as the difference between the area under the concentration-response relationships in the control and the SNP groups as well as in the IBTX and the IBTX + SNP groups. n = 8; $ - $p < 0.05$ (Welch's t-test).

at low levels of contractility, the anticontractile effect of SNP was larger in the presence of iberiotoxin than in its absence; that at higher levels of contractility, the anticontractile effect of SNP was smaller in the presence of iberiotoxin than in its absence; and that at high levels of contractility, no difference in the anticontractile effect of SNP was detected in the presence and absence of iberiotoxin. These findings were reproduced in three other vessels, the saphenous artery and the left and right coronary arteries, where at low levels of contractility the anticontractile effect of SNP was larger in the presence of iberiotoxin than in its absence, and at higher levels of contractility, the anticontractile effect of SNP was smaller in the presence of iberiotoxin than in its absence.

Of note, NO-donors such as SNP are widely used in experimental studies and in clinical practice (Napoli and Ignarro, 2003; Miller and Megson, 2007). In the present study, SNP was used to evoke an anticontractile effect. It has been shown that the effect of SNP is very similar to the effects of NO released from the endothelium (Wanstall et al., 2001). SNP can induce effects that are independent of NO (Napoli and Ignarro, 2003). However, the NO scavenger hydroxocobalamin (Kruszyna et al., 1998), abolished the SNP-induced increase in BK_{Ca} currents (Gagov et al., 2022) and SNP-evoked vasorelaxation on rat tail arteries (Schubert et al., 2004; Schmid et al., 2018). SNP can also release cyanide (Bates et al., 1991) and/or generate nitroxyl (HNO) (Filipovic et al., 2013). However, neither substance was involved in the effect of SNP (Schubert et al., 2004; Schmid et al., 2018). The anticontractile effect of SNP is therefore most likely mediated by NO released from SNP.

In the present study, the NO-donor SNP reduced methoxamine-induced contractile responses of several arteries, which is referred as the anticontractile effect of SNP. The anticontractile effect of SNP is consistent with the well-established effect of NO as a vasodilator derived from endothelial cells (Zhao et al., 2015). BK_{Ca} channels have been shown to facilitate NO-induced vasodilation in many vascular beds (Williams et al., 1988; Khan et al., 1993; Robertson et al., 1993), and have sometimes been reported to be resistant to NO-induced regulation (Tykocki et al., 2017) (additional studies listed and discussed in (Tanaka et al., 2004; Tykocki et al., 2017)). Recently, it has been proposed that BK_{Ca} channels limit the anticontractile effect of NO (Schmid et al., 2018). The present study shows that the two roles of BK_{Ca} channels, as facilitators and as limiters of the effect of NO, co-exist, at least in the four arteries studied.

Thus, a common observation in the four vessels studied was that the anticontractile effect of SNP was larger in the presence of iberiotoxin than in its absence at lower levels of contractility, i.e., functionally active BK_{Ca} channels limit the anticontractile effect of

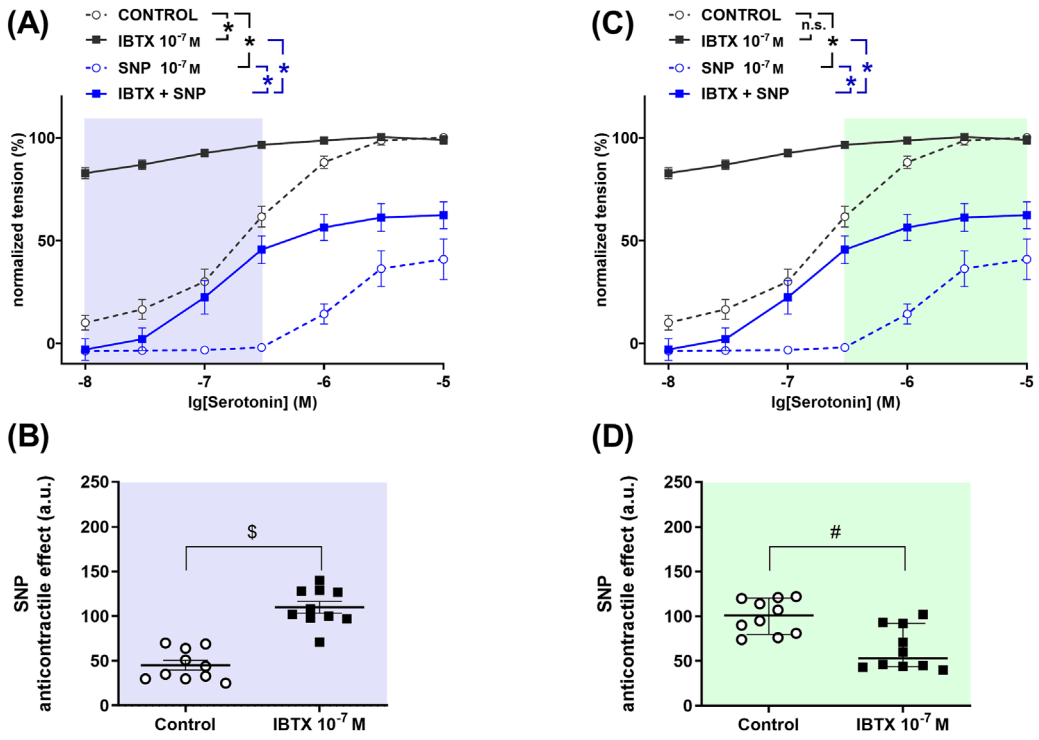

FIGURE 4
Anticontractile effect of SNP in the absence and presence of BK_{Ca} channel blockade at different levels of contractility in rat left coronary arteries. **(A, C)** Concentration–response relationships for serotonin in the absence of any additional substances (control), in the presence of iberiotoxin (0.1 μM, IBTX), sodium nitroprusside (0.1 μM, SNP) or iberiotoxin together with sodium nitroprusside (IBTX + SNP). Data analysis was limited to the respective highlighted areas corresponding to low **(A)** and high **(C)** levels of contractility. n = 10;* - $p < 0.05$ (repeated measures ANOVA with two-stage linear step-up procedure of Benjamini, Krieger and Yekutieli). **(B, D)** Anticontractile effect of SNP in the absence (circles, Control) and in the presence of IBTX (squares, IBTX), presented as the difference between the area under the concentration-response relationships curves in the control and the SNP groups as well as in the IBTX and the IBTX + SNP groups. n = 10; $ - $p < 0.05$ (Welch's t-test), # - $p < 0.05$ (Mann-Whitney test).

SNP. This finding reproduces a recent report in which the role of the BK_{Ca} channel as a limiter of the effect of NO was described for the first time (Schmid et al., 2018). However, that study investigated the overall effect of NO on the full range of contractility. The data of the present study extend the previous findings by showing that the limiting role of the BK_{Ca} channel in NO-induced vasodilation is confined to lower levels of contractility. Furthermore, the present study suggests that this limiting role of the BK_{Ca} channel in NO-induced vasodilation is a more generalized property of the BK_{Ca} channel, as it was observed in four different vessels. This suggestion is supported by the observation that this role of the BK_{Ca} channel was observed in tail arteries from different species, the rat and the mouse (Schmid et al., 2018).

In a previous study (Schmid et al., 2018), data were presented showing that the limiting role of the BK_{Ca} channel in NO-induced vasodilation is mediated by the GC/PKG pathway and by an NO-induced reduction of calcium influx via L-type calcium channels. Thus, the limiting role of the BK_{Ca} channel in NO-induced vasodilation has a specific mechanistic explanation: NO exerts two simultaneous effects on BK_{Ca} channels: a PKG-mediated activation of BK_{Ca} channels, which has long been established by a number of studies (Alioua et al., 1995; Schubert and Nelson, 2001; Kyle et al., 2013), and a deactivation of BK_{Ca} channels mediated by a decrease in the intracellular calcium concentration. It was suggested that, at lower levels of contractility, the PKG-mediated activation of BK_{Ca} channels is weaker than the $[Ca^{2+}]_i$ decrease–mediated deactivation of BK_{Ca} channels. This leads to an overall decrease in BK_{Ca} channel activity, which defines the role of BK_{Ca} channels as limiters of the effect of NO.

Alternatively, the observed shifts in methoxamine-induced concentration response relationships could be explained by an NO-induced increase in BK_{Ca} channel activity that overcomes the iberiotoxin-induced decrease in BK_{Ca} channel activity. However, this explanation seems unlikely. Recently we reported (Ma et al., 2020) that iberiotoxin was able to completely block the shift of the methoxamine-induced concentration response relationship induced by the BK_{Ca} channel opener NS19504. Thus, although NS19504, like NO, increases BK_{Ca} channel activity, this increase in channel activity was not able to overcome the iberiotoxin-induced decrease in BK_{Ca} channel activity. More importantly, we have recently published data on BK_{Ca} currents (Gagov et al., 2022), showing that SNP does not change the BK_{Ca} current in the presence of iberiotoxin, although SNP alone produces a more than sixfold increase in BK_{Ca} channel current. Thus, although SNP alone considerably increases BK_{Ca} channel activity, this increase in channel activity was not able to overcome the iberiotoxin-induced decrease in BK_{Ca} channel activity.

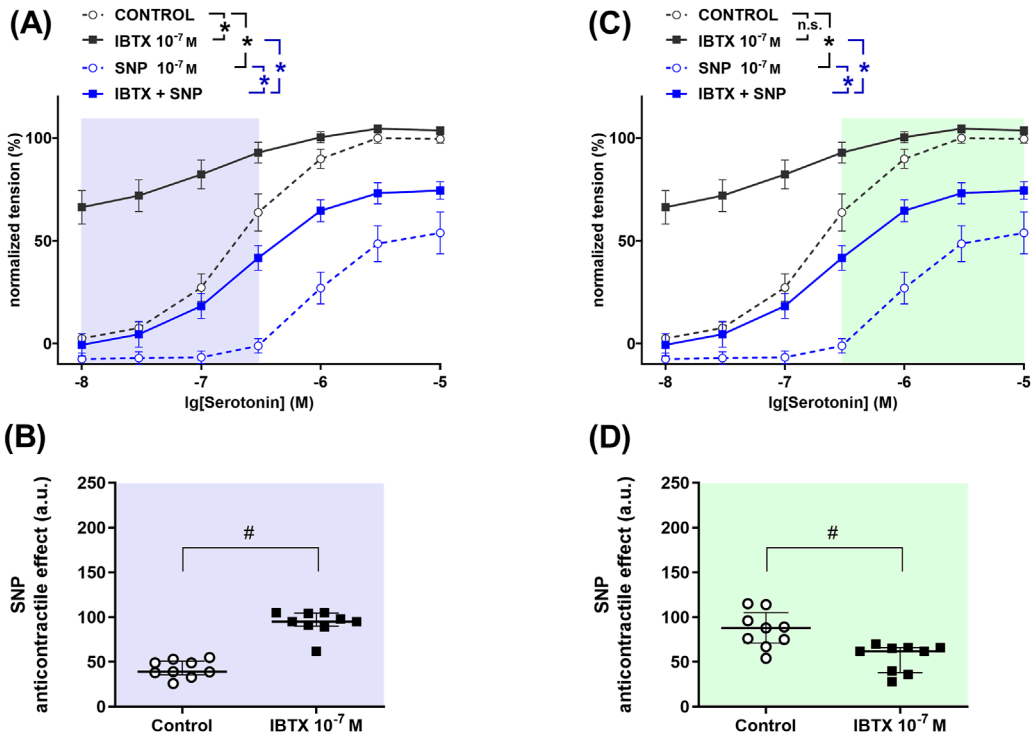

FIGURE 5
Anticontractile effect of SNP in the absence and presence of BK_{Ca} channel blockade at different levels of contractility in rat right coronary arteries. **(A, C)** Concentration–response relationships for serotonin in the absence of any additional substances (control), in the presence of iberiotoxin (0.1 μM, IBTX), sodium nitroprusside (0.1 μM, SNP) or iberiotoxin together with sodium nitroprusside (IBTX + SNP). Data analysis was limited to the respective highlighted areas corresponding to low **(A)** and high **(C)** levels of contractility. n = 9;* - $p < 0.05$ (repeated measures ANOVA with two-stage linear step-up procedure of Benjamini, Krieger and Yekutieli). **(B, D)** Anticontractile effect of SNP in the absence (circles, Control) and in the presence of IBTX (squares, IBTX), presented as the difference between the area under the concentration-response relationships in the control and the SNP groups as well as in the IBTX and the IBTX + SNP groups. n = 9; # - $p < 0.05$ (Mann-Whitney test).

In conclusion, our data suggest that the observed effects represent a physiological mechanism.

Another common observation in the four vessels studied was that the anticontractile effect of SNP was smaller in the presence of iberiotoxin than in its absence at higher levels of contractility, i.e., functionally active BK_{Ca} channels facilitate the anticontractile effect of SNP. This finding is consistent with a large number of studies showing that BK_{Ca} channels facilitate NO-induced vasodilation in many vascular beds (Williams et al., 1988; Khan et al., 1993; Robertson et al., 1993), although they are sometimes reported to be resistant to NO-induced regulation (Tykocki et al., 2017), (additional studies listed and discussed in (Tanaka et al., 2004; Tykocki et al., 2017)). The data of the present study extend previous findings by showing that the facilitating role of the BK_{Ca} channels in NO-induced vasodilation is confined to higher levels of contractility. Indeed, most previous studies have investigated the effect of NO and the role of BK_{Ca} channels herein at higher levels of contractility. This was due to the fact that the experimental protocols used required pre-constriction of the arteries before the effect of the vasodilator NO could be tested. Usually, this pre-constriction was chosen to achieve higher levels of contractility as this provides more stable conditions. However, this was most likely the reason why the limiting role of the BK_{Ca} channel in NO-induced vasodilation observed at lower levels of contractility was not previously described. Thus, opposing conclusions reported in this and in previous studies do not indicate a contradiction, but are due to the fact that a common mechanism was studied under different conditions of pre-constriction.

Of note, the mechanistic framework that explains the role of the BK_{Ca} channel as a limiter of the effect of NO also explains the role of the BK_{Ca} channel as a facilitator of the effect of NO. Again, this role is mediated by the GC/PKG pathway and by an NO-induced reduction of calcium influx via L-type calcium channels, with NO exerting two simultaneous effects on BK_{Ca} channels: a PKG-mediated activation of BK_{Ca} channels, long established by a number of studies (Alioua et al., 1995; Schubert and Nelson, 2001; Kyle et al., 2013), and a deactivation of BK_{Ca} channels mediated by a decrease in the intracellular calcium concentration. It has been suggested that, at higher levels of contractility, the PKG-mediated activation of BK_{Ca} channels is stronger than the $[Ca^{2+}]_i$ decrease–mediated deactivation of BK_{Ca} channels. This leads to an overall increase in BK_{Ca} channel activity, which defines the role of BK_{Ca} channels as facilitators of the effect of NO.

Regarding the activity of BK_{Ca} channels, RyR-mediated opening of BK_{Ca} channels by calcium sparks has been described in cerebral and coronary artery smooth muscle cells (Nelson et al., 1995; Bychkov et al., 1997; Knot et al., 1998). However, BK_{Ca} channel activity has been shown to be independent of calcium sparks in other

vessels (Szado et al., 2001; Westcott and Jackson, 2011), including the tail artery examined in the present study (Iozzi et al., 2013). Thus, the data of the present study show that the dual role of the BK_{Ca} channel in NO-induced relaxation is observed both in the presence as well as in the absence of calcium spark coupling to BK_{Ca} channels. Thus, the question of how activator calcium, supplied by calcium sparks or alternative pathways like voltage-gated calcium channels, and NO-induced signaling converge at the BK_{Ca} channels is a rather complex issue that requires a detailed and comprehensive investigation in the future.

Our previous study (Schmid et al., 2018) suggests a mechanistic framework for both the limiting and the facilitating role of BK_{Ca} channels in NO-induced vasodilation. Strictly speaking, the mechanistic explanations are limited to the tail artery, the vessel from which most of the data were obtained in the previous study (Schmid et al., 2018). Although we consider it likely that similar mechanisms are operating in the other vessels tested - at least we currently have no evidence that this is not the case - the question of whether the proposed mechanisms are common for different vessels has to be addressed. This should be done in future studies.

With our data, we were able to demonstrate a facilitator and a limiter role of the BK_{Ca} channel under conditions of vasoconstrictor-induced tone and confirm the hypothesis that BK_{Ca} channels both facilitate and limit NO-induced vasorelaxation in multiple vessels. Whether, and if so to what extent, this dual role can also be observed under other conditions (pressure-induced tone, interaction with active endothelium etc.) and ultimately *in vivo* requires further investigation.

5 Conclusion

In conclusion, the present study shows that BK_{Ca} channels can play a dual role, namely, as facilitators and as limiters of the effect of NO. Remarkably, both roles coexist in the same artery, albeit at different levels of contractility. The BK_{Ca} channels limit NO-induced vasodilation at lower levels of contractility, but facilitate NO-induced vasodilation at higher levels of contractility. The simultaneous presence of the dual role of BK_{Ca} channels in the same artery seems to be a general phenomenon, as it has been observed in different species, the rat and the mouse (Schmid et al., 2018) and in several different arteries (this study).

Data availability statement

The raw data supporting the conclusions of this article will be made available by the authors, without undue reservation.

Ethics statement

Ethical approval was not required for the study involving animals in accordance with the local legislation, institutional requirements and German law.

Author contributions

AS: Conceptualization, Data curation, Formal Analysis, Writing–original draft, Writing–review and editing. DG: Conceptualization, Data curation, Formal Analysis, Writing–original draft, Writing–review and editing. JS: Formal Analysis, Writing–original draft, Writing–review and editing, Investigation. PW: Investigation, Writing–original draft, Writing–review and editing, Formal Analysis. IS: Investigation, Writing–original draft, Writing–review and editing, Formal Analysis. RS: Writing–original draft, Writing–review and editing, Conceptualization, Data curation, Formal Analysis, Project administration, Resources.

Funding

The author(s) declare that no financial support was received for the research and/or publication of this article.

Conflict of interest

The authors declare that the research was conducted in the absence of any commercial or financial relationships that could be construed as a potential conflict of interest.

Generative AI statement

The author(s) declare that no Generative AI was used in the creation of this manuscript.

Publisher's note

All claims expressed in this article are solely those of the authors and do not necessarily represent those of their affiliated organizations, or those of the publisher, the editors and the reviewers. Any product that may be evaluated in this article, or claim that may be made by its manufacturer, is not guaranteed or endorsed by the publisher.

References

Alioua, A., Huggins, J. P., and Rousseau, E. (1995). PKG-I alpha phosphorylates the alpha-subunit and upregulates reconstituted GKCa channels from tracheal smooth muscle. *Am. J. Physiol. Cell. Mol. Physiol.* 268, L1057–L1063. doi:10.1152/ajplung.1995.268.6.L1057

Bates, J. N., Baker, M. T., Guerra, R., and Harrison, D. G. (1991). Nitric oxide generation from nitroprusside by vascular tissue. *Biochem. Pharmacol.* 42, S157–S165. doi:10.1016/0006-2952(91)90406-U

Bychkov, R., Gollasch, M., Ried, C., Luft, F. C., and Haller, H. (1997). Regulation of spontaneous transient outward potassium currents in human coronary arteries. *Circulation* 95, 503–510. doi:10.1161/01.CIR.95.2.503

Filipovic, M. R., Eberhardt, M., Prokopovic, V., Mijuskovic, A., Orescanin-Dusic, Z., Reeh, P., et al. (2013). Beyond H2S and NO Interplay: Hydrogen Sulfide and nitroprusside React directly to give nitroxyl (HNO). A New Pharmacological Source of HNO. *J. Med. Chem.* 56, 1499–1508. doi:10.1021/jm3012036

Gagov, H., Gribkova, I., Serebryakov, V., and Schubert, R. (2022). Sodium nitroprusside-induced activation of vascular smooth muscle BK channels is mediated by PKG rather than by a Direct interaction with no. *Int. J. Mol. Sci.* 23, 2798. doi:10.3390/ijms23052798

Iozzi, D., Schubert, R., Kalenchuk, V. U., Neri, A., Sgaragli, G., Fusi, F., et al. (2013). Quercetin relaxes rat tail main artery partly via a PKG-mediated stimulation of KCa1.1 channels. *Acta Physiol.* 208, 329–339. doi:10.1111/apha.12083

Khan, S. A., Mathews, W. R., and Meisheri, K. D. (1993). Role of calcium-activated K+ channels in vasodilation induced by nitroglycerine, acetylcholine and nitric oxide. *J. Pharmacol. Exp. Ther.* 267, 1327–1335. doi:10.1016/s0022-3565(25)39397-3

Knot, H. J., Standen, N. B., and Nelson, M. T. (1998). Ryanodine receptors regulate arterial diameter and wall [Ca2+] in cerebral arteries of rat via Ca2+-dependent K+ channels. *J. Physiol.* 508, 211–221. doi:10.1111/j.1469-7793.1998.211br.x

Kruszyna, H., Magyar, J. S., Rochelle, L. G., Russell, M. A., Smith, R. P., and Wilcox, D. E. (1998). Spectroscopic studies of nitric oxide (NO) interactions with cobalamins: reaction of NO with superoxocobalamin(III) likely accounts for cobalamin reversal of the biological effects of NO. *J. Pharmacol. Exp. Ther.* 285, 665–671. doi:10.1016/s0022-3565(24)37434-8

Kyle, B. D., and Braun, A. P. (2014). The regulation of BK channel activity by pre- and post-translational modifications. *Front. Physiol.* 5, 316–410. doi:10.3389/fphys.2014.00316

Kyle, B. D., Hurst, S., Swayze, R. D., Sheng, J., and Braun, A. P. (2013). Specific phosphorylation sites underlie the stimulation of a large conductance, Ca2+-activated K+ channel by cGMP-dependent protein kinase. *FASEB J.* 27, 2027–2038. doi:10.1096/fj.12-223669

Lu, T., Wang, X., He, T., Zhou, W., Kaduce, T. L., Katusic, Z. S., et al. (2005). Impaired arachidonic acid-mediated activation of large-conductance Ca2+-activated K+ channels in coronary arterial smooth muscle cells in Zucker Diabetic Fatty rats. *System* 54, 2155–2163. doi:10.2337/diabetes.54.7.2155

Ma, D., Gaynullina, D., Schmidt, N., Mladenov, M., and Schubert, R. (2020). The functional availability of arterial Kv7 channels is suppressed considerably by large-conductance calcium-activated potassium channels in 2- to 3-month old but not in 10- to 15-day old rats. *Front. Physiol.* 11, 597395–597418. doi:10.3389/fphys.2020.597395

McGahon, M. K., Dash, D. P., Arora, A., Wall, N., Dawicki, J., Simpson, D. A., et al. (2007). Diabetes downregulates large-conductance Ca2+-activated potassium β1 channel subunit in retinal arteriolar smooth muscle. *Circ. Res.* 100, 703–711. doi:10.1161/01.RES.0000260182.36481.c9

Miller, M. R., and Megson, I. L. (2007). Recent developments in nitric oxide donor drugs. *Br. J. Pharmacol.* 151, 305–321. doi:10.1038/sj.bjp.0707224

Mulvany, M. J., and Halpern, W. (1977). Contractile properties of small arterial resistance vessels in spontaneously hypertensive and normotensive rats. *Circ. Res.* 41, 19–26. doi:10.1161/01.RES.41.1.19

Napoli, C., and Ignarro, L. J. (2003). Nitric oxide–Releasing drugs. *Annu. Rev. Pharmacol. Toxicol.* 43, 97–123. doi:10.1146/annurev.pharmtox.43.100901.140226

Nelson, M. T., Cheng, H., Rubart, M., Santana, L. F., Bonev, A. D., Knot, H. J., et al. (1995). Relaxation of arterial smooth muscle by calcium sparks. *Sci.* 270, 633–637. doi:10.1126/science.270.5236.633

Robertson, B. E., Schubert, R., Hescheler, J., and Nelson, M. T. (1993). cGMP-dependent protein kinase activates Ca-activated K channels in cerebral artery smooth muscle cells. *Cell. Physiol.* 34, C299–C303. doi:10.1152/ajpcell.1993.265.1.C299

Schmid, J., Müller, B., Heppeler, D., Gaynullina, D., Kassmann, M., Gagov, H., et al. (2018). The unexpected role of calcium-activated potassium channels: Limitation of no-induced arterial relaxation. *J. Am. Heart Assoc.* 7, 1–14. doi:10.1161/JAHA.117.007808

Schubert, R., Krien, U., Wulfsen, I., Schiemann, D., Lehmann, G., Ulfig, N., et al. (2004). Nitric oxide donor sodium nitroprusside dilates rat small arteries by activation of inward rectifier potassium channels. *Hypertension* 43, 891–896. doi:10.1161/01.HYP.0000121882.42731.6b

Schubert, R., and Nelson, M. T. (2001). Protein kinases: tuners of the BK Ca channel in smooth muscle. *Trends Pharmacol. Sci.* 22, 505–512. doi:10.1016/s0165-6147(00)01775-2

Shvetsova, A. A., Gaynullina, D. K., Tarasova, O. S., and Schubert, R. (2019). Negative feedback regulation of vasocontraction by potassium channels in 10- to 15-day-old rats: Dominating role of Kv7 channels. *Acta Physiol.* 225, 131766–e13218. doi:10.1111/apha.13176

Shvetsova, A. A., Gaynullina, D. K., Winkler, P., Wohlfart, P., and Schubert, R. (2025). Potassium channel-mediated NO-induced vasodilation during maturation: Dominance of Kv7 channels. *FASEB BioAdvances*, 1–18. doi:10.1096/fba.2024-00178

Szado, T., McLarnon, M., Wang, X., and Van Breemen, C. (2001). Role of sarcoplasmic reticulum in regulation of tonic contraction of rabbit basilar artery. *Am. J. Physiol. - Hear. Circ. Physiol.* 281, 1481–1489. doi:10.1152/ajpheart.2001.281.4.h1481

Tanaka, Y., Koike, K., and Toro, L. (2004). MaxiK channel roles in blood vessel relaxations induced by endothelium-derived relaxing factors and their molecular mechanisms. *J. Smooth Muscle Res.* 40, 125–153. doi:10.1540/jsmr.40.125

Tykocki, N. R., Boerman, E. M., and Jackson, W. F. (2017). Smooth muscle ion channels and regulation of vascular tone in resistance arteries and arterioles. *Compr. Physiol.* 7, 485–581. doi:10.1002/cphy.c160011

Wanstall, J. C., Jeffery, T. K., Gambino, A., Lovren, F., and Triggle, C. R. (2001). Vascular smooth muscle relaxation mediated by nitric oxide donors: a comparison with acetylcholine, nitric oxide and nitroxyl ion. *Br. J. Pharmacol.* 134, 463–472. doi:10.1038/sj.bjp.0704269

Westcott, E. B., and Jackson, W. F. (2011). Heterogeneous function of ryanodine receptors, but not IP3 receptors, in hamster cremaster muscle feed arteries and arterioles. *Am. J. Physiol. Heart Circ. Physiol.* 300, H1616–H1630. doi:10.1152/ajpheart.00728.2010

Williams, D. L., Katz, G. M., Roy-Contancin, L., and Reuben, J. P. (1988). Guanosine 5'-monophosphate modulates gating of high-conductance Ca2+-activated K+ channels in vascular smooth muscle cells. *Proc. Natl. Acad. Sci.* 85, 9360–9364. doi:10.1073/pnas.85.23.9360

Zhao, Y., Vanhoutte, P. M., and Leung, S. W. S. (2015). Vascular nitric oxide: beyond eNOS. *J. Pharmacol. Sci.* 129, 83–94. doi:10.1016/j.jphs.2015.09.002

Frontiers in Physiology

Understanding how an organism's components work together to maintain a healthy state

The second most-cited physiology journal, promoting a multidisciplinary approach to the physiology of living systems - from the subcellular and molecular domains to the intact organism and its interaction with the environment.

Discover the latest Research Topics

See more →

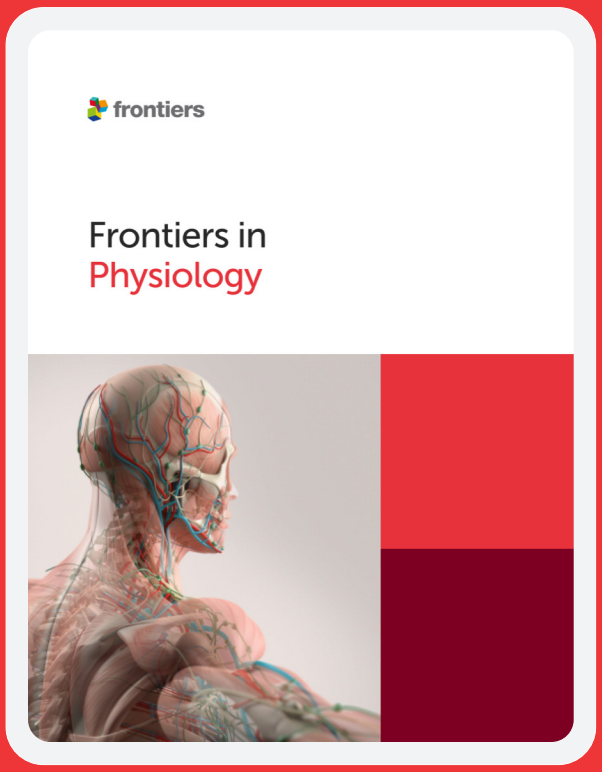

Frontiers

Avenue du Tribunal-Fédéral 34
1005 Lausanne, Switzerland
frontiersin.org

Contact us

+41 (0)21 510 17 00
frontiersin.org/about/contact